2016

Multidimensional Room-Temperature Fluorescence Microscopy for the Nondestructive Analysis of Forensic Trace Textile Fibers

Nirvani Mujumdar
University of Central Florida

MULTIDIMENSIONAL ROOM-TEMPERATURE FLUORESCENCE MICROSCOPY FOR THE NONDESTRUCTIVE ANALYSIS OF FORENSIC TRACE TEXTILE FIBERS

by

NIRVANI MUJUMDAR

B.A. Texas Tech University, 2008
M.S. Texas Tech University, 2010
M.S. University of Central Florida, 2013

A dissertation submitted in partial fulfillment of the requirements for
the degree of Doctor of Philosophy
in the Department of Chemistry in
the College of Sciences
at the University of Central Florida
Orlando, Florida

Fall Term
2016

Major Professor: Andres D. Campiglia

ABSTRACT

The purpose of this dissertation is to advance nondestructive methodology for forensic fiber examination. Non-destructive techniques that can either discriminate between similar fibers or match a known to a questioned fiber – and still preserve the physical integrity of the fibers for further court examination - are highly valuable in forensic science. A challenging aspect of forensic fiber examinations involves the comparison of fibers colored with visually indistinguishable dyestuffs. This is not an uncommon situation, as there are numerous indistinguishable fibers pre-dyed with commercial dyes of virtually identical colors. Minimal chemical structural variations are actually encouraged by the dye patent process and commercial competition.

The common denominator to forensic methodology is the fact that fiber analysis primarily focuses on the dyes used to color the fibers and do not investigate other potential discriminating components present in the fiber. This dissertation explores a different aspect of fiber analysis as it focuses on the total fluorescence emission of fibers. In addition to the contribution of the textile dye (or dyes) to the fluorescence spectrum of the fiber, we consider the contribution of intrinsic fluorescence impurities – i.e. impurities imbedded into the fibers during fabrication of garments - as a reproducible source of fiber comparison. Although fluorescence microscopy is used in forensic labs for single fiber examination, measurements are made with the aid of band-pass filters that provide very limited information on the spectral profiles of fibers. We take the non-destructive nature of fluorescence microscopy to a higher level of selectivity with the collection of room-temperature fluorescence excitation emission matrices (RTF-EEMs).

The information contained in the EEMs was first used to select the best excitation wavelength for recording first order data, i.e. two-dimensional fluorescence spectra. Pairwise comparisons involved the following visually indistinguishable fibers: nylon 361 pre-dyed with acid

yellow (AY) 17 and AY 23, acrylic 864 pre-dyed with basic green (BG) 1 and BG 4, acetate satin 105B pre-dyed with disperse blue (DB) 3 and DB 14, and polyester 777 pre-dyed with disperse red (DR) 1 and DR 19. With the exception of acrylic 864 fibers dyed with BG1 and BG4, the comparison of two-dimensional spectra via principal component analysis (PCA) provided accurate fiber identification for all the analyzed fibers.[1] The same approach was later applied to the investigation of laundering effects on the comparison of textile fibers. The presence of brighteners and other detergent components adsorbed in the fibers provided spectral fingerprints that enhanced the fiber identification process.[2, 3]

The full dimensionality of EEMs was then explored with the aid of parallel factor analysis (PARAFAC), a second order algorithm capable to determine the number of fluorescence components that contribute to an EEM along with their individual excitation and emission profiles. The application of PARAFAC was carried out unsupervised and supervised by linear discrimination analysis (LDA). The classification performances of PARAFAC and LDA-supervised PARAFAC were compared to the one obtained with supervised discriminant unfolded partial least squares (DU-PLS). The best discrimination was obtained with the supervised DU-PLS, which allowed the pairwise differentiation of the four pairs of investigated fibers.[1]

DU-PLS was then used to investigate weathering effects on the spectral features of cotton 400 pre-dyed with DB1, nylon 361 pre-dyed with AY17 and acrylic 864 pre-dyed with BG4. The investigated fibers were exposed to humid (Florida) and dry (Arizona) weathering conditions for three, six, nine and twelve months. In all cases, this algorithm was unable to differentiate non-exposed acrylic fibers from exposed acrylic fibers. DU-PLS was able to differentiate non-exposed cotton and nylon fibers from exposed fibers to Florida and Arizona weathering conditions. It was possible to determine the period of exposure to either Florida or Arizona conditions. It was also possible to discriminate between fibers exposed to Florida or Arizona weathering conditions for the

same period of time.[4] These results provide the foundation for future studies towards a non-destructive approach capable to provide information on the history of the fiber.

Abstract references:

1. de la Pena, A. M.; Mujumdar, N.; Heider, E. C.; Goicoechea, H. C.; de la Pena, D. M.; Campiglia, A. D. Nondestructive Total Excitation-Emission Microscopy Combined with Multi-Way Chemometric Analysis for Visually Indistinguishable Single Fiber Discrimination. *Analytical chemistry*, **2016**, *88*, 2967.
2. Mujumdar, N.; Heider, E. C.; Campiglia, A. D. Enhancing Textile Fiber Identification Using Detergent Fluorescence. *Applied Spectroscopy*, **2015**, *69*, 1390.
3. Heider, E. C.; Mujumdar, N.; Campiglia, A. D. Identification of Detergents for Forensic Fiber Analysis. *Analytical Bioanalytical Chemistry*, **2016**, 408 (*28*), 7935-7943.
4. Mujumdar, N.; de la Pena, A. M.; Campiglia, A. D. Classification of Pre-dyed Textile Fibers Exposed to Weathering and Photodegradation Using Fluorescence Microscopy Paired with Discriminant Unfolded-Partial Least Squares, **2016**, *Analytica Chemica Acta*, in review.

This work is dedicated to my family and friends

To my beloved parents, Mr. Ghanshyam Mujumdar and Mrs. Sulochana Mujumdar for constantly motivating me during this journey. To my dear brother, Omkar Mujumdar, for being my biggest strength and support at all times. To Dadaji, for showering me with endless blessings and showing me the way. You allowed me to believe in my dream and follow it. And to Jessy, we all miss you.

To my best friend and partner, Gourab, for always being there by my side with so much positivity; and to my little love, Tofu, for being the sunshine of my life.
You both made me a better person that I am today.

And to my friends who became my family away from home: Prachi, Bhoomi, Sindhu, Jill, Jinka, Shammi, Erica, Stanisha, Orielyz, Fiona, Carolina, and my Bangla Gang.
I will always cherish the unforgettable moments spent together.

Thank you everyone for the wonderful times, and for your constant support, motivation and love.
This has been possible because of you all.
☺

ACKNOWLEDGMENTS

First and foremost, I would like to express my sincere gratitude towards my academic advisor, Professor Andres D. Campiglia, for giving me the opportunity to become a part of his research group, to develop as a researcher and extend my knowledge in the field of forensic fiber analysis. His encouragement and guidance all along the way allowed me to gather invaluable research experience along my journey in accomplishing my Ph.D. I would also like to thank my committee members, Dr. Michael Sigman, Dr. James Harper, Dr. Matthew Rex and Dr. Robert Peale for their useful feedbacks and ideas. It has been an honor to have the opportunity to present my research to them and benefit from their knowledge. I am extremely grateful to Dr. Emily Heider and Dr. Arsenio Munoz de la Peńa for imparting their valuable knowledge and time towards my research projects, and for inspiring me to learn everything about chemometrics.

Special thanks to all my former and current lab-mates, for their support, advices, constructive criticisms and good times: Dr. Krishnaveni Appalaneni, Dr. Brent Wilson, Dr. Anthony Moore, Dr. Bassam Al-Farhani, Dr. Alaa Alhaddad, Maddie Johnson, Hugh Hayes, Maha Al-Tameemi, Khang Trieu and Luciano. Furthermore, I would like to acknowledge the following organizations for financially supporting all our research projects – U.S. National Institute of Justice (Grant # 2011-DN-BX-K553), UNL and CONICET, Ministerio de Economia y Competitividad of Spain (CTQ2014-52309-P and DPI2013-48243-C2-2-R) and Gobierno de Extremadura (GR15090-Research Group FQM003), where the last two grants were co-financed by European FEDER funds. Lastly, cheers UCF. Go Knights!

TABLE OF CONTENTS

LIST OF FIGURES

LIST OF TABLES

CHAPTER 1. FORENSIC FIBER ANALYSIS – A REVIEW

1.1. Background

Since decades forensic science has been an integral part of criminal investigations around the world. At present, nearly 400 laboratories dedicated to forensic science have been accredited under the American Society of Crime Laboratory Directors/Laboratory Accreditation Board (ASCLD/LAB) in the United States[1]. Crimes such as robbery, burglary or any types of assault, which could probably leave trace levels of physical or biological evidence behind, may now provide evidence linking the offender to the crime[2]. Trace evidence can comprise of a variety of materials such as hair, fibers (from clothing, car seat, carpet, etc.), paint chips, soil, glass pieces, pollen, dust, etc.[3,4]. Their forensic significance arises from the fact that transfer of trace material can provide valuable insight on the relationship between an offender (suspect) and a victim or a crime scene. The likelihood of establishing a partnership based on prior contact is based on Locard's exchange principle which suggests that whenever two objects come into contact, each of them transfer apart of its own material on to the other object[5]. Hence, while conducting forensic examination of textile fibers, examiners are interested in the comparison of individual fibers recovered from the crime scene and from an unknown source, with other fibers obtained from clothes obtained from a suspected individual who might possibly be related to the crime scene[5-7].

Out of all the forensic laboratories in the USA, 85% reported of having between 1 to 3 fiber analysts; out of which, 75% spend 30% or less time on fiber analysis[8]. This gets reflected on the average number of cases solved or worked upon each year, which is 27 cases per analyst

per year[8]. Wiggins further states that it is likely that with so many cases being crimes against an individual within the USA, very little (if any) time is available for an examiner to deal with less serious cases where fiber contact may have occurred. However, textile fibers are considered as one of the most important forms of trace evidence because they are ubiquitous and can be transferred easily[2,9]. Moreover in a criminal investigation, trace textile fiber evidence have a high evidential value because, although produced in large numbers, they are not homogenous or indistinguishable products[9,10], meaning that if fibers are recovered from a crime scene, it is possible to analyze them and distinguish them based on their characteristics. Fibers can be a part of direct (primary) or indirect (secondary) transfer, and forensic laboratories can examine such transferred fibers by comparing them with a standard or a known source to discover the possible common origins[3,4,11] . In other words, when a fiber is transferred from a fabric directly onto a person's clothing, it is known as a direct or primary type of transfer; whereas a secondary or indirect transfer occurs when previously transferred fibers from one person's clothing gets transferred to another person's clothes. Although, the value of fiber transfer evidence has been well accepted in the forensic community, research and further examination is mostly conducted on primary transfer[12].

Fibers have several characteristics such as material type, texture, dyes of a variety of colors and shades used to dye the fibers, etc. that could make them distinguishable from one another, and also play a crucial role in fiber analysis. Fibers are the smallest units or components used to manufacture textiles for clothing, household furniture, upholsteries, floor coverings, rugs and carpets, car seats, tents, sails, ropes, cordages, etc.[4,9]. Even though several other classifications and subtypes of fibers exist, they can essentially be classified as either natural or

man-made[9,13]. Natural fibers such as wool, cotton, silk, asbestos, etc. occur or are produced in nature, whereas man-made fibers are manufactured by humans from either naturally occurring fiber-forming polymers (e.g. viscose) or synthetic fiber-forming polymers (e.g. polyester)[9]. Further, natural fibers are divided into animal (protein), vegetable (cellulose) or mineral (asbestos) origin; whereas man-made fibers are classified into either synthetic polymers (polyvinyl, polyamide, polyester, etc.), natural polymers (viscose, acetate, etc) or other types of fibers (glass, metal, carbon, etc.), depending on their base material[4,9,13,14].

Another crucial aspect of forensic fiber analysis involves the analysis of dyestuffs or pigments used for imparting color on to the textile fibers[15] . Since different types of dyes have different types of affinities for the substrate on to which they are being applied, dyeing is the process employed by industries to imparting a certain color to a textile material by the interaction between the fabric substrate and a dye[3]. In short, a dye is a colored chemical compound used to evoke the visual sensation of a specific color by permanently adhering to a substrate (textile fiber), so that it is able to absorb and reflect certain wavelengths of light in the visible (vis) region of the spectrum ranging from 400-700 nm[3,16,17]. The ability of a dye to absorb a particular wavelength of light is based on its molecular structure, which depends on the chromophores present within the dye and their degree of unsaturation. As the degree of conjugation or the number of conjugated double bonds increase, the maximum wavelength of absorption also increases[18]. Chromophores include double bonds (C=C) and are the components within dye molecules that absorb UV-vis radiation and are responsible for color emission from the dye[16-19]. When the molecule is exposed to light, the structure of chromophore oscillates, light is absorbed and color becomes visible[19]. In contrast to dyes, a pigment is a compound having no affinity for

the textile fiber substrate, hence it is incorporated into the fiber while manufacturing it, or bonded to the surface[3,20]. Pigments are seen as colorants in a variety of fiber types (e.g. polypropylene, viscose, acrylic, polyamide, polyester, etc.). Since pigments do not have any affinity for fibers, they are generally added in the melt or while production, and are therefore not subsequently extractable[20].

There are various ways of classifying fiber dyes, including their method of application, chemical class, or the type of fiber substrate onto which they are applied. The important or major classes of dyes are: acid, basic, direct, disperse, azoic, metallized, reactive, sulfur and vat dyes[3,4,19]. Acid dyes are applied under acidic conditions so that the basic functional groups (e.g. amino) on the fiber substrate get protonated and positively charged. These groups form ionic bonds with the deprotonated functional groups (e.g. sulfonate) of the dye molecule[3,19,20]. Basic dyes are also applied under acidic conditions where the protonated functional groups on the dye form ionic bonds with the negatively charged functional groups on the fiber substrate. In the presence of heat and an electrolyte, direct dyes are directly incorporated into the cellulose during fiber production; whereas disperse dyes are also incorporated directly into synthetic fibers by linking with the substrate through weak van der Waal's force and some hydrogen bonding[3,19,20]. In brief, different dyes are bound to the fibers either through covalent and ionic bonding, Van der Waals forces or impregnation of colloidal dye particles into the fiber substrates[19,20]. Some of the important fiber dye classes and the fiber types to which they are applied are summarized in Table 1.1, with a detailed discussion associated with different fiber dye classes and their applications in the literature[20].

Table 1.1. Different types of dye classes and the fiber substrates to which they are applied

Dye class	Fiber substrate
Acid	Wool, silk, polyamide, protein, polyacrylonitrile, polypropylene
Basic	Polyacrylonitrile, acrylic, polyester, polyamide
Direct	Cotton, viscose
Disperse	Polyester, polyacrylonitrile, polyamide, polypropylene, acetate
Reactive	Cotton, wool, polyamide
Sulfur	Cotton
Vat	Cotton
Azoic	Cotton, viscose
Metallized	Wool, polypropylene

In 2012, the global fiber production was reported to be around 85.9 million metric tons (MT), out of which man-made fibers consisted of 58.6 MT (68%), 26.3 MT (31%) of it comprised of cotton and 1.07 MT (1%) was wool[21]. Synthetic or man-made fibers are the largest subgroups of fibers, and polyester fibers are the most popular among synthetic fibers[4]. In the studies related to international fiber population, cotton was reported as one of the most consumed textiles in the world, with blue and black/grey colored cotton being the most commonly encountered combination[22]. The world-wide production of man-made fibers during 2012 is presented in Table 1.2[4].

Table 1.2. Global man-made (synthetic) fiber production in 2012

Synthetic fiber material	Million metric tons	Percentage of production
Polyester	43.30	75 %
Cellulosic	4.95	9 %
Polyamide	4.01	7 %
Polypropylene	2.43	4 %
Polyacrylic	1.92	3 %
Others	0.91	2 %

As stated earlier, fibers are mass produced and are used in large quantities. Forensic examiners must be able to examine transferred fibers and compare them with a standard or a known fiber source to discover the possible common origins. Previous studies on fiber persistence have concluded that a very high proportion (about 80%) of fibers may be lot during the first 4 hours after the initial transfer; hence there should not be a delay in collecting fiber evidence[3,4,23]. Some factors – such as type of fibers transferred, the type of receiving material and the extent of the usage of receiving material after transfer – influence how the transferred fibers adhere to the receiving material (clothes)[11]. Therefore, it is very important for examiners to analyze or characterize the questioned fibers in as much details as possible to prove whether the fibers belong to the same source or not[24]. The 'analytical aspects' of a crime-related case can be optimized by adopting some strategies such as: (i) choosing the best target fibers, (ii) using the most efficient method for recovering fibers from a crime scene, (iii) examining the most relevant exhibits first, and (iv) using the most discriminating analytical techniques appropriate for the type of fibers recovered from a crime scene[25]. The upcoming sections will provide a detailed review on the various fiber recovery methods as well as different analytical techniques used till date for the forensic identification, comparison and examination of trace textile fiber evidence.

1.2. Analytical methods used for forensic fiber examination

The determination of evidential value, i.e. the extent to which trace fibers of different origins can be differentiated, is directly related to the analytical methods used for their analysis. These methods could either be destructive or nondestructive in nature; hence, if a sample size is limited, nondestructive methods must be exhausted before subjecting the sample to any destructive tests (e.g. pyrolysis, HPLC, etc.)[26]. On the other hand, nondestructive methods of

fiber comparison and analysis (e.g. microscopy) provide information about the fiber polymer (or the substrate), refractive indices, luster, birefringence, elemental composition of fibers[4], and also aid in discriminating between different classes and subclasses of fibers (single fiber comparison) by comparing specific spectral features[10,27]. Some other techniques (SEM) can be used primarily to examine the elemental contents of the fibers. A standard forensic examination of trace textile fiber evidence, according to their types (e.g. synthetic polymer) and subtypes (e.g. nylon), are based on the principles of microscopy, spectroscopy, chromatography (for separations), and mass spectrometry (MS)[3,4]. Several different analytical techniques that have been reported earlier and applied towards the forensic examination of fibers will be discussed in this review and are presented in Figure 1.1.

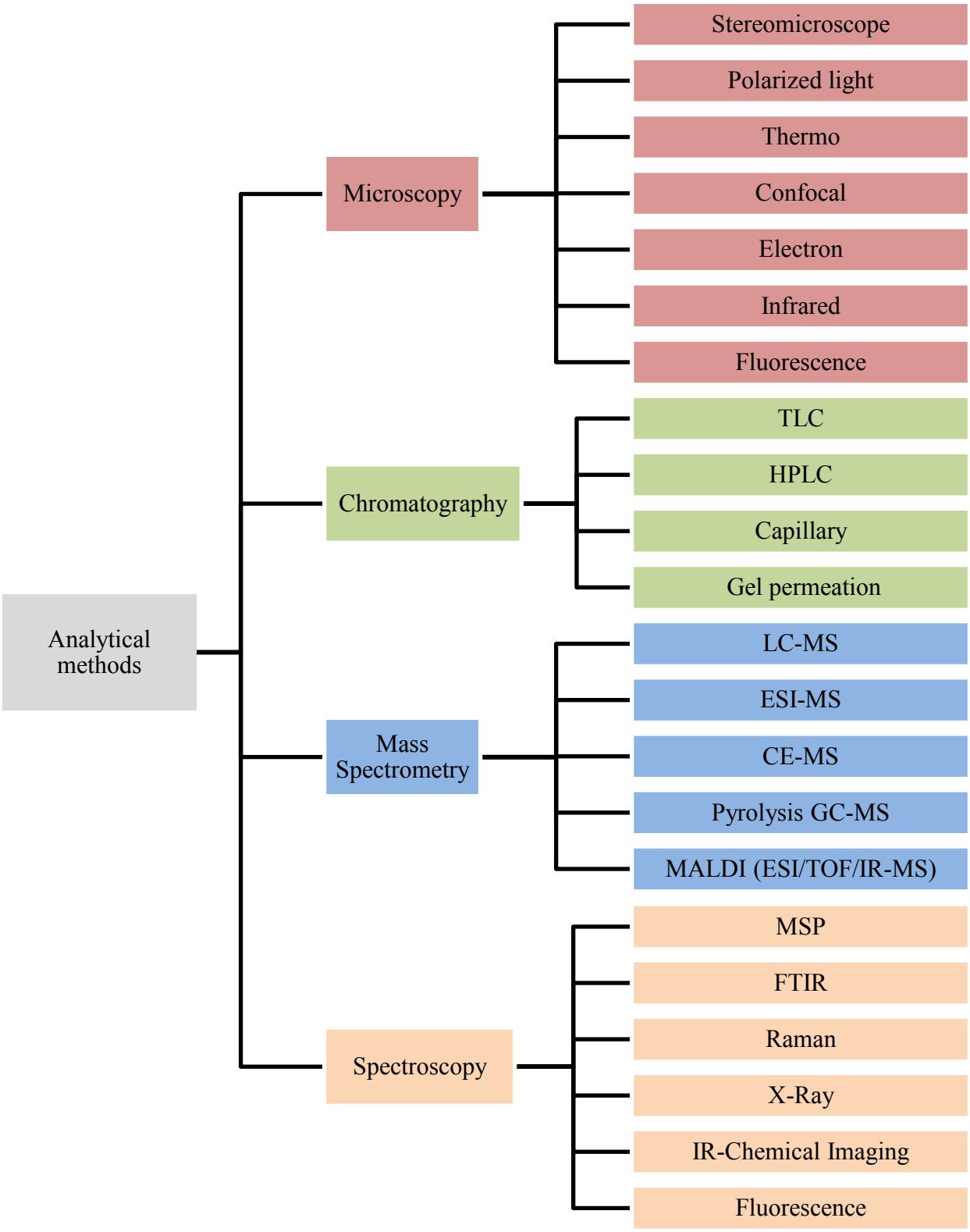

Figure 1.1. Analytical techniques applied towards the analysis of forensic fiber evidence

1.3. Microscopy

Several decades ago, the identification and comparison of fibers in forensic science laboratories were at a relatively simple level but relied heavily on microscopy[23]. The application of microscopy in the field of forensic fiber analysis is unlimited and holds a lot of importance. This is mainly due to the ability of microscopes to identify, image and resolve a single tiny piece of fiber without any structural modification. For example, a trace analyst uses microscopes for comparison of trace evidences such as fibers, hairs, soil/dust, paint, glass etc.; a firearms specialist compares marks or striations on bullets, tools, weapons, etc., a document examiner studies ink line patterns and crossings; whereas a serologist studies bloodstains and their patterns using different types of microscopes. Evidences such as ink, bloodstains, or bullets require no further treatment as they can directly be analyzed using appropriate microscopes. Sample preparation is required for other types of evidences prior to microscopic examination. Different kinds of microscopes are available and used in well-equipped forensic laboratories. In short, microscopic examinations remain a key tool for various types of comparisons of trace evidences[10]. Microscopy is an important analytical tool in the field of forensic fiber analysis, and is mainly useful for the analysis of unrelated polymer fibers. It is also used to examine fraying and cuts in the identification of characteristic features of a polymer such as striations, crimps, and cross-sectional shapes[28].

1.3.1. Stereomicroscopy

A stereomicroscope can record several characteristics of fibers such as size, crimp, color, luster[3], striations and cross-sectional shapes[28]. It is a type of an optical microscope that is designed for observation of a sample at lower magnification, and typically uses a light reflected

from the surface of an object or sample rather than transmitting through it. Preliminary evidence examination should include an overall viewing of all items in question, which can be accomplished through stereomicroscopy. In contrast to the restricted stage-objective distance in compound microscopes, the open stage area of a stereomicroscope allows for viewing large amount samples[29]. In an experiment conducted by De Wael et. al., stereomicroscopy aided in calculating the % recovery, or the total amount of fibers retrieved by tape-lifting method[30].

1.3.2. Polarized light microscopy (PLM)

A PLM is used to compare manufactured and synthetic dyed fibers, because it reveals the polymer class or the substrate based on the rotation of incident polarized light by the fiber[3,4,31] . PLM involves the usage of a polarized light to investigate the optical properties of a sample. Polarized filters are used to obtain polarized light, and to configure the movement of light waves and forcing their vibration in a single direction. Being omnidirectional, light waves will vibrate out at an angle perpendicular from the direction in which it is transmitted. A polarizer is used to allow a beam of light to move in one direction only, causing all light passing through to be blocked except for the light waves that vibrate in parallel with their privileged (light passing) directions[32,33].

This method can differentiate between common synthetic and regenerated fibers based on the characteristics of a fiber's surface and diameter, their optical properties by means of relative refractive index, birefringence, determination of the sign of elongation[27]. Goodpaster[3] stated that PLM can be used to detect dichroism in cases where dye molecules are linear and oriented along the axis of a fiber, and also to distinguish two fibers based on characteristics such as fluorescence

of the dyes, or optical brighteners added to the fibers. A target fiber study using cinema and car seat fibers determined that fluorescence microscopy was more accurate compared to white light microscopy while comparing the number of apparent matches with green cotton target fibers[34].

1.3.3. Confocal microscopy

Confocal microscopy can capture fiber images of the cross section at any point in the field of view along the length of a fiber. It is an optical imaging technique used for increasing the optical resolution and contrast of a micrograph by adding a spatial pinhole placed at the confocal plane of the lens to eliminate any light that is out of focus. It creates a three-dimensional structure from the obtained images by collecting sets of images at different depths (optical selection) from a sample[35]. An excitation light or laser source is used where the blue light reflects off a dichoric mirror. From there the laser hits two mirrors which are mounted on motors; these mirrors scan the beam of light across the sample. The dye from the sample fluoresces and the emitted light (green) gets de-scanned by the same mirrors that are used to scan the excitation light (blue) from the light source. The emitted light then passes through the dichroic and gets directed to the pinhole, later on measured by a detector such as a photomultiplier tube (PMT)[36].

Since it is a fluorescence-based technique it is destructive in nature, and the images obtained are auto-fluorescence of the specimen, meaning that fluorescence staining is not required[37]. Lepot et al. previously coupled a confocal microscope to Raman spectrometer for forensic fiber analysis caseworks [38]. The study of dye-diffusion or fluorescein dye uptake (as a function of time) into nylon 66 fibers was studied using laser scanning confocal microscopy[39].

Using a 408 nm excitation source, it takes under 5 minutes to cross-section a range of man-made fibers (with a thickness of 130 mm) such as nylon, acrylic, polyester, and acetate; as well as natural fibers such as linen, cotton and silk using confocal microscopy. No specific mounting technique is needed; hence this method can be performed on fibers that have been prepared for other forensic microscopic examinations[37].

1.3.4. Thermo-microscopy

Thermo-microscopy has previously been reported, to have aided in the differentiation of synthetic fibers (e.g. nylon and olefin carpet fibers) by measuring their melting points. Thermo microscope or hot stage microscope is a microscope coupled with a hot-stage accessory (either open or closed), which provides valuable information regarding the physical characteristics of a sample. It is an analytical technique that combines the properties of microscopy and thermal analysis to enable the solid state characterization of materials as a function of temperature. A sample under investigation is placed onto a microscopic stage which consists of a large area of temperature control element with excellent heating and cooling systems with temperature varying from -200 °C to 500 °C. A color camera is attached to the microscope to observe visual changes, and the hot stage controller (which is attached to the system) monitors the temperature program as well as transmits the thermal results to a computer for further data analysis[40,41]

The melting points of nylon 6 and nylon 6,6 are around 213 °C and 250 °C, respectively. Polythene olefin melts at around 135 °C whereas polypropylene melts at 170 °C[42]. After thermo-microscopic analysis, if all the characteristics for the two fibers being compared are identical, the next step is to conduct an examination using comparison microscope[26]. A comparison

microscope is used to identify and compare the questioned fibers to the ones obtained from a crime scene. This technique has a comparison bridge that rests on two microscopes, has two sets of optics built in one instrument, and is used to compare features such as color, crimp, pigmentation, thickness, luster and cross-sectional shapes[8,26,42]. Fiber identification, sub-classification of the fiber type, and identification and differentiation of fiber subclass based on differences in their melting points – are the three most common reasons for observing the thermal behavior of fibers via thermal microscopy[27].

1.3.5. Electron microscopy

These microscopes have an advantage over other conventional microscopes, as they have a wide range of magnification, resolving capacity, and the ability to perform elemental analysis when equipped with an energy dispersive X-ray spectrometer[4]. Scanning electron microscopy (SEM) coupled with energy dispersive spectrometry (SEM-EDS) is used primarily to examine the elemental contents of the fibers, by analyzing the inorganic materials arising from the residues of the manufacturing process, additives, or environmental contaminants[3,43]. SEM is useful in revealing the morphological features of the surface, cross-section or the tips of a fiber[44]. Moreover, surface imaging using SEM was previously reported to have aided in the identification of animal hair structure[45], and can also help in the detection of trace debris on a fiber surface[44]. A study was conducted for the recognition and identification of modified acrylic fibers from unmodified acrylics, using SEM in conjugation with energy dispersive X-ray analysis (SEM-EDX). 'Teklan' acrylic fibers showed a strong chlorine peak, 'Acribel' acrylics of various compositions tested showed a complete absence of chlorine, and 'Elura' modac fibers

showed the presence of bromine[46]. In short, modified acrylics could be distinguished from one another, based on the manufacturing companies.

1.3.6. Infrared (IR) microscopy

An IR microscopy or microspectroscopy is widely used in forensic laboratories for the identification, comparison and analysis of single fibers[31]. IR microscopy can easily be performed on fibers less than 100 μm long. The infrared spectra of different types of acrylic fiber samples have previously been examined by using a scanning IR microscopy, where 20 different varieties of undyed acrylic fiber types could be spectrally differentiated[47]. It is a minimally destructive technique, where the physical morphology of a fiber is altered when a sample is flattened prior to analysis[31,48]. Identification of generic classes (e.g. nylon, acrylic) and sub-generic classes (e.g. polyacrylonitrile, nylon 6,6) of fibers is possible this kind of microscopy[31]. Given the polymeric nature of synthetic and natural fibers, if the sample size is small, then pyrolysis coupled to gas chromatography (GC) or mass spectrometry (MS) is an informative and a minimally destructive technique[49].

1.3.7. Fluorescence microscopy

Another practical and convenient method of fiber comparison is the use of fluorescence microscopy. Several dyed fibers exhibit a surprising effect of fluorescence – when illuminated with light with shorter wavelengths (near UV region) they emit light of a longer wavelength than that with which they were excited. This phenomenon of the emission stopping when the exciting radiation is cut off, is known as fluorescence[27]. Macrae et al. reported the importance of adding fluorescence examination in the UV region to increase the discriminating power of fiber

comparisons from about 50% for white light bright field comparison microscopy to as much as 80% with the addition of UV fluorescence[10,50]. A few years ago, our research group conducted single textile fiber dye identification from two pairs of single indistinguishable fibers, using fluorescence microscopy; where an epifluorescence microscope was fiber-optically coupled to a commercially available spectrofluorimeter[51]. More recently, our group again used the same method for the discrimination of four different pairs of visually indistinguishable single fibers colored with dyes with very similar molecular structures[52]. More details are provided in the spectroscopy section (section 1.6.6). Dyes and pigments frequently fluoresce, and since a fiber's color is usually achieved by adding more than one colorant, we can expect that some of these components will fluoresce. Normal dyes fluoresce in a variety of colors with different excitation wavelengths, hence a complete range of excitation wavelengths should be employed and all the emission spectra must be recorded[27].

1.4. Chromatography

Chromatography is the science of separating and identifying mixtures of substances into their individual components. Figure 1.2 represents a schematic diagram of a typical chromatographic system[53]. Color or dye comparison is a critical factor to relate between a fiber collected from a crime scene and a fiber obtained from a suspect or a known source. The color of a fiber, present naturally or imparted through dyes or pigments, can be extremely discriminating for forensic examiners. Even though they are partially destructive in nature, chromatographic methods of analysis are regularly used by forensic scientists to compare and examine fibers because they can provide a much greater degree of discrimination than physical or optical methods alone. This section will provide an overview of various chromatographic methods

implemented towards the analysis of dyes in a fiber such as thin layer chromatography (TLC), high performance liquid chromatography (HPLC) and reverse-phase HPLC, capillary electrophoresis (CE), ultra-performance liquid chromatography (UPLC) and gel permeation chromatography (GPC).

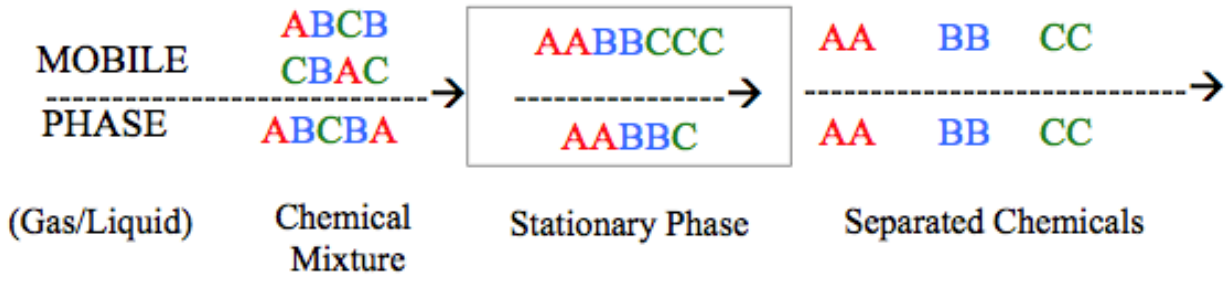

Figure 1.2. Schematic diagram of a basic chromatographic system.

1.4.1. Thin Layered Chromatography (TLC)

For over 25 years, TLC has been used to compare control and recovered fibers from crime scenes, and is a commonly used tool for the comparison of fiber dyes and the separation of dye classes in several forensic laboratories[20]. It can be coupled with techniques such as microscopy and UV-vis MSP for more specific comparison of fibers[54-56]. A typical TLC separation involves application of a solution of the sample to be analyzed as a discrete spot or smear upon the stationary (chromatographic) plate, typically coated with silica gel or alumina. Once the solvent in which the sample was applied has evaporated, the plate is developed by allowing a mobile phase to move by capillary action upwards through the stationary phase thus leading to separation[53]. The characteristics of the eluted compounds can be reported as R_f values, which are a measure of the relative distance travelled by each compound from the original spot

with respect to the solvent front[57]. In short, if a mixture (in a solution) is applied to a TLC plate and a solvent is allowed to pass across it, different components from the mixture will travel with the solvent at different rates depending on their physical and chemical properties. Visually similar looking colors can be made of different dye components and hence can be easily and quickly distinguished using TLC. Owing to the spectral properties of dye molecules and their high absorptivities, the detection levels required can generally be achieved by the human eye[20]. TLC eluent systems have been previously used for separating dyes used fibers such as polyester, nylon, acrylic[58], cotton[59,60], cellulosic[61], polypropylene[62], and wool[63].

As mentioned earlier, fibers are most likely to be dyed with a combination of several different types of dyes; hence the first step in the analytical process is the extraction of dye(s) from the fiber. Several different extraction methods utilizing a variety of solvents have been reported previously[58,61-67]. Multiple solvent system was used to separate several classes of dyes such as acid, basic, disperse and reactive. These enabled researchers to select the most appropriate pair of solvent or extraction systems for a particular dye class[59,68]. A summary of the extraction solutions used for different types of fibers and varied classes of dyes is listed in Table 1.3[20,57]. Wiggins et al. employed the TLC method to examine the dye batch variations in textile fibers, and reported that in many instances, TLC highlighted the variations between dye batches that were not detected with microscopy or visible spectroscopy[55]. Additional literature specified using TLC for the analysis of reactive colored (blue, black and red) dyes in wool and cotton fibers, where TLC provided additional information (compared to comparison microscopy and UV-vis MSP) and gave greater individuality to the fibers[56,69]. In short, comparison microscopy and UV-vis MSP are used for primary analysis and comparisons of dyes that are encountered in

textile fibers in the field of forensic science. If relatively large quantities of dyes are extracted from fibers, TLC could extensively be used as an additional comparative technique for forensic fiber analysis because it is cheap, and with practice, relatively easy to perform[4,20].

Table 1.3. Extraction solutions commonly used for fiber-dye analysis

Dye class	Fiber Type	Extraction Solution
Acid	Wool, silk, polyamide, protein, polypropylene, polyacrylonitrile	Pyridine/water (4:3 v/v)
Azoic	Cotton, viscose	Pyridine/water (4:3 v/v)
Basic	Polyacrylonitrile, modified acrylic Polyamide, polyester	Formic acid: water (1:1 v/v) Pyridine/water (4:3 v/v)
Direct	Cotton, viscose	Pyridine/water (4:3 v/v)
Disperse	Polyacrylonitrile, polyester, acetate, polyamide, polypropylene	Pyridine/water (4:3 v/v)
Metallized	Triacetate Wool, polypropylene	Pyridine/water (4:3 v/v) Aqueous oxalic acid (2%) then pyridine/water (4:3 v/v)

1.4.2. High Performance Liquid Chromatography (HPLC)

HPLC has been in use since the late 1960s and is arguably the most widely used of all the analytical separation or chromatographic techniques. Its popularity lies in its applicability in several fields and to a wide range of analytes such as amino acids, proteins, nucleic acids, carbohydrates, drugs, metabolites, pesticides, steroids, explosives, dyes, inks, etc[57,70]. A typical HPLC system consists of a solvent reservoir containing the mobile phase, pump, injection system, separation column (3-25 cm long; 3-5 mm internal diameter), detector and a data recording system. The mobile phase is pumped through the stationary phase at high pressure (up

to 6000 psi) with flow rates of 0.1-10 ml/min. A sample containing a mixture of compounds is introduced into the separation column via the injection system. Components of a mixture are resolved in the column depending on their selectivity towards either the stationary or the mobile phase contained within the column, known as retention time. A detector records the separation in form of a graph or a chromatogram, which is further analyzed by the data recording system[57,70]. A schematic diagram of a typical HPLC system is presented in Figure 1.3.[57]

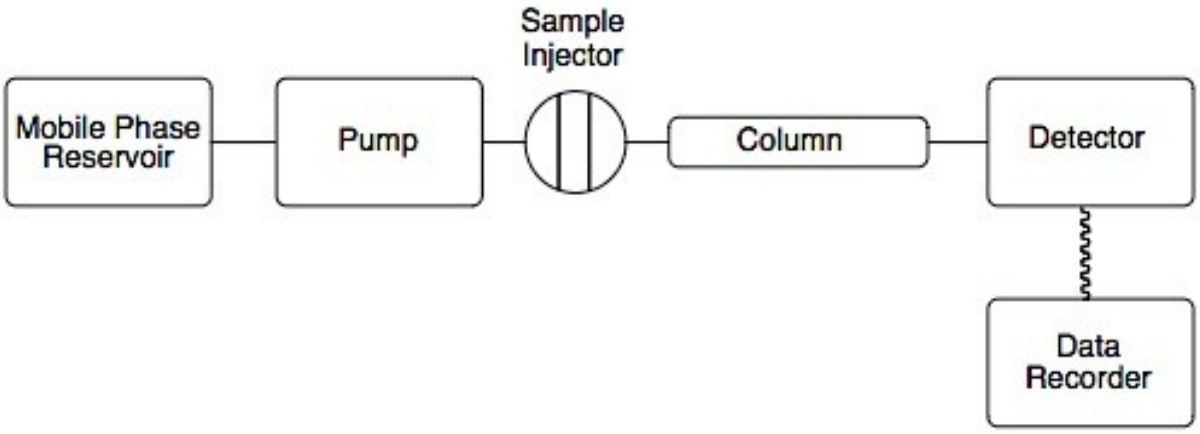

Figure 1.3. Schematic diagram of the components of a typical HPLC system

(Adapted from *Identification of Textile Fibres* by Houck, M. M.; 1st ed.; Woodhead Publishing Ltd. Cambridge, UK, 2009; Chapter 11: Analysis of dyes using chromatography, pg. 16)

HPLC has advantages over MSP and TLC for dye analysis, because MSP is limited when attempting to analyze highly absorbing dark colored fibers and TLC requires relatively large quantities of dyes and different eluent systems for various classes of dyes. On the other hand, HPLC exhibits better chromatographic resolution, greater sensitivity and can be used for qualitative and quantitative analysis[3,4]. There are different forms of HPLC depending on the retention mechanism involved. Partition chromatography is the most common type, where the

stationary phase is chemically bonded to silica particles, and can further be divided into normal phase and reverse phase chromatography. In normal phase chromatography, the stationary phase is relatively polar, allowing the non-polar compounds to elute first; whereas in reverse phase chromatography, the stationary phase is non-polar and allows polar compounds to elute first[57].

There are several considerations to make while developing an HPLC system for fiber dye analysis, such as the general chemical nature of the dye (acid, basic or neutral), probable extraction solvents to use, and the possibility of sample degradation. For example, organic solvents used for dye extraction can interfere with a UV-vis detector[70]. Some of the extracted dye classes might degrade at high temperatures, hence lower temperatures, or the use of antioxidants are necessary[70]. A summary of the HPLC separation systems developed for the analysis of acid, basic and neutral and other types of dyes is tabulated for these purposes[71]. For example, organic solvents used to extract dyes can interfere with the UV-vis detector. Some dyes can degrade at higher temperatures, hence low extraction temperatures and/or antioxidants must be used.

Reverse phase HPLC was used earlier for the separation of dyes belonging to the charged-dye class, and anionic dyes were separated more successfully compared to cationic dyes. Basic dyes can be separated efficiently by employing a separation system based on the ion-exchange property of silica. HPLC by itself can only characterize a dye based on its retention time; hence a sensitive and specific detection method must be incorporated along with chromatography. Using a multiwavelength detector helps in obtaining a complete UV-vis spectrum from dyes, determining peak purity, and assisting in generating a spectral database[3,4]. The powerful combination of HPLC coupled with mass spectrometry has previously been

reported and applied to forensic fiber dye analysis. Petrick et al.[72] combined HPLC with electrospray ionization mass spectrometry (discussed in the next section) for separating a mixture of 15 basic and 13 disperse dyes extracted from acrylic and polyester fibers of 0.5 cm length. Combining HPLC with different detection methods enables the determination of molecular structure information of the eluted bands, hence providing an extra dimension of information[4].

In a recent study, a highly sensitive chromatographic instrumentation method (HPLC) coupled with diode array detector (DAD) and a mass spectrometer, or HPLC-DAD-MS, was implemented towards the separation and detection of nine different types of dyes, their varieties ranging from neutral, positively and negatively charged dyes; dyes with single and/or multiple charges; hydrophilic and hydrophobic dyes; and dyes with a wide range of sizes and molecular masses; all in a single analytical run[73]. A single set of chromatographic conditions was applied to separate dyes of nearly all relevant fiber dye classes (from fibers as small as 1mm in length) such as acidic, basic, direct, disperse and reactive dyes. The authors reported this method to have a very high specificity due to analysis by high-resolution MS and a DAD, and were able to analyze single textile fibers of a length of few millimeters or less. Previous studies reporting fiber-dye analysis using HPLC was preferred on synthetic fibers due to easy extraction of dyes from these fibers, however, besides synthetic fibers (such as polyamide, polyester, acrylic and regenerated cellulose) Carey et al. used natural fibers for their study, such as cotton, wool. Three different digeston procedures were implemented to isolate the dye molecules from fibers[73]. Kretschmer et al. reported a combination of HPLC methods such as size exclusion liquid chromatography (SEC) and reversed-phase chromatography (RPC) for the analysis and differentiation of six different types of PET polyester fibers obtained from different

manufacturers. Chromatograms obtained from these fibers differed insignificantly in terms of their peak structure and area distribution. Data obtained was subjected to principle component cluster analysis, which was successful in differentiating the classes of fibers based on the manufacturing company[74].

van Bommel et al.[75] reported using chromatographic and spectroscopic methods for the analysis of 65 synthetic dyestuffs that were developed and used in the 1800s. For the HPLC analysis, two different solvent systems (mobile phase of the first system consisted of a gradient of water, methanol and 5% phosphoric acid in water; whereas the second system used a water and methanol gradient with a 5mM tetra butyl ammonium hydroxide) were evaluated. Detection was performed using a 996 photodiode array detection (DAD) system. The combination of UV-Vis spectra (ranging from 200–700 nm) along with chromatographic analysis of the colorants is a very strong tool for identification. Limits of quantitation (LOQs) were calculated at a signal-to-noise (S/N) of 10 at the maximum adsorption wavelengths of the dyes in the visible region. Dyes were not only distinguished from one another by their retention times, but also were identified by their unique UV-Vis absorption spectra[75].

Another technique for the sensitive comparison of dyes extracted from fibers is ultra-performance liquid chromatography (UPLC). According to the van Deemter equation, as the sample size decreases to less than 2.5 μm, there a significant gain in efficiency and it does not diminish at increased flow rates or linear velocities. By using smaller particles, the elution speed and peak capacity (number of peaks resolved per unit time in gradient separations) can be extended to new limits, which is UPLC[76]. Rapid analysis can be performed by UPLC by using high pressure pumps (<15,000 psi) capable of moving samples and mobile phases through

columns packed with increasingly smaller diameter (1.7 μm) stationary phase particles[77]. Hence, this technique is able to achieve rapid separation at a very high resolution in a very short analysis time (<5 min). Decreased band-broadening, sharper peaks and higher signal-to-noise ratio measurements are possible to achieve using UPLC[77].

1.4.3. Capillary Electrophoresis (CE)

Separation of components in a chemical mixture occur in a narrow bore capillary under the influence of an electric field, and is based upon the differential migration of charged species through a fused silica capillary filled with electrolyte[57]. Detection is typically carried out by using UV-vis absorbance spectrophotometry, resulting in a graph or an electropherogram which looks similar to a chromatographic separation. Details pertaining to the composition of the capillary columns and the mechanism are explained elsewhere[78]. A schematic diagram of a typical CE instrument is shown in Figure 1.4.[57,78]

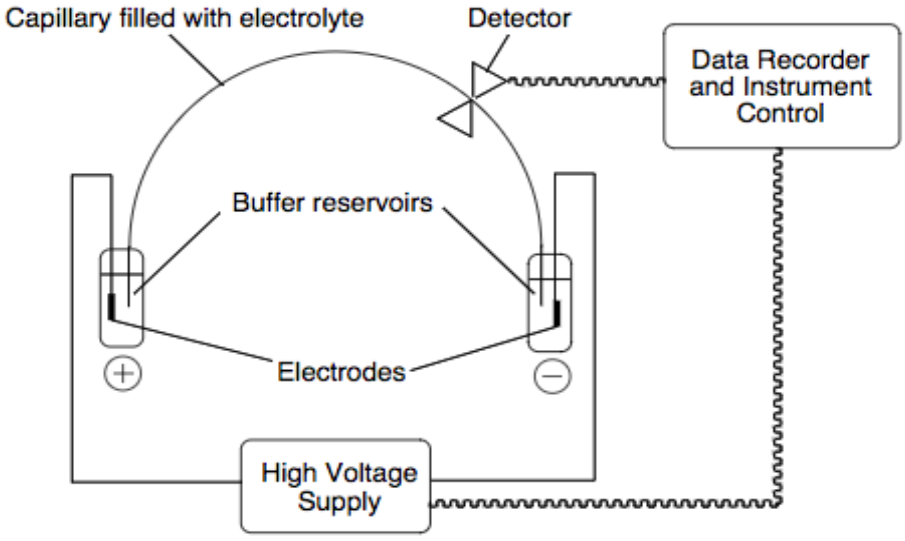

Figure 1.4. Schematic diagram of a CE system

(Adapted from *Identification of Textile Fibres* by Houck, M. M.; 1st ed.; Woodhead Publishing Ltd. Cambridge, UK, 2009; Chapter 11: Analysis of dyes using chromatography, pg. 17)

CE analysis is highly popular in the field of forensics due to its exceptional separation power, rapid analysis, low sample requirement (<50 nl) and minimal sample preparation[4]. As reported earlier in various literature articles[79-81], CE was employed for the examination of acidic, basic and reactive dyes, and was successful in separating them with a high resolution of separation. However, it was also reported that earlier attempts to develop rigorous CE methods for fiber-dye analysis were unsuccessful due to lack of reproducible migration times, poor sensitivity and the inability to separate non-ionizable dyes[70]. Hence, the introduction of micelles into the buffer now allows for separation of water-insoluble dyes; this modification is known as micellar electrokinetic chromatography (MEKC), and is reported in details elsewhere[78]. Initiaily reported by Terabe et al.[82], MEKC provides a method where neutral molecules can be resolved. Li et al. reported the ability of MEKC to separate different ionic species based on their M/Z ratio, hydrophobicity, and charge interactions at the surface of micelles[83]. Natural dyes such as flavonoids and anthraquinones were extracted from wool samples and analyzed using MEKC[84]. On the other hand, disperse dye (on polyester) and vat dye (on cotton) were difficult to ionize and separate using CE[85,86].

Oxspring et al. compared the selectivity of two techniques namely – reversed-polarity capillary electrophoresis and adsorptive stripping voltammetry (AdSV) – for the separation and identification of various reactive textile dyes[87]. Anionic reactive dyes have an electrophoretic mobility towards the anode, which is opposite to the electroosmotic flow (EOF); hence they have long migration times compared to cations and neutral species. Hence, reversing the polarities of the electrodes by applying a negative voltage to the capillary reverses the direction of EOF and changes the order in which species migrate through the capillary to anions eluting first, followed

by neutral and cationic species. The dyes now migrate against the EOF, towards the anode and are detected using a UV/Vis diode array detector. Using this technique, it was possible to separate the dyes according to differences in their electrophoretic mobilities[87]. Stripping voltammetry using a hanging mercury drop electrode (HMDE) was also employed for the separation and determination of reactive dyes by Oxspring and group where cell current was measured as a function of electric potential. Adsorptive stripping measurement is based on the formation, accumulation and reduction of the absorbed species by differential pulse voltammetry[87]. To summarize, the authors reported that reversed-polarity CE could effectively analyze and separate all the six textile dyes under investigation, and provided a fast method of analysis with all the six dyes eluting from the capillary within 7.5 minutes. On the other hand, AdSV was shown to be a very sensitive technique to monitor individual dyes, but lacked the selectivity to deal with a complex mixture of samples[87].

1.4.4. Gel Permeation Chromatography (GPC)

GPC or size exclusion chromatography is a type of liquid chromatography (using a solid stationary phase and a liquid mobile phase), which separates analytes based on their size[88]. In the late 1970s, GPC was first used as an analytical tool for the forensic identification and discrimination of polymer products, and to determine the molecular weight distribution of polymers[88,89]. In short, GPC is used to either characterize polymers and/or separate mixtures into discrete fraction e.g. polymers, oligomers, monomers, etc. Evaluation of the molecular weight distribution amongst PET fibers was reported in previous literatures[90,91], where various solvent mixtures such as m-cresol/chloroform, o-chlorophenol/chloroform and 1,1,2,2-tetrachlorothane/nitrobenzene were used as a GPC solvent for PET fibers. Also, 1,1,2,2,3,3-

hexafluoroisopropanol was described as an effective solvent for determining molecular weights of PET and nylon-6,6 fibers[92]. Farah et al. employed GPC for the analysis of 14 PET fibers and used hexafluoroisopropanol to dissolve the fibers. Results showed that distinct differences in the molecular weight of different fiber samples were found which may have potential use in forensic fiber comparison[93]. PET fibes with average molecular weights between 20,000-70,000 g/mol were determined, and the detection limits for this method were tested by using samples with concentrations as low as 1 μg/ml. Molecular analysis of PET fibers by GPC allowed for fiber comparison that could not be otherwise distinguished with high confidence, and this method can be extended to forensic comparison of other synthetic fibers such as acrylics and polyamides[93].

1.5. Mass Spectrometry

Classical forensic science depends on the fact that there cannot be a crime without the suspect leaving behind some sort of evidence – that every interaction leaves a trace behind, whether it is the minute fragment of a skin cell, a microscopic piece of fiber from carpet or clothes, the least remnant of a lingering poison in the smallest bit of blood, glass splinters, paint flakes, etc[10]. The field of forensic science has drastically evolved due to the development of increasingly sophisticated instrumentation techniques that are able to detect and analyze the smallest samples of these remnants of criminality. Also, forensic examination must be done in a manner that will stand up in court, or at least provide sufficiently reliable evidence to direct the court of a police investigation. In order to discern between two trace fibers colored either with different ratios of the same dye constituents, or with a dye similar in color but not identical in chemical structure, a high level of sensitivity and discrimination power is required. Mass-spectral-based detection methods provide for a more definitive comparison between two fibers

(mainly dyed) based on the molecular ion mass (MS) and/or the parent-mass structure (MS/MS)[15]. Mass spectrometry or MS provides examiners with unique valuable information such as molecular mass (separation is based on the mass to charge or m/z ratios), structural information and quantitative data of the molecule, all at high sensitivity[94].

MS is an analytical technique that can provide both qualitative (structural) as well as quantitative (molecular mass/concentration) information of the analyte molecules after their conversion to ions[95]. The analyte of interest is firstly introduced into the ionization chamber of the MS, where they are first ionized to acquire positive or negative ions; which further travel through the analyzer at different speed depending on their mass to charge (m/z) ratios. It is important to place reliance on this method to examine the physical identity of these infinitesimal fragments of evidence. MS is a scientific method of analyzing a sample of material to determine its molecular makeup. An examiner can ionize a sample and cause it to separate into its individual ions, allowing for the analysis and categorization of those ions to determine the sample's composition. Hence, MS has become a valuable tool in forensic science, where it can provide clues from the simplest traces left by a suspect at a crime scene. Coupling of different kinds of instrumentations and/or techniques such as LC, ESI, MALDI, CE, pyrolysis, etc. with mass spectrometry have been reported by several researchers previously, and will be reviewed.

1.5.1. Liquid chromatography mass – mass spectrometry (LC-MS)

LC-MS is a highly sensitive and selective analytical method used for the identification and characterization of dye extracts from textile fibers, according to their molecular structures[96]. Interfaces using the combination of LC-MS were developed in the early 1970s and involved

techniques of evaporating the solvent and splitting the flow from LC columns to admit the eluted compounds into the higher vacuum of the spectrometer[94]. Electrospray ionization (ESI) is a soft ionization technique used in mass spectrometry to produce ions using an electrospray, in which a high electric voltage is applied to a liquid sample to generate aerosol. Coupled with HPLC for molecular separation prior to mass spectrometric analysis, HPLC-ESI-MS has become a powerful method that is capable of analyzing small and large molecules of various polarities in a complex biological matrix[95].

Huang and coworkers[96] used LC-MS to identify different classes of dyestuffs (acid, basic, direct and disperse) extracted from 'forensic-size' textile fiber samples by connecting a UV-vis absorbance detector in series before the electrospray ionization (ESI) – MS quadrupole detector (LC-ESI-MS). A comparison of mass spectra obtained from extracted dyes was made by matching them with database of reference samples for all types of dyes that were analyzed. In another study, Huang et al.[97] used LC-ESI-MS to differentiate between seven pairs of commercial dyes having nearly identical UV-vis absorption profiles, with an absorption maxima within 5 nm. The authors reported that this method was able to discriminate between two pairs of cotton fibers that were indistinguishable via MSP, thus demonstrating the potential of LC-MS for discriminating between known and questioned fibers where the dyes are different at molecular level. Petrick et al[72] used HPLC-UV-vis-ESI MS to separate and identify a mixture of 15 basic and 13 disperse dye standards, and also reported that this method allowed for the detectinon and analysis dyes extracted from acrylic and polyster fibers of 0.5 cm. In summary, LC-ESI-MS with in-line UV-vis detection allows for the analysis of dyes extracted from textile fiber samples similar in size to what could be obtained in real forensic cases. The UV-vis absorption detector is

a good monitor for the chromatographic elution of colored dyes, whereas the LC-MS paired with ESI allows for the distinction between indistinguishable dyes[97].

Coupling the separation efficiency of HPLC with the sensitivity and specificity of MS was reported initially[98] using thermospray (TSP) ionization source for the identification and quantification of dyes in various matrices, this technique was abbreviated as TSP-HPLC-MS. TSP is a form of atmospheric pressure ionization in mass spectrometry where ions are transferred from liquid to gaseous phase for analysis[99]. Disperse and basic dyes were extracted from single fibers and placed in capillary tubes and then injected into the instrument. The mass spectra obtained from the extracted dyes matched with the previously published database for standard reference dyes[98].

1.5.2. Electrospray ionization – mass spectrometry (ESI-MS)

This technique is coupled with MS to produce ions using an electrospray source, where a high voltage is applied to a liquid to create an aerosol. The liquid containing the analyte(s) of interest (usually the dye extract from fibers) is dispersed by electrospray, into a fine aerosol[100]. Tuinman et al.[101] used electrospray ionization-mass spectrometry (ESI-MS) for the quantitative and qualitative analysis of trace nylon fibers (less than 1mm in length) dyed with acidic dyes, as well as dye extracts from nylon fibers. Qualitative identity was mainly established by comparing the observed masses for each peak in the ESI-MS of each fiber extract, whereas quantitative analysis was performed by comparing the relative intensities of the individual dye peaks which provided a measure of the concentration of each dye in each of the fibers. To absolutely confirm that any two fibers in comparison come from the same origin, it is important to demonstrate that

their dye components are identical, and that those dyes are present in the same proportion in each piece of fiber. The coupling of ESI- MS provided qualitative as well as quantitative information needed for such fiber comparisons in forensic caseworks. ESI is a so-called 'soft ionization' technique, because very little fragmentation occurs. This can be advantageous in the sense that the molecular ion of interest is always observed, however very little structural information can be o from the simple mass spectrum obtained. This disadvantage can be overcome by expanding the technique to include tandem mass spectrometry (ESI-MS/MS). For dyes with unknown origin, ESI-MS/MS analysis can help with providing information regarding the chemical structures of the compound[101].

1.5.3. Capillary electrophoresis – mass spectrometry (CE-MS)

Earlier reports suggest that CE coupled with MS was successful in discriminating textile fibers with dyed with different colored dyes[102]. In this study, different types of fibers (such as cotton, acrylic, nylon and polyester) were treated with different solvents to extract dyes from them. To ensure that the solutes were negatively charged, a high pH buffer was used to extract anionic acid, direct, reactive and dyes from cotton and nylon fibers. A reducing agent was used to extract the insoluble vat dyes from cotton and a low pH buffer was required for the CE analysis of basic cationic dyes. A diode array detector was used for the analysis of peak migration times as well as the UV-vis spectra of dye extracts. The sensitivity of the CE-MS system allowed for the precise analysis of fibers as small as 2 mm. Natural dyes were analyzed with CE paired with MS as a detection method and 11 natural dyes from plant and insect origin were quickly separated with low detection limits[84].

1.5.4. Pyrolysis-GC–mass spectrometry (Py-GC-MS)

Beyond microscopy but still under the category of minimally destructive techniques is pyrolysis coupled to a combination of gas chromatography (Py-GC) and/or mass spectrometry (Py-MS), or both. Pyrolysis is defined as the cleavage of large, nonvolatile polymeric molecules into smaller, volatile molecules by the rapid input of thermal energy[103]. This technique is capable to compare the polymeric nature of synthetic and natural fibers at expenses of partial sample consumption[49]. Pyrolysis is the high-temperature fragmentation of a substance where the thermal decomposition produces molecular fragments, usually characteristic of the composition of the sample being analyzed[49]. Py-GC and Py-MS both start with the pyrolytic breakdown of a sample. In Py-GC, the pyrolysate is swept into a gas chromatograph and the analytical information is provided by the chromatograms or pyrograms after separation. On the other hand, with Py-MS the pyrolysate enters the mass spectrometer without separation, and upon ionization several mass spectral scans are obtained. By using different data processing facilities, a composite and characteristic mass spectrum/program is plotted after spectral integration[104].

Causin et al.[105] used Py-GC-MS for the differentiation of undyed polyacrylonitrile fibers with similar morphology, where several degradation products deemed most useful for discrimination of samples. Byproducts were separated based on differences in their molecular weights, the lower ones eluted faster whereas higher molecular weight compounds had a higher retention time. Single peaks obtained from chromatograms were analyzed by principal component analysis (PCA), aiding in the differentiation of acrylic fibers with very similar structure and properties. Similarly, different types of synthetic fibers such as acetate, acrylic, nylon, polyester, rayon, vinyl, etc. were analyzed using py-GC-MS by Armitage et al.[106].

Embedding fibers in a graphite matrix and indirectly pyrolyzing them facilitated with the molecular characterization of samples due to the high spatial resolution and selectivity of Nd:YAG laser microprobe (λ_{exc} = 1064 nm) combined with GC-MS detection. Synthetic fibers were readily distinguished by their pyroprobe pyrolysate distributions that eluted at different retention times, and over 100 pyrolysates were detected from analyzed forensic fiber samples.

The polyolefinic fiber chromatogram showed characteristic peaks at m/z 57 (saturated aliphatics) and m/z 69 (unsaturated, branched and cyclic aliphatics). In particular, nylon and polyolefinic fibers were highly susceptible to thermal pyrolysis and produced large numbers of products in high abundance over a wide molecular weight range[106]. Hughes et al. employed Py-MS for the analysis of three different subtypes of nylon (synthetic) fibers, to check for its potential in the field of forensics[104]. These three subtypes of nylon fibers (nylon 4, nylon 6 and nylon 66) could be properly differentiated based on the different M/E peaks obtained in their mass pyrograms.

1.5.5. Matrix-assisted laser desorption/ionization (MALDI)

MALDI is a soft ionization technique that consists of three steps, where firstly, a sample is mixed with a suitable matrix and applied on a metal plate. Secondly, a pulsed laser source irradiates the sample triggering causing ablation and desorption of the sample as well as the matrix. Lastly, after the analyte molecules gets ionized in the hot plume of the ablated gas, they move forward into whichever mass spectrometer is used to analyze them[107]. Previously, MALDI was applied in different fields of studty such as proteomics[108], metabolomics[109], lipidomics[110], pharmacodynamics[111], etc. However, the application of MALDI towards analyzing certain

samples became limited due to its extensive sample preparation procedure, hence the introduction of desorption electrospray ionization (DESI) signified the trend towards native sample analysis[112]. Since the introduction of DESI, which allows for the analysis of samples directly from a surface with little or no sample preparation, many new ambient ionization techniques have been introduced such as matrix-assisted laser desorption electrospray ionization (MALDESI), IR-MALDESI, MALDI-time-of-flight (MALDI-TOF). MALDESI was the first ambient ionization technique to combine atmospheric pressure matrix-assisted laser desorption with electrospray post-ionization[113]. Mass spectrometry (MS) has become one of the most important tools in the field of analytical and forensic sciences and is an exceptional technique due to its sensitivity, selectivity and versatility. Hence, different MALDI-related techniques were further paired with MS and applied towards trace forensic textile fiber analysis, and the various outcomes that have been reported elsewhere will be described in this article.

A detail of MALDI and its ion-separation process that is based on time-of-flight principle is described in several other literatures[114-116]. Single textile fiber analysis was performed where acidic and basic dyes could be instantly distinguished by examining both positive and negative ion mass spectra, and additionally, this method allowed examiners to obtain results with highly accurate mass determination[117]. Soltzberg et al. further mentioned that the comparison of positive and negative ion spectra provided structural information about the dye or pigment class, and in certain cases, the spectra could distinguish between isomers.

Different classes of dyes can directly be examined from several fabrics or fibers to identify the dye masses. Previously, fiber polymers were reported to have been analyzed in a

significantly shorter period of time by using infrared or IR-MALDESI coupled with MS[28,118]. The IR-MALDESI source has been described in greater details in previous publications[119-121]. Direct analysis of dyed textile fabrics was conducted using the IR-MALDESI as a source for MS, where an IR laser source tuned to 2.94 μm was used to desorb the dyes from fabric samples with water as the matrix. The desorbed dye molecules were then post ionized by electrospray ionization or ESI, allowing for the analysis of a variety of dye classes (such as acid, basic, disperse, pigment, vat and reactive dyes) from different fibers types (such as nylon, acetate, polyester and cotton) with little or no sample preparation needed. This allowed the research group to identify the dye masses and in some cases, the fiber polymers. Details about this study include dye-detection in either positive or negative ion modes, with their observed m/z, and also showing the theoretical monoisotopic mass of the analyzed dyes with their mass accuracies[28]. In summary, direct analysis of textile fibers and dyes with IR-MALDESI is advantageous since no dye-extraction is required. Moreover, fibers can be used for multiple analyses because a very small amount is sufficient for analysis using this technique, which is rapid and takes only a few seconds to analyze the fiber and dye. Sample preparation takes minimal time where spotting a few drops of water on the fabric is needed to absorb laser energy and facilitate dye desorption.

Cochran et al. used IR-MALDESI as a source for mass spectrometry imaging (MSI) for a dyed nylon fiber cluster and single fiber[118]. Their goal was to determine how small of a sample could be used to still obtain specific m/z information about the dye and fiber polymer down to the single fiber level, and in the end, information was obtained from a single fiber which was in the order of 10 μm in diameter. This study was conducted directly from the surface of a tape lift of the fiber, with a background containing extraneous fibers. Characterization results obtained

from MSI did not identify the dyes directly since no database has yet been developed, however the authors stated that this information could be used for exclusion purposes. Using a polarity switching experiment to image the samples in both positive and negative polarity (in a single experiment) would allow for the observation of species that may preferentially ionize in either mode[118]. Lastly, the authors stated that fibers may incur minimal damage during laser pulsing, which could be minimized by using ice as an exogenous matrix.

1.6. Spectroscopy

Microscopic screening is essential to discriminate between fibers obtained from the clothes of a victim or a suspect at a crime scene. However, beyond microscopic analysis, sometimes fibers could still be indistinguishable; and in such cases spectroscopic techniques are required for further examination. Spectroscopy is the study of interactions between a matter or a sample and electromagnetic radiation and the spectral measurement devices are commonly known as spectrometers or spectrophotometers[18]. Such techniques are used to identify the type of polymer or substrate, along with their composition. Due to the wide range of samples available at a crime scene, a variety of spectroscopic techniques have previously been employed for their identification in a forensic investigation. During recent years, the application of spectroscopy to the identification and discrimination of textile fibers has increased gradually. Some of the important spectroscopic techniques such as Fourier transformed infrared spectroscopy (FTIR), Raman spectroscopy (RS) and micro-spectrophotometry in the UV-Vis region (UV-Vis MSP) are used in the study and analysis of textile fibers, mainly man-made polymers such as polyester, polyamides and polyacrylics[4]. Also, there are other less used spectroscopic techniques such as X-

Ray fluorescence spectroscopy (XRFS) and infrared chemical imaging (IRCI), which are emerging in the field of forensic fiber analysis[5].

1.6.1. Microspectrophotometry (MSP)

MSP is a special method within the UV-vis spectroscopy category, where a microscope collects light from a sample and transmits it to a UV-vis spectrometer[3,16]. This technique is more suitable for the discrimination of dyed fibers and is more suitable for dyed fibers that appear similar to the naked eye[4]. Since dyes are substances with conjugated systems of excitable electrons, UV-vis spectroscopy in general but MSP in particular is the suitable method for the analysis of different dyes on fibers. Hence, in forensic science, MSP has been established as one of the important methods for analysis because it is a rapid, repeatable and a non-destructive method (with little or no sample preparation needed) for examining trace evidence which consists of colored microscopic samples such as fibers, paints and inks[16]. MSP can distinguish between indistinguishable colored fibers by identifying the spectral characteristics two fibers in comparison, based on difference in the molecular structures of their chromophores and also on the environment in which the chromophore is found[3,4,122].

Color can be a highly discriminating feature in forensic fiber comparison, and the advent of visible MSP increases an examiner's ability to objectively discriminate color over and above microscopic comparisons. Even though further fiber discrimination was attained in the UV spectral range and reported in several literatures previously[123-129], there has been little published data on the validation of analytical parameters and protocols for UV-vis MSP in forensic fiber analysis. Fibers of fabrics such as wool, silk, polyester and acrylics with methylvinylpyridine

(MVP) are not suitable for analysis in the UV range below 300 nm due to the polymer absorbance interference[130,131]. However, colored fibers with no polymer interference such as cotton, viscose, olefin and acrylics without MVP are suitable for analysis and colored fibers could be differentiated[132]. Morgan et al. employed fluorescence MSP in addition to UV-vis MSP on 4 types of yellow and 3 types of red fibers (indistinguishable under light microscopy), since fluorescence was found to add considerable discrimination even without common fiber class/color combinations[102]. Multivariate statistical methods of spectral analysis such as unsupervised principal component analysis (PCA) and supervised linear discriminant analysis (LDA) were used to evaluate the discrimination between similar fibers of various textile fiber types (nylon, acrylic, polyester and cotton)[102]. Was-Gubala et al. used this method for discriminating single cotton fibers dyed with reactive dyes coming from the same manufacturer, and confirmed that all of the analyzed samples were distinguishable between each other with the use of MSP, mostly in the visible, and also in ultraviolet range[133].

1.6.2. Fourier Transform Infrared (FTIR) spectroscopy

This method is used classically to compare fibers in forensic and industrial analysis due to its sensitivity to minor variations in the polymer structure. FTIR is commonly used for the determination of a fiber's composition (natural versus synthetic, organic versus inorganic); class (such as polyester, polyamides and acrylics); or subclass (nylon 6, nylon 6,6, etc.)[134-137] but not for identifying the types of dyes used to color a fiber [3,31]. This is due to the fact that inherently there are low concentrations of dyes found in most textiles (less than 5% of total weight of the fiber). However, a modified version of this technique known as diffuse reflectance infrared Fourier transform spectroscopy (DRIFTS) has been reported as being more successful in

characterizing fiber dyes. DRIFTS has the advantage of not following Beer's law, hence reflectance measurements are more sensitive than transmission at lower dye concentrations[138]. Previously, this method was described to have successfully discriminated between both dye color and reactive dye state on cotton fibers[139,140]. Some advantages of the FTIR method are that it is rapid, easy, selective, and non-destructive in nature[4], meaning that other analytical methods can be implemented further after FTIR analysis. The only disadvantage is that FTIR analysis cannot be accomplished if a fiber has a diameter thicker than 30 μm, since the IR light is poorly transmitted[137]. Hence, fibers are flattened before analysis, changing their morphology. Hence, IR is a very powerful tool for the discrimination of fiber types, and to enhance the evidential value of a sample obtained at a crime scene.

Polyethylene terephthalate (PET) is the most common type of polyester fibers, and these fibers can be differentiated based on the evaluation of two features in the IR spectra: (i) the trans-gauche conformation, and (ii) the O-H end-group content of the molecule[141]. Initially, trans-conformers of the PET molecules produced Raman peaks at 846, 973, and 1340 cm^{-1}; and subsequently the ratios of the last two peaks were calculated because this is where the gauche conformation originates. The end-group content was estimated by calculating the ratios of peaks at 3340 and 874 cm^{-1}. By calculating the relative standard deviation of the polyester fibers, a way for sub-classifying PET fibers was reported[6,141]. Causin et al. utilized IR spectroscopy for the quantitative differentiation of undyed acrylic fibers by obtaining the absorbance peaks from functional groups such as nitrile (2240 cm^{-1}), carbonyl (1730 cm^{-1}) and C-H (1370 cm^{-1}). Ratios of A_{1730}/A_{2240} and A_{1730}/A_{1370}, a relative measure of the co-monomer content in the fiber, were used to differentiate the samples[142].

1.6.3. Raman Spectroscopy

Also known as vibrational spectroscopy, this is a very good analytical technique for the efficient discrimination between different dyes used for coloring textile fibers, as the molecular structures of many dyes are characterized by non-polar bonds[5]. Most of the Raman band from dyed fibers come from the dye themselves, meanwhile there are only a few weaker signals obtained from textile polymer substrates. Jochem et al. reported that Raman spectra in the visible region provided detailed data on the pigments but gave little or no information about the sub-class or types within the polymer; and on the contrary, the opposite holds true for IR spectroscopy which was well suited for characterizing the polymer but failed to provide useful data on the pigments[143].

By comparing the Raman spectra obtained from cotton (natural) versus rayon (synthetic) fibers, major difference between these fibers were reported at Raman peak at 650 cm^{-1}, obtained from rayon spectrum (the C-S-C stretch)[6]. This could possibly result from incomplete regeneration of xanthate derivative back into the form of cellulose during manufacturing rayon[144]. Rayon fibers are man-made and regenerated from wood cellulose and have an identical chemical structure to cotton (which is made up of cellulose); yet Raman spectroscopy was able to distinguish between these two fiber types[5,6]. Moreover, differentiation between two animal (natural) fibers such as wool and silk was reported[6], indicating that the main difference between them is the disulphide bond (S-S) which is present in silk, exhibiting a Raman peak at 523 cm^{-1}. Additional differentiation of polymer subtypes was successful after the principal spectral differences were reviewed between the three most common subtypes of nylon (nylon 6, nylon 6.6 and nylon 6.12) and also acrylic subtypes (acrylic Creslan 61 and modacrylic)[6]. These

findings agree with the results obtained by Miller et al., where subgeneric fiber identification and differentiation by Raman analysis was possible for undyed fibers such as nylon 6 and nylon 6,6[137]. It was also indicated that the differences between the nylon subtypes were more visible in Raman than in IR spectra. Several such studies have been conducted previously, reporting detailed differences between Raman bands obtained from nylon, acrylic, polyester and other subtypes of fibers[6,7,137,143,145,146].

A study conducted to discriminate between linen and jute[147] reported that a specific Raman band was obtained from jute samples at 1736 cm^{-1} and another band from linen at 1578 cm^{-1}. Real caseworks have been reported by Lepot et al. where Raman spectroscopy efficiently categorized questioned fibers to the set of known fibers, while also characterizing a detailed dye spectrum from all the questioned fibers. These are some of the examples of the highly specific identification capabilities of Raman spectroscopy. This method is of special interest to analyze natural fibers, where cotton fibers are often encountered from crime scenes. Since dye composition is the only characteristic feature of these fibers, Raman measurements could be useful in improving the discriminating power of these fiber types[38].

Raman spectroscopy has also been successfully in distinguishing between several types of synthetic/man-made fibers. Polyester is a generic term that comprises of different man-made textile materials, where synthetic fibers are usually produced from polyethylene terephthalate (PET)[5]. By studying the relative Raman band intensities from 350 - 1100 cm^{-1}, it is possible to observe variances between different subtypes of PET fibers that have similar spectral features[5,6]. During a real case, molten end colorless polyester fibers were searched in a suspect's blue denim

textiles. These fibers had forensic intereste because they are rarely present in blue denim textiles. Raman analysis of the colorless part of these fibers confirmed these fibers belonged to PET polymer class[148]. In a murder case, the suspect's sweat shirt with flock printing was the garment of interest. A particular fiber type known as mauve polyamide caught the examiner's attention, because several of these fibers were present on the victim. These mauve polyamide fibers produced reproducible and resolved Raman bands at 1400 cm^{-1}. Lepot et al. were able to differentiate between three undyed fibers such as cotton, polyester (PET) and polyamide (PA6.6)[38].

The implications of Raman spectroscopy mainly for the study of dyes onto the fibers, and for the examination of natural and manufactured fibers has been extensively performed in the past. In the research conducted by Jochem et al., Raman bands were obtained from dyed and undyed polyacrylonitrile (PAN) fibers. Undyed fibers provided only a few bands at the excitation wavelengths used, whereas spectra from strongly pigmented fibers were solely attributed to the pigment or dye on the fiber (without bands from the matrix or undyed fibers)[143]. Raman bands of dyes exhibited strong/intense peaks at low uptake, and increased in intensity at medium uptake, however intensity of bands decreased at high dye uptake – indicating an optimum concentration for observing the spectrum[5]. A collaborative study of the evaluation of Raman spectroscopy was conducted by Massonnet et al. on two red colored acrylic fibers (with different polymer types) using 9 different laser wavelengths ranging from blue (λ = 458 nm) to near IR (λ = 1064 nm). Results stated that red lasers (λ = 633 and 685 nm) gave the poorest spectral quality due to fluorescence interference, near IR (785, 830 and 1064 nm) lasers provided average results, whereas blue (488 nm) and green (532 nm) lasers provided spectra with best quality[146].

Thomas et al. used a laser with excitation wavelength of 632.8 nm provided the best results with little acquisition time and no spectral degradation[22]. Overall, a Raman instrument equipped with multiple lasers is recommended to analyze forensic fiber samples, since certain excitation wavelengths can cause fluorescence to interfere with the spectra. Quality of spectra obtained greatly depends on the laser wavelength that is selected, which must be an important parameter to consider while choosing a Raman instrument. To summarize, Raman spectroscopy has been established as a method for fiber analysis, and identified as a priority research area by the European Fibers Group (EFG)[149]. Even though techniques such as MSP, IR and Raman are used as nondestructive methods to measure color, very little information is gained about the specific dye. Raman is well suited for analyzing colored fibers since it requires no sample preparation, is a no-contact technique, needs only a small sample size, reproducible results can be obtained in less than a minute, and multiple tests can be performed on the same fiber[3-6]. Raman measurements are insensitive to water or moisture, hence it can be used to examine even a wet sample through a plastic pack or even in a glass container without interference[4]. Lastly, fluorescence interference can be reduced, or removed, by mathematically post-processing of the data, by altering the laser wavelengths, or using other techniques such as surface enhanced resonance Raman spectroscopy (SERRS), which increases the signal by several orders of magnitude while reducing the background noise or fluorescence[3,146].

1.6.4. X-Ray Fluorescence (XRF) Spectroscopy

XRF is a powerful quantitative and qualitative analytical tool used for the elemental characterization and composition determination of fibers. This method is fast, accurate, non-destructive, and usually requires minimum sample preparation[150-152]. When elements in a certain

sample are exposed to a high intensity X-ray source, the fluorescent X-rays will be emitted from the sample at energy levels unique to those elements[153]. During the study of a hit-and-run case, Sano et al. employed XRF spectroscopy to analyze the inorganic contents from smooth surface artificial leather fibers. Results showed important differences in the detected elements and characteristic X-ray intensities, even for samples with similar color[152].

Another study focused on analyzing fibers of different textile materials (polyester, viscose and wool) using total-XRF spectroscopy, yielding a 'fingerprint-type' trace elemental pattern[151]. Prange et al. stated that there are trace-element patterns present in textile fibers, allowing examiners to clearly distinguish not only between different fiber materials, but also between sub-groups of fibers made from the same material type. Total XRF is able to analyze samples as small as 3 mm in length and mass of less than 1μg[151]. Koons used energy dispersive (ED-XRF) for the elemental characterization of individual carpet fibers from various automobiles. It is common to find several metallic elements in automotive carpet fibers, which are less frequently obtained from residential carpet fibers; allowing for source classification of the questioned fibers[150]. Results indicated that automotive and residential fibers could be differentiated based on the presence of certain transition metals (such as Co, Cr and Zn) which were obtained from automotive fibers. This method could provide promising classification results for nylon fibers, which typically do not contain metallic elements when intended for residential use[150]. Quantitative identification of many elements introduced into cotton textiles by addition or modification can be accomplished using X-ray fluorescent spectra, and almost all elements (metal or nonmetal) in the periodic chart can be detected, identified or quantitatively analyzed using this method [154]. Moreover, elemental analysis was conducted on chemically

modified cotton textiles using x-ray fluorescence for the quantitative determination of several elements such as P, S, Cl, Ca, K, Al, Mg, etc.[155].

1.6.5. IR-Chemical Imaging (IRCI) Spectroscopy

Certain tools for sample mapping and generation of chemical images present significant advantage in the field of forensic science, by providing alternate visualization methods that enable the access to scientific information. In order to elaborate the chemical images, multiple spectra are recorded using a variety of excitation wavelengths. Such imaging techniques provide information about the distribution of the chemical species along sample surfaces, aiding in the identification of its components[5]. Flynn et al. utilized IRCI spectroscopy for the analysis of bi-component fibers, which essentially are a special class of manmade fibers that comprise of two polymers of different chemical and/or physical properties and exist within the same filament. In short, bi-component fibers are a combination of two or more polymeric materials and present a great value as forensic evidence, due to their low frequency in the population and the specific spatial configuration of their components[156]. The authors stated that IRCI has been established as method useful to recognize and provide spatially resolved chemical information for those types of bi-component fibers where it is likely to detect spectral differences between the two components present.

When one component is flattened over the other, a laser passes through both the components at the same time, providing characteristic IR spectra of each component, along with providing images that illustrate the side-by-side configuration of two components of a fiber. The two side-by-side components were clearly observed for Monvelle fibers, whose IR chemical

images were produced from the integrated spectral intensity under bands near 1641 cm^{-1} (amide I in polyamide) and 1735 cm^{-1} (C=O in polyurethane). Fibers such as Belson F040 and Cashmilon G4K also had a side-by-side configuration, since both were formed by PAN-MA-AA and PAN-MA subtypes of polyacrylic material[156].

1.6.6. Fluorescence Spectroscopy

Techniques used for the non-destructive analysis of fibers (such as diffuse reflectance infrared Fourier transform spectroscopy (DRIFTS), FTIR or Raman spectroscopy) base fiber comparisons on spectral characteristics of textile dyes imbedded in the fibers. When coupled to chemometric algorithms for spectral interpretation such as principal component analysis (PCA) and soft independent modeling of class analogies (SIMCA), DRIFTS was reported to be able to discriminate both dye color and reactive dye state on cotton fabrics[138-140]. Attempts to distinguish between single fibers were however not reported. Raman microprobe spectroscopy was able to characterize dyes in both natural and synthetic fibers via a combination of Fourier transform-Raman spectra and PCA analysis[143,157,158]. Due to the inherently weak nature of the infrared absorption signal and the Raman signal, the identification of minor fiber dyes via FTIR and Raman spectroscopy has not been possible. The inability to detect smaller dye concentrations that could add valuable information to the signature of fibers certainly reduces the discrimination power of these techniques. The weak nature of their signals also poses serious limitations in the analysis of lightly dyed fibers[6,16,43,50,146,159,160].

Details on the principles of fluorescence spectroscopy is reported elsewhere[161]. To the extent of our literature search, investigation of the full potential of fluorescence microscopy for

forensic fiber examination has not been reported. Most fluorescence microscopy articles report measurements made with excitation and emission band-pass filters[34,62], i.e. an approach that takes no advantage of the information content that exists in the spectral signatures of textile fibers. A highly discriminating approach based on fluorescence microscopy which focuses on the total fluorescence emission obtained from dyed and undyed fibers will be described in this dissertation. In addition to the contribution of the textile dye(s) to the fluorescence spectrum of the fiber, our research group has examined the contribution of intrinsic fluorescence impurities – i.e. impurities imbedded into the fibers during fabrication of garments - as a reproducible source of fiber comparison. Fiber comparison is made via acquiring data formats known as room-temperature fluorescence excitation-emission matrices (RTF-EEM). Collection of 2D fluorescence emission spectra and 3D EEMs directly from the fiber is carried out using an epi-fluorescence microscope coupled with a commercial spectrofluorimeter using fiber optic probes. Statistical figures of merit for correct identification of fiber dyes via principal component cluster analysis have been reported so that matching single evidential fibers to other single fibers, threads, or bulk materials may be accomplished with 99 % confidence[51].

Single textile fiber dye identification was carried out by our research group using excitation-emission fluorescence spectroscopy. It is a non-destructive technique where no dye extraction from the fibers is required for analysis. Two pairs of fibers with closely matched dye pairs namely acid blue 25 and 41, and direct blue 1 and 53 were analyzed, compared and differentiated with high accuracy using principle component analysis, and no false-positive identifications were observed[51]. More recently, our group was successfully able to discriminate between four pairs of visually and microscopically indistinguishable fibers using non-destructive

total excitation-emission fluorescence spectroscopy paired with multi-way chemometric analysis[52]. The four pairs of visually indistinguishable fibers consisted of nylon 361 dyed with acid yellow 17 and acid yellow 23, acetate satin 105B dyed with disperse blue 3 and disperse blue 14, polyester 777 dyed with disperse red 1 and disperse red 19, and acrylic 864 dyed with basic green 1 and basic green 4. Different chemometric algorithms were employed to process the fluorescence data obtained from the selected dyed fibers. To summarize, the ability of these algorithms to distinguish between two pairs of fibers excludes the possibility that the visually indistinguishable fibers originated from a common source[52].

Fluorescence microscopy was more recently employed by our research group for enhancing textile fiber identification using fluorescence spectra obtained from various fibers after sequentially laundering them with commercially available detergents[162]. This technique aided in the examination of the alterations in the fluorescence spectral fingerprints of single textile fibers resulting from exposure to commonly used laundry detergents that contain fluorescent whitening agents. Lastly, PCA was used to determine that the spectra of laundered fibers are distinct from the spectra of dyed and unwashed fibers such as cotton, nylon and acrylic. More recently, discriminant unfolded partial least squares (DU-PLS) method – a chemometric algorithm for data analysis – was used to analyze the 3D EEMs obtained from different dyed fibers, and to investigate the effects of weathering on the spectral features of these fibers. The fibers investigated were cotton 400 pre-dyed with DB1, nylon 361 pre-dyed with AY17 and acrylic 864 pre-dyed with BG4. The investigated fibers were exposed to humid (Florida) and dry (Arizona) weathering conditions for a time period of zero, three, six, nine and twelve months. In all cases, this algorithm was unable to differentiate non-exposed acrylic fibers from exposed acrylic fibers.

DU-PLS was able to differentiate non-exposed cotton and nylon fibers from exposed fibers to Florida and Arizona weathering conditions. It was possible to determine the period of exposure to either Florida or Arizona conditions. It was also possible to discriminate between fibers exposed to Florida or Arizona weathering conditions for the same period of time. In summary, these results provide the foundation for future studies towards a non-destructive approach capable to provide information on the history of the fiber.

1.7. Other methods reported for forensic fiber analysis

Thermal techniques, such as differential thermal analysis (DTA) and thermogravimetric analysis (TGA) were employed by Gray et al. for the characterization of polymers and fibers[163]. A particular thermal characteristic from a fiber specimen may provide fingerprinting information for forensic characterization purpose. Features of a fiber sample that can be identified include the glass transition temperature; % crystallinity; melting temperature; cold-crystallinity temperature; thermal process associated with the release of water, additives or other solvent residues; phase transformations; and thermal degradation[163]. The authors stated that TGA is useful for observing the thermal events that occur with loss of fiber mass (e.g. associated with release of adsorbed water or thermal degradation); whereas other thermal events such as glass transition, melting or solid-phase transformations can be observed using DTA. Differences in spectral features between natural (linen, wool, rayon, silk) and synthetic (nylon, vinyon, olefin, spandex, modacrylic) fibers were observed from the thermograms that were obtained from thermal analysis of the selected fibers. These thermal techniques helped Gray et al. to observe the thermal behavior of synthetic fiber properties, which was in sharp contrast with that of natural fiber materials[163].

1.8. Conclusion

The importance of the analysis of trace textile fiber evidence in forensic crime scene investigations has stimulated a substantial amount of research by examiners using several microscopic and other analytical instrumentation techniques. Since the identification and discrimination of fiber evidence is crucial, different methods have become available over the past few decades for fiber analysis ranging from simple visualization or microscopic techniques to the use of advanced analytical instrumentation techniques as described throughout this chapter. Chromatographic (e.g. HPLC) and mass-spectrometric (e.g. GC-MS) techniques are selective yet destructive in nature; however they are employed when fibers cannot be discriminated via non-destructive methods. In such cases, a reasonable procedure would be to perform analysis by comparing questioned and known fibers via dye extraction. Chromatographic techniques primarily focus on the dyes used to color the fibers and do not investigate other potential discriminating components present on the fiber. Once a dye is extracted from a fiber, the original integrity of the sample is lost. Differentiating among commercial dyes with very similar chromatographic behaviors and almost identical absorption spectra and/or fragmentation patterns could be a challenging task. Most of the microscopic techniques are non-destructive and are used by investigators to examine the physical properties of fibers. IR and thermo-microscopy are destructive because for the former method, the physical morphology of a fiber is altered when a sample is flattened prior to analysis, whereas in the later, a hot stage is used to hold the sample and to comparing melting points of different fibers; both these methods destroy the fibers.

Spectroscopic techniques on the other hand are generally non-destructive in nature, meaning they preserve the integrity of a sample, and fibers can be used again for further

examinations. For example, Raman, FTIR, MSP and fluorescence spectroscopy have been reported to be non-destructive, and have an advantage of requiring only a small sample for analysis, and these methods need no time for sample preparation. Our research group was successful in accomplishing the non-destructive analysis of several fibers with an instrumental set-up combining a commercially available spectrofluorimeter and an epi-fluorescence microscope, a technique known as fluorescence. With the 40X visible objective lens, the open pinhole diameter corresponds to a 6000 μm (6 mm) fiber length, which is considerably shorter than the ~2mm fiber length typically encountered in crime scenes. A smaller pinhole diameter (400 μm or 0.4 mm) was utilized for analyzing several dyed and undyed fibers, and the results are reported in various articles elsewhere[51,52,162]. Investigation of spectral changes that could occur in textile fibers as a result of exposure to different environmental conditions such as repetitive launderings and altering weather conditions over various time intervals was conducted using fluorescence microscopy. Moreover, four different pairs of visually and microscopically indistinguishable fibers with similar dye colors and molecular structures were successfully differentiated from one another using this method paired with different chemometric algorithms[52]. Such examinations conducted on forensic trace textile fibers can provide us with a better understanding of the physical, chemical and spectral changes that might affect textile fibers after they are analyzed, compared and differentiated using the nondestructive approach of fluorescence microscopy paired various chemometric algorithms for data analysis.

CHAPTER 2. FLUORESCENCE MICROSCOPY

2.1. Background

Textile fibers are a key source of trace evidence[3,14] and the ability to reliably identify or discriminate them is very important for forensic scientists worldwide during crime-scene cases. Microscopy, polarized light microscopy[164] , microspectrophotometry (MSP)[50,54,123-125], infrared microscopy[141,165,166] and scanning electron microscopy (SEM) paired with energy dispersive spectrometry[167] are some of the microscope-based techniques that have been reported for forensic fiber comparison and analysis, and have also been utilized to differentiate fibers with at least one distinguishable characteristic. Generally an analyst only gets a limited number of fibers to work with, sometimes only one. The advantage of these methods is that they are non-destructive in nature, meaning that they preserve the physical integrity of the fibers that could be used later on during court examination.

Beyond microscopy, there is a minimally destructive technique – pyrolysis coupled to gas chromatography – that is capable to compare the polymeric nature of synthetic fibers, by partial consumption of the sample[168]. There are several other analytical techniques reported in the past, which have been implemented towards the analysis of forensic fibers, such as UV-vis absorption spectrometry[10,15], HPLC[96], TLC[15], and CE[81,84], some of which have been reported and mentioned in the previous section, of being able to separate and identify colored dyes extracted from fibers. Preliminary attempts to develop CE methods for fiber dye analysis resulted in non-reproducible migration times, inability to separate non-ionizable dyes and poor sensitivity[169].

An alternate method of analyzing the forensic fibers is to use techniques that extract the dyes from the questioned and known fibers, in which case the samples can no longer be retrieved. Methods such as solvent extraction[170], alkaline[60,69] and enzymatic hydrolysis[56,69] have been previously used to extract the dyes from various different types of fibers. TLC has been an established technique for the separation of common classes of dye from various fibers, where silica gel is typically used as a stationary phase. Although the discriminating ability of techniques such as TLC and HPLC works the best with situations where the chromatographic and/or optical behavior of dyes from a questioned and known fibers are different, their selectivity has a drawback in differentiating between fibers with similar dyes. Moreover, there are several commercially available dyes having indistinguishable colors, similar molecular structures, indistinguishable UV and absorption spectra and similar chromatographic retention times; making it even more challenging for the forensic scientists to analyze such fibers.

The combination of liquid chromatography and mass spectrometry (LC-MS) is perhaps a well-suited method to analyze fibers with similar dyes. This approach provides a high distinguishing power and helps in identifying textile dyes that cannot adequately be distinguished using UV-visible absorption profiles[97,171]. The discrimination power of mass spectrometry (MS) has been demonstrated by coupling it with several analytical instruments such as thermospray HPLC (TSP-HPLC-MS)[98], electrospray ionization HPLC (ESI-HPLC-MS)[72,86,101,170], MALDI-TOF-MS[117], IR-MALDESI-MS[28] and time-of-flight secondary ionization (TOF-SIMS)[172]. Unfortunately MS-coupled techniques destroy the fiber evidence like all other previously mentioned methods that provide chemical information from the extracted dyes[98].

Non-destructive techniques that can either differentiate between similar fibers, or match a fiber in question to a known source – yet be able to preserve the physical integrity of such fibers without destroying them – are highly valuable in the field of forensic science. Out of such non-destructive techniques currently available for analyzing dyes extracted from textiles, newer approaches such as Fourier transform infrared spectrometry (FTIR) and Raman spectrometry have been reported to be promising. Both these techniques base their comparisons on spectral characteristics of textile dyes imbedded in the fibers. Attempts to differentiate and analyze single fibers have not been reported. However, due to the inherent weak nature of IR and Raman absorption signals, these techniques have limitations in analyzing light-colored dyes as well as detecting small concentration of dyes[22,50,146,159,160,173].

To the extent of our literature search, there have been no reports published on efforts made to investigate the total potential of fluorescence microscopy for forensic fiber examination. Most articles regarding fluorescence microscopy report measurements made with excitation-emission band-pass filters[34,62,174], i.e. an approach that does not take any advantage of the information that lies within the spectral signatures of the dyes of textile fibers. This dissertation will focus on the analysis of the total fluorescence emission spectra obtained from numerous dyed and undyed fibers, and will describe a highly discriminating methodology based on fluorescence microscopy. In addition to the contribution of the textile dyes on the total fluorescence spectrum of fibers, the contribution of intrinsic fluorescence impurities embedded into the fibers during garment fabrication or manufacture were also examined, as a potential source of fiber comparison. Fluorescence spectral data were collected in the form of 2D spectra as well as 3D excitation emission matrices (EEMs) using an epi-fluorescence microscope

coupled with a commercially available spectrofluorimeter via excitation-emission fiber optic probes. Statistical figures of merits for fiber analysis were calculated using several methods for chemometric analysis, such as: principle component cluster analysis (PCA), parallel factor analysis (PARAFAC), PARAFAC supervised by linear discriminant analysis (LDA) and discriminant unfolded partial least squares (DU-PLS). These methods have been described in details so that matching single evidential fibers to other fibers can be accomplished with 99% confidence.

2.2. Principles of fluorescence and phosphorescence

Figure 2.1 illustrates the Jablonski diagram that represents an energy diagram arranged with the energy on vertical axis, and explains the phenomena of fluorescence and phosphorescence[175]. The first transition is the absorbance of a photon of a particular energy by the molecule of interest, where the electrons within the molecule get promoted from lower to higher energy level. Once a molecule absorbs energy in the form of electromagnetic radiation, there are multiple ways as to which it can return back to the ground state. During absorption, high energy (short wavelength) light or a photon excites the system and promotes electrons within the molecule to a higher transition level from the ground electronic state (S_0) to one of the excited electronic states (S_n). Fluorescence occurs when a photon emission occurs between states of the same spin state (e.g. $S_1 \rightarrow S_0$). In short fluorescence is described as an occurrence where a molecule system absorbs and then emits light. It occurs at a shorter wavelength, and has a higher energy. Photon absorption is very rapid and takes approximately 10^{-14} to 10^{-15} s. In the excited state, the photon will rapidly (within picoseconds) relax to the lowest available energy state. After a period of delay of several nano-seconds (fluorescence lifetime), the electrons will relax

back to the ground state, releasing their stored energy in an emitted photon. However, if the spin states of the initial and the final energy levels are different (e.g. $T_1 \rightarrow S_0$), the emission or the loss of energy is known as phosphorescence. It occurs at a longer wavelength, and has lower energy than fluorescence. The lifetime of phosphorescence states are longer, ranging from 10^{-4} s to minutes or even hours (the glow remains for a longer time).

There are three important nonradiative deactivation phases during the photoluminescence process: internal conversion (IC), intersystem crossing (ISC) and vibrational relaxation (VR). IC is an intermolecular transition that occurs between energy levels of the same spin state, without the emission of radiation[176]. ISC is another radiationless transition of the excited molecule, which occurs between energy levels of different spin states. Here, the multiplicity of the molecule changes from the first excited singlet state to the lowest excited triplet state. Vibrational relaxation, which occurs very rapidly (less than 10^{-12} s), is enhanced by physical contact of the excited molecule with other particles, through which the energy (in the form of vibrations and rotations) can be transferred through collisions[176].

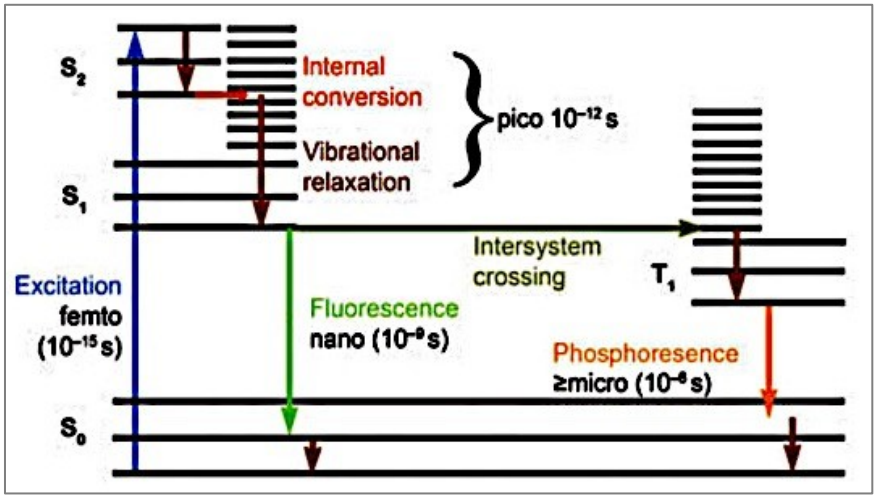

Figure 2.1. Jablonski diagram describing the various electronic processes of photoluminescence.

Fluorescence emission intensity is directly proportional to the quantum yield (φ_F), and is defined by the ratios of the rate of fluorescence (Φ_F) to the rate of absorption (Φ_A). Here $\Phi_F = k_F n_{S1} V$ and $\Phi_A = k_A n_{S0} V$; where V is the volume of sample illuminated, n_{Sx} is the number of molecules occupied in a given electronic state x, and k_F and k_A represent the rate of fluorescence and absorption respectively. Under steady state conditions, $n_{S1} = n_{S0} k_A/(k_F+k_{nr})$; where k_{nr} is the sum of the rates of all the nonradiative processes. Using these relationships, the fluorescence quantum yield is defined by the following equation:

$$\varphi_F = \frac{k_F}{k_F + k_{nr}} \tag{2.1}$$

Equation 2.1 demonstrates that enhanced fluorescence is attained when the contribution from nonradiative transitions are minimized. The structure of the analyte molecule is the main factor contributing to the magnitude of k_F. Molecules with rigid, fused ring structures exhibit increased fluorescence.

2.3. Excitation-emission matrices (EEMs)

A typical procedure for recording fluorescence data involves the measuring of emission spectrum at a fixed excitation wavelength, providing researchers with two-dimensional (2D) data plots. Similarly, 2D emission spectral profiles can be measured by monitoring the excitation wavelength at a fixed emission or fluorescence wavelength. Maximum fluorescence intensity can be obtained at the maximum excitation wavelength of a certain fluorophor. However, recording 2D spectrum from a mixture of samples consisting of several fluorescence components could provide partial information regarding the total fluorescence of the mixture. In short, where a 2D spectrum only provides partial information on the fluorescence of a sample, a three-dimensional

(3D) EEM gives the possibility of collecting the total fluorescence of that sample. A contribution from individual fluorophors to the total fluorescence spectrum of a sample depends on the fluorescence quantum yields of the fluorophors and quenching due to synergistic effects. Hence, for a sample with an unknown composition, variations in the fluorescence spectral profiles along with distinctions in the excitation wavelengths suggests that there could be more than one fluorescent component present in the sample.

The total fluorescence of a sample can be collected in a single data format known as excitation-emission matrix (EEM)[177,178]. Experimental procedure of recording EEM data is straightforward, wherein fluorescence spectra along various excitation wavelengths are acquired and plotted simultaneously. The resulting *I* x *J* matrix (EEMs) is composed from an array of 2D fluorescence spectra as the excitation wavelengths are increased incrementally after each scan[179,180]. An EEM consists of several measurement combinations obtained from a sample, where excitation wavelength is on one axis, emission wavelength on the second and fluorescence intensity is plotted on the third axis[1]. Each *I* row in the EEM corresponds to the emission spectrum at the i^{th} excitation wavelength, whereas each *J* column represents the excitation spectrum at the j^{th} emission wavelength. For a single species emitting fluorescence within the sample, the constituents of the EEM are represented by the following equation:

$$M_{ij} = 2.303\varepsilon(\lambda_i)bc\Phi_F I_0(\lambda_i)\gamma(\lambda_j)k(\lambda_j) \quad (2.2)$$

Where $I_0(\lambda_i)$ is the intensity of the incident light that excites the sample in the units of quanta/s; $2.303\varepsilon(\lambda_i)bc$ represents the sample's optical density, resulting from the product of the molar absorptivity of the analyte $\varepsilon(\lambda_i)$, the optical path-length b, and the concentration of the emitting

species c; Φ_F is the fluorescence quantum yield; $\gamma(\lambda_j)$ is the fraction of the fluorescence photons emitted at wavelength λ_j; and $k(\lambda_j)$ is the instrumental factor representing the wavelength dependence of the spectrofluorimeter's sensitivity[179]. Equation 1.2 is based on the assumption that the optical densities of the analytes (i) are low enough so that the condition $2.303\varepsilon(\lambda_i)bc << 1$ is satisfied for all λ_i. The condensed version of equation 1.2 can be expressed as:

$$M_{ij} = \alpha x_i y_j \tag{2.3}$$

Where $\alpha = 2.303\Phi_F bc$ is a wavelength independent factor containing all of the concentration dependence, $x_i = I_0(\lambda_i)\varepsilon(\lambda_i)$ and $y_j = \gamma(\lambda_j)k(\lambda_j)$. The observed relative fluorescence excitation spectrum may be represented by x_i, the wavelength sequenced set, and thought of as a column vector, x_i in λ_i space. The wavelength sequenced set, y_j, may be thought of as a row vector y in λ_j space, representing the observed fluorescence emission spectrum. Thus, for a single component, M can be represented as:

$$M = \alpha xy \tag{2.4}$$

Where M is the product of x and y multiplied by the compound specific parameter α. When data is taken from a sample that contains several, r, different species, M is represented by:

$$M = \sum_{k=1}^{r} \alpha_k x^k y^k \tag{2.5}$$

Where *k* is used to detail the species. For the observed M, analyzing the data then depends on obtaining r, α_k, x^k and y^k.

Schematic representations of 2D and 3D EEM graphs are demonstrated in Figures 2.2 and 2.3 respectively, where in the 2D plot, the excitation and fluorescence emission are shown along the sides (X and Y axis) of the EEM plot. The third axis represents the fluorescence emission intensity, or in other words, the fluorescence intensity is plotted as a function of excitation and emission wavelengths either as a 2D (contour map) or 3D data format. Within the defined contour levels, the fluorescence profile of the compound does not change with the excitation wavelength, and vice-versa. As observed from the EEM graph, the center of the contour plot corresponds to the maximum excitation and emission wavelengths of the fluorescent components from the analyzed sample.

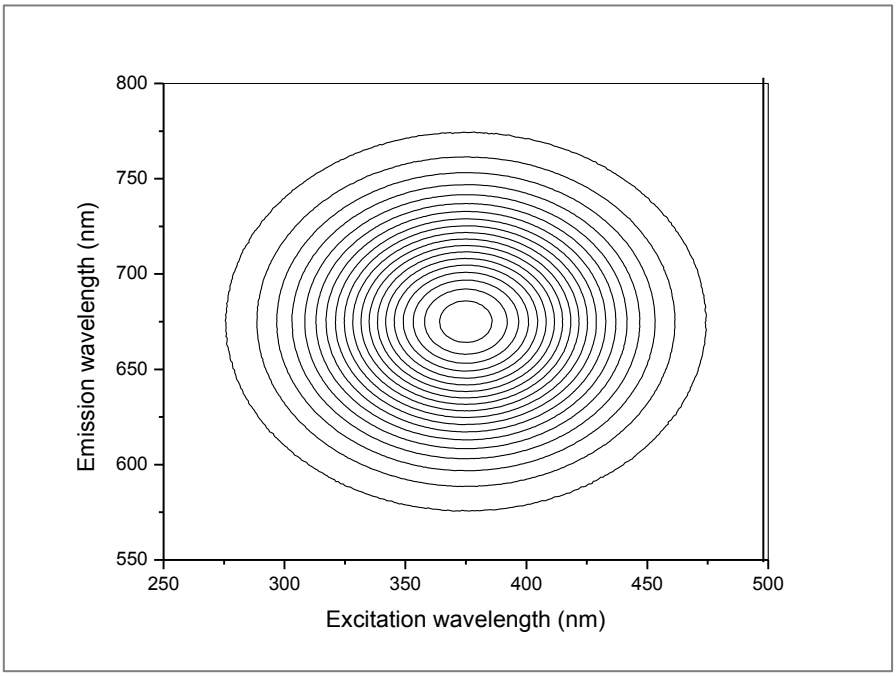

Figure 2.2. Example of a 2D counter plot, where the center of the contour circle represents the excitation wavelength at which maximum intensity of fluorescence emission is achieved.

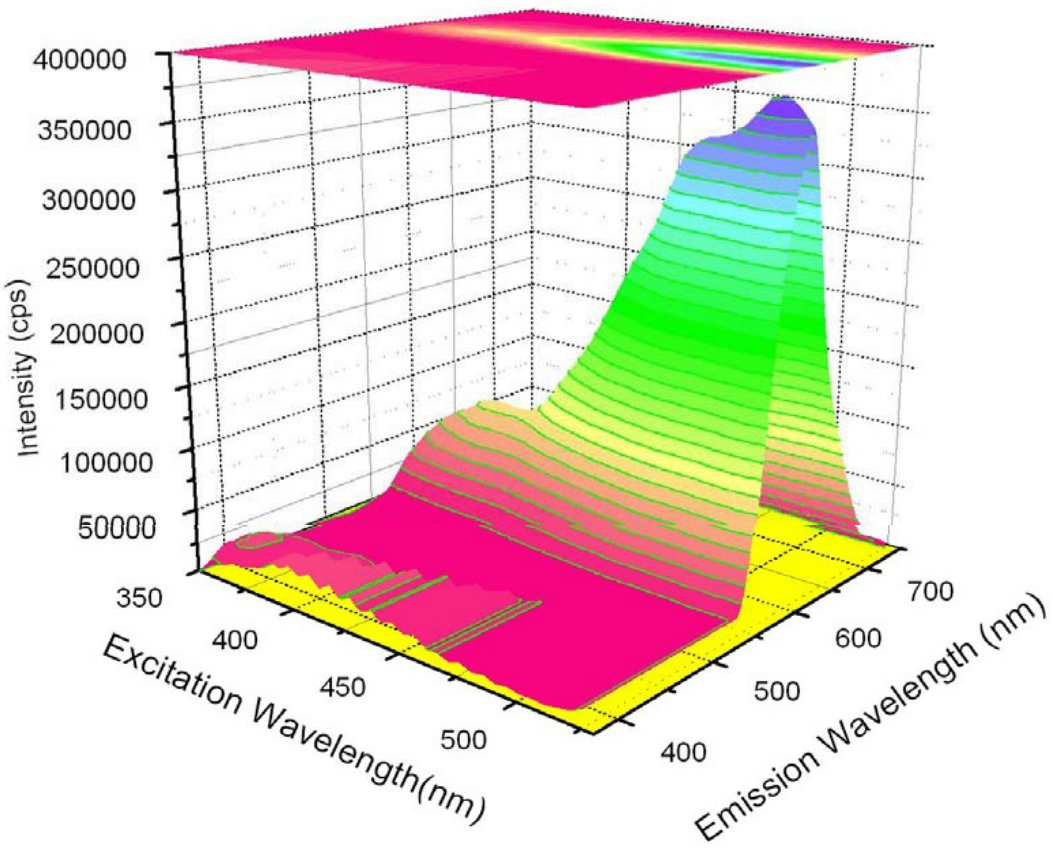

Figure 2.3. Example of an EEM graph plotted in 3D, where fluorescence emission intensity is plotted as a function of excitation wavelength and emission wavelength.

Figure 2.3 illustrates a more complex EEM recorded from a multicomponent mixture exhibiting fluorescence. The multicomponent nature of such a mixture becomes evident when multiple changes in the emission profile are observed due to variations in the excitation wavelengths. The same holds true for the variations in the excitation spectra as the emission wavelengths are changed. The number of changes noted in the excitation or emission profile provides visual indication of the number of fluorescent components or impurities present in such a mixture.

CHAPTER 3. INSTRUMENTATION AND EXPERIMENTAL PROCEDURE FOR FIBER ANALYSIS

A commercially available spectrofluorimeter (Fluoromax-P from Horiba Jobin-Yvon) was fiber-optically coupled to an epifluorescence microscope (BX-51 from Olympus) and was used to obtain 2D fluorescence emission spectra in the visible and the UV spectral regions. The spectrofluorometer is equipped with a 100 W continuous pulsed xenon arc lamp with a 200-2000 nm illumination. Excitation and fluorescence spectra were acquired with two spectrometers with the same reciprocal linear dispersion of 4.25 nm/mm and same accuracy of ± 0.5 nm with 0.3 nm resolution. Both the diffraction gratings had 1200 grooves per mm and were blazed at 330 nm excitation and 550 nm emission wavelengths. A photomultiplier tube (from Hamamatsu, model R928) with a spectral response from 185-800 nm was used for detecting the fluorescence, operating at room temperature in the photo-counting mode. Commercially available software (DataMax) was used to obtain all the spectral data and computer-control the instrument.

The microscope and the spectrofluorometer were connected together using commercially available fiber-optic bundles (Figure 3.1). The sample compartment of the spectrofluorometer optimized the collection efficiency via two concave mirrors, and was equipped with a fiber-optic platform (from Horiba Jobin-Yvon). The microscope is equipped with two 50/50 beam splitters, one for the UV and the other for the visible spectral region. Two objective lenses, 10x and 40x (from Olympus, UplanSApo) were used for light collection in both the spectral regions. A rotating pinhole wheel, with various diameters ranging from 100 μm to 6000 μm, is located between the 50-50 beam splitter and the mirror that directs fluorescence emission to the charge-

coupled device (CCD) camera (iDS UI-1450SE-C-HQ, USB-camera) of the microscope or the emission fiber optic bundle of the spectrofluorometer.

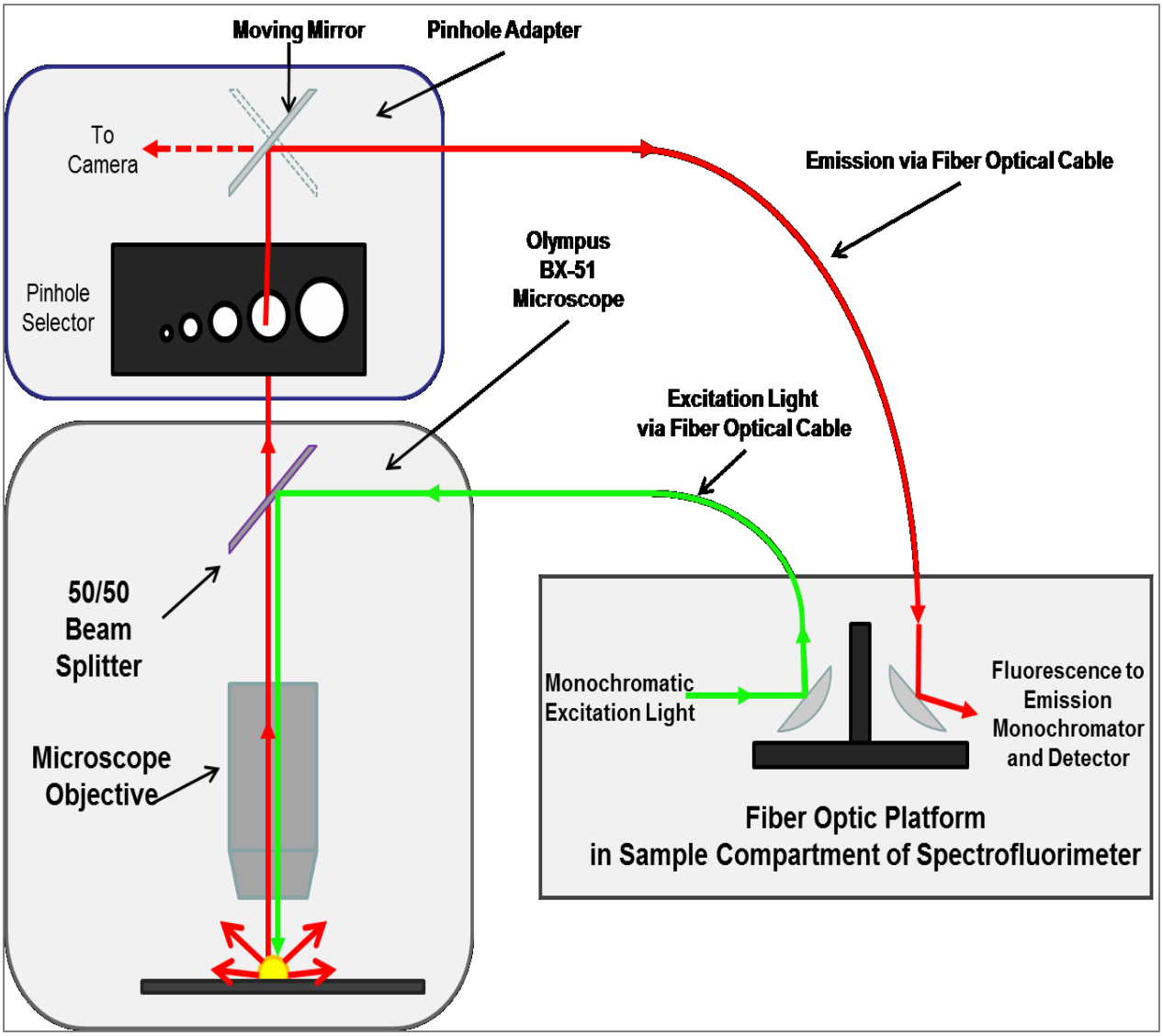

Figure 3.1. Schematic diagram displaying the microscope connected to fiber optic mount of spectrofluorimeter via fiber optic bundles

Optimization of instrumental parameters was performed by monitoring the fluorescence intensity and signal-to-background ratio recorded from single fibers as a function of pinhole size and excitation-emission band-pass. The examined fibers are listed in Table 3.1 (see appendix B for detailed results). All the examined fibers showed maximum fluorescence emission in the visible region. The combination of a 400 μm pinhole diameter and a 40X visible-objective provided the best signal-to-background ratio (S/B) for all the investigated fibers. Two experimental procedures commonly employed for forensic fiber examination were tested, namely the slide and coverslip[38,57] and the tape lift[181-183] methods. Since the tape lift method provided the worst S/B ratios, all further studies were performed via the cover slip method.

Table 3.1. Dyed fibers used for S/B optimization of instrumental parameters

Type of dyed fiber	*Best ex/em λ*	*Objective*	*Magnification*	*Method*
Basic red 9	305/380 nm	UV	10x	Slide/cover-slip
Basic red 9	305/380 nm	UV	40x	Slide/cover-slip
Basic red 9	305/380 nm	UV	40x	Tape-lift
Basic green 4	380/475 nm	Vis	10x	Slide/cover-slip
Basic green 4	380/475 nm	Vis	40x	Slide/cover-slip
Basic green 4	380/475 nm	Vis	40x	Tape-lift
Disperse red 4	309/385 nm	UV	40x	Tape-lift
Disperse red 4	513/576 nm	Vis	40x	Tape-lift
Acid green 27	410/686 nm	Vis	40x	Tape-lift
Direct blue 53	587/692 nm	Vis	40x	Tape-lift

CHAPTER 4. ENHANCING TEXTILE FIBER IDENTIFICATION WITH NONDESTRUCTIVE EXCITATION-EMISSION SPECTRAL CLUSTER ANALYSIS

4.1. Background on previous work

Currently, several methods for fiber dye analysis have been developed for cases where the material composition of the fiber doesn't provide exclusive information for its identification purposes. As discussed in the earlier chapter, some of the highly selective and sensitive methods for dye analysis from single textile fibers include electrospray ionization mass spectrometry[97,101], surface enhanced Raman spectroscopy[184,185] and capillary electrophoresis[81]. Even though it is possible to perform single fiber analysis using these techniques, a pretreatment[185] or a dye-extraction step[81,101] is required, which can potentially damage the evidence or a fiber sample. This chapter discusses an attempt made by our research group to develop a novel method that was employed towards the acquisition of 3-dimensional excitation-emission luminescence data from different dyed fibers. The goal was to come up with a non-destructive technique that could be able to distinguish these single fiber pairs dyed with dyes with very similar molecular structures. Such identification methods for single textile fibers are in demand for forensic applications, and non-destructive methods (such as fluorescence microscopy) with minimal sample pretreatment have a great potential for utility.

To demonstrate the applicability of this technique, four dyes from two different classes such as acid blue (AB) 25 and 41 and direct blue (DB) 1 and 53 were selected for this study. In

other words, two pairs of indistinguishable fibers such as AB25 and AB41 from a nylon fabric (8”x10”) and DB1 and DB53 from a cotton fabric (8”x10”) were chosen for this study. Their corresponding dyes were purchased from Sigma-Aldrich (excluding acid blue 41 which was purchased from acros organics) at reagent grade level. Table 4.1 lists the % composition of dye in the reagent standard and the type of fabric used in dying process.

Table 4.1. Commercial sources and purity of dyes along with the corresponding type of fibers used for the dyes

Fiber type	*Dye*	*Commercial source*	*% purity of the dye*
Spun nylon 361	Acid blue 25	Sigma Aldrich	45 %
Spun nylon 361	Acid blue 41	Acros Organics	NA
Cotton 400	Direct blue 1	Sigma Aldrich	80 %
Cotton 400	Direct blue 53	Sigma Aldrich	75 %

Two commercially available instruments were combined together: a fluorimeter which was fiber-optically coupled with an epi-illumination Olympus microscope (the instrumental setup will be discussed in the next section). These pairs of dyed fibers were selected mainly because of the difficulty in distinguishing their spectra from one another, and because they represent two of the eight major classes of dyes (acid, basic, azoic, direct, disperse, sulfur, reactive and vat dyes)[3]. Our research group published a rigorous statistical comparison of visually and microscopically indistinguishable fibers based on the 3D excitation-emission matrices (EEMs) recorded from several spots on these single fibers[51]. Ten spots along the length of the fiber were sampled and EEMs were obtained, which served as a training set for comparison to other fibers, threads and regions of a fabric.

EEM acquisition for non-destructive analysis of dyes from single textile fibers can provide highly valuable identification information[51]. Coupling of the two commercially available instruments enhances the luminescence capabilities above that of other individual instruments, and allows for the acquisition of a complete training set for fiber dye identification from an individual fiber. Accounting for the alterations in the EEM spectra from different locations along the length of a fiber delivered a useful training set that was used as a basis for data analysis performed via principle component cluster analysis (PCA). The statistical approach to identification was demonstrated using dyed fibers with similarities both in 2D absorbance spectra and in 3D EEM data.

4.2. Detergent fluorescence used for fiber identification

Single textile fibers can be an essential form of trace evidence, and characterization of evidential fibers has been accomplished by examining fiber composition[136,137,141,186], molecular structure of the fiber dye[187-189], color[190], absorption[191], Raman signal[192] and fluorescence[51,193]. Identification using characteristics such as these is essential since forensic fibers can be transferred and subsequently examined to discover common origins. Because the composition of the fiber is infrequently useful for exclusive discrimination (cotton, wool and other synthetic fibers are widely available), secondary information, for example dye composition or color must also be utilized. Previously, we reported the identification of single fibers using fluorescence excitation-emission data of visually indistinguishable dyed fibers[51]. While that approach provided high accuracy in fiber identification, the analysis utilized the presence of fluorescent dyes on the fiber- a feature that may not always be available.

Chemical or mechanical modifications to textiles – following manufacture and distribution – are of increasing interest, since modifications to the fibers after mass manufacture can provide more exclusive identification. For example, Bowen et al. reported a method for removal of small (1-50 μm) particles adhering to carpet fiber surfaces, and the analysis of the particles using scanning electron microscopy coupled with energy-dispersive X-ray spectrophotometry[194]. Others have utilized X-ray fluorescence of metal contaminants that were introduced to cotton fibers as flame retardants or for water resistance[195]. In both cases, solvent extraction was required that could damage the sample and the expensive techniques could be cost prohibitive to routine analysis. Alternatively, alteration in fiber color or dye characteristics due to laundering remains a relatively unexploited characteristic for fiber identification, and could be inexpensively and nondestructively assessed on both dyed and undyed fibers. The goal of this work was to determine if fluorescence spectra of laundered textiles could be utilized to distinguish washed fibers from unwashed fibers. The fluorescence spectral characteristics of detergents adhered to textile fibers were exploited for identification.

Fluorescent whitening agents (FWAs) are used in laundry detergents[196] to achieve visual whitening because they fluoresce in the blue when exposed to near UV radiation. As a result, their accumulation on fibers due to sequential washings can influence the optical characteristics of the fiber and fiber dyes. Early work by Stana et al.[197] monitored the adsorption of anionic whitening agents (sulfonated stilbene derivatives) on cellulose fibers using zeta potential and calorimetry measurements. Their report of increasing zeta potential with whitening agent concentration up to a concentration of 0.8% indicates that adsorption of the FWA onto the negatively charged cellulose fiber may facilitate FWA fluorescence-based fiber identification.

More recent publications have detailed the kinetics of color change via perception[198] and spectrophotometric[199] measurements upon sequential launderings. In case of spectrophotometric analysis of fibers with exposure to detergents[199], it was reported that cotton, polyester and acrylic fibers showed no statistically significant alteration in transmittance (at the wavelength of minimum transmittance); wool fibers did indicate changes in the transmittance at a select wavelength correlating to minimum transmittance. Here, expansion of the wavelengths studied to a complete spectral profile (rather than the wavelength of minimum transmittance) and use of statistical methods for fiber comparison provides a rigorous comparison of fibers using FWA fluorescence measurements.

The emission spectra of fluorescent dyes and brighteners on single fibers are measured with fluorescence microscopy, and used to determine that the presence of brightening agents due to laundering enhances the fiber identification process. Three fiber types (acrylic 864, cotton 400, and nylon 361) both dyed (basic green 4, direct blue 1, and acid yellow 17, respectively) and undyed were examined before and after laundering between 0-6 times with the commercially available detergents: All, Cheer, Oxiclean, Tide (liquid), Tide (powder), Wisk and Purex. The first six detergents contain the FWA disodium diaminostilbene disulfonate, while Oxiclean contains the FWA tinopal. Although the fibers are not visually distinguishable after sequential washings, changes in the fluorescence emission spectra were characterized by measuring the spectral components due to the fiber itself (undyed and unwashed), the dye bound to the fiber, and the detergent adhered to the fiber. Spectra of washed fibers were fit using the component spectra and changes in the spectra with repeated washings were quantified. The spectral distinctions between fibers with adhered detergent components, and unwashed fibers, provide a

detergent fingerprint that is utilized to distinguish unlaundered from laundered fibers using principal component cluster analysis.

4.3. Experimental

4.3.1. Reagents and materials

The dyes, including basic green 4 (90% purity), direct blue 1 (80% purity), and acid yellow 17 (60% purity) were purchased from Sigma-Aldrich (www.sigma-aldrich.com). Quartz coverslides (75 x 25 x 1 mm) and coverslips (19 x 19 x 1 mm) were purchased from Chemglass (www.chemglass.com). Nanopure water was prepared using a Barnstead Nanopure Infinity water purifier. Fabrics were acquired and dyed by Testfabrics, Inc (West Pittston, PA). The dye concentrations were 3% for BG4 on acrylic 864, 2% DB1 on cotton 400, and 2% of AY17 on nylon 361.

4.3.2. Instrumentation

A detailed description of the instrument employed for fluorescence microscopy has been reported previously[51], and explained in chapter 3. Fluorescence measurements form liquid detergents were carried out by placing the liquid solution into a standard quartz cuvette (spectral data from absorbance readings is provided in Figure D1, appendix D).

4.3.3. Textile preparation

Detergents were selected using the market research of Hendel et al[200], showing that the top-selling liquid detergents in the Midwest United States were Tide, All, Wisk, Purex and Cheer. The most commonly used powder detergent was Tide. These detergents were utilized for this study; Oxiclean was also included for diversity in fluorescent whitening agents. Textile samples

were cut into 3.0”x 2.25” swatches and immersed into 40 mL centrifuge tubes containing the detergent solutions made in nanopure (18 MΩ·cm) water. Detergent concentrations were prepared according to manufacturer’s recommendations, assuming a 40L washing solution volume. The liquid detergent and concentrations were: All (1.31 mL/L), Purex (1.11 mL/L), Tide (1.53 mL/L), Wisk (1.15 mL/L) and Cheer (1.15 mL/L). The powder detergent and concentrations were: Oxiclean (0.94 g/L), and Tide (1.29 g/L). The centrifuge tubes were then placed on a Thermolyne Maxi-Mix III (type M 65800) rotary shaker at 800-1000 rotations per minute (RPM) for 20 minutes. After each wash, the detergent solution was discarded and the cloth piece was rinsed copiously with nanopure water. After washing, the cloth pieces were air-dried overnight and then 10 fibers were collected, uniformly sampling the swatch. The fibers were placed on a quartz slide and covered with a quartz cover-slip and the spectra recorded with a fluorescence microscope. The manufacturers of all the detergents are listed in the Table 4.2.

Table 4.2. Detergents selected for this study and their manufacturing companies

Detergent	*Manufacturer*
All	The Sun Products Corporation
Cheer	Proctor & Gamble
Oxiclean	Church & Dwight Co., Inc.
Purex	The Dial Corporation
Tide (liquid and powder)	Proctor & Gamble
Wisk	The Sun Products Corporation

4.3.4. Spectral analysis

Fluorescence emission data were collected for dyed, undyed, laundered and unwashed fibers with 350 nm excitation wavelength. The emission wavelength range was 390-650 nm. For

laundered, dyed fibers, the 2D emission spectra were fit to a linear combination of the spectra from the undyed fiber ($I_{\text{fiber}}^{\text{undyed}}$), the dye on the fiber ($I_{\text{fiber}}^{\text{dye}}$) and the spectrum of the detergent on the fiber ($I_{\text{fiber}}^{\text{detergent}}$)according to the equation:

$$I_{\text{washed}}^{\text{dyed}} = AI_{\text{unwashed}}^{\text{undyed}} + BI_{\text{fiber}}^{\text{dye}} + CI_{\text{fiber}}^{\text{detergent}} \quad (4.1)$$

The spectra for the dye on the fiber were measured by subtracting the average of 10 spectra of undyed, unlaundered fibers from the spectra of 10 dyed, unlaundered fibers. The resulting spectrum of the dye *on the fiber* ($I_{\text{fiber}}^{\text{dye}}$) was obtained by averaging the 10 difference spectra. The spectra of the detergents on the fiber ($I_{\text{fiber}}^{\text{detergent}}$) were the residuals from a nonlinear least-squares fit of the combination of $I_{\text{fiber}}^{\text{undyed}}$ and $I_{\text{fiber}}^{\text{dye}}$ to the spectra of dyed fibers that had been laundered six times. The constraint in the fit was that the combination of $I_{\text{fiber}}^{\text{undyed}}$ and $I_{\text{fiber}}^{\text{dye}}$ could not exceed the signal of the dyed, laundered fibers. The fitted spectrum was subtracted from the raw dyed, laundered fiber spectrum to obtain the spectrum of the detergent on the fiber ($I_{\text{fiber}}^{\text{detergent}}$). Once the individual spectra of $I_{\text{unwashed}}^{\text{undyed}}$, $I_{\text{fiber}}^{\text{dye}}$, and $I_{\text{fiber}}^{\text{detergent}}$ were measured or calculated, the spectra of dyed, washed fibers were fit to determine the fractional components given by A, B and C in equation 4.1. For clarity, examples of spectra for AY17-dyed nylon 361 washed with Tide (liquid) detergent can be visualized in Figure 4.1. After the spectra were fit to assess the detergent contribution to the spectrum with laundering, the comparison of means t-test was used to compare the fractional contribution of the detergent spectra to the spectral profile after each sequential wash.

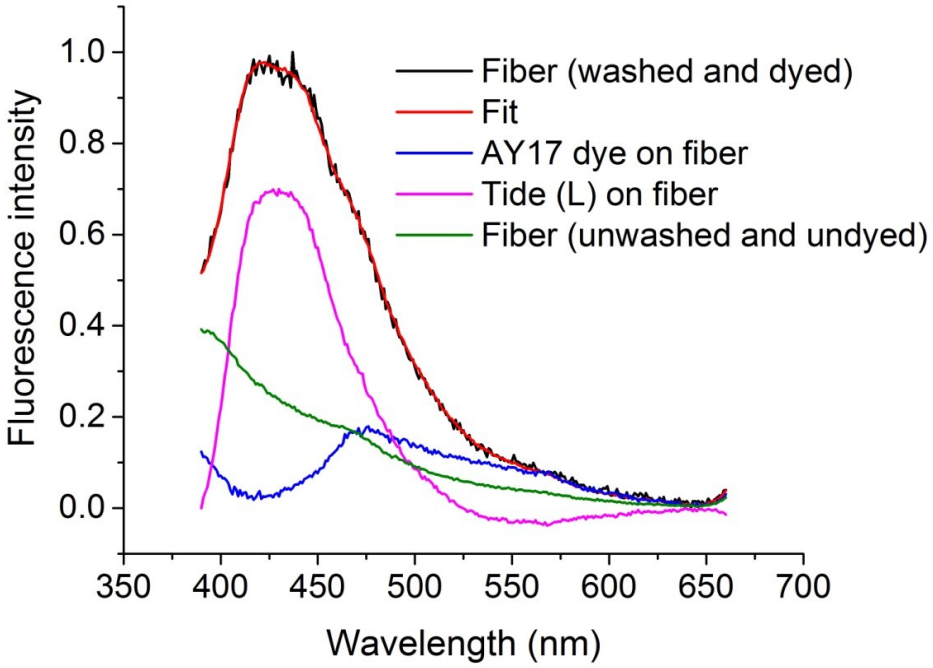

Figure 4.1. Fluorescence emission spectrum of AY17 dyed nylon 361 fiber washed four times with Tide (liquid). The fit to the spectrum is a combination of the spectra of the dye on the fiber, the detergent on the fiber, and the undyed fiber.

4.3.5. Principle component cluster analysis (PCA)

Since the fitted data did not always provide unambiguous capability to determine whether or not the fiber was washed, principal component cluster analysis was also employed. This approach has been described previously[51,201]. Briefly, a training set for each fiber type was comprised of fluorescence data for unwashed fibers and fibers washed with each of the seven detergents. The training set data matrix contained intensity of fluorescence emission at each wavelength in the columns and each row contained the spectrum for a different fiber. The spectra were baseline corrected and normalized prior to principal component analysis. A square

covariance matrix (**Z**) was calculated from the training set (**D**) by multiplying the data matrix by its transpose according to the equation:

$$\mathbf{Z} = \mathbf{D}^{T}\mathbf{D} \tag{4.2}$$

Matrices of eigenvectors ($\mathbf{Q}_0$) and eigenvalues ($\boldsymbol{\lambda}_0$) were calculated for the covariance matrix according to equation 4.3:

$$\mathbf{Q}_0^{T}\mathbf{Z}\mathbf{Q}_0 = \boldsymbol{\lambda}_0 \tag{4.3}$$

and the number of components assessed using the Fischer's F-ratio of the reduced eigenvalues, as detailed by Malinowski[202] and successfully employed in fiber analysis previously[51].

The spectra of washed and dyed fibers were projected onto the axes of the first two principal component vectors as principal component scores. The resulting clusters were inspected to determine whether clusters formed by unwashed fibers were sufficiently distinct from clusters formed by washed fibers. To aid in this inspection, the clusters were fit to a rotated ellipse (equation 4.4) for which an ellipse with center (*h,k*) is rotated by angle α. The standard deviation along the major axis is *a*, and the perpendicular axis standard deviation is *b*.

$$\frac{\cos^2\alpha}{a^2}+\frac{\sin^2\alpha}{b^2}\ (x-h)^2+2\cos\alpha\sin\alpha\ \frac{1}{a^2}-\frac{1}{b^2}\ x-h\ y-k\ +\ \frac{\sin^2\alpha}{a^2}+\frac{\cos^2\alpha}{b^2}\ (y-k)^2=1 \tag{4.4}$$

To visually discriminate between clusters, a boundary was drawn around each cluster with the borders of the ellipse representing three standard deviations scatter of the two perpendicular ellipse axes formed by the training clusters. In some cases, the borders of the

washed and unwashed training clusters are well resolved, but validation data are required to characterize the identification utility of the method.

Spectra from additional validation fibers were also plotted as scores along the principal component vector axes and the distances from the centers of the training clusters to the validation points were calculated (d_i) using the two-point distance formula. The vector from the center of the cluster to the validation point was determined and the variance of the training cluster in the direction of that vector was obtained by simultaneously solving the equation for the ellipse that is fit to the training set, and the equation for the line formed by validation point and the center of the training cluster. An F-ratio was calculated to determine whether the validation point should be included with the training cluster:

$$\mathrm{F} = \frac{d_{\mathrm{i}}^2}{d_{\mathrm{ellipse}}^2} \tag{4.5}$$

With a critical F-value of 7.71 and 95% confidence, F-ratios for validation points indicated whether the point would be correctly classified with its parent training cluster, falsely excluded from the parent cluster (false negative) or falsely included with an erroneous cluster (false positive).

4.4. Results and Discussion

4.4.1. Fluorescence spectra of laundered fibers

The exposure of textile fibers to laundering cycles can change the fluorescent properties of the fiber and dye; Figure 4.2 shows the emission spectra for nylon 361 fibers dyed with AY17 (Figure 4.2-A), acrylic 864 dyed with BG4 (Figure 4.2-B), and cotton 400 fibers dyed with DB1

(Figure 4.2-C) that have been washed sequentially with some selected detergents. Complete spectra for all the tested detergents are included in the supplemental information section for this chapter (appendix C). The addition of the detergent features in the spectra are quantified by treating the spectra as a linear combinations of unwashed, undyed fiber (with scaling A), the dye on the fiber (with scaling B) and the detergent on the fiber (scaling C) (shown in equation 4.1). The fractional contributions of each spectral component are plotted in figure 4.2D for nylon 361 fibers dyed with AY 17, figure 4.2E for acrylic 864 fibers dyed with BG4, and 4.2F for cotton 400 fibers dyed with DB1. Component plots for all the fitted spectra are included in the supplemental information section (appendix C).

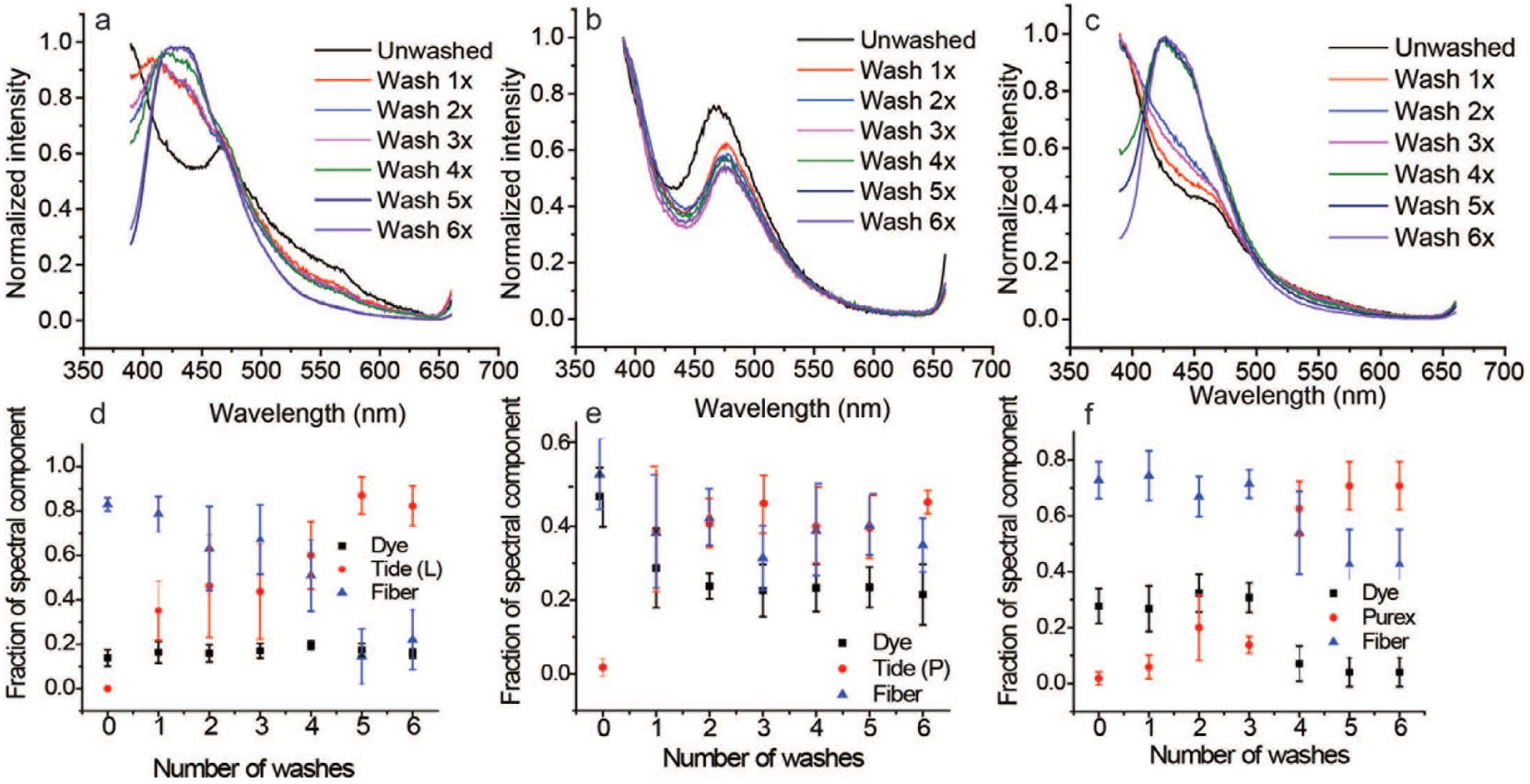

Figure 4.2. Emission spectra of A) Nylon 361 dyed with AY17 and sequentially washed with Tide (L), B) Acrylic 864 dyed with BG4 and sequentially washed with Tide (P), C) Cotton 400 dyed with DB1 and sequentially washed with Purex. Parts D-F show the fit of the fiber, dye and detergent component in the spectra of A-C. Error bars represent the standard deviation measured from 10 fiber samples.

Evaluation of the number of washes required to show statistically meaningful differences in the spectra was accomplished using a comparison of means t-test for the spectral contribution of the detergent to the fiber spectrum. For example, the scaling contribution of the detergent component (C in equation 4.1) was compared for an unwashed fiber and a fiber washed once, using a pooled standard deviation. This t-test was repeated for a fiber washed once or twice, and so on. Number of washes required before the detergent signal is distinguishable from no signal is shown in Table 4.3.

It is apparent that the detergent spectra on acrylic 864 are not usually detectable using this approach. For cotton and nylon, washing only once provides statistically different spectra from unwashed fibers in eight of the fourteen cases. For all detergents on cotton 400 and nylon 361, fibers washed at least five times showed the greatest deviation from the unwashed fiber, as indicated by the large value of the detergent fraction component for detergent spectra. For most cases, the detergent components for the fifth and sixth wash were within the error of each other. For this reason, the spectra from fiber for the fifth wash were used to compare unwashed to washed fibers using principal component cluster analysis.

Table 4.3. Number of sequential washes[a] required for the detergent spectral component to be distinct from an unwashed fiber evaluated using a comparison of means t-test.

	All	Cheer	Oxiclean	Purex	Tide (Liquid)	Tide (Powder)	Wisk
AY 17 dyed Nylon 361	4	4	1	1	1	5	1
BG4 dyed Acrylic 864	X	X	2	X	X	X	X
DB1 dyed Cotton 400	1	1	1	2	1	5	4

[a] An X indicates that there were no statistically meaningful differences in the washed detergent component of the fiber spectrum relative to the unwashed fiber.

4.4.2. PCA

Small differences in spectra can be visualized by reduction of the data and removal of the noise, calculating the eigenvectors of the training data and plotting the spectra as scores on perpendicular axes. This approach is demonstrated in Figure 4.3, for which spectra from the three fiber types are plotted in eigenspace. Fibers washed five times with the detergents were used to construct the plots shown here. The boundaries plotted around each cluster represent elliptical fits to the cluster data with three standard deviations used to describe the long and short axes.

The clusters in Figure 4.3-A show that after a nylon fiber has been washed five times, the spectra of washed fibers appear to be distinct from unwashed fibers, while acrylic 864 laundered fibers do not appear to form distinct clusters (Figure 4.3-B). Clusters formed by unwashed cotton 400 fibers (Figure 4.3-C) appear to be distinct from most washed fibers, but to determine how accurate fiber classification would be using this approach, validation spectra from five fibers of each washed and unwashed condition and fiber type were projected onto the axes of the training set and the distances calculated for the validation point to the center of the training clusters. This distance was then compared to the average distances of the training cluster points in the direction of the validation point. These distances were used to calculate an F-ratio to determine if the validation points could be correctly classified as washed or unwashed, and to determine if the unwashed fibers would be falsely classified as washed (as well as the reverse case).

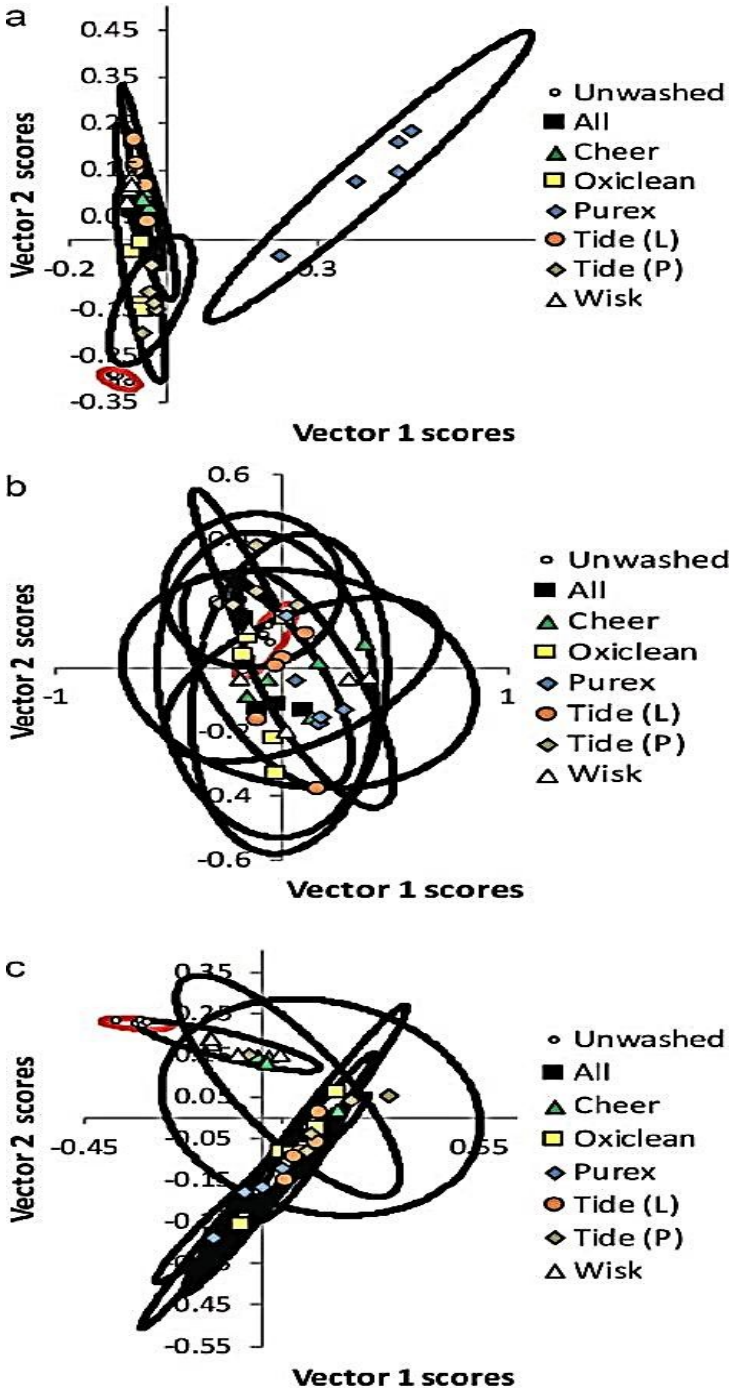

Figure 4.3. Principal component clusters from spectra of fibers washed 5 times, with elliptical boundaries drawn from fitting the standard deviation in the long and short axis of each cluster. Clusters formed by unwashed fiber spectra are outlined in red. A) Clusters from nylon 361 fibers dyed with AY17, B) Clusters from acrylic 864 fibers dyed with BG4, C) Clusters from cotton 400 fibers dyed with DB1.

If a washed validation fiber was excluded from its matching washed training cluster using the F-ratio with 95% confidence (critical F-value 7.7), it was classified as a false negative result. If a washed fiber were incorrectly matched to the unwashed cluster, it was considered a false positive result. In the case of washed fiber classification, the results are summarized in Table 4.4, for each of the three fiber types. Similarly, classification of unwashed fibers was assessed and summarized in Table 4.5. If an unwashed fiber were incorrectly excluded from the unwashed fiber training cluster, it was classified as a false negative. A false positive result was reported when an unwashed validation fiber was misclassified as a washed fiber.

Table 4.4. Dyed validation fibers percent accuracy/false negative/false positive results for washed fiber validation points compared to both washed fiber training clusters and unwashed fiber training clusters.

Dye	Wash	All	Cheer	Oxiclean	Purex	Tide (L)	Tide (P)	Wisk
AY 17	Wash 5x	100/0/0	20/80/0	100/0/0	40/60/0	100/0/0	80/20/0	20/80/0
AY 17	Wash 6x	60/40/0	80/20/0	100/0/0	80/20/0	100/0/0	60/40/0	100/0/0
BG4	Wash 5x	80/20/20	80/20/0	100/0/0	80/20/0	100/0/0	100/0/0	100/0/20
BG 4	Wash 6x	80/20/0	100/0/0	100/0/20	100/0/0	100/0/40	60/40/0	100/0/0
DB 1	Wash 5x	80/20/0	60/20/0	80/20/0	80/20/0	60/40/0	80/20/0	0/100/0
DB 1	Wash 6x	100/0/0	100/0/0	80/20/0	100/0/0	100/0/0	60/40/0	60/40/0

These data indicate that both AY 17 dyed nylon 361 fibers and DB 1 dyed cotton 400 fibers that have been laundered are never falsely classified as unwashed fibers (no false positives). Depending on the detergent used, some washed fibers are falsely excluded from their training cluster and are false negative classifications. For BG 4 dyed acrylic 864, the clusters are so overlapped as to yield frequent false positive classification of laundered fibers as unwashed, and unwashed fibers as washed (Table 4.5). This result indicates that nylon 361 fibers and cotton 400 fibers may be of greater utility in fiber identification with detergent-based spectra; however, acrylic 864 fibers do not possess sufficiently distinct spectra after laundering to provide accurate comparison.

Table 4.5. Undyed validation fibers percent accuracy/false negative/false positive results for unwashed fiber validation points compared to both unwashed fiber training clusters and washed fiber training clusters

.

Fiber	Wash	All	Cheer	Oxiclean	Purex	Tide (L)	Tide (P)	Wisk
Nylon	Wash 5x	100/0/0	100/0/0	100/0/0	100/0/0	100/0/0	100/0/0	100/0/0
Nylon	Wash 6x	100/0/0	100/0/0	100/0/0	100/0/0	100/0/0	100/0/0	100/0/0
Acrylic	Wash 5x	80/20/100	80/20/80	80/20/100	80/20/100	80/20/100	80/20/100	80/20/100
Acrylic	Wash 6x	80/20/0	80/20/100	80/20/100	80/20/0	80/20/0	80/20/40	80/20/0
Cotton	Wash 5x	100/0/0	100/0/0	100/0/0	100/0/0	100/0/0	100/0/0	100/0/0
Cotton	Wash 6x	100/0/0	100/0/0	100/0/0	100/0/0	100/0/0	100/0/0	100/0/0

The difference in fluorescence spectral distinctions on nylon and cotton compared to acrylic may be attributable to likelihood of FWA adsorption onto the fiber. The whitening agent is commonly a derivatized sulfonated stilbene, which has a high affinity for the cellulose structure of cotton, as indicated by the distinct fluorescence emission spectrum of the whitening agent on the undyed fiber. There appears to be no unique fluorescence of the whitening agent on the acrylic 864, which could be caused by several factors. The acrylic fiber is composed of the polymer, polyacrylonitrile, which could not form hydrogen bonds or ionic attractions to a sulfonated stilbene FWA, minimizing the probability of accumulation of the FWA on the fiber. For cotton 400 fibers, the small contribution of detergent fluorescence in some cases on the dyed cellulose fiber may be attributable to the presence of the sulfonated direct blue dye – the FWA would have to compete for unoccupied sites on the fiber if the dye is present in high concentrations. Depletion of the dye would allow for substitution of the FWA on the fiber. With multiple washings, this may be the case, as indicated by the slight increase in the contribution of the FWA fluorescence to the dyed, washed fiber and corresponding diminished dye contribution (Figure 4.2, parts C and F). Alternatively, quenching of the direct blue dye with the fluorescent whitening agent may occur and result in diminished dye signal if the FWA has adsorbed to the surface. In one study, quenching of the FWA has been reported to occur at high concentrations[197]; however, the data reported here are not sufficient to conclude the mechanism responsible for the dye/FWA interaction and further research is required.

4.5. Conclusion

Adsorption of fluorescent whitening agents in detergents to textile fibers alters the fluorescence spectral profile of the fibers and dyes. Collection of a library of spectra from fibers washed 0-6 times with popularly utilized detergents has enabled characterization of the spectral contribution of the detergent to the overall spectrum of the fiber, dye and detergent. In most cases, the detergent signal reaches its maximum after a textile has been washed five times. Distinction of washed from unwashed fibers using principal component cluster analysis was accomplished. In the case of nylon 361 fibers dyed with AY 17 and cotton 400 fibers dyed with DB1, laundered fibers are never misclassified as unwashed. Acrylic 864 fibers have little detergent contribution to the spectra and so are not recommended to be utilized for classifying fibers as washed or unwashed. Future characterization of fibers based on the detergents used in laundering would be a powerful extension of this work and would potentially enable identification of a detergent used on textiles without solvent extraction or destruction of the fiber.

Supplemental information in Appendix C

Fibers from three different textiles were washed sequentially with seven different laundry detergents. The emission spectra with 350 nm excitation were collected from individual fibers and are shown in Figures C1, C2 and C3. The spectral components of the undyed fiber, dye on the fiber and detergent on the fiber were fit to the spectra and the contribution of each component is plotted in Figures C4, C5 and C6. Absorbance recordings from all the seven detergent solutions are shown in Figure C7.

CHAPTER 5. IDENTIFICATION OF DETERGENTS FOR FORENSIC FIBER ANALYSIS

5.1. Introduction

Trace fibers have been of critical evidential value in many cases[203,204], and for decades, research efforts have been applied to determining the composition[205], color and dye structure using nondestructive methods[186,205-210]. Even with sophisticated methods for identification of inherent fiber characteristics[3], additional techniques are reported for identification of exogenous features introduced to the fiber following mass production and distribution. Methods to determine structural changes to the fiber (i.e., due to heat[211]) or chemical contaminants on evidential fibers have been developed. For example, cocaine was identified in single rayon fibers using nanomanipulation-coupled nanospray mass spectrometry[212], and lipstick smears on textiles were identified using HPLC with UV detection[213]. In the interest of limiting human exposure to toxins, Luongo et al.[214] developed a solvent extraction and mass spectrometry approach to detect quinolone and derivatives in commercially obtained textiles. More recently, Antal et al. revealed the presence of nonylphenol ethoxylates, phthalates, and amines (among many other chemicals) on clothing items using mass spectrometry – chemicals of concern if they are released into wastewater with repeated laundering[215].

Although identifying a fiber contaminant independent of the fiber composition is valuable, additional insight could be gained if the fiber contaminant provided some utility in comparing a trace fiber sample to a proposed bulk specimen of origin. Detection and identification of exogenous substances present in both the trace and bulk sample may aid in the process of identifying fiber origins. Fluorescent whitening agents (FWAs) are chemical species added to detergents that

fluoresce in the visible blue spectrum to cause laundered textiles to appear whiter and brighter. FWAs are generally found in detergents at concentrations ranging from 0.02-0.50 mass percent can be identified in detergent bulk samples using HPLC[216]. As early as 1977, Loyd theorized the possibility of detergent identification on laundered fibers and employed a thin-layer chromatographic approach to qualitatively compare FWAs; the method required solvent extraction that could potentially damage the fibers[217]. Hartshorne et al. scrutinized the fluorescence lifetime decay for FWAs with the goal of using the half-lives for identification, but the observed second-order rate decay behavior added unexpected complexity and uncertainty to the conclusions[218]. More recently, Shu and Ding[219] developed an extraction, ion-pair chromatographic separation, and fluorescence detection method to quantify five fluorescent whitening agents in large (10 g) samples of infant clothes and paper textiles.

Recently, we reported that fluorescence microscopy can be used, in some cases, to determine whether a fiber had been laundered with one of seven commercially available detergents containing fluorescent whitening agents[162]. Here, we describe the direct measurement of the FWA fluorescence spectra on single fibers with the aim of identifying which detergent was used in a laundering process. For this proof-of-concept study, dyed and undyed nylon 361 and acrylic 864 fibers were examined. The dyes applied to the fibers were acid yellow 17 (on nylon fibers) and basic green 4 (on acrylic fibers). Fibers washed with different detergents during laundering appear visually indistinguishable (example of images are shown in Figure 5.1). The detergents used were All, Cheer, Oxiclean, Purex, Tide (liquid), Tide (powder), and Wisk. They contained either the FWA tinopal (found only in Oxiclean) or disodium diaminostilbene disulfonate (all other detergents) – their molecular structures are shown in Figure 5.2. Principal component cluster

analysis from the detergent fluorescence spectra of single textile fibers was employed to achieve detergent identification. In some cases, this approach yields reproducible identification of the detergent, although limitations were found for some fiber and dye types, as well as differences in selectivity between dyed and undyed fibers. The nondestructive analysis described here was conducted without fiber pretreatment or solvent extraction.

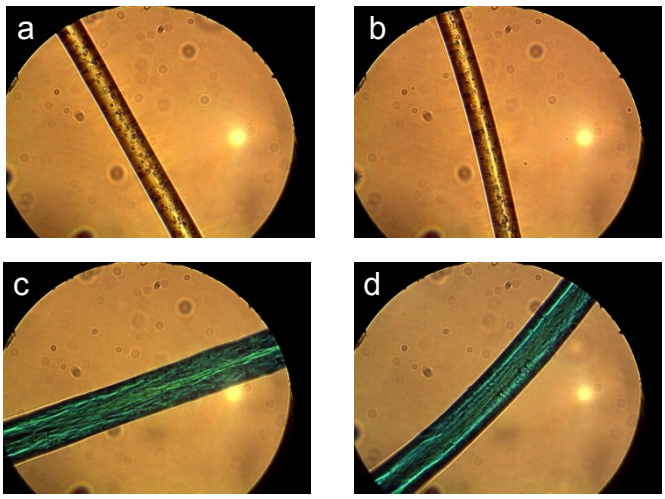

Figure 5.1. Microscope images of single textile fibers after laundering five times with different detergents. Nylon 361 fibers dyed with acid yellow 17 are washed with Tide liquid (a) and Wisk (b). Acrylic 864 fibers are dyed with basic green 4 and washed with Purex (c) and Tide powder (d).

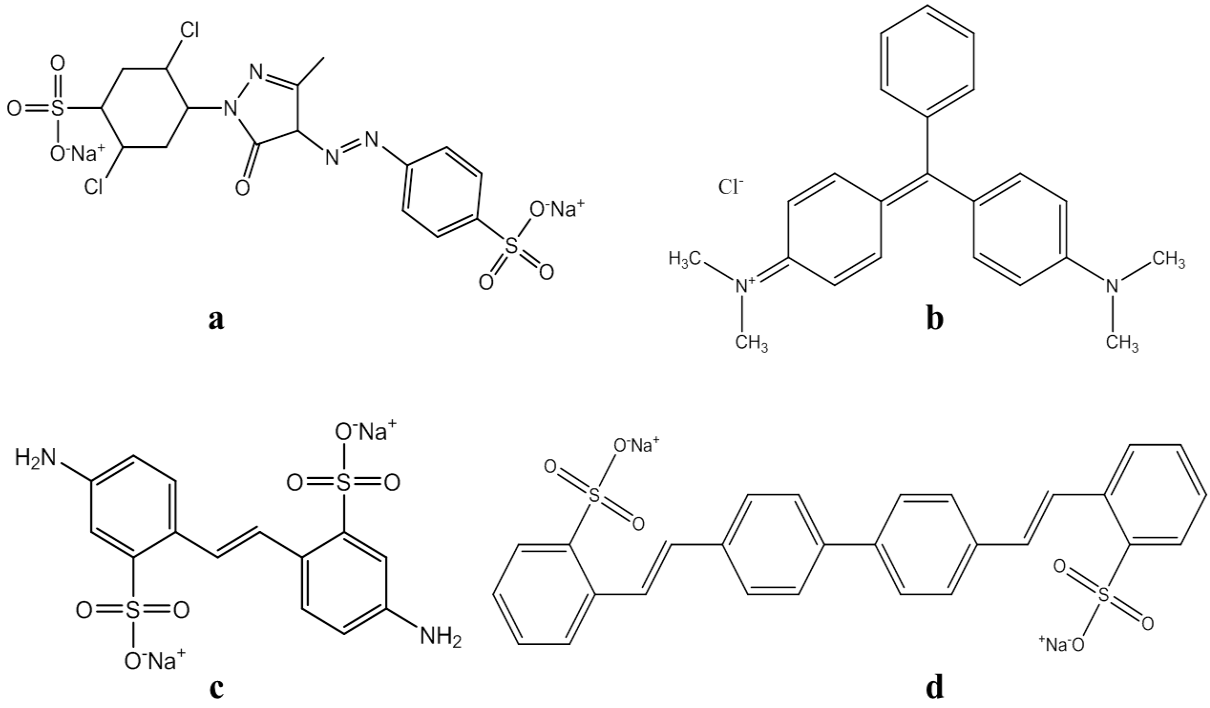

Figure 5.2. Chemical structures for dyes and FWAs used. Acid yellow 17 dye (a), Basic green 4 dye (b), disodium diaminostilbene disulfonate (c) and tinopal (d)

5.2. Experimental

5.2.1. Materials

Acrylic 864 and nylon 361 fabrics were dyed (without prior brightener application) by Testfabrics, Inc (West Pittston, PA) with dyes that were purchased from Sigma-Aldrich (St. Louis, MO). The dyes were basic green 4 (90% purity) and acid yellow 17 (60% purity); for experiments on dyed fibers, these dyes were used to attain concentrations of 3% for basic green 4 on acrylic 864 and 2% acid yellow 17 on nylon 361. For undyed fibers, the nylon and acrylic textiles were subjected to wash cycles without any further pretreatment. Quartz slides (75 x 25 mm x 1 mm) and coverslips (19 x 19 x 1 mm) were supplied by Chemglass (Vineland, NJ). Nanopure water was prepared using a Barnstead Nanopure Infinity water purifier was used to prepare nanopure (18 MΩ·cm) water.

5.2.2. Textile preparation

Detergent solutions were made to suit the recommendations of the manufacturer, assuming a 40 L washing solution volume. The concentrations of the powder detergent and concentrations were: Oxiclean (0.94 g/L), and Tide (1.29 g/L) in nanopure water. The concentrations of the liquid detergents were: All (1.31 mL/L), Purex (1.11 mL/L), Tide (1.53 mL/L), Wisk (1.15 mL/L) and Cheer (1.15 mL/L). Textile swatches with dimension 3.00” x 2.25” were cut and immersed in a test tube containing the detergent solutions. The centrifuge tubes were agitated with 800-1000 RPM for 20 minutes using a Thermolyne Maxi-Mix III (type M 65800) rotary shaker. Subsequently, the detergent solution was decanted and the cloth piece was rinsed copiously with nanopure water. The swatches were then air-dried for 12 hours or overnight, and then fiber samples were collected and

the textile was washed again, up to six times. Ten fibers were collected from the laundered swatch with uniform sampling. To image the fibers and collect emission spectra, the fibers were placed on a quartz slide and covered with a quartz cover-slip.

5.2.3. Instrumentation

The instrument employed here has been described in previous work[51], and details are provided in chapter 3 of this dissertation.

5.3. Data analysis

Fluorescence emission spectra from the laundered textile fibers were recorded with 350 nm excitation, with emission collected from 390-660 nm. Absorbance spectra for the detergents in solution are included in the supplementary material, showing that each of the detergents absorb at 350 nm. Emission spectra for the undyed fibers, detergent on the fibers and dyed fibers can be found elsewhere[162].

Our research group previously reported that when the fibers are washed sequentially, the maximum detergent signal is reached at (or before) the fiber has been washed five times[162]. For this reason, fibers laundered five times were selected to comprise the training set, with the validation set comprising fibers washed both five times and six times. The validation set containing the six-times-washed fibers was included to determine if subsequent washing of the fiber sample would distort the classification of the detergent based on a five-wash training set.

Although discriminant analysis is a powerful approach to class discrimination, PCA has been shown to outperform LDA in cases when the number of samples per class is small, as in the case when a single fiber is used to provide the training set[220]. Hence, PCA was employed here. The

use of principal component calculations and analysis of clusters arising from spectra has been validated and applied elsewhere[51,201]. For convenience, the analytical approach is briefly summarized here. The emission spectra were background corrected and normalized and then the training set matrix comprised of spectra from two sets of detergents was created (separate training sets with all possible detergent pairs were created). Each row represented the spectrum of a single fiber, and each column, the wavelength. Before calculating eigenvectors and eigenvalues from the training set (D), the data were made into a square covariance matrix (Z) by multiplying the data matrix by its transpose according to the equation:

$$Z = D^T D \tag{5.1}$$

Next, equation 2 was used to calculate eigenvectors (Q_0) and eigenvalues (λ_0):

$$Q_0{}^T Z Q_0 = \lambda_0 \tag{5.2}$$

The number of components was assessed using the Fisher's F-ratio of the reduced eigenvalues, described by Malinowski[221], and utilized in fiber analysis previously[51]. To calculate principal component scores, the data matrix was multiplied by a truncated eigenvector matrix that contained only the first two eigenvectors from the covariance matrix. Before the scores were plotted on the axes in eigenspace, they were mean-centered and normalized. Plots were constructed to evaluate the clusters formed by the individual detergents in the training set. The shapes formed by the clusters were elliptical, so each cluster was fit to an equation that described the shape of a rotated ellipse. The average of the x- and y- coordinates provided the center of mass for the ellipse. The angle of rotation was determined by fitting the slope a line through the data cluster, which was the tangent of the skewed angle of the ellipse. The boundaries of the ellipse were calculated from

the standard deviation of the cluster, both in the direction of the skew angle (to provide the major axis) as well as perpendicular to the skew angle (to provide the radius along the minor axis). To guide the eye in identifying the clusters in the plots in Figure 5.4, ellipses are drawn around the training set. The two radii drawn in the plot were three times the standard deviation of the training set scores in those directions. The ellipses in the plot are not intended for statistical classification; rather they are intended to help visually identify the clusters.

Using spectra from fibers different from those used to construct the training set, validation spectra were projected onto the principal component axes in eigenspace formed by the training set data. Knowing the equation for the ellipse provided an important parameter for determining if validation points (for fibers washed either five or six times) were correctly classified with the appropriate cluster, falsely excluded from the correct training cluster (a false negative result), or – in the worst case – falsely identified with the incorrect detergent cluster (a false positive result). Cluster plots are useful for rapid visual inspection to determine if a validation point is clustered appropriately with its corresponding training set. However, a figure of merit is essential for determining if a point should be statistically included or excluded from a cluster. Here, the distance (d_i) of a validation point from the center of the cluster was calculated, and compared to the distance ($d_{ellipse}$) from the center of the training cluster to the boundary formed by the ellipse around the training cluster that was defined in terms of one standard deviation of the training set along the major and minor axis of the ellipse. An F-ratio was calculated using the square of those distances:

$$F = \frac{d_i^2}{d_{ellipse}^2} \tag{5.3}$$

Using a 95% confidence F-ratio of 7.71, the F-ratios for validation points allowed classification of a validation point – if it were falsely excluded from the matching detergent training cluster, it was classified as a false negative. If it were falsely included with an alternative detergent cluster, it was classified as a false positive.

5.4. Results and Discussion

Adsorption of fluorescent whitening agents and other detergent components to textile fibers during laundering results in the emission of fluorescence spectra that can be measured directly from the fiber. Figure 5.3 shows emission spectra from the detergents on single fibers after the textiles were laundered five times. Although the spectra exhibit some visual distinction, identification without a statistical figure of merit would prove challenging. To aid in identification, principal component scores were calculated from training sets composed of spectra from fibers washed with one of two detergents – the spectra were projected onto the principal component axes, and example cluster plots are shown in Figure 5.4. Every combination of two detergents were compared for nylon 361 fibers (both undyed and dyed with acid yellow 17), as well as acrylic 864 fibers (both undyed and dyed with basic green 4). With seven detergents, 21 different cluster plots were constructed for each different fiber type. Complete cluster plots (to identify between two detergents) are included in the supporting material section of this chapter (appendix D).

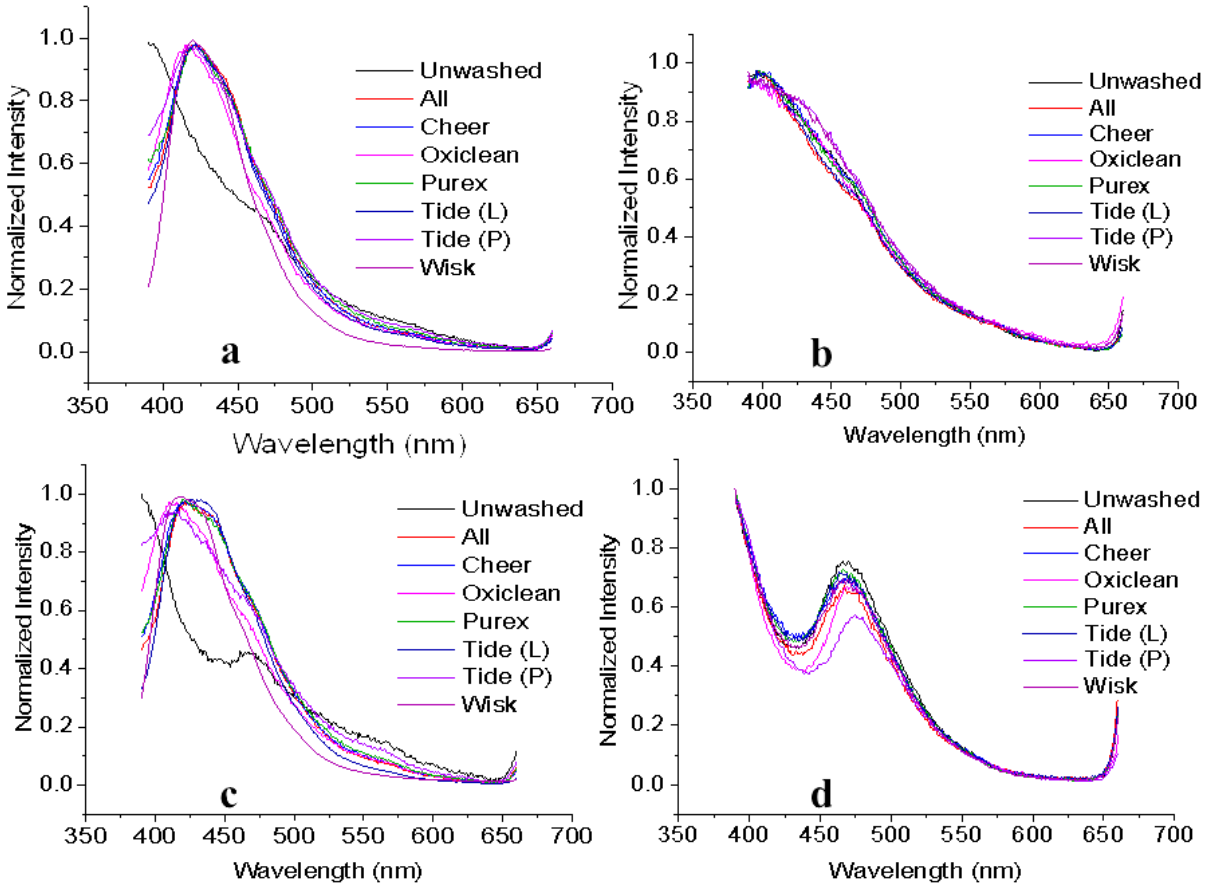

Figure 5.3. Fluorescence emission spectra with 350 nm excitation of fluorescent whitening agents measured on textile fibers after laundering five times with the indicated detergent. Undyed, and AY 17-dyed Nylon 361 fibers are shown in parts A and C, respectively. Undyed and BG 4-dyed acrylic 864 fibers are shown in parts B and D, respectively.

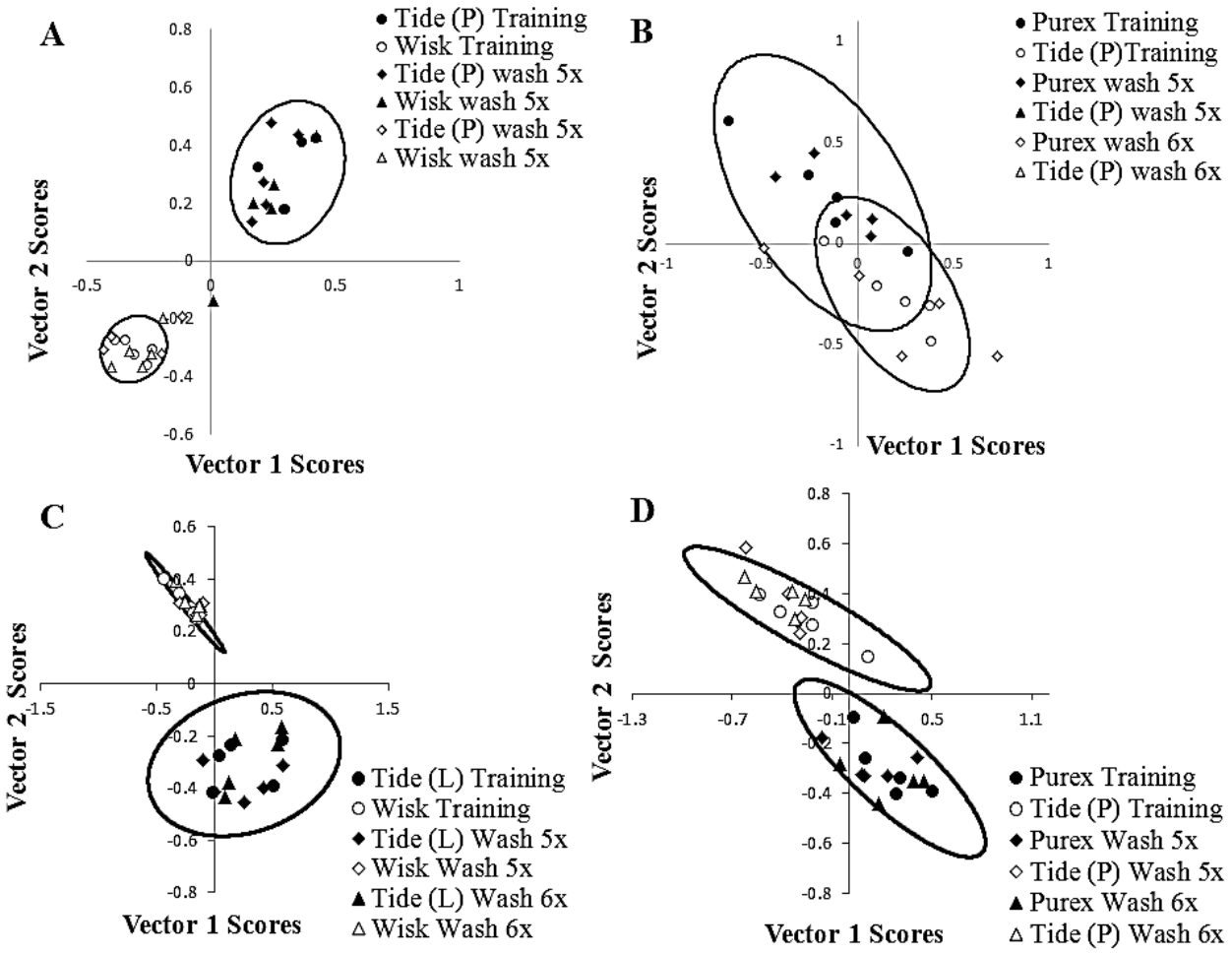

Figure 5.4. Cluster plots formed by principal component scores of fluorescence emission spectra of fluorescent whitening agents on single textile fibers. Boundaries for the clusters were determined by calculating three times the standard deviations of the training set along the major and minor axes of an ellipse. Clusters from emission spectra of washed nylon 361 fibers are shown in A (undyed) and C (dyed with AY17). Clusters from emission spectra of washed Acrylic 864 fibers are shown in B (undyed) and D (dyed with BG 4).

For undyed fibers, the ability to identify a detergent on a fiber was minimal. Nylon 361 fibers washed with Wisk formed clusters that were well resolved, as determined by the absence of overlap from the ellipses fit to the training sets. Remarkably, for undyed acrylic fibers, there was no

combination of detergents that could be resolved from one another. Identification of detergents on dyed fibers yielded many more detergent pairs that could be reproducibly identified from each other. Of the 21 possible detergent combinations on dyed nylon fibers, 8 cluster combinations of two detergents could be resolved within three standard deviations of the training set elliptical boundaries. For the dyed acrylic fibers, 6 of the 21 detergent combinations could be resolved, notably increased from the undyed fiber results.

The increased ability to achieve resolution of detergents on dyed fibers compared to undyed fibers indicates the importance of the role of the endogenous fluorescence of the fibers and the fluorescence of the dyes themselves. While the dyed fiber spectra are shown in Figure 5.3, spectra from the undyed fibers and the background of the quartz slide are included in the supplementary section (appendix D). By visual comparison, the spectra of the nylon undyed fiber, dyed fiber, and washed dyed fibers exhibit pronounced differences. By contrast, the emission of the acrylic dyed fibers dominates the emission with little variation due to washing. The increasing contribution of the detergent fluorescence on the fibers with repeated washing has been reported previously and shown to vary for both fiber types and detergents – a more detailed discussion of that variation can be found elsewhere[162]. In contrast, this research focuses on the variation of the signal that arises from the different detergent types.

Distinctly resolved clusters formed by a training set alone do not conclusively demonstrate the potential for identifying the detergent on a fiber in question, or characterize the reproducibility in classification. Spectra from validation fibers that had also been washed five times were projected on the principal component axes and are also shown in Figure 5.4. The distance of the validation

point to the center of the training cluster, combined with the distance from the center to the edge of the elliptical boundary, were used to calculate an F-ratio. This F-test allowed the questioned validation fiber to be compared to the cluster of fibers washed with the same detergent, as well as the cluster washed with a different detergent. This allowed for classification of the questioned fiber – whether it was correctly classified with the training cluster, falsely excluded from the training cluster, or falsely included with the opposite detergent training cluster. Using this approach, the undyed nylon validation fibers could be used to reproducibly identify Wisk from all other detergents (100% correct identification of validation fibers washed five times with Cheer, Oxiclean and Tide (P) and 80% correct classification of fibers washed with All, Purex and Tide (L)). All cases of inaccurate exclusion from the correct training cluster were also tested for inaccurate inclusion with the opposite cluster (a false positive). There were no false positive identifications observed for undyed fibers. Those data are tabulated in Table 5.1.

Table 5.1. Undyed Nylon 361 fibers washed 5 times with the indicated detergents. An "x" indicates that the clusters for the two compared detergents on the fiber could not be resolved. The numbers indicate the percentage of correctly classified/false negative exclusion/false positive inclusion, respectively, with the detergent listed in the row.

	All	Cheer	Oxiclean	Purex	Tide (L)	Tide (P)	Wisk
All		x	x	x	x	x	60/40/0
Cheer	x		x	x	x	x	60/40/0
Oxiclean	x	x		x	x	x	60/40/0
Purex	x	x	x		x	x	40/60/0
Tide (L)	x	x	x	x		x	40/60/0
Tide (P)	x	x	x	x	x		80/20/0
Wisk	80/20/0	100/0/0	100/0/0	80/20/0	80/20/0	100/0/0	

In addition to the undyed fibers tested, dyed validation fibers were also examined for reproducibility in classification. The identification results are summarized in Table 5.2 for nylon fibers and Table 5.3 for acrylic fibers. When spectra from validation fibers washed five times with a detergent listed in a column is compared to the training set for the detergent in the rows, the clusters are either unresolved (indicated with an x) or resolved within three standard deviations of the training clusters. For those that are resolved, the percent of validation fibers correctly classified/falsely excluded from the correct training cluster/falsely included with the other detergent training cluster are listed. A blank in the table occurs when the two detergents listed for comparison are the same.

Table 5.2. Nylon 361 fibers dyed with acid yellow 17 and washed 5 times with the indicated detergents. An "x" indicates that the clusters for the two compared detergents on the fiber could not be resolved. The numbers indicate the percentage of correctly classified/false negative exclusion/false positive inclusion with the detergent listed in the row.

	All	Cheer	Oxiclean	Purex	Tide (L)	Tide (P)	Wisk
All		x	x	x	x	x	40/60/0
Cheer	x		60/40/0	x	x	x	40/60/0
Oxiclean	x	80/20/0		80/20/0	80/20/0	x	x
Purex	x	x	20/80/0		x	x	80/20/0
Tide (L)	x	x	100/0/0	x		x	100/0/0
Tide (P)	x	x	x	x	x		60/40/0
Wisk	60/40/0	60/40/0	x	60/40/0	80/20/0	40/60/0	

Table 5.3. Acrylic 864 fibers dyed with basic green 4 and washed 5 times with the indicated detergents. An "x" indicates that the clusters for the two compared detergents on the fiber could not be resolved. The numbers indicate the percentage of correctly classified/false negative exclusion/false positive inclusion, respectively, with the detergent listed in the row.

	All	Cheer	Oxiclean	Purex	Tide (L)	Tide (P)	Wisk
All		x	x	x	x	100/0/0	x
Cheer	x		x	x	x	40/60/0	x
Oxiclean	x	x		x	x	x	x
Purex	x	x	x		x	100/0/0	x
Tide (L)	x	x	x	x		80/20/0	x
Tide (P)	80/20/0	40/60/0	x	80/20/0	80/20/0		40/60/0
Wisk	x	x	x	x	x	60/40/0	

In some cases, the correct classification of the validation fibers is highly reproducible (i.e., nylon fibers washed with Oxiclean or Tide (liquid) is correctly classified in at least 80% of cases, and up to 100%). Several detergents have frequent rates of false negative classification. This indicates the need in future studies to expand the training set. Importantly, there are no false positive classifications for any detergent or fiber type. A false positive misidentification of a detergent could have more profound and damaging consequences (i.e. inculpatory evidence) than a false negative (exculpatory evidence). In contrast to the detergent identification on nylon fibers, most detergents on acrylic fibers cannot be resolved. Previous work reports that in most cases, a laundered acrylic fiber was indistinguishable from an unlaundered fiber[162]. The use of Tide powder detergent, however, is an exception to this trend on acrylic; in most cases that detergent can be correctly identified when compared to other detergents.

It is possible that in an application of this approach, a fiber could be detached from a bulk textile specimen, and the bulk material subsequently laundered. To interrogate the extent to which subsequent laundering would influence identification in the comparison of the bulk sample and detached fiber, the textiles were laundered a sixth time and spectra from individual laundered fibers compared to the training clusters formed by the fibers that had been laundered only five times. The results from this comparison are summarized in Table 5.4 for dyed nylon 361 fibers and Table 5.5 for dyed acrylic 864 fibers. As with those validation fibers that were laundered five times, few cases show perfect identification, and most have at least 20% false negative exclusion from the correct training set detergent. However, there are no false positive misidentifications of a six-times laundered fiber with the incorrect training set.

Table 5.4. Nylon 361 fibers dyed with acid yellow 17 washed 6 times and compared to the training set created by fibers washed 5 times.

	All	Cheer	Oxiclean	Purex	Tide (L)	Tide (P)	Wisk
All		x	x	x	x	x	20/80/0
Cheer	x		100/0/0	x	x	x	60/40/0
Oxiclean	x	60/40/0		80/20/0	80/20/0	x	x
Purex	x	x	60/40/0		x	x	40/60/0
Tide (L)	x	x	100/0/0	x		x	100/0/0
Tide (P)	x	x	x	x	x		80/20/0
Wisk	80/20/0	60/40/0	x	80/20/0	80/20/0	80/20/0	

Table 5.5. Acrylic 864 fibers dyed with acid yellow 17 washed 6 times and compared to the training set created by fibers washed 5 times.

	All	Cheer	Oxiclean	Purex	Tide (L)	Tide (P)	Wisk
All		x	x	x	x	100/0/0	x
Cheer	x		x	x	x	40/60/0	x
Oxiclean	x	x		x	x	x	x
Purex	x	x	x		x	100/0/0	x
Tide (L)	x	x	x	x		80/20/0	x
Tide (P)	80/20/0	40/60/0	x	80/20/0	80/20/0		40/60/0
Wisk	x	x	x	x	x	60/40/0	

5.5. Conclusion

Seven different detergents were used to launder two different dyed textile materials, nylon 361 and acrylic 864. For nylon fibers, eight different detergent combinations could be successfully resolved with by principal component analysis of the detergent emission spectra. In the case of acrylic fibers, only five different detergent combinations could be resolved. When spectra from validation fibers (washed either five or six times) were tested, there were no false positive classifications of one fiber with an incorrect detergent cluster. It is remarkable that the ability to identify detergents increased when dyed fibers were studied compared to undyed fibers, particularly in the case of acrylic fibers. The alteration in the spectra that arises when both dye and FWA are present indicates that an interaction between the dye, the FWA, and detergent components (rather than the fiber and the FWA) may be the mechanism for variation in the spectra. More insight into the variation of the spectra, and perhaps increased ability to resolve the different detergent could be achieved by examining the emission of the fibers over many different excitation wavelengths, or

even using complete excitation-emission matrices (EEMs). Analysis of EEMs (to resolve otherwise indistinguishable dyes) has been successfully reported[52] and the application of this method to detergent fluorescence is the subject of future work. An additional variation of this work includes investigating the effect of less controlled conditions (e.g. tap water rather than nanopure water) where external contaminants have the possibility of adding additional distinguishing features to the spectra.

It is curious that detergents that contain the same whitening agent can, in some cases, produce different spectra on the same fiber type. While the comparison of Oxiclean (the only detergent to contain the whitening agent tinopal) formed distinct clusters separate from three other detergents, even greater success in identification with respect to other detergents was achieved with Wisk, which contained the same FWA as other detergents. Even when two detergents are produced by the same manufacturer their spectra can be resolved, as in the case of Tide powder distinguished from Tide liquid on acrylic fibers (a table showing the manufacturers of the detergents can be found in the supplementary material). It appears that interaction of the dye, the whitening agent, and the other detergent components combine to produce the ultimately observed spectrum from the fiber. Many manufacturers report the ingredients of their detergents, which often include bleaching agents and coloring agents in addition to whitening agents. Further analysis of the composition of the fiber with the detergent components adsorbed could provide more exclusive insight into the origin of the differences in the spectra.

Note: See appendix D for supplemental information

CHAPTER 6. NON-DESTRUCTIVE TOTAL EXCITATION-EMISSION FLUORESCENCE MICROSCOPY COMBINED WITH MULTI-WAY CHEMOMETRIC ANALYSIS FOR VISUALLY INDISTINGUISHABLE SINGLE FIBER DISCRIMINATION

6.1. Fiber identification using PCA

Excitation-Emission spectra or EEMs from ten spots on acrylic fibers dyed with Basic green 1 (BG1) or Basic green 4 (BG4) were used to construct a data matrix for cluster analysis. These dyes have very similar molecular structures, and the fibers that were sampled were indistinguishable to the naked eye, as well as under a microscope with 40X magnification using visible objective lens. The EEM spectral data (baseline-corrected and normalized) for a single spot were stacked into a single column for each spot, with a column for each spot and the number of emission wavelengths corresponding to the number of rows. This approach utilized entire emission data from the EEM to construct the data matrix in order to capture the complete variance in the EEM data to ideally illuminate the greatest differences between the spectra of BG1 and BG4 – dyed fibers. The stacked EEM spectra from each of the ten spots on the BG1 and BG4 fibers were combined to make a single data matrix. The remainder of the analysis has been described previously[51]. Briefly, a square covariance matrix was constructed by multiplying the data matrix by its transpose, and then diagonalizing the covariance matrix to determine the eigenvectors and eigenvalues. With the majority of the variance in the data described by the first two eigenvectors – as determined by Malinowski's[222] F-test of reduced eigenvectors - the stacked EEM spectra of the training set were projected onto those eigenvectors to calculate the principal component scores that are plotted in Figure 6.1.

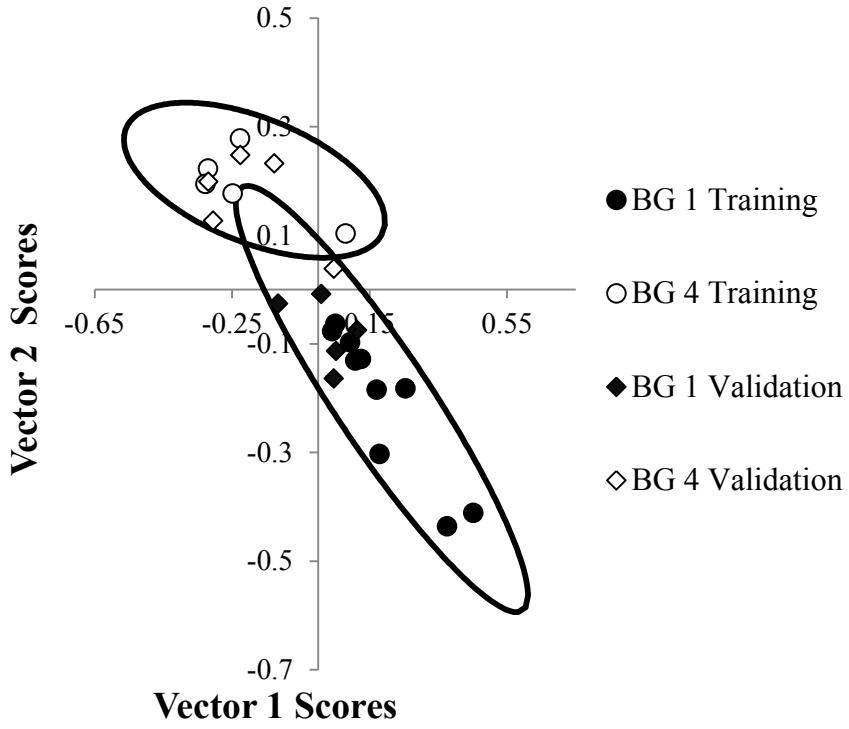

Figure 6.1. Principle component scores for BG1 and BG4 dyed acrylic 864 fibers

The clusters formed by the BG1 and BG4 spectra in Figure 6.1 are distinct, but insufficiently resolved. The boundaries depicted around each cluster represent the fit of the data to ellipses for which the axes lengths are determined from the standard deviation of the clusters along the major and minor axes. It can be seen in Figure 6.1 that, although the validation BG1 and BG4 spectra acquired from 10 different fiber samples, are grouped correctly with their parent cluster, the overlap of the clusters could result in misidentification of the dye on the fiber. This is a case where PCA was unable to discriminate between visually indistinguishable fibers. Hence, the next sections of this chapter will focus on the other types of chemometric methods that were used for data analysis, with which we could successfully discriminate between indistinguishable fibers.

6.2. Introduction

The analysis of fibers from clothes is of paramount importance in forensic science, when investigating a crime scene. Trace fiber evidence has been probative in cases ranging from the 1963 JFK assassination[223], to the Atlanta Child murders[224] of the early 1980s, or the 2002 Washington, DC, sniper case[225]. The fiber examiner typically performs a series of comparisons of the questioned fiber to a known fiber in an attempt to exclude the possibility that a questioned fiber and known fiber could have originated from a common source. If the two fibers are considered to be substantially different, then the hypothesis that the two fibers originated from a common source can be disregarded. The extension to which fibers of different origins can be discriminated is related to the analytical method used for their analysis[226]. A challenging aspect of forensic fiber examinations involves the comparison of fibers colored with visually indistinguishable dyestuffs. This is not an uncommon situation, as there are numerous indistinguishable fibers pre-dyed with commercial dyes of virtually identical colors. Minimal chemical structural variations are actually encouraged by the dye patent process and commercial competition.

Microscopy based techniques currently used in forensic science labs include polarized light microscopy, IR microscopy[123,165], micro-spectrophotometry[123-125], fluorescence microscopy[227] and scanning electron microscopy coupled to energy dispersive spectrometry[167]. Differences in cross-sectional shape, type of fiber material (natural or synthetic), weave and color often make possible to rule out a common source for the two samples. The main advantage of these techniques is their non-destructive nature, which preserves the physical integrity of the fibers for further court examination. Beyond microscopy - but still under the category of minimally destructive techniques – is pyrolysis

coupled to GC. This tool is capable to compare the polymeric nature of synthetic and natural fibers at expenses of partial sample consumption[168].

When fibers cannot be discriminated by non-destructive tests, the next step is to extract the questioned and the known fiber for further dye analysis. Thin-layer chromatography (TLC)[228,229], high-performance liquid-chromatography (HPLC)[230] and capillary electrophoresis (CE)[231,232] have been used to separate and identify colored dyes in fiber extracts. Additional selectivity is possible with the use of multichannel wavelength detection systems that record real-time absorption spectra for comparison of eluted components to spectral databases. The ultimate selectivity belongs to mass spectrometry (MS) coupled to either HPLC or CE. HPLC-MS and CE-MS are able to differentiate textile dyes with similar molecular structures that provide similar elution times and optical spectra[170,233-236]. Unfortunately, MS techniques destroy the fiber just like all the other methods that provide chemical information based on previous dye extraction.

Research reports on the non-destructive analysis of fibers have proposed the use of diffuse reflectance infrared Fourier transform spectroscopy (DRIFTS) and Raman spectroscopy. When coupled to chemometric methods for spectral interpretation such as principal component analysis (PCA) and soft independent modeling of class analogies (SIMCA), DRIFTS was able to discriminate both dye color and reactive dye state on cotton fabrics[138-140]. Raman spectroscopy was able to characterize dyes in both natural and synthetic fibers via a combination of Fourier transform-Raman spectra and PCA analysis[22,143,146].

Our group has focused on room-temperature fluorescence (RTF) spectroscopy. Although fluorescence microscopy is currently used in forensic labs for single fiber examination[237,238],

measurements are made with the aid of band-pass filters that provide very limited information on the spectral profiles of fibers. Our approach takes fluorescence microscopy to a higher level of selectivity with the collection of excitation emission matrices (EEMs)[51,162]. EEMs – which refer to a series of emission spectra recorded at various excitation wavelengths – were recorded with the aid of a microscope coupled to a spectrofluorimeter. The subtraction of EEMs from visually indistinguishable fibers provided the best excitation wavelength for recording two-dimensional fluorescence spectra (first order data). The comparison of fluorescence spectra via PCA resulted in the accurate identification of fibers with no false positives[51]. The same approach was later applied to investigate laundering effects on textile fibers. The spectral fingerprints of brighteners and other detergent components adsorbed on the fibers improved fiber discrimination via RTF-EEMs-PCA[162]. Reproducibility of EEMs acquired from ten spots on a single fiber is shown in appendix E.

Herein, we focus on the total fluorescence content of the EEMs. The entire data sets of fluorescence spectra recorded at various excitation wavelengths are compared with the aid of parallel factor analysis (PARAFAC). This second-order algorithm determines the number of fluorescence components that contribute to each EEM along with their individual excitation and emission profiles. The application of PARAFAC is carried out unsupervised and supervised by linear discrimination analysis (LDA). Supervision refers to the provision of information about sample types to the model when studying a training set of samples, followed by a prediction step. LDA is based on the determination of linear discriminant functions. By maximizing the ratio between-class variance, LDA supervised methods achieve maximum separation among classes, and, therefore, superior classification performance than non-supervised methods. PARAFAC and

PARAFAC-LDA are then compared to the supervised discriminant unfolded partial least squares (DU-PLS) method for classification purposes.

6.3. Theory

The theoretical considerations involved in the application of PCA to the differentiation of visually indistinguishable fibers have been covered in recent publications[51,162]. Herein, a brief description of the theoretical aspects pertinent to the application of PARAFAC, LDA and DU-PLS will be described.

6.3.1. PARAFAC

This algorithm often achieves the decomposition of three-dimensional data arrays into two-dimensional spectral profiles for both qualitative and quantitative purposes[239]. If EEMs are arranged in a three-way array $\boldsymbol{X}$ of dimensions *I x J x K*, where *I, J, and K* are the number of samples, number of emission wavelengths, and number of excitation wavelengths, respectively, PARAFAC attempts to decompose it into three matrices **A** (scores), **B**, and **C** (loadings) with elements a_{in}, b_{jn}, c_{kn}, respectively, where *n* indicates the component number. An element of $\boldsymbol{X}$ is given by:

$$x_{ijk} = \sum_{n=1}^{N} b_{jn} c_{kn} + e_{ijk} \qquad (6.1)$$

where x_{ijk} is the fluorescence intensity for sample *i* at the emission wavelength *j* and excitation wavelength *k* and e_{ijk} indicates an element of the array $\boldsymbol{E}$, which collects the variability not accounted by the model. For a given component *n*, the elements a_{in}, b_{jn}, and c_{kn} are arranged in the score vector $\mathbf{a}_n$ (whose elements are directly proportional to its concentration in each sample) and

the loading vectors $\mathbf{b}_n$ and $\mathbf{c}_n$, which estimate its emission and excitation profiles. The array of EEMs data is fitted to equation 6.1 by least-squares.

6.2.2. LDA

This algorithm calculates a surface separating sample groups by establishing a linear discriminant function that maximizes the ratio of the between-class and the within-class variances

Categories are supposed to follow a multivariate normal distribution and be linearly separated. With the **A** score matrix of PARAFAC and the $I \times g$ dummy matrix **Y** of binary digits representing the group assignments (g is the number of categories), the best representation is obtained if the ratio of the between-class variance **B**c matrix and the within-class variance **W**c matrix is maximized. Suitable expressions for the matrices **B**c and **W**c are given by the following expressions[240]:

$$\mathbf{B}c = (g-1)^{-1}\ \mathbf{A}^T\ \mathbf{Y}\ (\mathbf{Y}^T\ \mathbf{Y})^{-1}\ \mathbf{Y}^T\ \mathbf{A} \tag{6.2}$$

$$\mathbf{W}c = (I-g)^{-1}\ [\mathbf{A}^T\ \mathbf{A} - (g-1)\ \mathbf{B}c] \tag{6.3}$$

The canonical variate (CV) scores contain the successively maximized ratios between-groups variance/within-groups variance. They are obtained by PCA of the matrix ($\mathbf{W}c^{-1}\mathbf{B}c$) and projection of the data matrix **A** onto the first loadings. The samples are then plotted on a two- or three- dimensional space defined by the first CV scores for each sample.

6.3.3. DU-PLS

Although the mathematical foundations of U-PLS were originally developed for multivariate calibration purposes[241], its application to the classification of samples has been reported

extensively[242-244]. The main difference between U-PLS and discriminant U-PLS (DU-PLS) consists in the building of the dependent variable **y.** For model calibration purposes, the variable **y** contains concentrations values. For discriminant analysis purposes, **y** contains a coding integer representing the class label of the samples. PLS regression is conducted between the instrumental response in **X** block (built with the unfolded original second-order matrix data) and the class label in **y** block using training samples, and the optimal number of latent variables is chosen based on the error rate by cross-validation[245]. The final model for A latent variables is used to predict the class label in the test set according to:

$$y_{test} = \mathbf{t}_{test}^{T}\mathbf{v} \tag{6.4}$$

where y_{test} is the label class predicted, $\mathbf{t}_{test}^{T}$ area the scores of test samples obtained by projection of $\mathbf{x}_{test}$ onto the training loadings and **v** is the vector of the regression coefficients. In the ideal case scenario, the calculated values of y_{test} - for two classes of samples – are 1 or 2; in practice, y_{test} values are often close to 1 and 2. Therefore, in order to assign a test sample to a given class, it is necessary to establish thresholds for the y_{test} predicted values. This can be accomplished with the aid of re-sampling techniques such as the bootstrap[246] or the Bayes theorem[247]. The latter assumes that the predicted values for the training set follow relatively normal distributions that are comparable to those observed with future samples. The threshold is defined as the value that minimizes the number of false positives and false negatives[248].

6.4. Experimental section

6.4.1. Reagents and materials

Acetate satin 105B, nylon 361, polyester 777 and acrylic 864 fabrics were acquired and dyed at Testfabrics, Inc. (West Pittston, PA). Textile dyes were purchased from Sigma-Aldrich (www.sigma-aldrich.com) at their highest available purity (% w/w). These included acid yellow 17 (AY17; 60%), acid yellow 23 (AY23; ≥ 85%), disperse blue 3 (DB3; 20%), disperse blue 14 (DB14; 97%), disperse red 1 (DR1; 95%), disperse red 19 (DR19; 97%), basic green 1 (BG1; ~ 90%) and basic green 4 (BG4; > 95%). Nylon 361 fabrics were dyed with AY17 and AY23; acetate satin 105B with DB3 and DB14; polyester 777 with DR1 and DR19; and acrylic 864 with BG1 and BG4 (bright field microscopic images of the selected fibers along with the molecular structures of the dyes used, are shown in Figures 6.2 to 6.5). All fabric samples were received in sealed packages and kept as received in the dark to avoid environmental exposure. Tweezers, blades, and scissors used to manipulate fabrics and isolate fibers were previously cleaned with methanol and visually examined under UV-light (254 nm) to avoid fluorescence contamination.

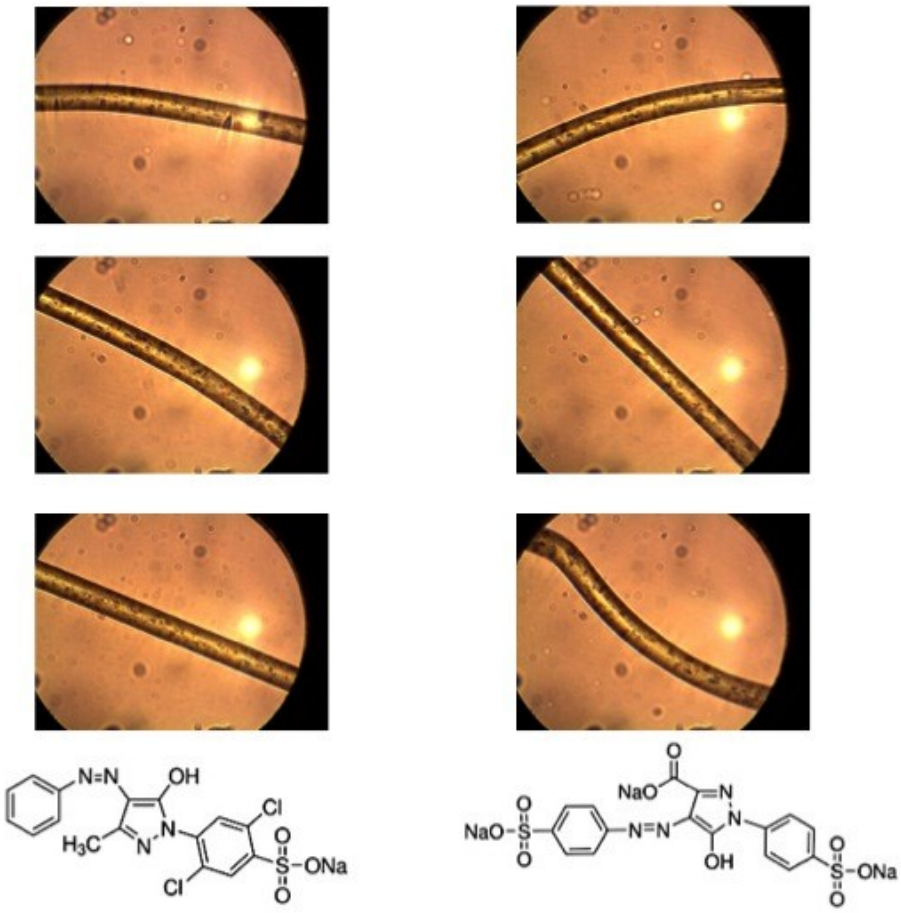

Figure 6.2. Bright field images of three single nylon 361 fibers dyed with AY17 (left) and AY23 (right).

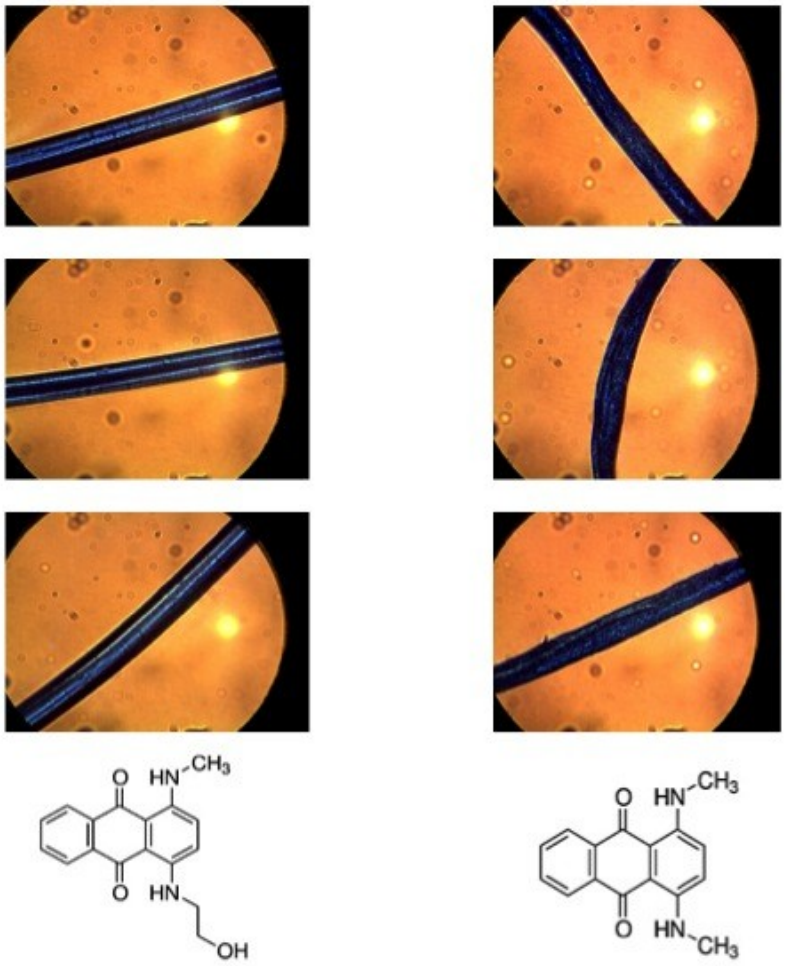

Figure 6.3. Bright field images of three single acetate satin 105B fibers dyed with DB3 (left) and DB14 (right).

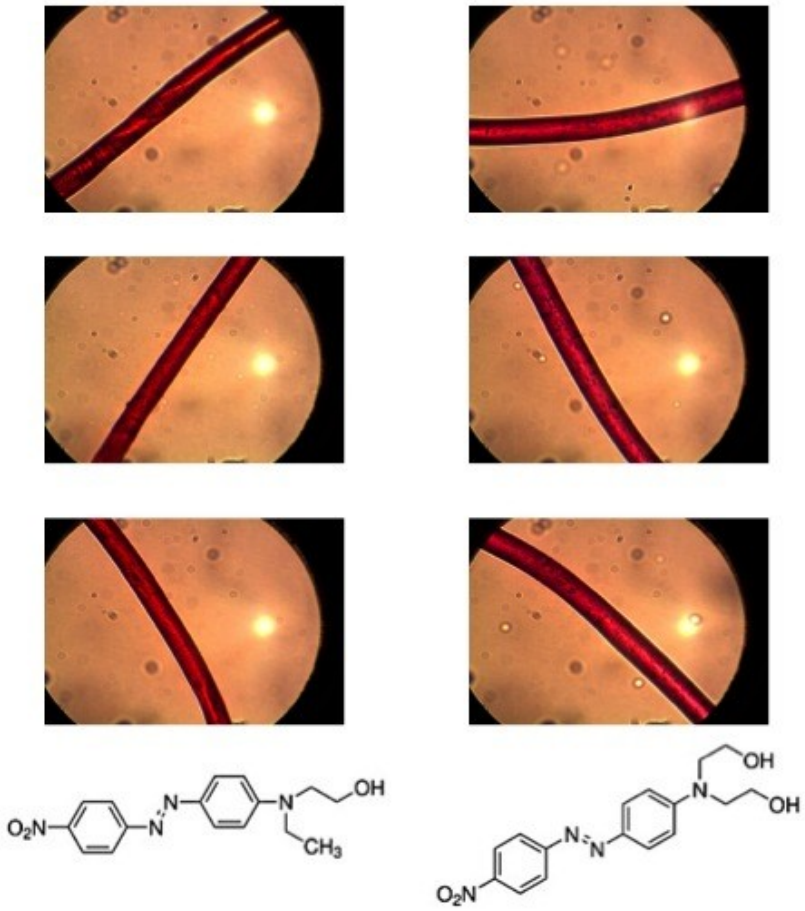

Figure 6.4. Bright field images of three single polyester 777 fibers dyed with DR1 (left) and DR19 (right).

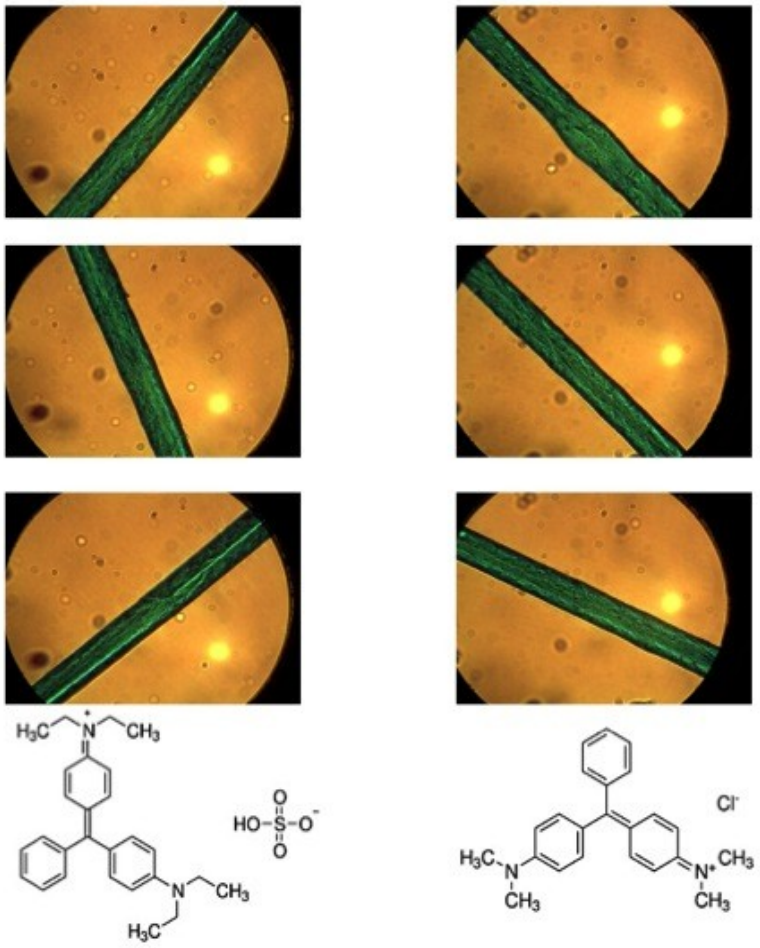

Figure 6.5. Bright field images of three single acrylic 864 fibers dyed with BG1 (left) and BG4 (right).

6.4.2. Fluorescence microscopy

A spectrofluorimeter (FluoroMax-P; Horiba Jobin Yvon) connected to an epifluorescence microscope (BX-51; Olympus) via a bifurcated fiber-optic probe (Horiba Jobin-Yvon) were used to acquire EEMs. The spectrofluorimeter was equipped with a continuous 100 W pulsed Xenon lamp with illumination from 200 to 1100 nm. Excitation and fluorescence emission spectra were recorded with two spectrometers holding the same reciprocal linear dispersion (4.25 nm/mm) and accuracy (± 0.5 nm with 0.3 nm resolution). Both diffraction gratings had the same number of grooves per unit length (1200 grooves nm^{-1}) and were blazed at 330 nm (excitation) and 500 nm (emission). A photomultiplier tube (Hamamatsu, model R928) with spectral response from 185 to 850 nm was used for fluorescence detection operating at room temperature in the photon-counting mode. The acquisition of EEMs was computer-controlled with commercial software (Datamax).

Collection of excitation and emission radiation between the two instrumental units was facilitated with the two concave mirrors of a fiber-optic platform located in the sample compartment of the spectrofluorimeter. The microscope was equipped with two 50/50 beam splitters, one for the ultraviolet and the other for the visible spectral region. A 40X Visible (Olympus UPlanSApo 40X) objective lens was used for light collection in the visible (435-800 nm, 90% transmittance) spectral region. A rotating pinhole wheel, with various diameters varying from 0 to1000 μm, was located between the 50/50 beam splitter and the mirror that directed fluorescence either to the CCD camera (iDS UI-1450SE-C-HQ USB-camera) of the microscope or the emission fiber bundle of the spectrofluorimeter. Image acquisition was computer-controlled with commercial software (DataMax).

6.4.3. Recording EEMs

Otherwise noted, EEMs were recorded within the 435-800 nm excitation-emission range using 5 and 1nm excitation and emission steps, respectively. Scatter interference from excitation radiation was avoided with the use of appropriate cut-off filters. EEMs from single fibers were recorded by placing the sample between two quartz glass slides. Each fiber was sampled 10 times by recording 10 EEMs from 10 spots randomly selected along the entire surface of the fiber.

6.4.4. Chemometric analysis

All chemometric calculations were done using Mat Lab 8.0. Routines for PARAFAC were available in the Internet thanks to Bro[239]. A useful Mat Lab graphical interface provided a simple means of loading the EEM data matrices into the Mat Lab working space before running and analyzing data via PARAFAC and DU-PLS[249,250]. An in house Mat Lab routine was used for LDA calculations[251].

6.5. Results and discussion

The focus of this research was placed on fibers containing structurally similar dyes that are not easily differentiated by visual inspection under the microscope. The similarity of the investigated fibers - nylon 361 fibers dyed with AY17 and AY23; acetate satin 105B fibers dyed with DB3 and DB14; polyester 777 fibers dyed with DR1 and DR 19; and acrylic 864 fibers dyed with BG1 and BG4 - is shown in Figures 6.2 – 6.5. In addition to the contribution of the textile dye to the fluorescence spectrum of the fiber, our approach considers the contribution of fluorescence impurities – i.e. impurities imbedded into the fibers during fabrication of garments – as a

reproducible source of fiber comparison[51,162]. Since the purity of all the reagent dyes is lower than 100%, the presence of unidentified fluorophores in the investigated fibers is possible.

The emission profile of a mixture with numerous fluorescence components varies with the excitation wavelength. Individual fluorophore contributions to the total fluorescence spectrum of the sample also depend on the fluorescence quantum yields of the fluorophores and possible quenching due to synergistic effects. EEMs gather all this information in a single data format that provides the true signature of the total fluorescence of a sample. Figures 6.6 and 6.7 shows EEMs recorded from AY17 and AY23 nylon fibers and BG1 and BG4 acrylic fibers. The similarity of the EEMs certainly challenges the pairwise discrimination of AY17/AY23 and BG1/BG4 fibers on the sole bases of visual comparison. Comparison of EEMs for purposes of fiber identification requires a statistical figure of merit that could be obtained from the chemometric algorithms proposed in the present study.

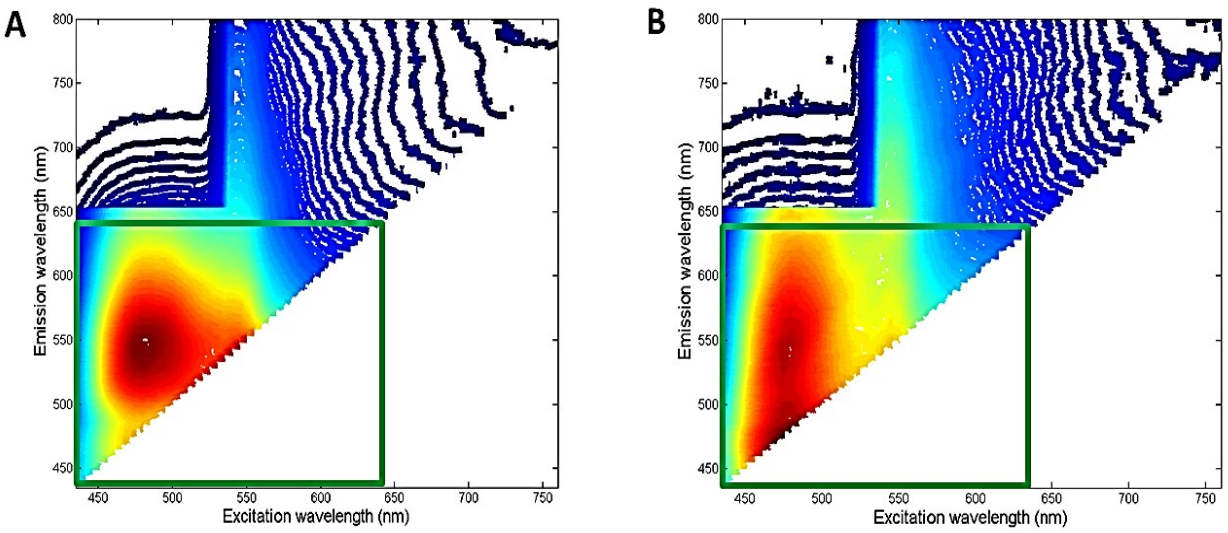

Figure 6.6. Contour plots of EEMs recorded from single AY17 (left) and AY23 (right) nylon 361 fibers. Each contour is the average of 10 EEMs recorded at different spots of each single fiber. Excitation range = 435 - 760 nm. Emission range = 435 - 800 nm. For the purpose of data analysis, the zones of the EEMs corresponding to Rayleigh dispersion were completed with NaN terms. The zones of the EEMs selected for PARAFAC are denoted in green (Exc. range = 435 – 630 nm; Em. range = 435 – 642 nm).

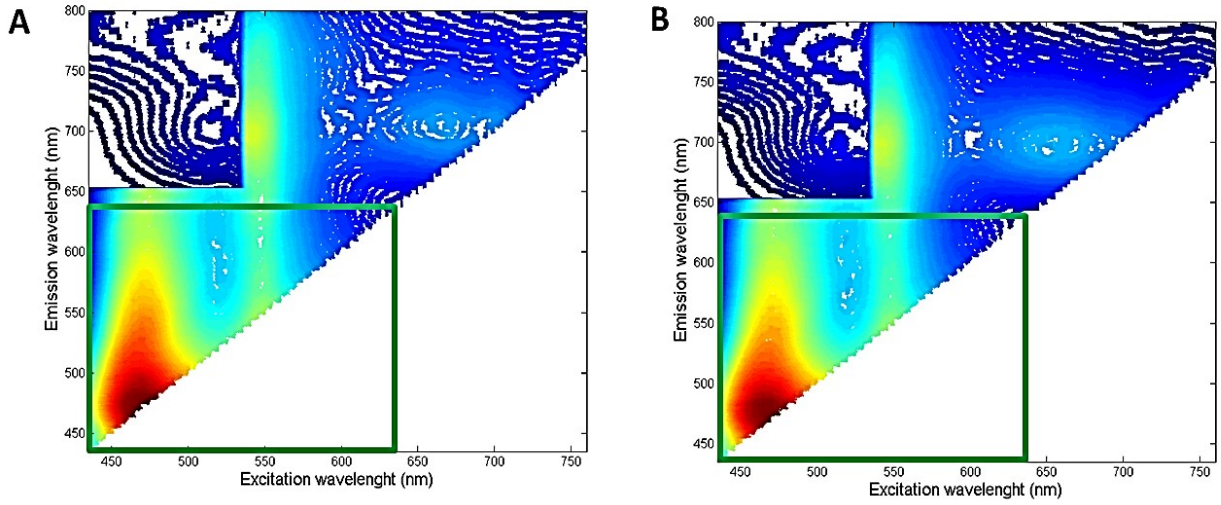

Figure 6.7. Contour plots of EEMs recorded from single BG1 (left) and BG4 (right) acrylic 864 fibers. Each contour is the average of 10 EEMs recorded at different spots of each single fiber. Excitation range = 435 - 760 nm. Emission = 435 - 800 nm. For the purpose of data analysis, the zones of the EEMs corresponding to Rayleigh dispersion were completed with NaN terms. The zones of the EEMs selected for PARAFAC are denoted in green (Exc. range = 435 – 630 nm; Em. range = 435 – 642 nm).

6.5.1. PCA

Differentiation of virtually identical EEMs was previously performed in our lab with the aid of PCA[51]. This algorithm provided accurate identification with no false positives for nylon 351 fibers dyed with acid blue 25 or acid blue 41 and cotton 400 fibers dyed with disperse blue 1 or disperse blue 53. The same approach was tested here for the discrimination of BG1 and BG4 acrylic fibers (discussed in brief in the section 6.1). As seen in Figure 6.1, the clusters formed by BG1 and BG4 spectra are distinct, but insufficiently resolved. The boundaries depicted around each cluster represent the fit of the data to ellipses for which the axes lengths are determined from three times the standard deviation of the clusters along the major and minor axes. Although the validation BG1 and BG4 spectra, acquired from 10 different fiber samples, are grouped correctly with their parent cluster, the overlap of the clusters could result in misidentification of the dye on the fiber.

To quantify the extent to which the overlapped clusters could result in misidentification, principal component scores from the spectra from 10 validation fibers were calculated, and their distances from the center of their parent cluster determined. The distance to the edge of the ellipse in the direction of the point was also calculated by fitting the training set scores to the equation for a rotated ellipse. In this case, the major and minor axes of the ellipse represented the standard deviation in along the angle of rotation, and perpendicular to the angle of rotation, respectively. The ratio of the distances (from the validation point to the center of the cluster, and the edge of the ellipse to the center of the cluster) could be used to calculate an F-ratio (equation 6.5), and determine if the difference in their distances was statistically meaningful and warranted exclusion (or inclusion) with the parent training cluster.

$$F = \frac{d_i^2}{d_{ellipse}^2} \quad (6.5)$$

If the F-ratio for a given validation point to the center of its training cluster was greater than the critical F-value (10.56, for 99% confidence), then the point was considered a false negative exclusion. If the F-ratio for a validation point to the center of the cluster with the opposite dye type, was less than the critical F-value, then it was considered a false positive inclusion. Table 6.1 shows the accuracy of classification using this approach. For fibers of forensic interest, a false negative identification would like provide exculpatory identification, which would be far less damaging than a false positive identification. In the case of BG4 fibers, which had a false positive identification as BG1 fibers in 30% of the cases, provide an unacceptably high rate of false, and potentially incriminating, identification.

Table 6.1. PCA classification of BG1 and BG 4 fibers

	Basic Green 1 Validation Fibers	Basic Green 4 Validation Fibers
Accuracy	100%	80%
False Negative	0%	20%
False Positive	0%	30%

6.5.2. PARAFAC

Ten EEMs were recorded from each of the investigated fibers. Excitation was made within 435 and 800 nm at 5 nm increments. Fluorescence was recorded between 345 and 800 nm at 1 nm increments. Under these parameters, each EEM resulted in a matrix with 66 x 366 data points (excitation x emission). As shown in Figures 6.6 and 6.7, those rather large data matrixes included

wavelength regions with either residual background fluorescence or no fluorescence data (Rayleigh scattering). These regions were excluded from calculations to optimize computational time. No significant loss was observed when data analysis time was further reduced by computing one fluorescence data point every 3 nm intervals. The resulting EEMs consisted of matrixes with 66 x 122 data points (excitation x emission). The wavelength regions selected for PARAFAC analysis are denoted as green rectangles in Figures 6.6 and 6.7. They included data points 1-40 in the excitation mode (435 – 650 nm) and data points 1 – 70 in the emission mode (432 – 642 nm). Missing data points due to Rayleigh scattering were completed with NaNs terms and handled by expectation maximization[239].

Spectral deconvolution of EEMs via PARAFAC was carried out with the four pairs of investigated fibers. Since 10 EEMs were recorded per single fiber, pairwise comparison was based on a total of 20 samples. PARAFAC was first applied without supervision. The model was estimated using certain constraints such as non-negativity on all three modes. The test provided the best fit for a three fluorescence components model in all cases[252,253]. The three fluorescence components improve the robustness of the modelling with the prior knowledge of the inexistence of negative fluorescence intensities. In all cases PARAFAC was initialized with the loadings giving the best fit after a small number of trial runs, selected from the comparison of the results provided by generalized rank annihilation and several orthogonal random loadings[254]. Convergence was achieved when the relative change in fit was 1×10^{-6}.

The number of PARAFAC components was analyzed by two different procedures: the statistical test of the core consistency diagnostic (CORCONDIA)[255] and the analysis of residuals[239].

The core consistency analysis consists in studying the structural model based on the data and the estimated parameters of gradually augmented models. Under this prospective, the model is considered appropriate when the addition of other combinations of components does not provide a considerable improvement of the fitting. An additional indication for the correct number of components is the dropping of the core consistency to value below 50[239]. On the other hand, the analysis of our data yielded three factors for each one of the analyzed fibers. Figure 6.8 shows the emission and excitation loadings of the three-component PARAFAC model for AY17 and AY23 nylon fibers. Analysis of residuals considers the residual fit of the PARAFAC model as a function of increasing number of factors. The appropriate model is the one which is not statistically different from the model leading to the minimum residual fit. We prefer to employ this criterion as it is more intuitively appealing than the rather complex core consistency. Additional indicators for reaching the correct number of components include the visual inspection of the retrieved profiles. Forcing PARAFAC to extract more components than the number of real constituents produces two different types of extra profiles, profiles composed of random noise and/or profiles that appear to repeat.

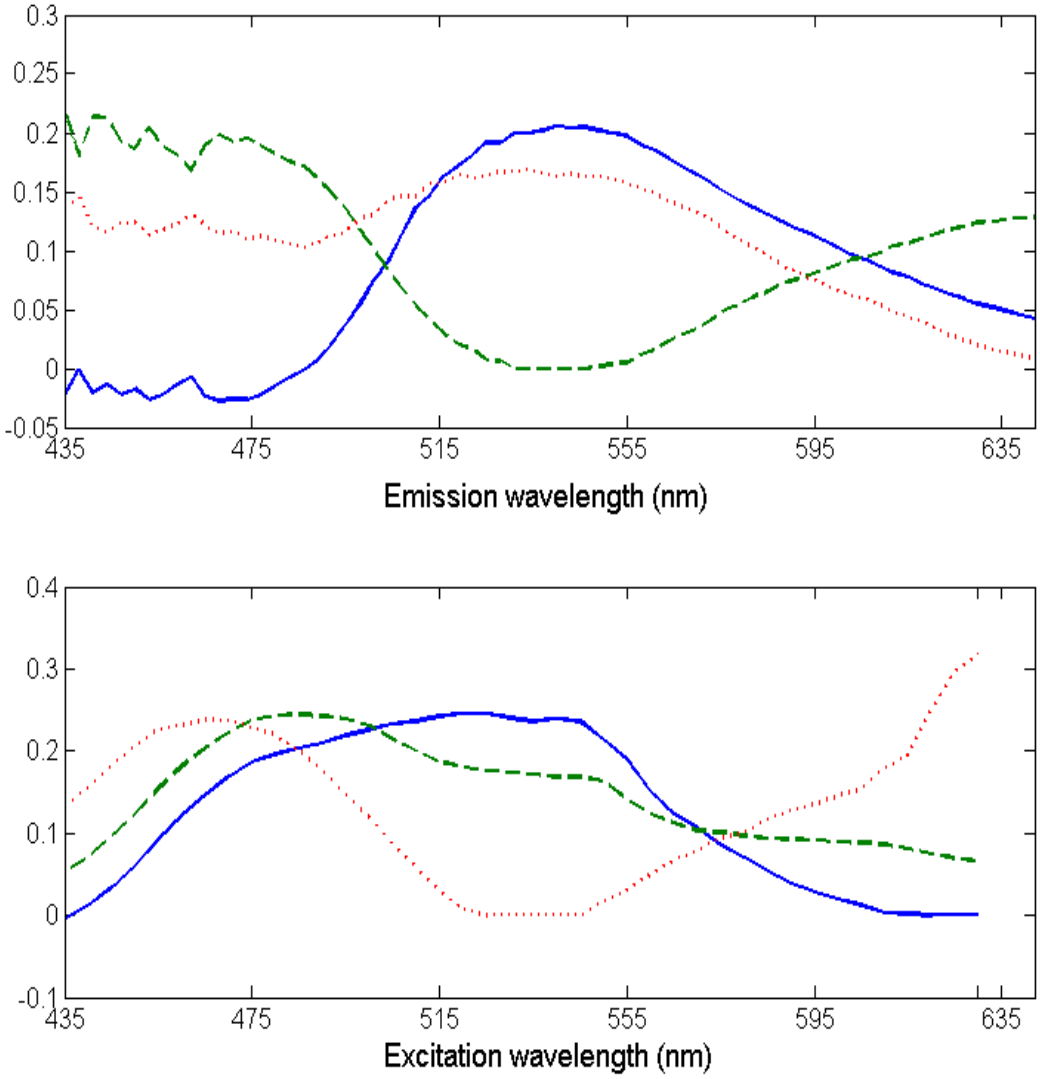

Figure 6.8. Extracted emission (top) and excitation (bottom) PARAFAC profiles taken from an AY17 and an AY23 nylon 361 fiber. Spectral profiles are based on ten EEM replicates per fiber.

Figure 6.8 shows the tridimensional plots of PARAFAC scores 1, 2 and 3 for each one of the investigated pairs. To facilitate the visualization of pairwise comparison, each plot includes the projections of the 95% confidence ellipses over the three planes defined by their corresponding axes. The prediction interval for the multivariate normal distribution yielded an ellipse consisting of **x** vectors satisfying the following equation:

$$\boldsymbol{x} - \mu \; ^{T}\sum^{-1} \; \boldsymbol{x} - \mu \; \leq \; \chi_k^2(p) \tag{6.6}$$

where μ is the mean, $\sum$ is the covariance matrix and $\chi_k^2(p)$ is the quantile function for probability *p* of the chi-squared distribution with k degrees of freedom, where k is the dimension of the data. The axes are defined by the eigenvectors of the covariance matrix and the radius of each axis is equal to 2.796 times the square root of the corresponding eigenvalue. The value 2.796 is obtained from the square root of the Chi-Square distribution with three degrees of freedom and 95% confidence interval[256].

As shown in Figure 6.9, pairwise discrimination was only obtained for AY17/AY23 and DR1/DR19 fibers. No significant improvement was observed with a number of components higher than the one suggested by the analysis of residuals. The inability of PARAFAC to differentiate DB3 from DB14 fibers and BG1 from BG4 fibers could be attributed to its non-supervised nature.

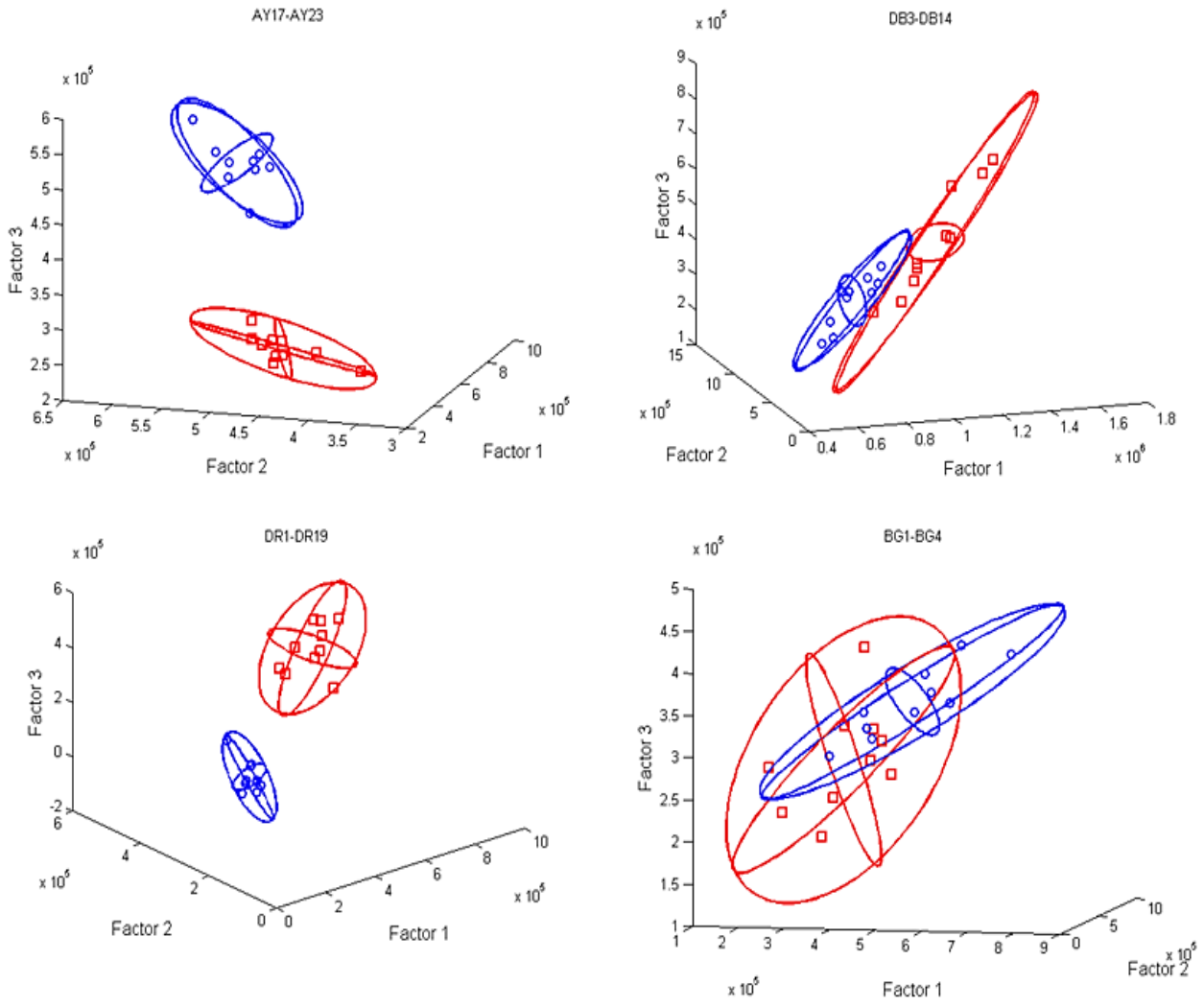

Figure 6.9. PARAFAC scores (3 components model) for 20 samples of (top left) AY17 (10 replicates; blue circles) and AY23 (10 replicates; red squares) nylon 361 fibers; (top right) DB3 (10 replicates; blue circles) and DB14 (10 replicates; red squares) acetate satin 105B fibers; (bottom left) DR 1 (10 replicates; blue circles) and DR19 (10 replicates; red squares) polyester 777 fibers; and (bottom right) BG1 (10 replicates; blue circles) and BG 4 (10 replicates; red squares) acrylic 864 fibers. The three-dimensional projection of the 95% confidence ellipse of the data collected from each type of fiber is included to facilitate visualization of the obtained results.

6.5.3. LDA

An approach that often improves the screening capability of PARAFAC is to submit the resulting scores to supervised LDA[222,252]. With this approach, it was possible to discriminate AY17 from AY23 fibers, DB3 from DB14 fibers and DR1 from DR 19 fibers (Figure 6.10). The inability of PARAFAC-LDA to differentiate between BG1 and BG4 fibers led us to attempt their discrimination via DU-PLS.

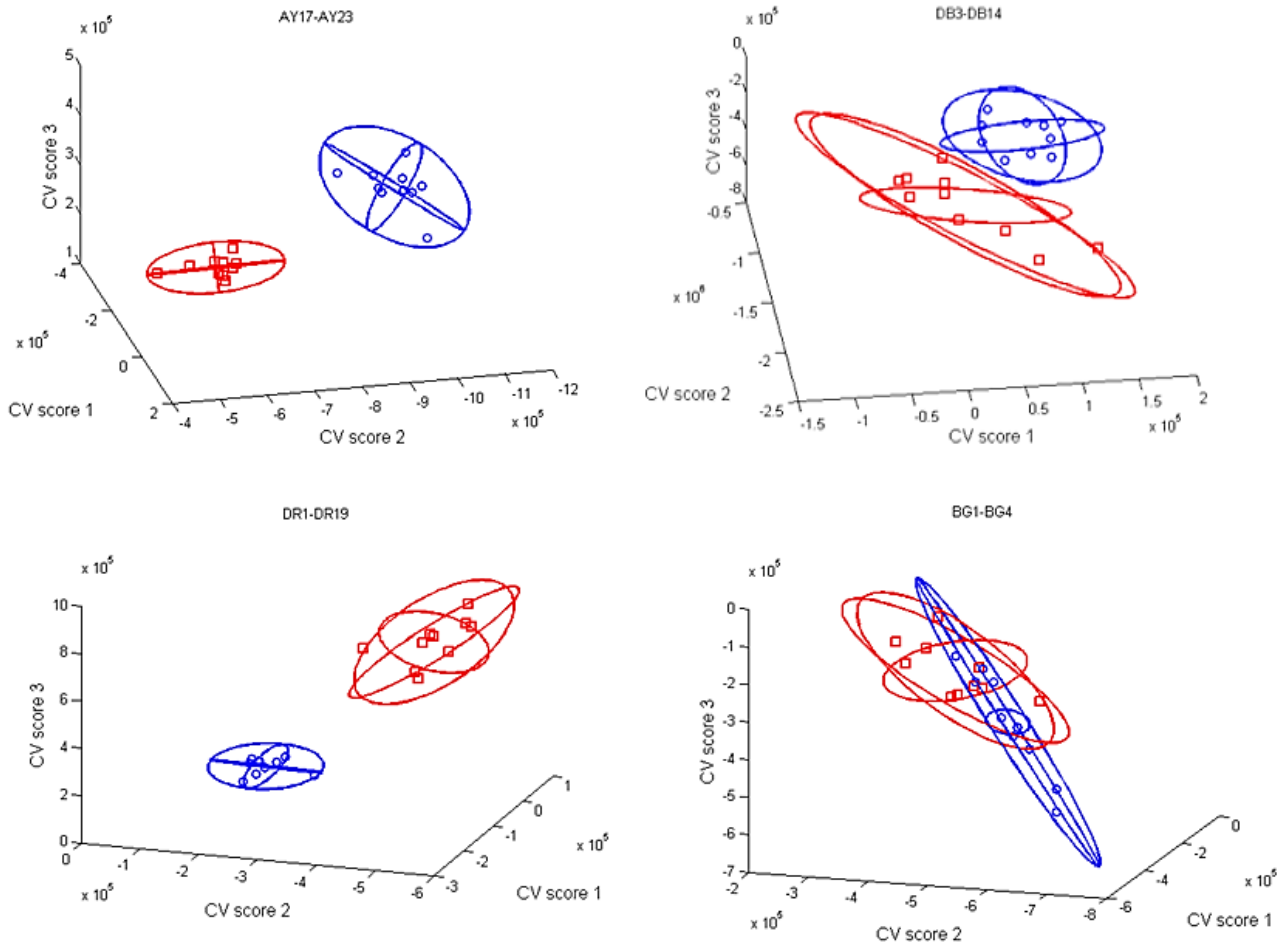

Figure 6.10. LDA CV scores (3 components model) for 20 samples of (top left) AY17 (10 replicates; blue circles) and AY23 (10 replicates; red squares) nylon 361 fibers; (top right) DB3 (10 replicates; blue circles) and DB14 (10 replicates; red squares) acetate satin 105B fibers; DR 1 (10 replicates; blue circles) and DR19 (10 replicates; red squares) polyester 777 fibers; and (bottom right) BG1 (10 replicates; blue circles) and BG 4 (10 replicates; red squares) acrylic 864 fibers. The three-dimensional projection of the 95% confidence ellipse of the data collected from each type of fiber is included to facilitate visualization of the obtained results.

6.5.4. DU-PLS

Since U-PLS is unable to process data files with NaN terms, the first step towards the application of DU-PLS was to select an appropriate range of sensors for each pair of fibers. Optimization of sensor ranges for each pair of fibers provided the following sensor data for the excitation and emission modes, respectively: 26 to 70 and 1 to 16 (AY17/AY23 fibers); 26 to 70 and 1 to 16 (DB3/DB14 fibers); 20 to 70 and 1 to 12 (DR1/DR19 fibers); and 10 to 70 and 1 to 5 (BG1/BG4 fibers).

The number of optimum latent variables (h) was estimated via the leave-one-sample-out cross-validation approach[257] using a 14-sample set per fiber pair; i.e. 7 samples from each type of fiber. The optimum h value was estimated with the ratio F(h) = PREES (h<h*)/PRESS(h*); where PRESS = $\sum(c_{i,act}-c_{i,pred})^2$, h was the trial number of factors and h* corresponded to the minimum PRESS. By selecting an h value that led to a probability of less than 75% that F>1, three factors were found for each pair of fibers.

The discriminant ability of DU-PLS was tested on 3 validation samples using the 14 samples as the calibration training set along with the coded values for each category of each pair of fibers. The predicted versus nominal code values are shown in Figure 6.11. The confidence interval for each category was estimated as the product of the calculated standard deviations of the results for the training samples – namely, 0.18 for AY17 and 0.13 for AY23; 0.14 for both DB3 and DB14; 0.13 for DR1 and 0.11 for DR19; and 0.17 for BG1 and 0.23 for BG4 - and the Student t-value with n-1 degrees of freedom ($t_{6,\ 0.05}$) = 2.45. Based on Figure 6.11, it is safe to state that the all the investigated fibers were clearly predicted and classified. Although the EEMs recorded from single

fibers belonging to the same fiber pair were almost identical, the prediction ability of the DU-PLS algorithm was enough to perform a successful supervised classification of samples.

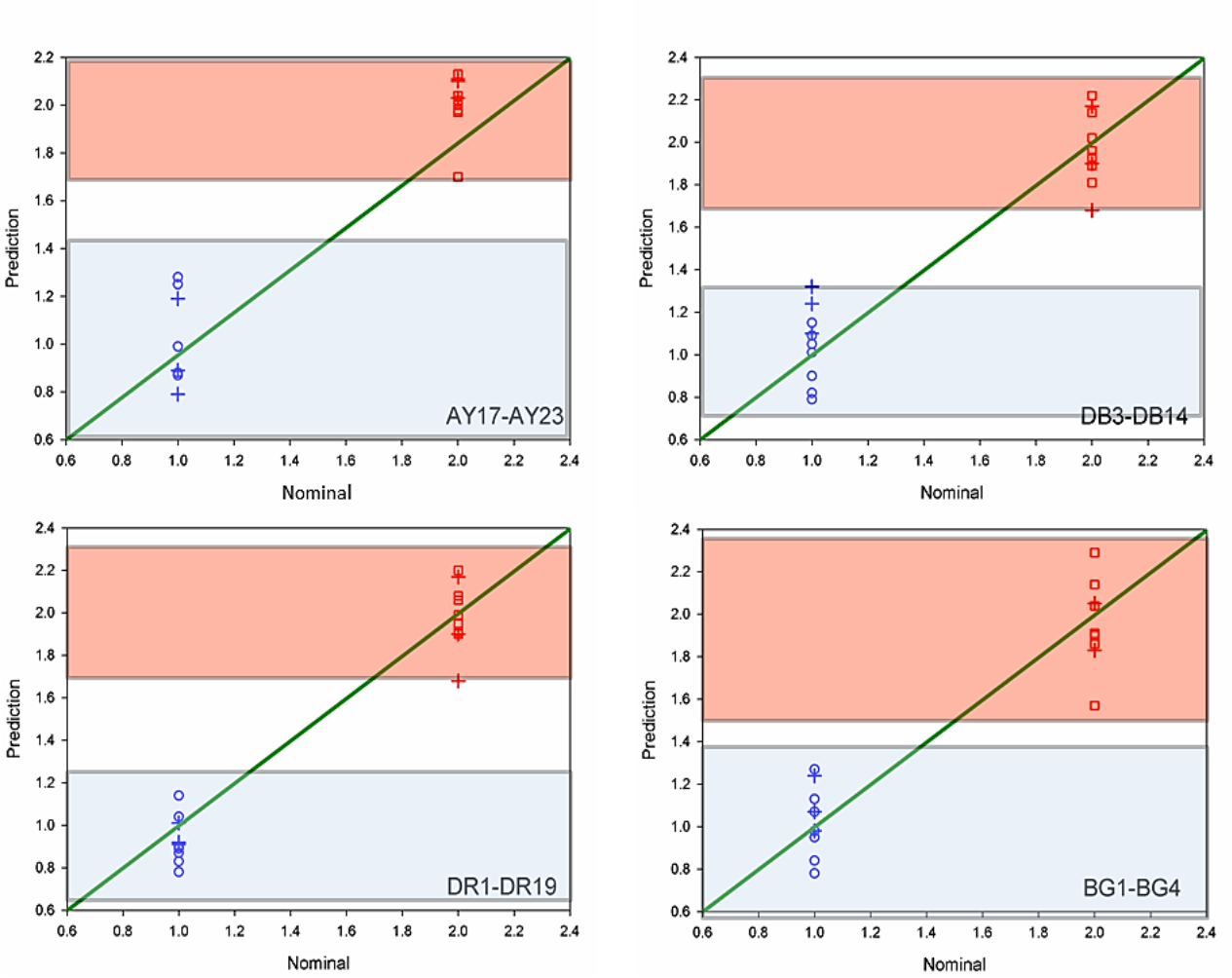

Figure 6.11. Plot of the DU-PLS (3 components model) predicted vs nominal coded values for 20 samples of (top left) AY17 (7 calibration samples = blue circles; 3 validation samples = blue crosses) and AY 23 (7 calibration samples = red squares; 3 validation samples = red crosses) nylon 361 fibers; (top right) DB3 (7 calibration samples = blue squares; 3 validation samples = blue crosses) and DB14 (7 calibration samples = red squares; 3 validation samples = red crosses) acetate satin 105B fibers; (bottom left) DR1 (7 calibration samples = blue circles; 3 validation samples = blue crosses) and DR19 (7 calibration samples = red squares; 3 validation samples = red crosses) polyester 777 fibers; and (bottom right) BG1 (7 calibration samples = blue squares; 3 validation samples = blue crosses) and BG4 (7 calibration samples = red squares; 3 validation samples = red crosses) acrylic 864 fibers.

6.6. Conclusion

Non-destructive techniques that can either discriminate between similar fibers or match a known to a questioned fiber – and still preserve the physical integrity of the fibers for further court examination - are highly valuable in forensic science. The work presented here provides a valuable data format for the fluorescence differentiation of visually indistinguishable fibers. In the case of virtually identical EEMs, an additional data treatment step involving an appropriate chemometric algorithm is necessary. Based on the obtained results, it can be concluded that LDA-supervised PARAFAC shows better discriminating potential than unsupervised PARAFAC. However, LDA-supervised PARAFAC was unable to discriminate between Acrylic 864 fibers dyed with BG 1 and BG 4. The best discrimination was obtained with the supervised DU-PLS model, which allowed the pairwise differentiation of the four pairs of investigated fibers.

CHAPTER 7. CLASSIFICATION OF PRE-DYED TEXTILE FIBERS EXPOSED TO WEATHERING AND PHOTODEGRADATION USING FLUORESCENCE MICROSCOPY PAIRED WITH DISCRIMINANT UNFOLDED-PARTIAL LEAST SQUARES

7.1 Introduction

Textile fibers are a key form of trace evidence, and the ability to reliably classify or discriminate them is important in forensic science. While different types of microscopic and analytical instrumentation methods can be implemented to understand the composition of these fibers, additional specificity is often obtained by analyzing the dye or the dye color on such fibers. This is mainly important if the fiber's bulk composition is relatively uninformative, as it is with cotton, wool or other natural fibers[3]. Non-destructive microscopic methods of analysis provide information about the fiber polymer (or substrate), refractive indices, luster, birefringence, and elemental composition of fibers[4], additionally aiding in the differentiation between different classes and subclasses of fibers (single fiber comparison) by comparing specific spectral features[31]. Similarly, Infrared (IR) spectroscopy has been reported earlier to determine the polymeric composition (natural vs. synthetic, organic vs. inorganic) of various fibers, and helps in identifying a generic class (e.g. polyester, polyamides, acrylics, etc.); or subclass (nylon 6, nylon 6,6, etc.) of such fibers[134-136]. Usually no dyes are detected using IR since the dye content of a fiber is in most cases lower than 5% of fiber weight. Alternatively, Raman spectroscopy, a complementary method to IR, was reported to provide information mainly about the dyes onto the fibers due to their enhancement by resonance.

Alternatively, a complementary method to IR known as Raman spectroscopy was reported to provide information mainly about the dyes onto the fibers due to their enhancement by

resonance[22,38,146]. Spectroscopic studies were also conducted to investigate the photo-oxidative degradation and weathering patterns of textiles like nylon, polyester, acrylic, cotton, etc. using Fourier transform infrared spectroscopy (FTIR)[258]. FTIR facilitated the characterization of photo-oxidation in the polymer or textile films, and to study the changes in the hydroxyl region (3700-3200 cm^{-1}) that took place during photo-irradiation or exposure of these fabrics to sunlight. IR spectral changes in various regions were examined and compared to observe the decomposition patterns of hydroperoxide/hydroxyl groups in the carbonyl groups[259]. However, some of the major drawbacks of the FTIR technique include labor-intensive sample preparation procedure, the possibility of losing the sample or fibers during mounting, and diffraction effects of the aperture leading to significant wavelength-dependent energy loss[260].

Forensic scientists are primarily interested in rapid, non-destructive, selective and sensitive examination methods, since they could face problems such as analyzing an extremely small sample size, destruction or loss of sample where a fiber cannot be retrieved back, complex dye composition onto the fiber, etc during fiber examination. The likelihood of fiber transfer between the suspect and the victim is highly possible at a crime scene. When a fiber is transferred from a fabric directly onto a victim's clothing, it is known as a direct or primary type of transfer; whereas a secondary or indirect transfer occurs when already transferred fibers on the clothing of a suspect transfer to the clothing of a victim[3,4,11]. Forensic laboratories are interested in examining such transferred fibers by comparing them with a questioned or known source to discover the possible common origins. There is a possibility that once a crime occurs, a criminal could escape and travel from one geographical region to the other, commonly known as crime scene getaway[261]. In such a situation, if there is a slightest chance of the suspect carrying any transferred fibers from the victim's clothing

onto theirs, it becomes important to be able to identify and relate a questioned fiber to a known source. More so, comparisons of transferred fibers can provide valuable information regarding their history or the source of origin. Environmental components such as solar irradiance, temperature, moisture and/or humidity are some of the critical weathering variables for many textile materials. Solar radiation on materials leads to fading, color change, surface erosion, and loss of gloss and numerous other deteriorations of textile fabrics[262].

Textiles such as nylon, polyester, polyethylene-terephthalate, etc. have previously been reported to be susceptible to photodegradation, resulting in a loss of physical properties and a change in the chemical properties of these fibers, when exposed to UV energy in unfiltered and filtered sun-sky radiation[263]. Photochemical degradation pattern of cellulosic fibers has been extensively investigated and reported earlier[264,265], while the degradation behavior of polyurethane coated nylon fabric and woven webbings made of nylon and polyester fibers when exposed to outdoor environment has also been studied[266,267]. Within the United States, extreme differences in atmospheric conditions occur due to the variations in the exposure to the intensity of sunlight, in the amount and distribution of precipitation, altitude and other such factors[267]. Weathering effect in two extremely different climate zones in Russia has previously been reported to examine the most rapid degradation of fabrics such as wool, polyester, cotton, etc.[262]. Effects of temperature on a weathering material include thermal oxidation degradations, subsequent reaction rates and other accelerating weathering reactions. The local climate of the Miami, FL area comprises of increased levels of critical weathering variables such as higher solar radiant exposure, increased temperatures and extreme humidity or moisture in the atmosphere. On the other hand, the local climate of the

Phoenix, AZ area contains increased levels of important weathering variables such as higher radiant exposure and extremely dry heat or temperature in the atmosphere [268].

Weather is made up of a number of factors which have an individual and combined effect on the behavior of a textile when the material is exposed outdoors. Factors such as heat, light, oxygen and humidity cause textile degradation which might lead to significant changes in the spectral features of fibers. Weathering trials in tropical and arid regions are more aggressive to materials due the higher levels of heat, temperature, humidity and solar radiation. Thus these climate conditions are often considered as a means of obtaining advanced information as the resistance of a material to temperate conditions. Arizona is an ideal environment for intense heat and low humidity, whereas due to the synergistic effect of intense sunlight, high ambient moisture, and high temperature, the tropical region of Florida has been established as the international benchmark for outdoor weathering.

The goal of this study was to investigate effects of weathering conditions on the spectral features of cotton 400 pre-dyed with DB1, nylon 361 pre-dyed with AY17 and acrylic 864 pre-dyed with BG4 – before and after exposure to humid (Florida) and dry (Arizona) weathering conditions for three, six, nine and twelve months. Nondestructive fluorescence microscopy[51,52,162] was employed for obtaining spectral data from single pre-dyed textile fiber exposed to weathering. The degradation pattern of Direct Blue 1 dyed Cotton 400 fibers, Acid Yellow 17 dyed Nylon 361 and Basic Green 4 dyed Acrylic 864 fibers was analyzed, and an attempt has been made to be able to differentiate and classify any two fibers compared together, before and after environmental exposure. The chosen pre-dyed textiles were exposed to natural and outdoor weathering at the

testing facilities of Atlas Weathering Services Group (located in Arizona and Florida). Spectral and chemometric analysis (of the 2D and 3D fluorescence emission spectra obtained from the exposed and non-exposed fibers) was performed using fluorescence microscopy in combination with a chemometric algorithm – discriminant unfolded partial least-squares (DU-PLS).

7.2. Principles of DU-PLS

There are several algorithms for partial least squares (PLS) and its enhancements for discriminant analysis. This chapter will focus on the DU-PLS algorithm where there are two groups of samples with an aim to decide which of the two groups a sample belongs to. PLS is regarded as a linear two-class classifier, a method that aims to find a line that divides a space into two regions[243]. For univariate calibration, before selecting linear or non-linear regression method to fit the data, it is important to know whether the signal varies linearly with the analyte concentration or not, Likewise, for a 2D matrix data, it is important to know whether the data is bilinear, for a 3D-dimensional (3D) data, whether the data is trilinear or not, etc. In short, bilinearity and trilinearity are important for multiway calibration, just as linearity is important in univariate calibration[250]. A three-way data array is built by joining data matrices for a group of samples, in such a way that if data matrices of size J x K are measured for I samples, they can be arranged into an object of size I x J x K. A three-way data array, X, built for a single constituent, is trilinear if its elements are given by the equation 7.1[243,250].

$$X_{ijk} = a_i b_j c_k \tag{7.1}$$

where a_i, b_j and c_k are elements of the profiles along the sample mode i, j and k respectively. For a mixture of N constituents generating trilinear signals, the overall signal is given by:

$$X_{ijk} = \sum_{n=1}^{r} a_{in} b_{jn} c_{kn} \quad (7.2)$$

where a_{in} is the value of an element in profile **a** for constituent n in sample i, and b_{jn} and c_{kn} are the respective values of the n^{th} constituents in the **b** and **c** profiles. Equation 7.2 suggests that n should be close to or ideally equal to the number of constituents in a mixture[52,243,250,269].

Some of the useful three-way/second-order calibration algorithms such as parallel factor analysis (PARAFAC), linear discriminant analysis (LDA) and multivariate curve resolution-alternating least-squares (MCR-ALS) have been reported elsewhere[52,269], and used for the convenient analysis of the second-order data. These algorithms are adequate for specifically processing trilinear data. Once a matrix is unfolded, the resulting vectors can be processed by a well-known technique, popular in the field of first-order calibration, such as the classical and highly useful partial least-squares (PLS) analysis. To calibrate second-order data, unfolding and PLS processing gives rise to the unfolded partial least-squares (U-PLS) methodology. This algorithm was implemented to discriminate between two groups of samples; hence it is also known as discriminant unfolded-partial least squares (DU-PLS). An advantage of implementing DU-PLS is that it is able to recognize a sample containing unexpected constituents and flag it as an outlier, indicating that the test sample data cannot be appropriately modeled using the current calibration method.

7.3. Experimental

7.3.1. Textile preparation

In order to cover a wide variety, textile fabrics chosen for this study were based on three criteria such as (1) material type such as Acrylic 864 (A864), Cotton 400 (C400) and Nylon 361

(N361); (2) different types of dyes such as acid, basic and direct; and (3) different dye colors such as yellow, blue and green. C400 fabrics were dyed Direct Blue 1 (DB1) dye, A864 fabrics were dyed with Basic green 4 (BG4) dye, and N361 with Acid Yellow 17 (AY17) dye. All fabric samples were separately stored in sealed packages, and kept in the dark to avoid any exposure to the environment. Blades, scissors and tweezers that were used to handle the fabrics and isolate the fibers were previously cleaned with methanol and tested for the presence of any fluorescence contamination under UV-light at 254 nm. The dyes, including BG4 (90% purity), DB1 (80% purity) and AY17 (60% purity) were purchased from Sigma-Aldrich (www.sigma-aldrich.com). The dye concentrations were 3% for BG4 on A864, 2% AY17 on N361 and 2% DB1 on C400. Fabrics were acquired and dyed by Testfabrics, inc. (West Pittson, PA). Further, Atlas Material Testing Solutions (www.atlas-mts.com) exposed these textiles (4.5 X 6.0 in) to the two weather conditions in Arizona and Florida.

Figure 7.1 displays the textiles exposed to humid environment, where exposure testing was performed in Miami, Florida (26°N) in accordance with governing standards at a tilt angle(s) of 5° from the horizontal facing south. The specimens were mounted unbacked on a 1643 x 3586 mm aluminum exposure rack, with grass groundcover, and the uncoded side facing the sun. Similarly, for textile exposed to desert environment, exposure testing was performed in New River, Arizona; in accordance with governing standards at a tilt angle(s) of 5° from the horizontal facing south. The specimens were mounted unbacked on a 1643 x 3586 mm aluminum exposure rack, with gravel groundcover, and the uncoded side facing the sun. Figures 7.2 to 7.4 show comparisons between the dyed fabric pieces before exposure and after various time intervals of exposure to both AZ and FL

weather conditions, whereas, as an example, figures 7.5 to 7.8 compare the microscopic images of DB1 and BG4 single fibers exposed to both climate conditions, under different time intervals.

Figure 7.1. Textiles exposed to Florida weather conditions in outdoor humid environment.

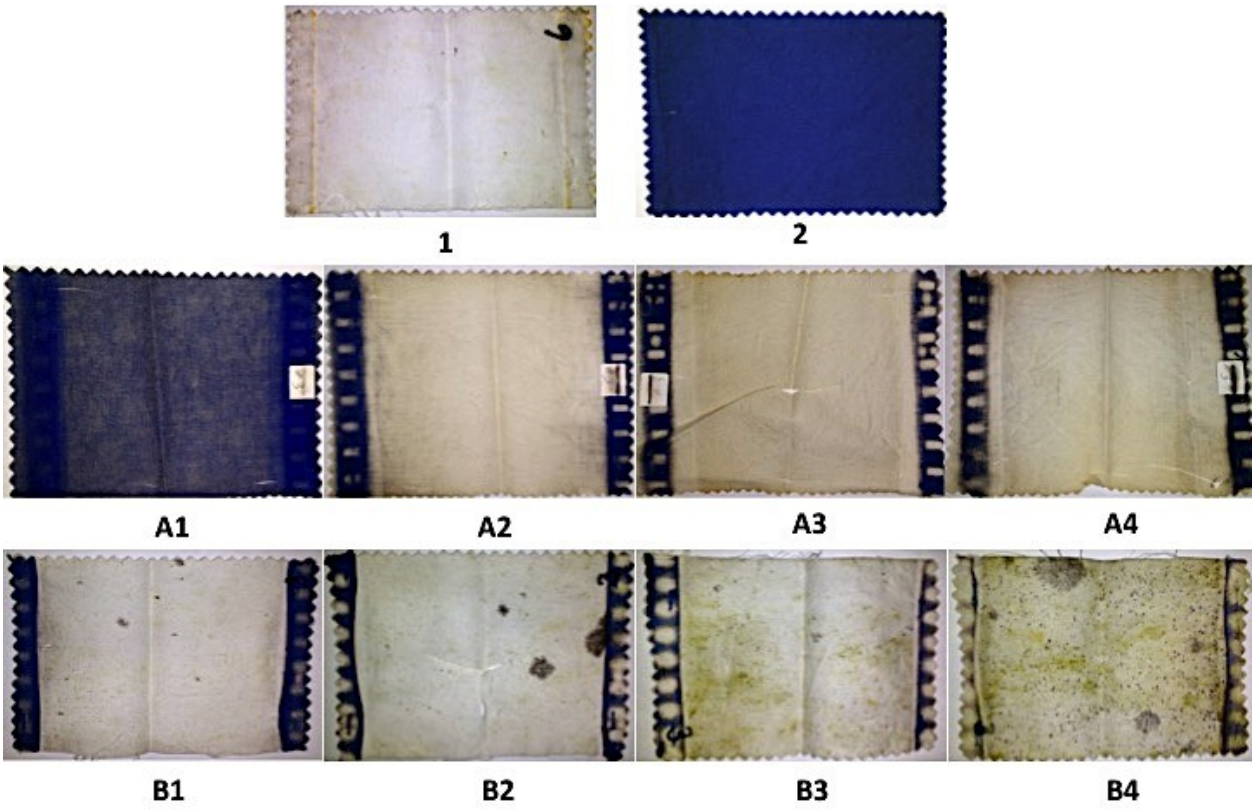

Figure 7.2. Direct blue 1 (DB1) dyed cotton 400 textile fabric pieces (4.5 in x 6.0 in) exposed to Arizona (dry) weathering for 3 months (A1), 6 months (A2), 9 months (A3) and 12 months; and to Florida (humid) weathering for 3 months (B1), 6 months (B2), 9 months (B3) and 12 months (B4). The top two cloth pieces are a comparison between non-weathered undyed cotton 400 fabric (1) and non-weathered cotton 400 fabric dyed with DB1 dye (2).

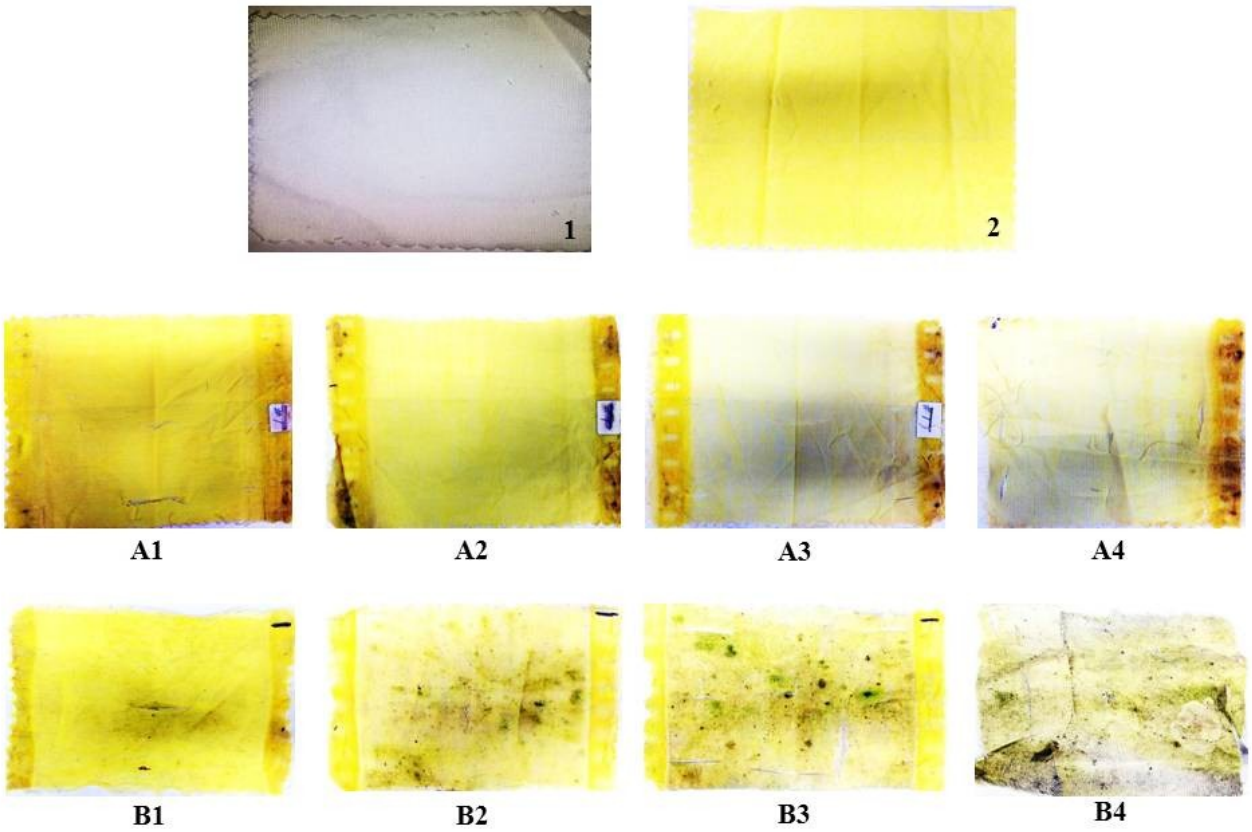

Figure 7.3. Acid yellow 17 (AY17) dyed nylon 361 textile fabric pieces (4.5 in x 6.0 in) exposed to Arizona or dry weather conditions for 3 months (A1), 6 months (A2), 9 months (A3) and 12 months; and to Florida or humid weather conditions for 3 months (B1), 6 months (B2), 9 months (B3) and 12 months (B4). Top two cloth pieces are a comparison between undyed nylon 361 fabric (1) and nylon 361 fabric dyed with AY17 dye (2).

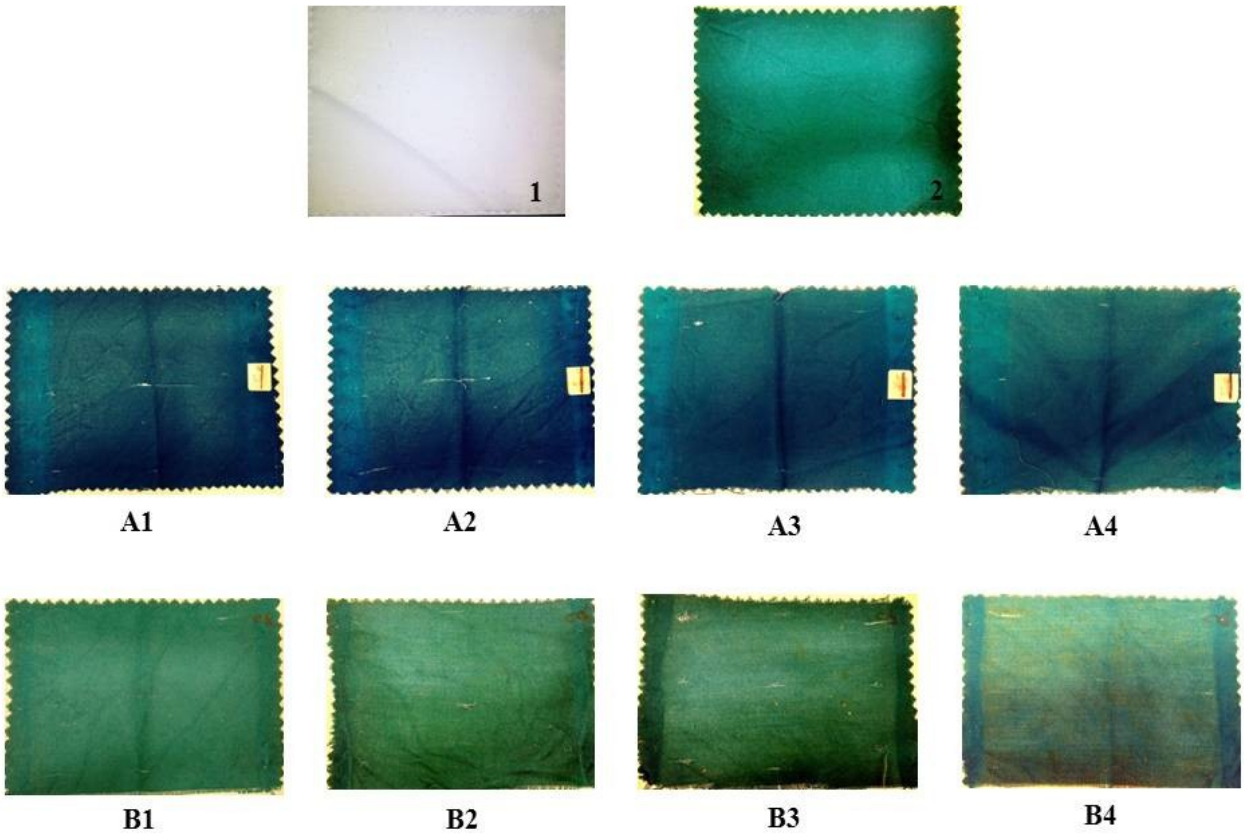

Figure 7.4. Basic green 4 (BG4) dyed Acrylic 864 textile fabric pieces (4.5 in x 6.0 in) exposed to Arizona or dry weather conditions for 3 months (A1), 6 months (A2), 9 months (A3) and 12 months; and to Florida or humid weather conditions for 3 months (B1), 6 months (B2), 9 months (B3) and 12 months (B4). Top two cloth pieces are a comparison between undyed Acrylic 864 fabric (1) and Acrylic 864 fabric dyed with BG4 dye (2).

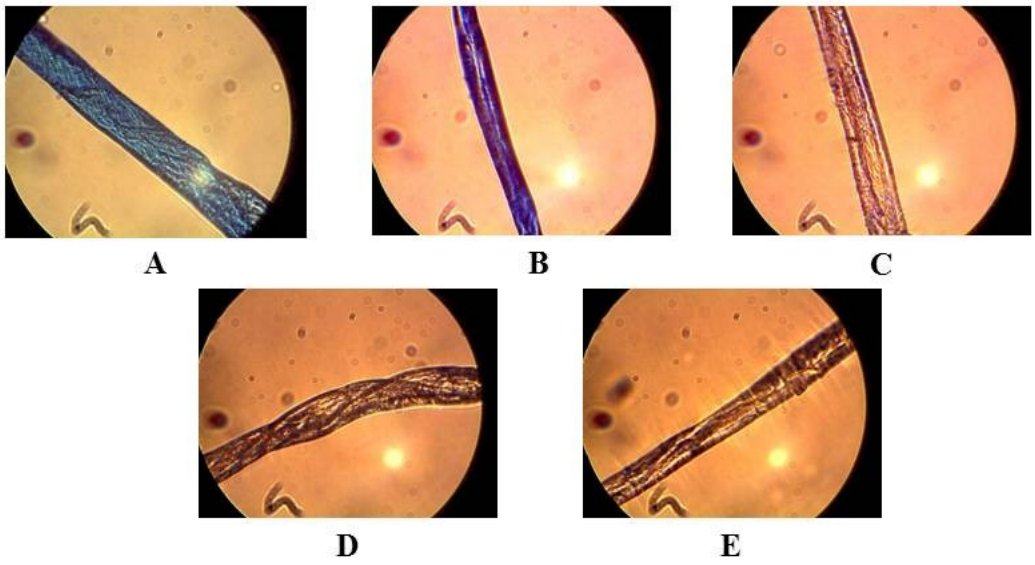

Figure 7.5. Microscope image of a single DB1 dyed fiber exposed to Arizona weathering for 0 months (A), 3 months (B), 6 months (C), 9 months (D) and 12 months (E).

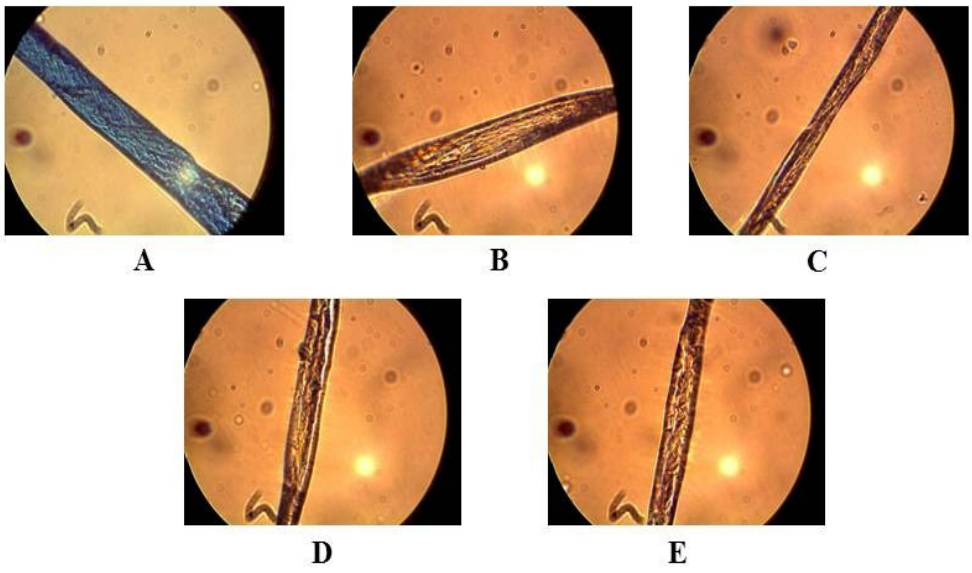

Figure 7.6. Microscope image of a single DB1 dyed fiber exposed to Florida weathering for 0 months (A), 3 months (B), 6 months (C), 9 months (D) and 12 months (E).

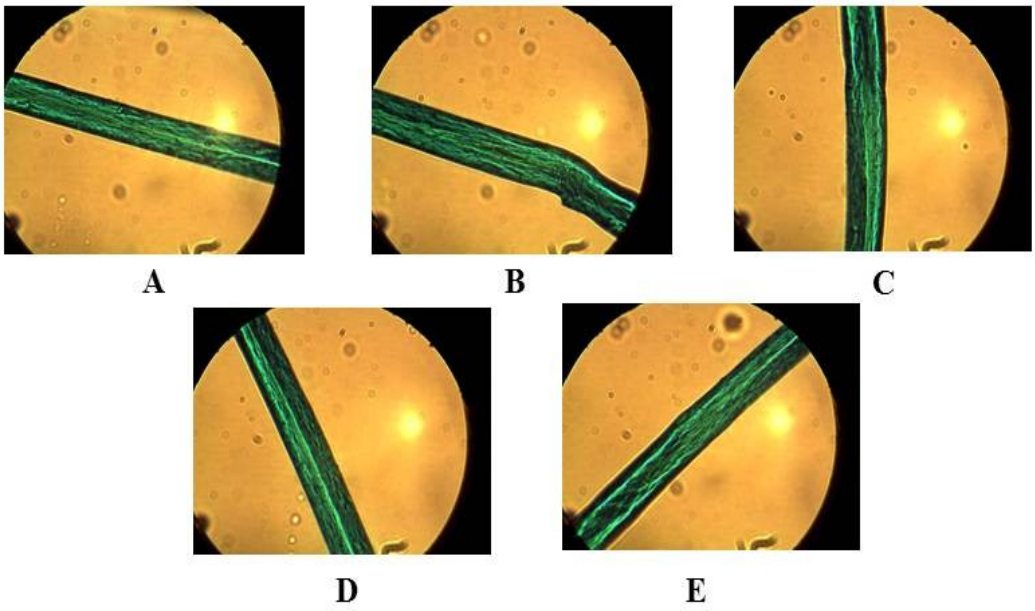

Figure 7.7. Microscope image of a single BG4 dyed fiber exposed to Arizona weathering for 0 months (A), 3 months (B), 6 months (C), 9 months (D) and 12 months (E).

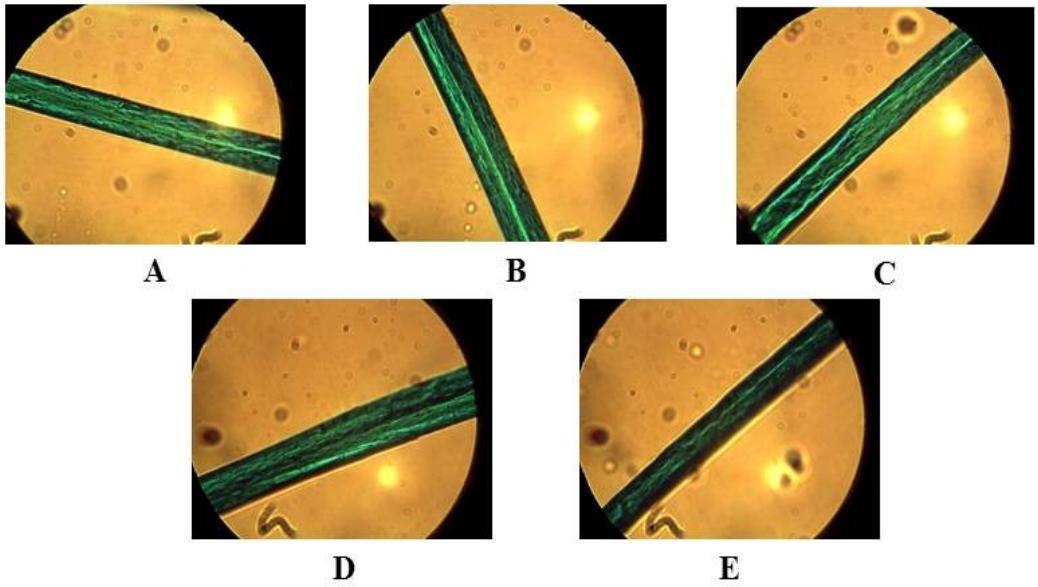

Figure 7.8. Microscope image of a single BG4 dyed fiber exposed to Florida weathering for 0 months (A), 3 months (B), 6 months (C), 9 months (D) and 12 months (E).

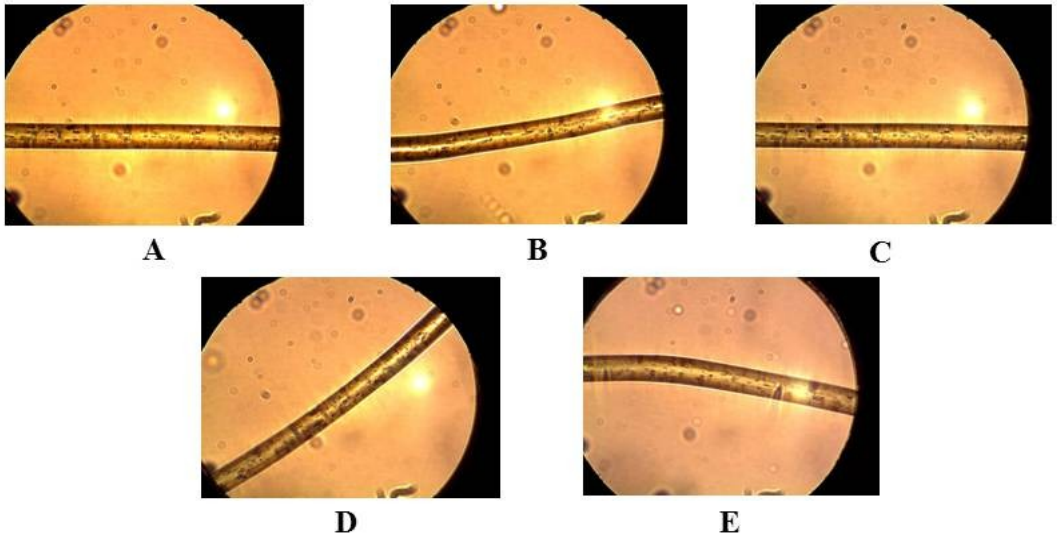

Figure 7.9. Microscope image of a single AY17 dyed fiber exposed to Arizona weathering for 0 months (A), 3 months (B), 6 months (C), 9 months (D) and 12 months (E).

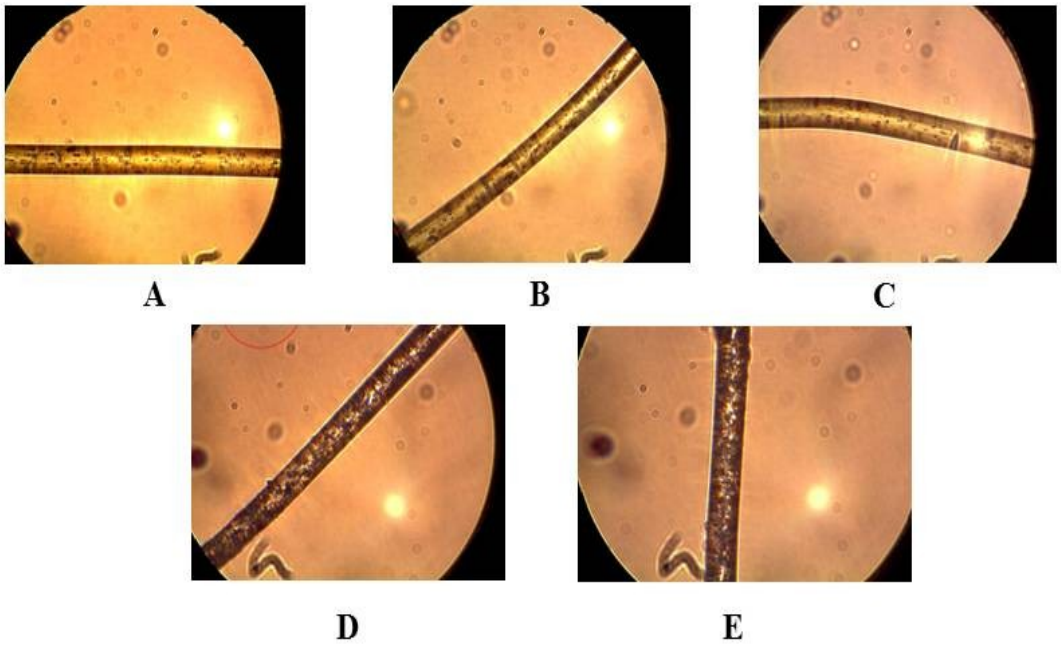

Figure 7.10. Microscope image of a single AY17 dyed fiber exposed to Arizona weathering for 0 months (A), 3 months (B), 6 months (C), 9 months (D) and 12 months (E).

7.3.2. Instrumentation

Details pertaining to the fluorescence microscopy instrumentation are provided in chapter 3 of this dissertation.

7.3.3. EEM Acquisition

With a 1 nm increment, fluorescence emission was recorded between 435 and 800 nm; where the excitation range was kept between 350 and 675 nm at 5 nm increments using suitable cutoff filters to avoid scatter interference from excitation radiation. Under the 40X visible microscopic objective, a pinhole diameter of 400 μm was used to expose an area of the fiber to the excitation light source. Ten fibers were uniformly sampled from each of the chosen textile fabric cloth pieces (6.0 in. x 4.5 in.) that were exposed to both dry and humid climate conditions, under various time intervals (such as 0, 3, 6, 9 and 12 months). To acquire EEM data from all the fibers, a single fiber was sampled or pulled from a cloth piece using tweezers, and placed in between a quartz slide and a quartz cover-slip which was later placed on a sample-holder underneath the microscope objective lens. Briefly, while analyzing a pair of fiber together (comparing two cloth pieces), a total of twenty fibers were examined together for DU-PLS analysis, out of which fourteen samples were used for calibration and six samples were used for validation.

One EEM was recorded from from one spot on a single fiber, providing a total of ten EEMs per textile fabric piece. In short, ten EEMs were collected from each of the ten fibers isolated from individual fabric cloth pieces exposed to three, six, nine and twelve months of Arizona as well as Florida weather conditions. EEMs were compared or evaluated for variations along the spectral profiles in different regions of the spectra. As an example, Figures 7.9 and 7.10 represent 3D

contour EEM plots belonging to AY17 dyed fibers exposed to Arizona and Florida weathering (respectively). Additional EEMs plots acquired from DB1 and BG4 dyed fibers exposed to weathering at different time intervals are shown in appendix G.

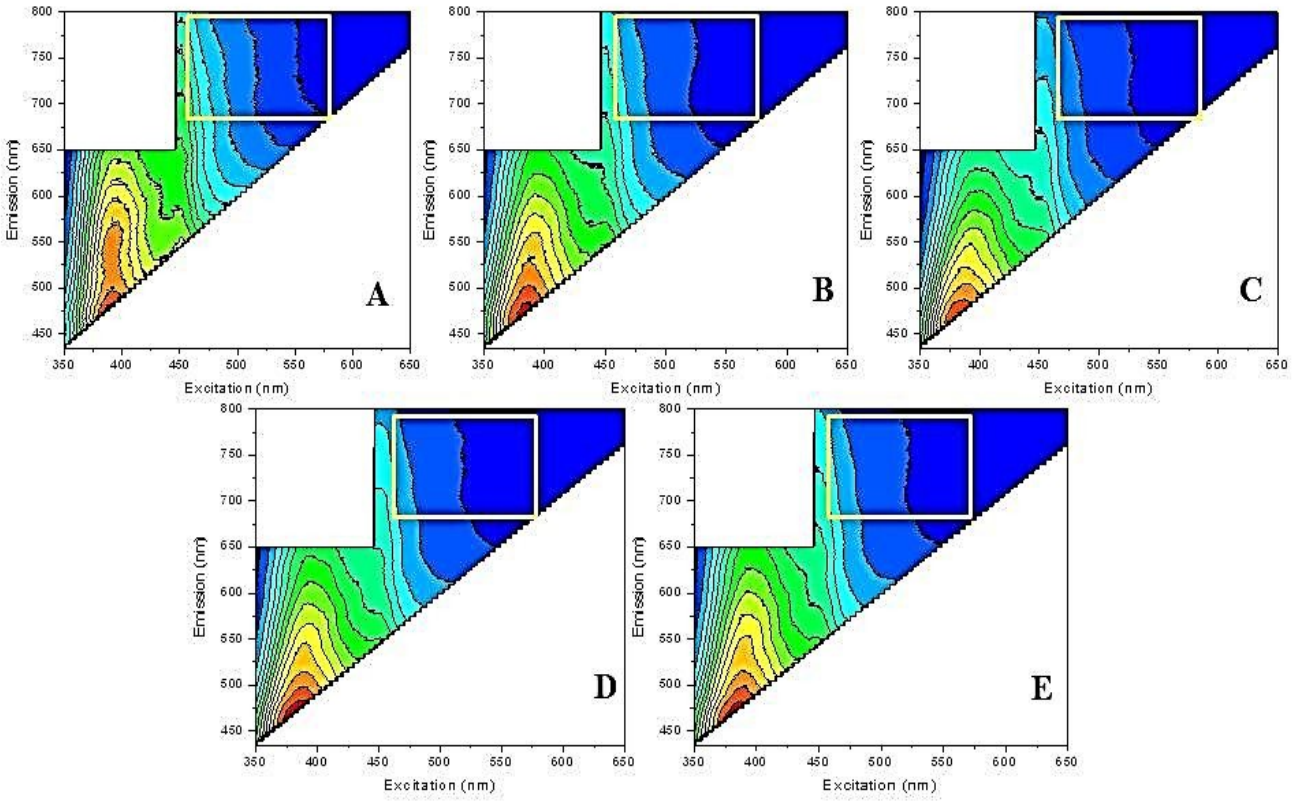

Figure 7.11. Contour plots of averaged EEMs from ten Acid Yellow 17 dyed Nylon 361 textile fibers exposed to Arizona (dry) weather condition for 0 months (A), 3 months (B), 6 months (C), 9 months (D), and 12 months (E).

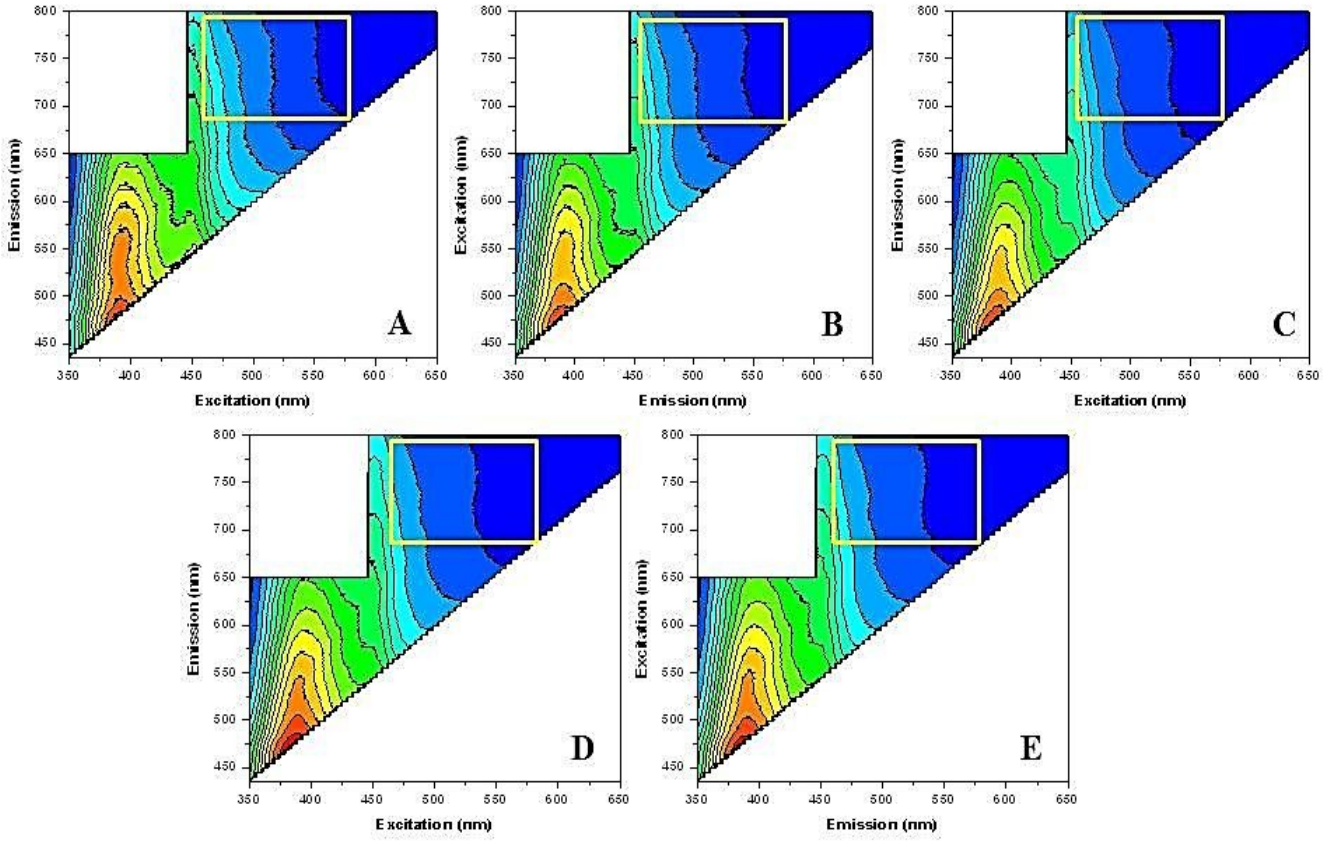

Figure 7.12. Contour plots of averaged EEMs from ten Acid Yellow 17 dyed Nylon 361 textile fibers exposed to Florida (humid) weather condition for 0 months (A), 3 months (B), 6 months (C), 9 months (D), and 12 months (E).

7.3.4. Data analysis

Excitation was recorded between 435 – 800 nm with increments of 5 nm, whereas fluorescence was obtained between 345 – 800 nm with 1 nm increments. Using these parameters, each EEM obtained resulted in a data matrix consisting of 66 × 366 data points (excitation × emission). As seen in Figures 7.9 and 7.10, these rather large data matrices include wavelength regions where there is no fluorescence data present due to Raleigh scattering. Hence, to optimize computational time, these regions were not included in the calculations. When the data analysis time was reduced further by computing one fluorescence data point at an interval of every 3 nm, no significant loss of data was observed. The new EEM consisted of matrices comprising of 66 × 122 data points (excitation × emission). The wavelength regions selected for DU-PLS analysis are denoted in yellow boxes in the above mentioned figures. These regions include data points 25 to 50 in the excitation mode (475 – 600 nm) and data points 75 to 100 in the emission mode (675 – 800 nm). All the missing data points from the Raleigh scattering were replaced by NaNs terms and handled by expectation maximization[239]. On visual comparison between EEMs recorded from the different fibers exposed to Arizona and Florida weathering, differences in the overall emission spectra were observed at 525 nm excitation wavelength (emission ranging from 610-800 nm). Hence, 2D fluorescence emission spectra comparing each time interval of exposure for DB1 dyed fibers was plotted in Figure 7.11.

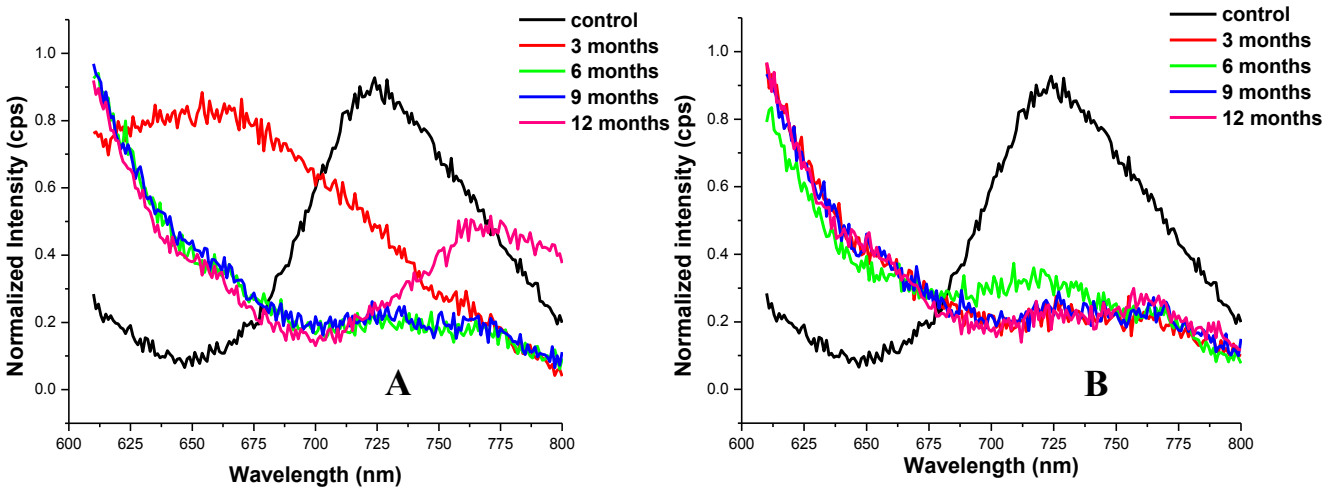

Figure 7.13. 2D fluorescence emission spectra at λ_{exc} = 525 nm from DB1 dyed cotton 400 fibers exposed to Arizona (A) and Florida (B) weather conditions before exposure and after various time intervals of exposure.

MATLAB 8.0 graphical interface was used to load the EEM data matrices prior to statistical analysis via DU-PLS. A detailed description for the DU-PLS theory/method has been reported earlier [52]. In brief, the main difference between U-PLS and discriminant U-PLS (DU-PLS) lies in the construction of a dependent variable 'y'. To calibrate a model, this variable y should contain concentration values. For discriminant analysis purpose, y must contain a coding integer that represents the class label of the sample. PLS regression is conducted in between the instrumental response in *X* block (built with the unfolded original second-order matrix data) and the class label in *y* block using training samples, and then the optimal number of latent variables is chosen depending on the rate of error after cross-validation. The final model for '*A*' latent variables is used to determine the class label in the test set according to the following equation: $y_{test} = (t_{test})^{T} * V$, where y_{test} is the predicted label class, t_{test}^{T} are the test sample scores obtained by projecting the x_{test} onto the training loadings, and v is the vector of regression coefficients. Ideally, the calculated y_{test} values

for the two classes of samples being compared are 1 or 2. However in reality, y_{test} values are often close to either 1 or 2. Hence, in order to allocate a test (validation) sample to a given (calibration) class, it is necessary to establish a threshold for the predicted values of y_{test}. This threshold is determined as a value that lessens the number of false positives and false negatives.

7.4. Discussion

Since U-PLS is unable to process the data files with NAN terms, the first step towards the application of the DU-PLS algorithm is to select an appropriate range of sensors for each fiber pair. After optimizing the sensor ranges for each pair of investigated fibers, the sensor data selected for the excitation and emission modes were 25 to 50 and 75 to 100 respectively. The number of calibration PLS latent variables *A* was estimated using a procedure known as leave-one-sample-out cross-validation, or CV for short[52,269]. Here, each sample was left out from the calibration set, and its concentration was predicted using a model built with the data from the remaining samples. The squared error for the prediction of the left out sample was then summed into a parameter called predicted error sum of squares (PRESS), as follows:

$$PRESS = \quad {}^{I}_{i=1}(y_{i,nominal} - y_{i,predicted})\text{^}2 \tag{7.3}$$

where *I* is the number of calibration samples. The optimum *A* value was estimated with the ratio:

$$F\ A\ = PRESS\ (A < A^{*})/PRESS\ (A^{*}) \tag{7.4}$$

Where A is the trial number of factors and A^{*} corresponds to the minimum PRESS. By selecting an *A* value that led to a probability of less than 75% stating that F > 1, three factors were found for each pair of fibers that were compared together[257].

For each pair of textile cloth pieces that were analyzed and compared together, 10 fibers from each fabric cloth piece were sampled and one EEM per fiber was obtained. This led to the accumulation a total of 20 EEMs per pair of fabric that was compared, out of which 14 samples were used as calibration training set and the discriminant ability of DU-PLS was tested on the remaining 6 validation samples, along with the coded values for each category of each pair of fibers.

DU-PLS was used to differentiate between textiles exposed to dry versus humid weather conditions, as well as to distinguish between samples exposed to different time intervals within dry condition or within humid weather condition. As an example, Figure 7.12 shows the differentiation between DB1 fibers exposed to Arizona versus Florida weathering, whereas Figures 7.13 and 7.14 represent the DU-PLS plots that discriminate between and classify DB1 fibers exposed to only the Arizona and Florida weather conditions, respectively. Each time interval of exposure was compared against one another to attempt to differentiate between any two fiber samples. In short, the predicted versus nominal code values for all types of DB1 fiber comparisons (within same climate conditions or after comparison between AZ versus FL weather) are shown in Figures 7.12 to 7.14. Similar analysis was performed for AY17 and BG4 dyed fibers (see appendix G for DU-PLS plots). The confidence interval for each category of comparison was estimated from the product of the calculated standard deviations (of the results of the training set samples) and the Student t-value with n-1 degrees of freedom for each category. On the basis of DU-PLS figures belonging to comparison between DB1 fibers (Figures 7.12 to 7.14), it was estimated that all the investigated fibers were clearly predicted, classified and distinguished from one another in their own category within their confidence interval limits (represented by bold red or blue lines within the DU-PLS graphs). Similar results were found for AY17 dyed fibers, DU-PLS plots are shown in appendix G.

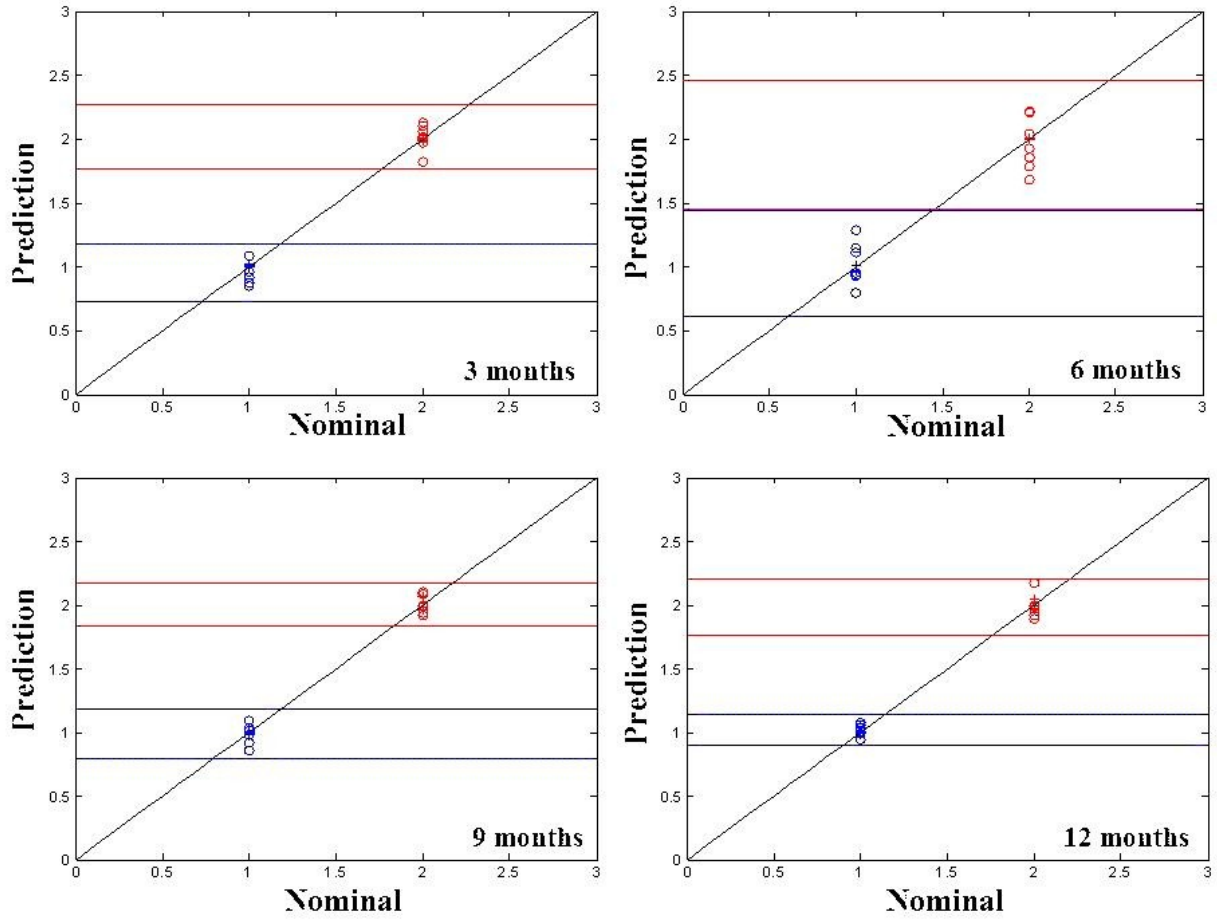

Figure 7.14. DU-PLS plots (3 component model) for the predicted versus nominal coded values for 10 fibers of DB1 dyed C400 exposed to Arizona (7 calibration samples = blue circles; 3 validation samples = blue crosses) versus 10 fibers of DB1 dyed C400 exposed to Florida (7 calibration samples = red circles; 3 validation samples = red crosses) weathering conditions under different time intervals of exposure.

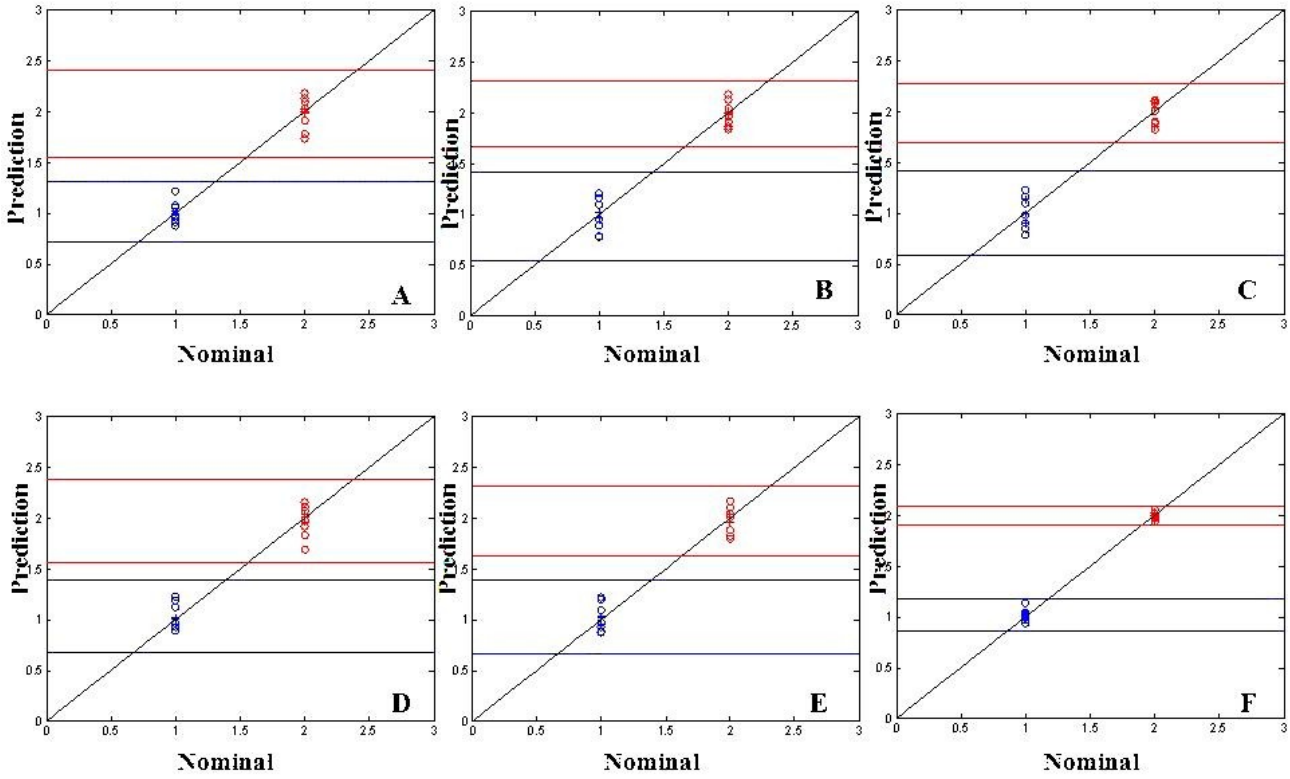

Figure 7.15. DU-PLS plots (3 component model) for the predicted versus nominal coded values of DB1 dyed C400 fibers exposed under different time intervals within Arizona's weathering conditions. 20 fibers were examined per exposure out of which 14 fibers were used as calibration samples (circles) whereas 6 fibers were used for validation (crosses). The plots represent: (A) 3 months (blue) versus 6 months (red); (B) 3 months (blue) versus 9 months (red); (C) 3 months (blue) versus 12 months (red); (D) 6 months (blue) versus 9 months (red); (E) 6 months (blue) versus 12 months (red); and (F) 9 months (blue) versus 12 months (red).

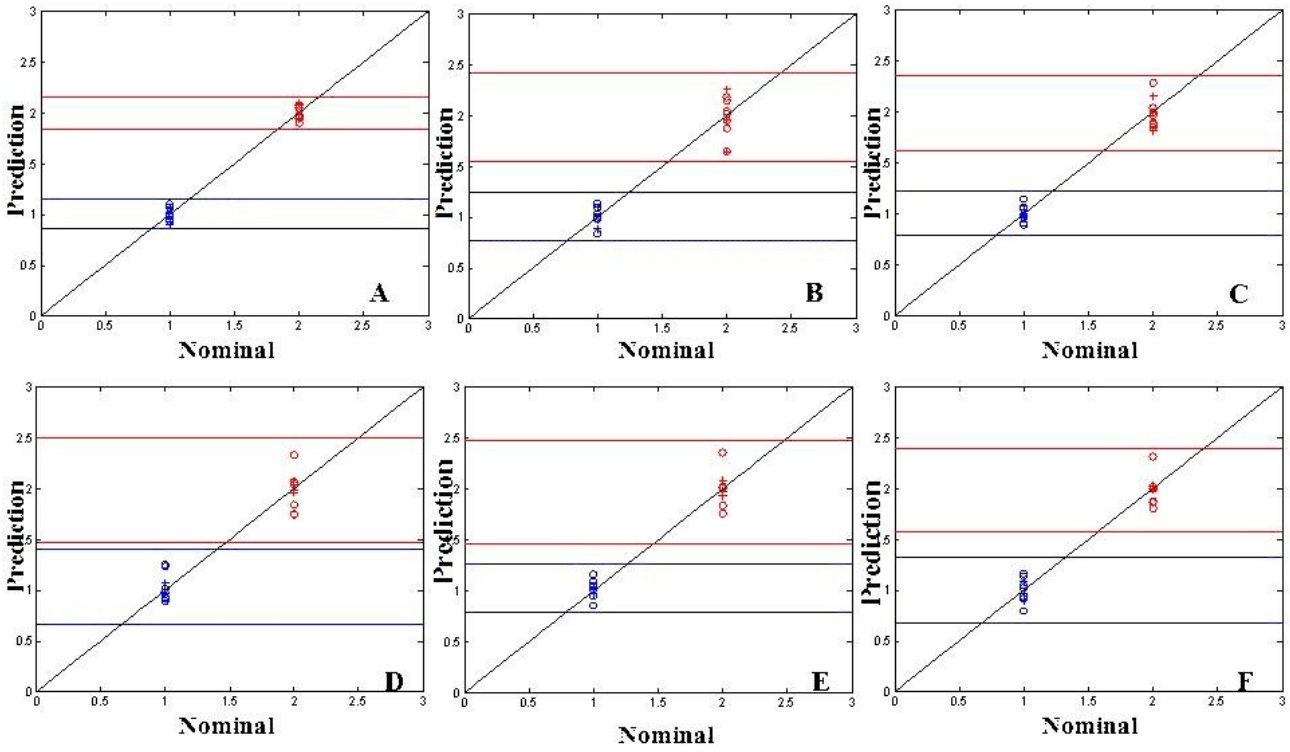

Figure 7.16. DU-PLS plots (3 component model) for the predicted versus nominal coded values of DB1 dyed C400 fibers exposed under different time intervals within Florida's weathering conditions. 20 fibers were examined per exposure out of which 14 fibers were used as calibration samples (circles) whereas 6 fibers were used for validation (crosses). The plots represent: (A) 3 months (blue) versus 6 months (red); (B) 3 months (blue) versus 9 months (red); (C) 3 months (blue) versus 12 months (red); (D) 6 months (blue) versus 9 months (red); (E) 6 months (blue) versus 12 months (red); and (F) 9 months (blue) versus 12 months (red).

In certain cases of AY17 dyed fibers, even though the recorded EEMs from two pairs of fibers were visually identical, the prediction ability of the DU-PLS algorithm was enough to perform a successful supervised classification of all the fiber samples (Tables 7.1 and 7.2). Lastly, DU-PLS showed little or no ability to discriminate between BG4 fibers exposed to different weathering (appendix G provides additional information for the DU-PLS plots obtained from classification of two fiber samples). For example, fibers exposed to Arizona versus Florida weathering could not be differentiated, and also fibers exposed within Arizona weathering could not be resolved (Table 7.3). In some cases within Florida's weathering, only some BG4 fiber samples could be differentiated (Table 7.4). A '✓' denotes a successful differentiation between two fiber samples that were compared and analyzed together, whereas a '×' denotes an unsuccessful differentiation. The DU-PLS plots belonging to BG4 fibers exposed to weathering is provided in appendix G.

Table 7.1. Differentiation between two of AY17 dyed N361 fibers or two DB1 dyed C400 fibers exposed to Arizona weather conditions under various exposure times in months

Exposure time	0 months AZ	3 months AZ	6 months AZ	9 months AZ	12 months AZ
0 months AZ	×	✓	✓	✓	✓
3 months AZ	✓	×	✓	✓	✓
6 months AZ	✓	✓	×	✓	✓
9 months AZ	✓	✓	✓	×	✓
12 months AZ	✓	✓	✓	✓	×

Table 7.2. Differentiation between two of AY17 dyed N361 fibers or two DB1 dyed C400 fibers exposed to Florida weather conditions under various exposure times in months

Exposure time	0 months FL	3 months FL	6 months FL	9 months FL	12 months FL
0 months FL	×	✓	✓	✓	✓
3 months FL	✓	×	✓	✓	✓
6 months FL	✓	✓	×	✓	✓
9 months FL	✓	✓	✓	×	✓
12 months FL	✓	✓	✓	✓	×

Table 7.3. Differentiation between two BG4 dyed Acrylic 864 fibers exposed to Arizona weather conditions under various exposure times in months.

Exposure time	0 months AZ	3 months AZ	6 months AZ	9 months AZ	12 months AZ
0 months AZ	×	×	×	×	×
3 months AZ	×	×	×	×	×
6 months AZ	×	×	×	×	×
9 months AZ	×	×	×	×	×
12 months AZ	×	×	×	×	×

Table 7.4. Differentiation between two BG4 dyed Acrylic 864 fibers exposed to Florida weather conditions under various exposure times in months.

Exposure time	0 months FL	3 months FL	6 months FL	9 months FL	12 months FL
0 months FL	×	×	×	×	×
3 months FL	×	×	×	×	✓
6 months FL	×	×	×	×	✓
9 months FL	×	×	×	×	✓
12 months FL	×	✓	✓	✓	×

7.5. Conclusion

In general, the initial rate of degradation in outdoor environment is higher and shows some levelling over a period of time. Different dyed textile fabrics were exposed to two different natural outdoor weathering conditions over a period of one year (May 2013 to April 2014), and samples were received by our laboratory after every three months. Comparisons between the EEM plots and the 2D fluorescence emission spectra suggest that photodegradation of the dyes occurs rapidly after the first three months of weathering. In cases where it was challenging to visually distinguish between spectra of AY17 dyed fibers subjected to six versus nine months of outdoor environmental exposure, the DU-PLS algorithm assisted in differentiating between these fibers by correctly classifying the validation clusters with the predicted values.

High irradiances coupled with extreme temperatures in a short time interval of dry weathering condition can lead to quicker textile material degradation compared to the same textile

material exposed in humid or tropical weathering. Temperature-irradiance interactions can create a unique degradation mechanism during the summer months in Arizona, whereas textiles exposed to Florida's climate provide lesser variation due to lower temperature-irradiance interactions. Addition of the moisture variable in Florida's environment to these interacting factors further differentiates these two reference environments which are extremely diverse from each other. These interactions in critical weathering variables result in dramatically different environments and ecologies. It is interesting to observe that the material degradation mechanism differs widely between these exposure environments.

Different polymers have different susceptibilities to photodegradation. Except for acrylics (in most cases), cotton and nylon showed sensitivity and vulnerability after exposure to both weathering conditions. Undyed cotton is photochemically activated by absorption of light energy in the UV region, but cotton dyed with certain 'active' dyes gets activated by the energy which the dye absorbs energy from the visible region of the spectrum. In case of cotton 400 textiles pre dyed with DB1, as the duration of outdoor exposure increased, the blue color on the fibers degraded rapidly. Similarly, nylon 361 textiles pre-dyed with AY17 faded away as the time of outdoor environmental exposure increased. This was not the case with acrylic textiles. Acrylic fibers are known to have good thermal stability, and some discoloration might occur when exposed to temperatures > 175 ^{0}C for a prolonged period. Because of its robustness, acrylics could not be differentiated when an attempt was made to compare and differentiate between exposures to Arizona versus Florida weathering conditions.

Recently, we could successfully discriminate between four pairs of visually indistinguishable single fibers using three different methods of multi-way chemometric analysis such as unsupervised PARAFAC, LDA-supervised PARAFAC and DU-PLS. Results indicated that LDA-supervised PARAFAC showed better discriminating potential than unsupervised PARAFAC, however the best discrimination was obtained with the supervised DU-PLS model, allowing for the pairwise differentiation of the investigated fibers[52]. Variations within the same type of fibers do not contribute to fiber discrimination, however discrepancies within two fibers from the same source (nylon and cotton) exposed to different weathering conditions can be differentiated and classified with DU-PLS. This algorithm was able to differentiate non-exposed cotton and nylon fibers from exposed fibers to Florida and Arizona weathering conditions. It was possible to determine the period of exposure to either Florida or Arizona conditions. It was also possible to discriminate between fibers exposed to Florida or Arizona weathering conditions for the same period of time. These results provide the foundation for future studies towards a non-destructive approach capable to provide information on the history of the fiber.

CHAPTER 8: OVERALL CONCLUSIONS

The objective of this research was to apply several different methods of chemometric analysis to forensic fiber identifications, comparisons and classifications; in order to develop a completely objective method of comparing fluorescence emission spectra collected from dyed and undyed textile fibers. In cases where fibers are colored with dyes having highly similar molecular structures, traditional methods of microscopic and visual comparisons of spectral profiles can fail to report the correct results or give rise to inconclusive decisions. Moreover, modifications to textile fibers after their production and distribution (be it chemical, mechanical or environmental), are of increasing interest since such modifications can provide additional and exclusive identification information of these trace textile fiber evidences. There are several other popular and widely used analytical techniques that have been applied towards forensic fiber investigation; however it is important for examiners to preserve the physical integrity of these fibers without destroying them for further court examinations.

The nondestructive analysis of fibers was accomplished (without any fiber pretreatment or solvent extraction) with an instrumental setup coupling a commercially available spectrofluorimeter with an epi-fluorescence microscope, a technique known as fluorescence microscopy. Optimization of this method was carried out by evaluating the behavior of both fluorescence intensity and signal-to-background ratio (from different dyed fibers that exhibited fluorescence when excited using ideal wavelengths – spectral data provided in appendix B) as a function of the instrumental parameters such as pinhole size and excitation-emission band-pass. The combination of a 400 μm pinhole and a 40X visible-objective appeared to be well suited for the fiber analysis. Using these parameters, fluorescence microscopy was employed for the nondestructive examination of trace fibers exposed to repetitive

launderings, contrasting weather conditions and also to distinguish between visually and microscopically indistinguishable fibers.

Laundry detergents contain fluorescence whitening agents, and sequential washings leads to their deposition onto the fibers chosen for the study. Adsorption of whitening agents and other detergent components to textile fibers during laundering results in the emission of fluorescence spectra that can be measured directly from the fiber. In most cases, after washing a textile for five times, the detergent signal reached its maximum. Principle component cluster analysis was used to distinguish between washed and unwashed fibers. Nylon fibers dyed with acid yellow 17 and cotton fibers dyed with direct blue 1 were never misclassified as unwashed; however, acrylic fibers have little or no detergent contribution to their fluorescence spectra. Clusters belonging to washed and unwashed acrylic fibers (dyed with basic green 4) could not be separated using PCA. With the goal of identifying the exact detergent used in a laundering process, direct measurement of fluorescence spectra obtained from whitening agents (when deposited on single fibers after washing) was conducted. Factors such as the dye on the fiber, the whitening agent, and other miscellaneous detergent components interact and combine together to produce the ultimately observed spectrum from the laundered fibers.

PCA was initially employed to distinguish between indistinguishable acrylic fibers dyed with basic green 1 and basic green 4 dyes; however, the spectral clusters could not be resolved sufficiently. Hence, besides PCA, other and more powerful chemometric methods of analysis such as unsupervised-PARAFAC, LDA-supervised PARAFAC and DU-PLS were used to discriminate between four pairs of indistinguishable fibers. Even though LDA-supervised PARAFAC had a better discriminating potential than unsupervised PARAFAC, it was able to distinguish between all

other chosen pairs of fibers, except for acrylic 864 dyed with BG1 and BG4. Overall, the best discrimination was obtained with the supervised DU-PLS model, which allowed the pairwise differentiation of all the selected four pairs of investigated fibers. Furthermore, the DU-PLS algorithm was again employed to examine and classify dyed acrylic nylon and cotton fibers exposed to two different (dry versus humid) weather conditions. Discrepancies within any two fibers from the same source (nylon and cotton in all cases, and acrylic in some cases) exposed to Arizona and Florida's environmental conditions were identified and these fibers were correctly classified (and distinguished from one another) in their own categories using DU-PLS.

In conclusion, fluorescence microscopy paired with different chemometric algorithms is a very strong, novel and a nondestructive approach that needs no fiber pre-treatment, and provides great potential towards forensic examination of trace textile fibers. Besides colleting two-dimensional fluorescence spectra while analyzing fibers, recording the total or three-dimensional excitation-emission matrices provides highly valuable information for fiber identification, differentiation and classification.

APPENDIX A: MOLECULAR STRUCTURES OF DYES USED FOR DYEING VARIOUS FIBERS

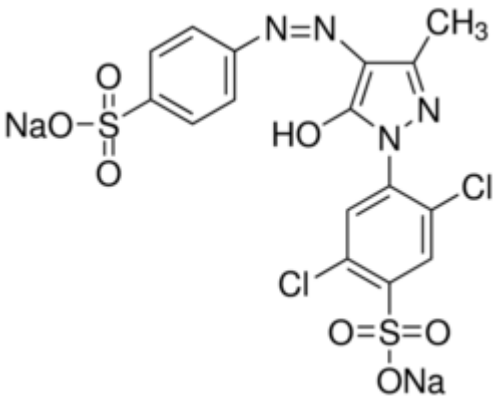

Acid yellow 17

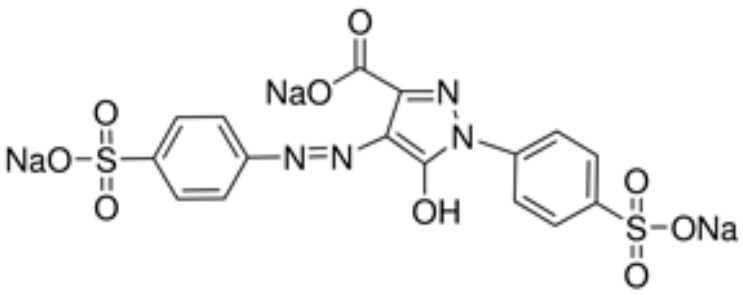

Acid yellow 23

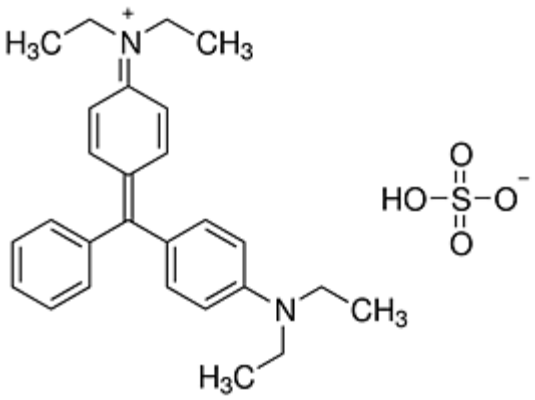

Basic green 1

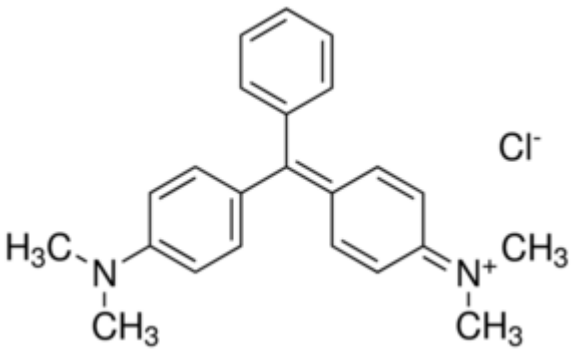

Basic green 4

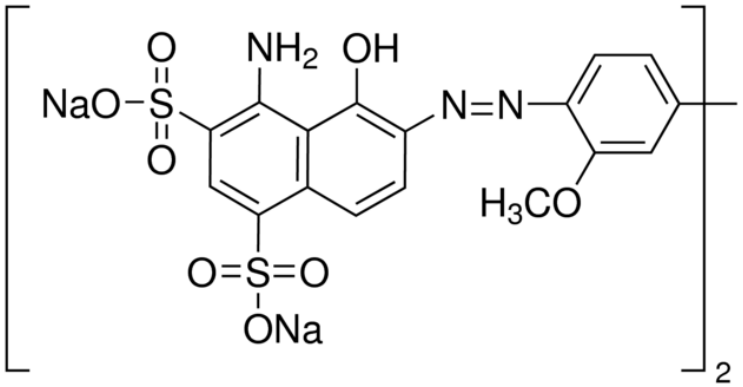

Direct blue 1

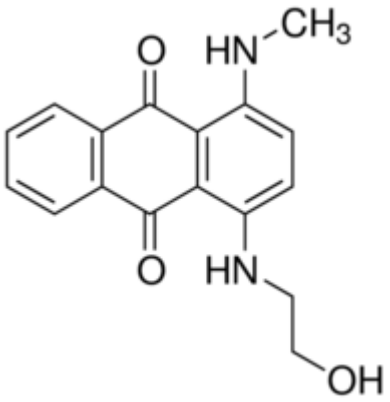

Disperse blue 3

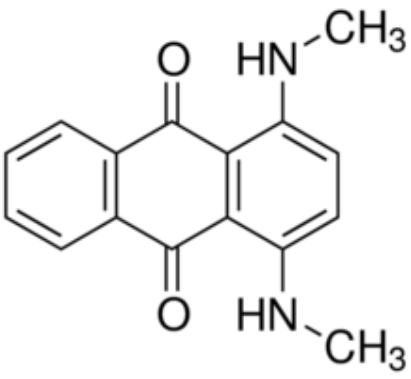

Disperse blue 14

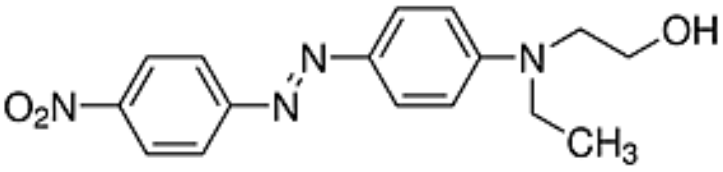

Disperse red 1

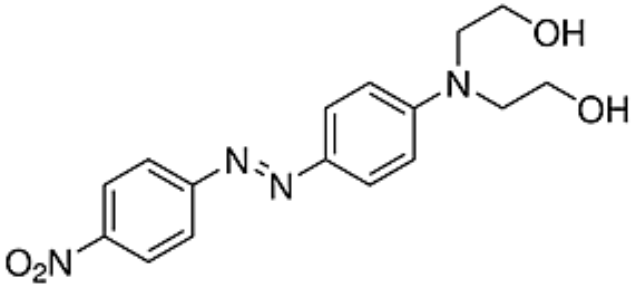

Disperse red 19

APPENDIX B: S/B OPTIMIZATION OF INSTRUMENTAL PARAMETERS

Table B1. S/B ratios recorded from P777-BR9 fiber with UV objectives

PD (µm)	*10X*		*40X*	
	DSA	*S/B*	*DSA*	*S/B*
100	10	1.033 ± 0.650	2.5	1.382 ± 0.148
200	20	1.150 ± 0.813	5	1.556 ± 0.067
400	**40**	**1.190 ± 0.744**	**10**	**4.713 ± 0.238**
600	60	1.300 ± 0.962	15	3.118 ± 0.056
800	80	1.214 ± 0.869	20	2.299 ± 0.024
1000	100	1.150 ± 0.855	25	2.210 ± 0.033
6000	600	1.070 ± 0.736	150	1.401 ± 0.037

Table B2. S/B ratios recorded from A864-BG4 fiber with visible objectives

PD (µm)	*10X*		*40X*	
	DSA	*S/B*	*DSA*	*S/B*
100	10	0.911 ± 0.099	2.5	2.035 ± 0.277
200	20	0.894 ± 0.060	5	2.345 ± 0.090
400	**40**	**0.864 ± 0.021**	**10**	**4.329 ± 0.082**
600	60	0.865 ± 0.022	15	3.221 ± 0.071
800	80	0.915 ± 0.024	20	2.836 ± 0.031
1000	100	0.920 ± 0.014	25	2.005 ± 0.026
6000	600	0.967 ± 0.009	150	1.157 ± 0.010

Table B3. S/B ratios recorded from N361-AG27 fiber with 40X-vis objective, tape-lift method.

PD (µm)	*DSA*	*S/B*
200	5	8.307 ± 0.287
400	**10**	**9.565 ± 0.706**
600	15	7.427 ± 0.046

Table B4. S/B ratios recorded from N361-BG4 fiber with 40X-vis objective, tape-lift method.

PD (µm)	*DSA*	*S/B*
200	5	1.751 ± 0.045
400	**10**	**4.141 ± 0.115**
600	15	3.483 ± 0.040

Table B5. S/B ratios recorded from C400-DB53 fiber with 40 X-vis objective, tape-lift method.

PD (µm)	***DSA***	***S/B***
200	5	6.982 ± 0.974
400	**10**	**12.474 ± 0.792**
600	15	7.128 ± 0.149

Table B6. S/B ratios recorded from P777-DsR4 fiber with 40 X-vis objective, tape-lift method.

PD (µm)	***DSA***	***S/B***
200	5	77.837 ± 3.362
400	**10**	**104.625 ± 5.563**
600	15	92.712 ± 4.416

Table B7. S/B ratios recorded from P777-BR9 fiber with 40X-UV objective, tape-lift method.

PD (µm)	***DSA***	***S/B***
200	5	2.987 ± 0.179
400	**10**	**5.564 ± 0.212**
600	15	3.956 ± 0.140

Table B8. S/B ratios recorded from P777-DsR4 fiber with 40X-UV objective, tape-lift method.

PD (µm)	***DSA***	***S/B***
200	5	3.218 ± 0.159
400	**10**	**6.708 ± 0.427**
600	15	3.814 ± 0.053

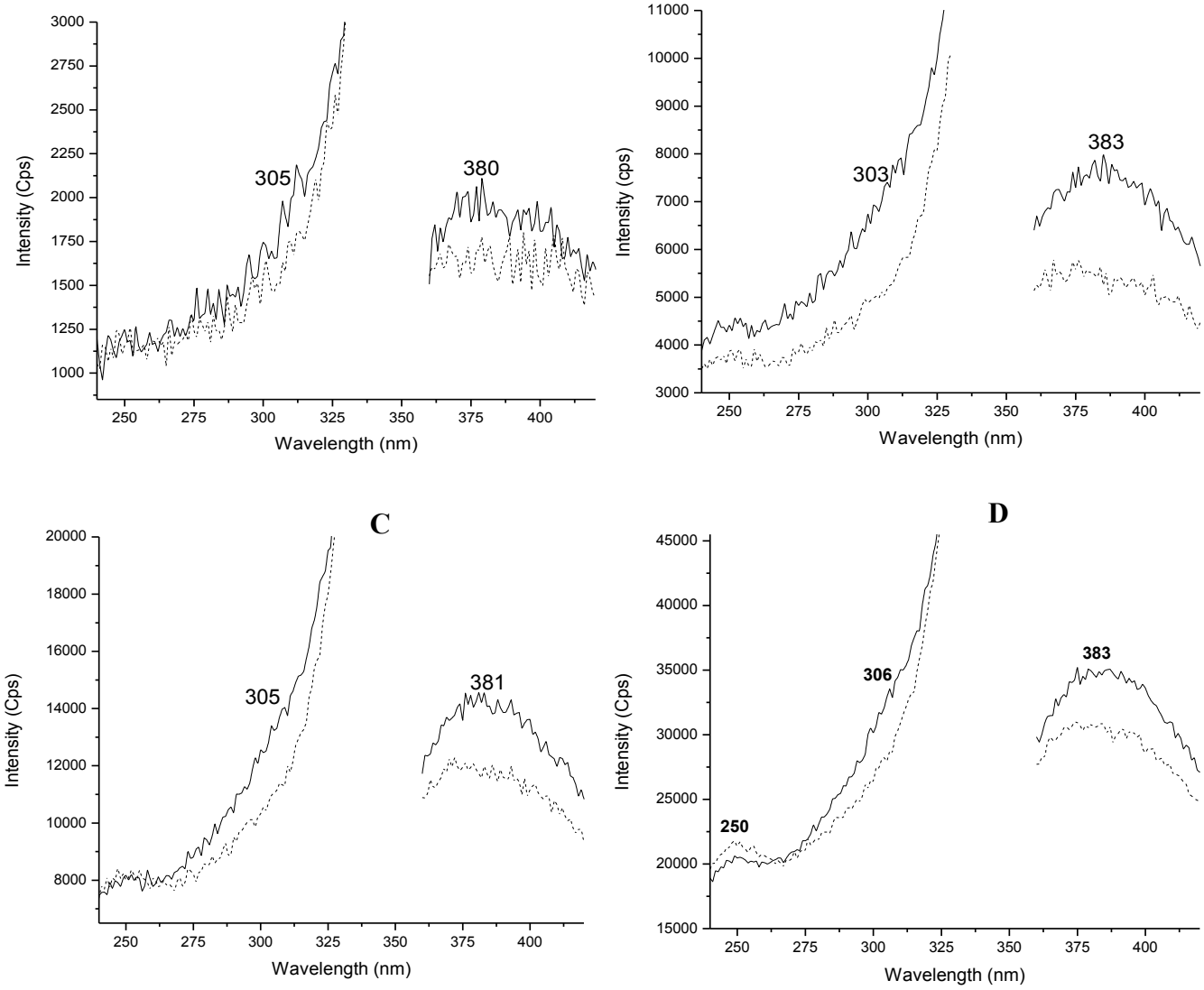

Figure B1. Comparison of excitation and emission spectra of a polyester 777 fiber dyed with Basic red 9 (–), and spectra collected from background (···), under a 10X UV objective lens, and using a pinhole diameter of (A) 200 µm, (B) 400 µm, (C) 600 µm, and (D) 1000 µm. Spectra were collected using $\lambda_{exc/em}$ = 305/380 nm, an excitation and emission band-pass of 25 nm, and using the glass slide and cover-slip method

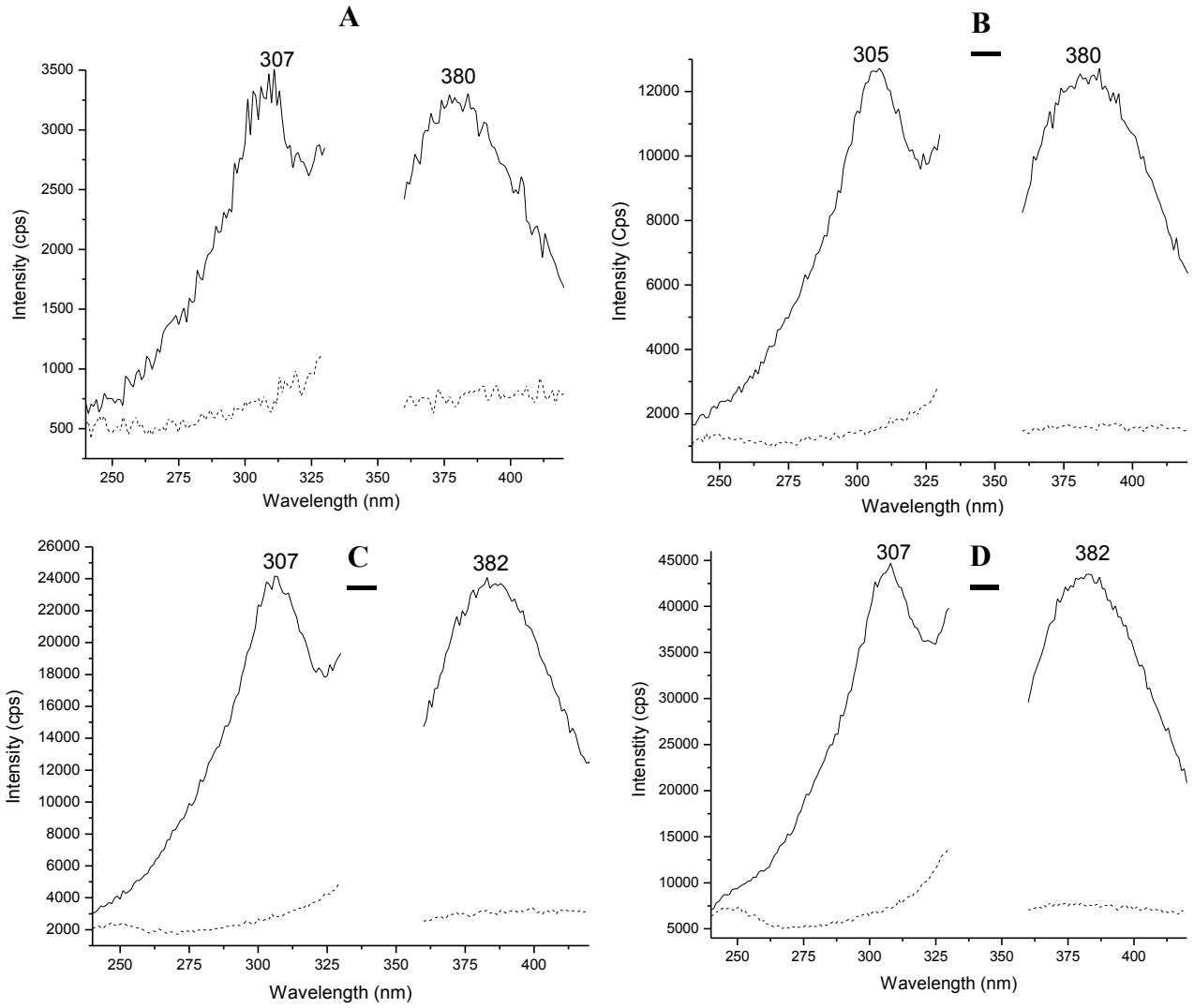

Figure B2. Comparison of excitation and emission spectra of a polyester 777 fiber dyed with Basic red 9 (–), and spectra collected from background (···), under a 40X UV objective lens, and using a pinhole diameter of (A) 200 µm, (B) 400 µm, (C) 600 µm, and (D) 1000 µm. Spectra were collected using $\lambda_{exc/em}$ = 305/380 nm, an excitation and emission band-pass of 25 nm, and using the glass slide and cover-slip method.

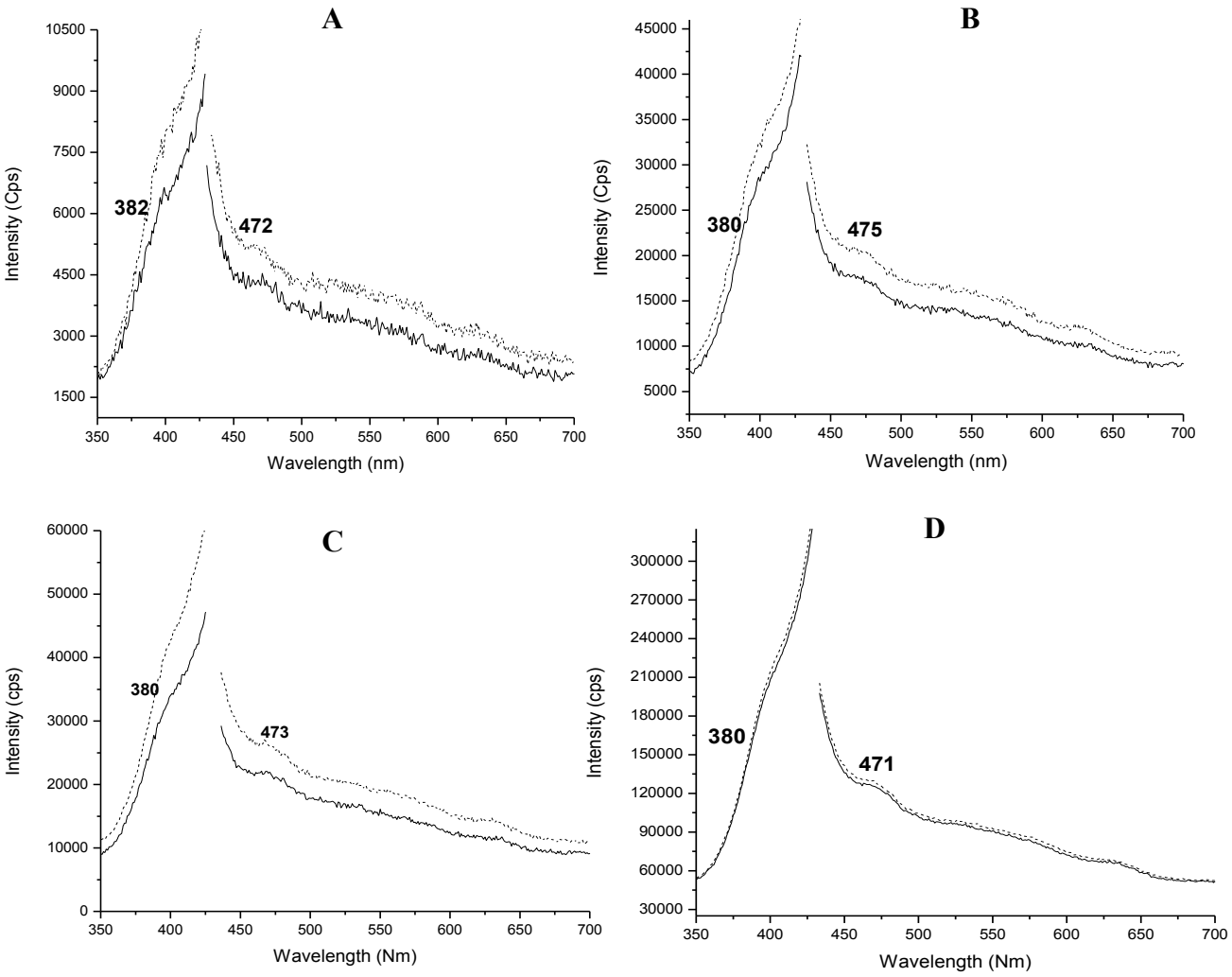

Figure B3. Comparison of excitation and emission spectra of an acrylic fiber dyed with Basic green 4 (–), and spectra collected from background (···), under a 10X Visible objective lens, and using a pinhole diameter of (A) 200 µm, (B) 400 µm, (C) 600 µm, and (D) 1000 µm. Spectra were collected using $\lambda_{exc/em}$ = 380/475 nm, an excitation and emission band-pass of 20 nm, and using the glass slide and cover-slip method.

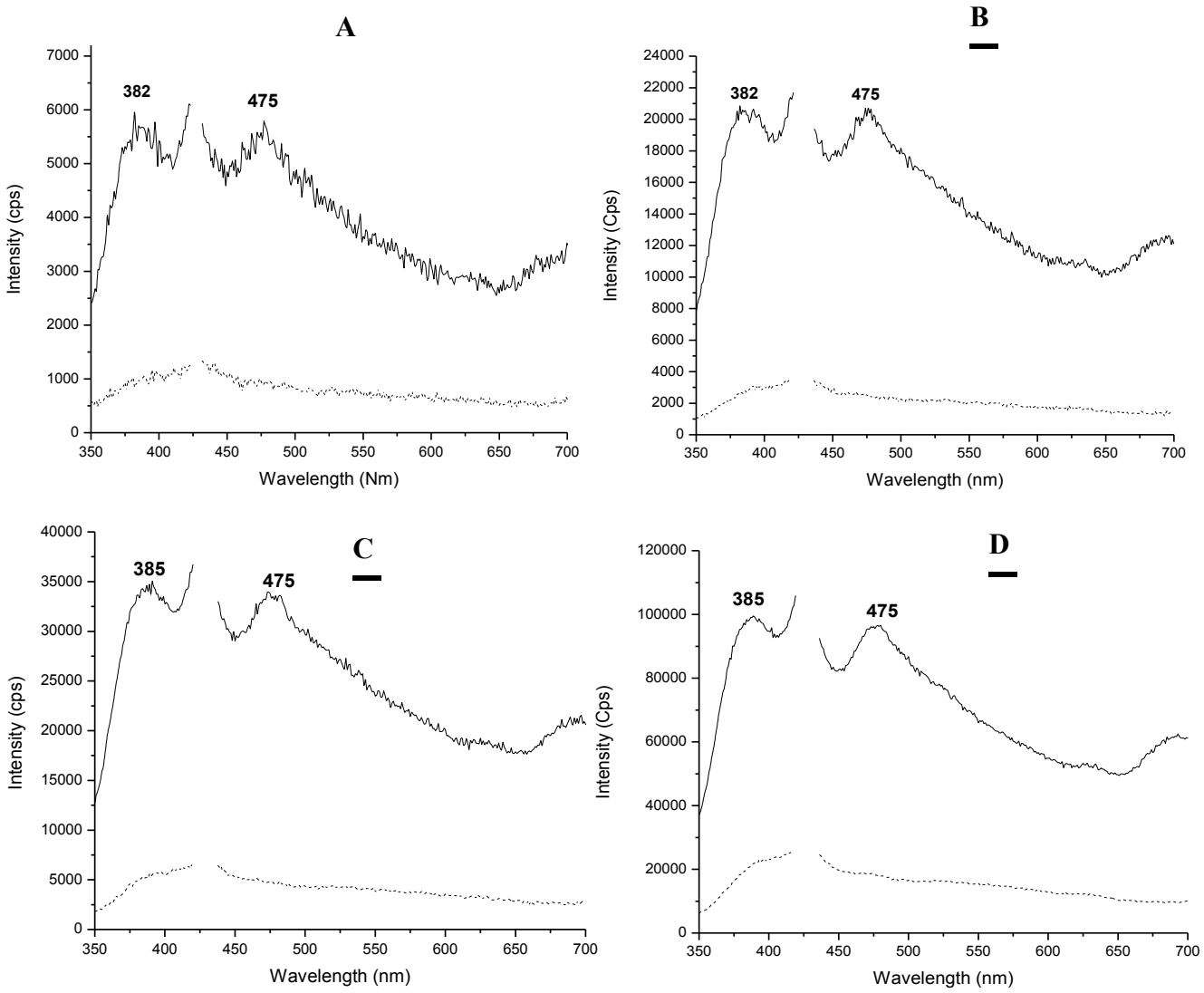

Figure B4. Comparison of excitation and emission spectra of an acrylic fiber dyed with Basic green 4 (–), and spectra collected from background (···), under a 40X visible objective lens, and using a pinhole diameter of (A) 200 µm, (B) 400 µm, (C) 600 µm, and (D) 1000 µm. Spectra were collected using $\lambda_{exc/em}$ = 380/475 nm, an excitation and emission band-pass of 20 nm, and using the tape-lift method.

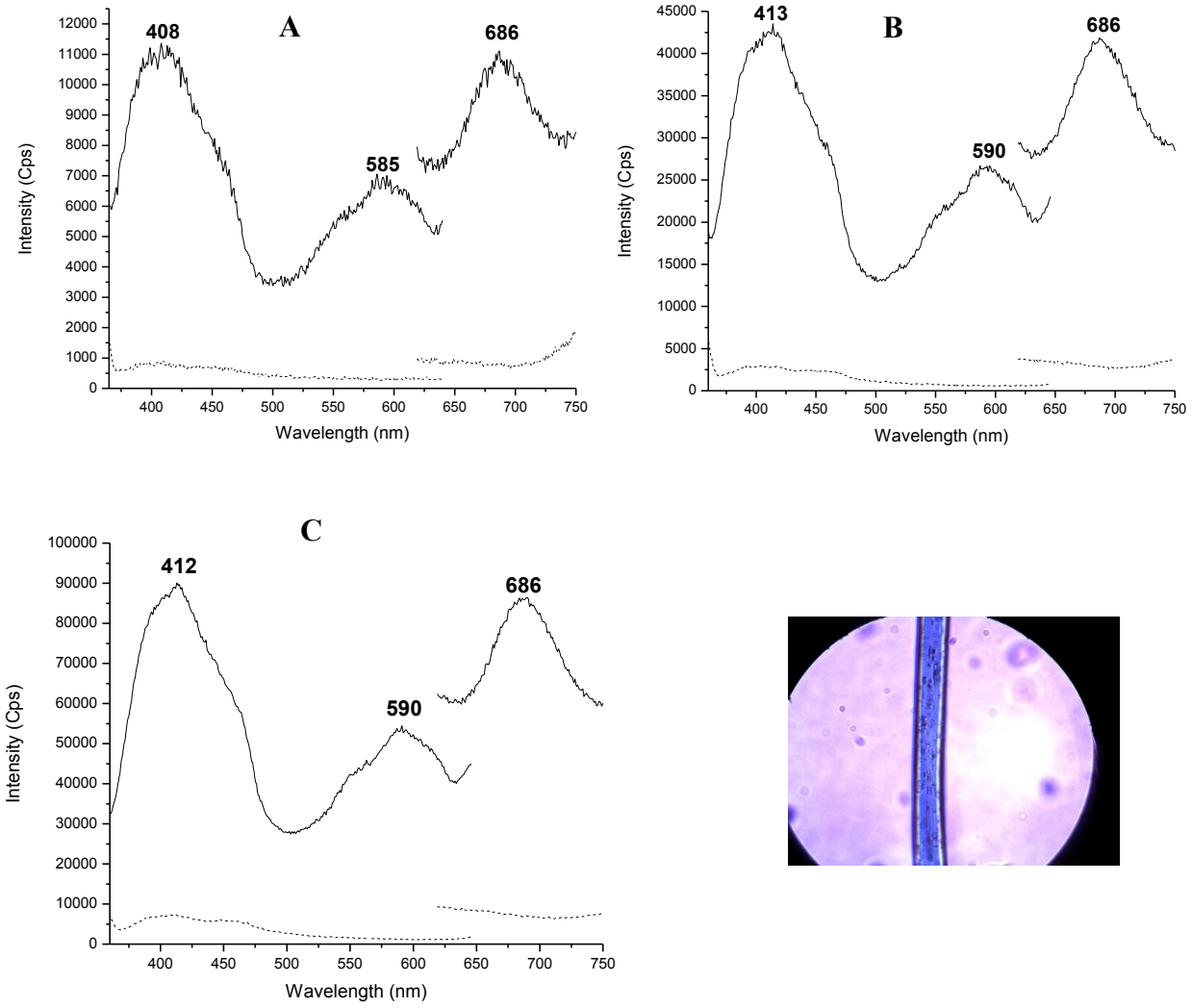

Figure B5. Comparison of excitation and emission spectra of nylon 361 fiber dyed with Acid green 27 (–), and spectra collected from the background (···), under a 40X visible objective lens, and using pinhole diameter of (A) 200 µm, (B) 400 µm, and (C) 600 µm. Spectra were collected using λexc/em = 410/686 nm, an excitation and emission band-pass of 20 nm, and using the tape-lift method.

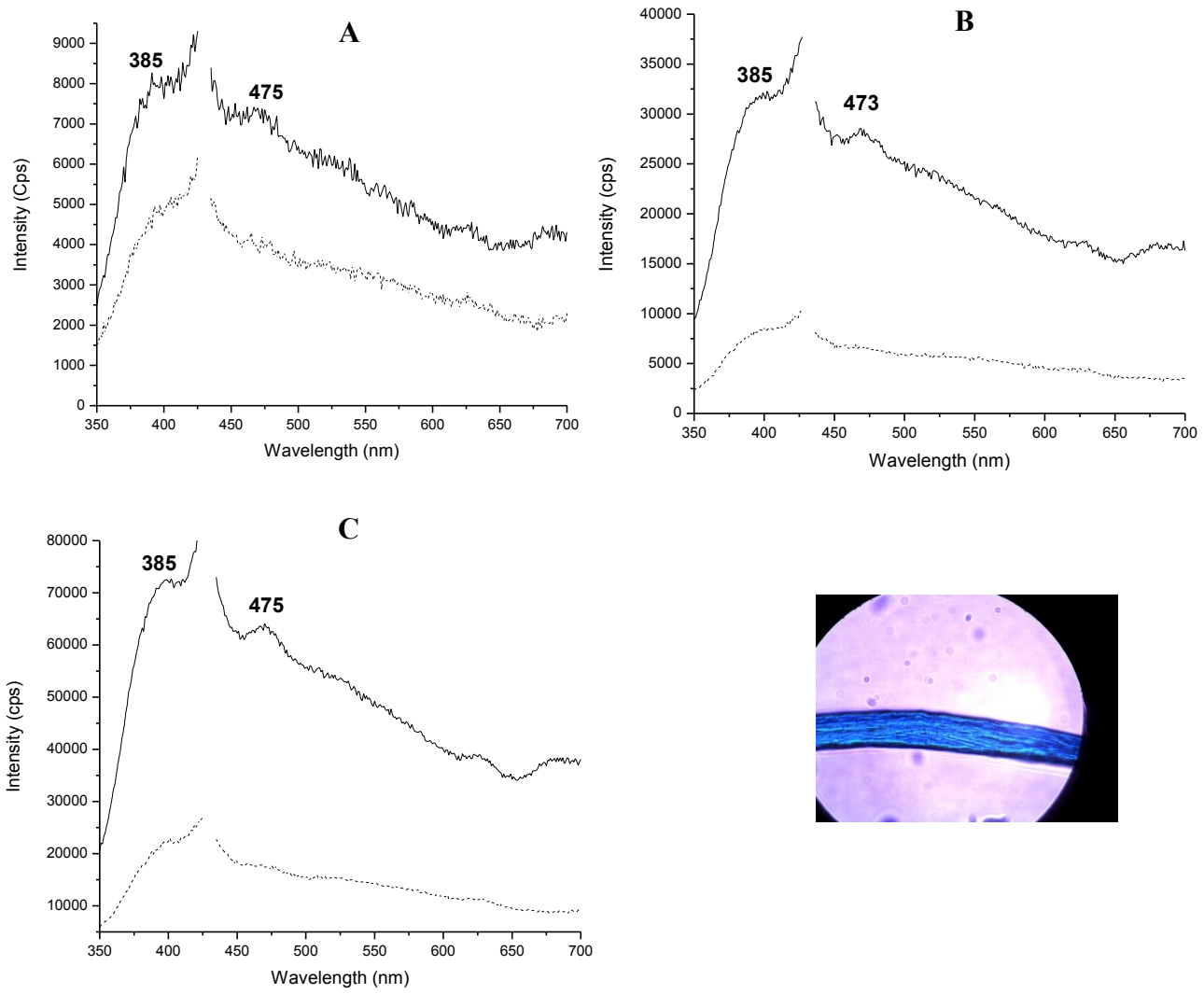

Figure B6. Comparison of excitation and emission spectra of an acrylic 864 fiber dyed with Basic green 4 (–), and spectra collected from the background (···), under a 40X visible objective lens, and using pinhole diameter of (A) 200 µm, (B) 400 µm, and (C) 600 µm. Spectra were collected using $\lambda_{exc/em}$ = 380/475 nm, an excitation and emission band-pass of 20 nm, and using the tape-lift method.

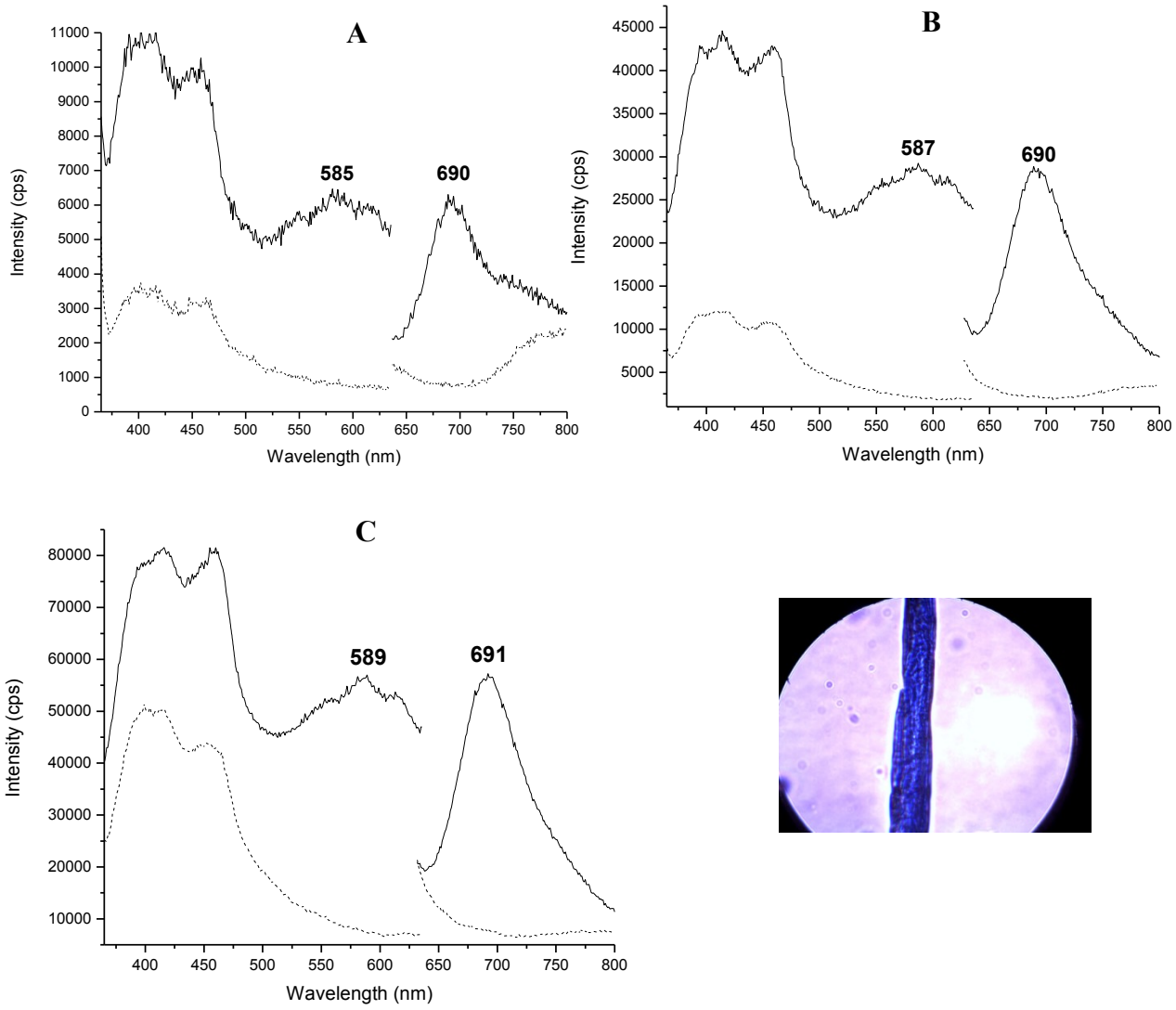

Figure B7. Comparison of excitation and emission spectra of cotton 400 fiber dyed with Direct blue 53 (–), and spectra collected from the background (···), under a 40X visible objective lens, and using pinhole diameter of (A) 200 µm, (B) 400 µm, and (C) 600 µm. Spectra were collected using a $\lambda_{exc/em}$ = 587/692 nm, an excitation and emission band-pass of 20 nm, and using the tape-lift method.

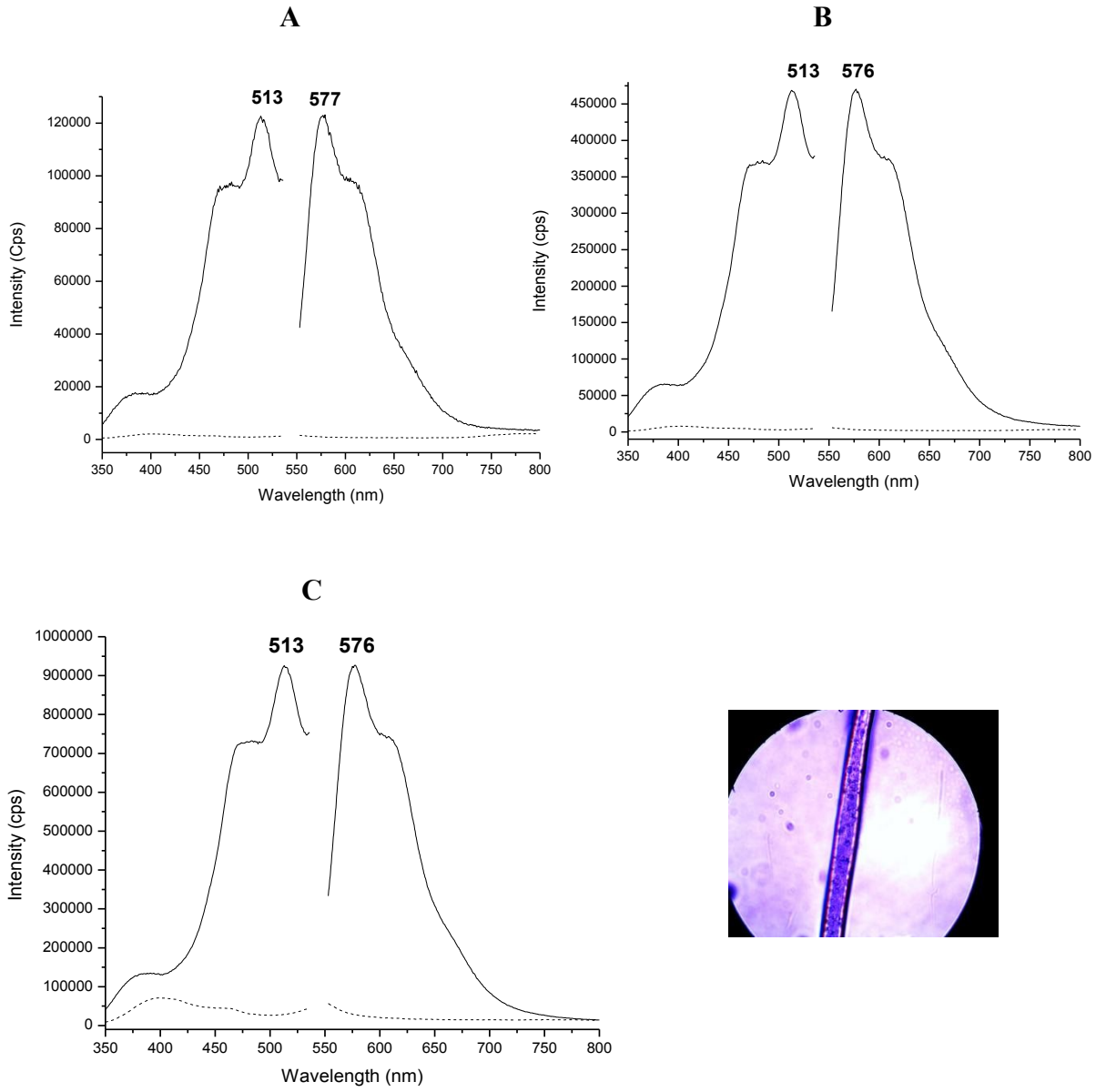

Figure B8. Comparison of excitation and emission spectra of polyester 777 fiber dyed with Disperse red 4 (–), and spectra collected from the background (···), under a 40X visible objective lens, and using pinhole diameter of (A) 200 µm, (B) 400 µm, and (C) 600 µm. Spectra were collected using λexc/em =513/576 nm, an excitation and emission band-pass of 20 nm, and using the tape-lift method.

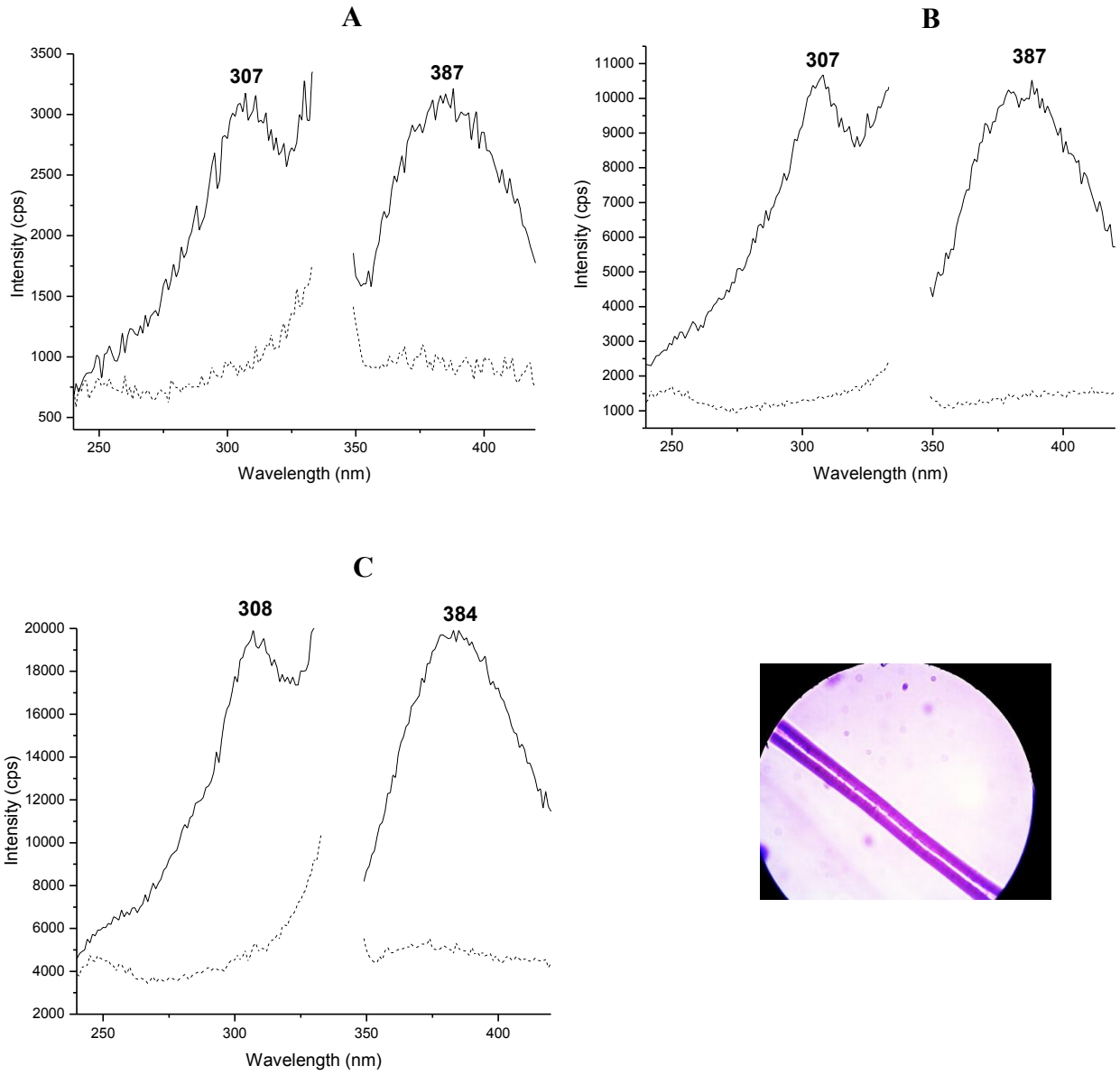

Figure B9. Comparison of excitation and emission spectra of polyester 777 fiber dyed with Disperse red 4 (–), and spectra collected from the background (···), under a 40X UV objective lens, and using pinhole diameter of (A) 200 µm, (B) 400 µm, and (C) 600 µm. Spectra were collected using a λexc/em = 309/385 nm, an excitation and emission band-pass of 25 nm, and using the tape-lift method.

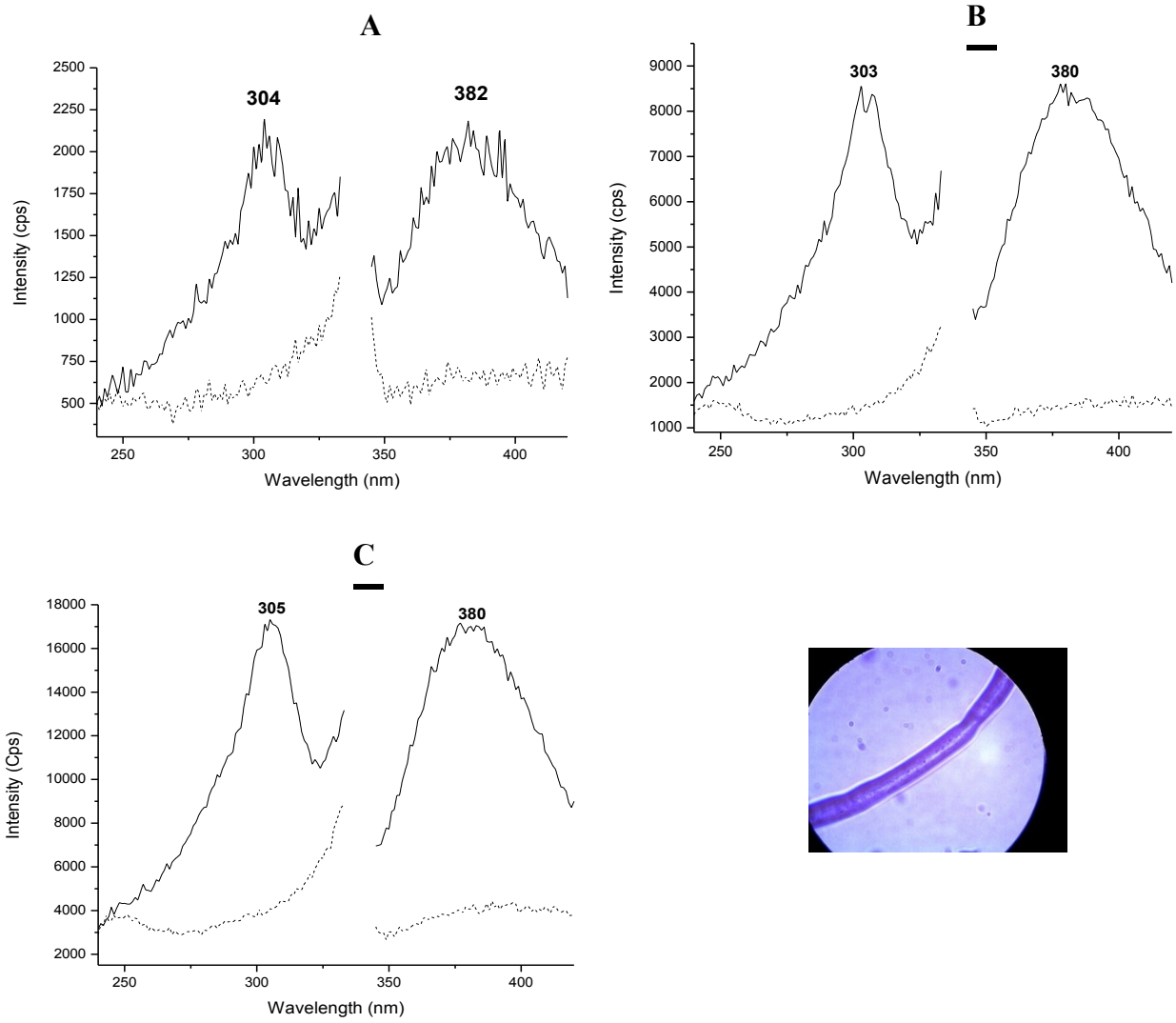

Figure B10. Comparison of excitation and emission spectra of polyester 777 fiber dyed with Basic red 9_(–), and spectra collected from the background (···), under a 40X UV objective lens, and using pinhole diameter of (A) 200 µm, (B) 400 µm, and (C) 600 µm. Spectra were collected using λexc/em = 305/380 nm, an excitation and emission band-pass of 25 nm, and using the tape-lift method.

APPENDIX C: SUPPLEMENTAL INFORMATION FOR CHAPTER 4

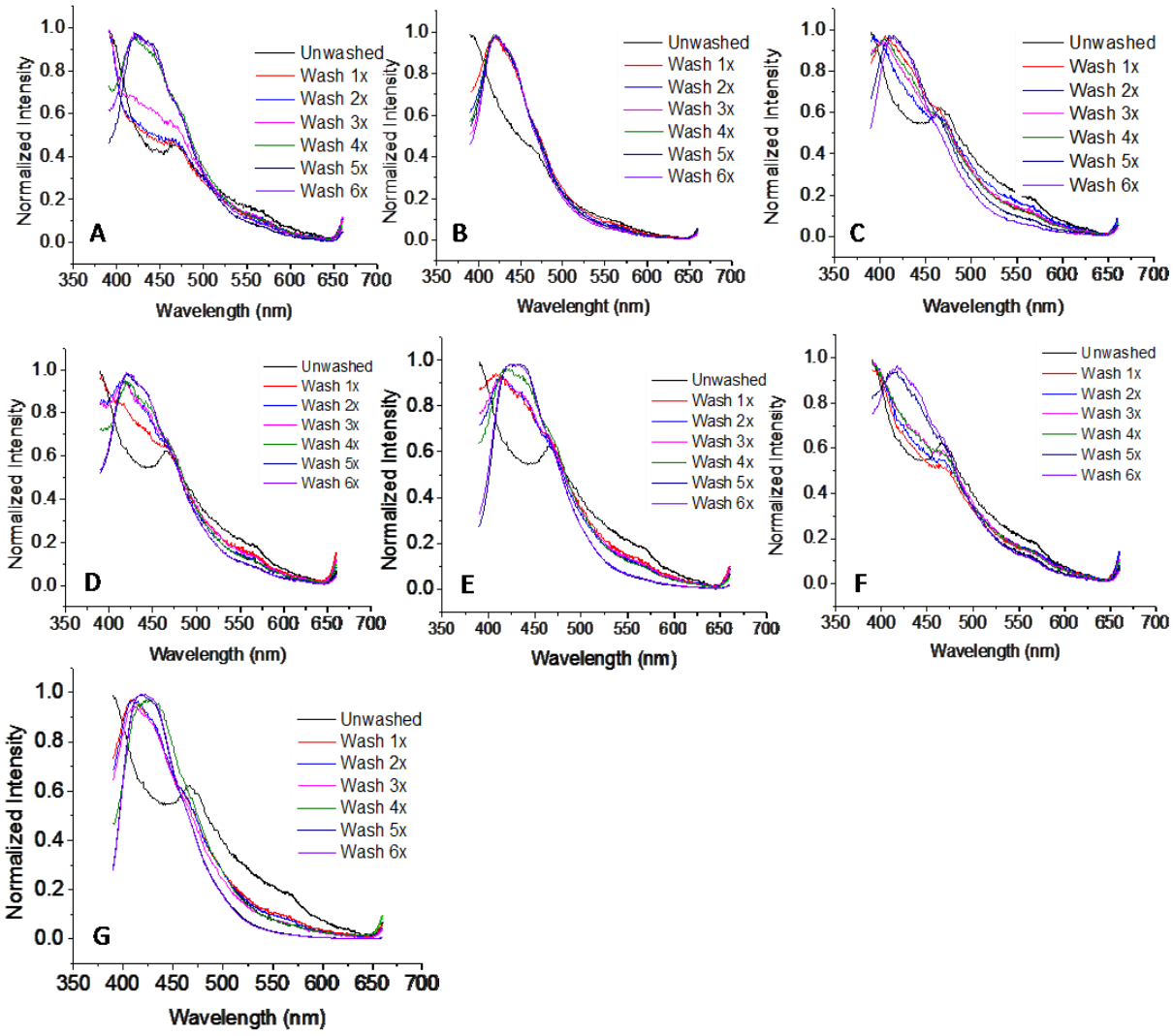

Figure C1. Emission spectra (350 nm excitation) of Nylon 361 fibers dyed with AY 17 and washed with A) All, B) Cheer, C) Oxiclean, D) Purex, E) Tide (L), F) Tide (P) and G)Wisk.

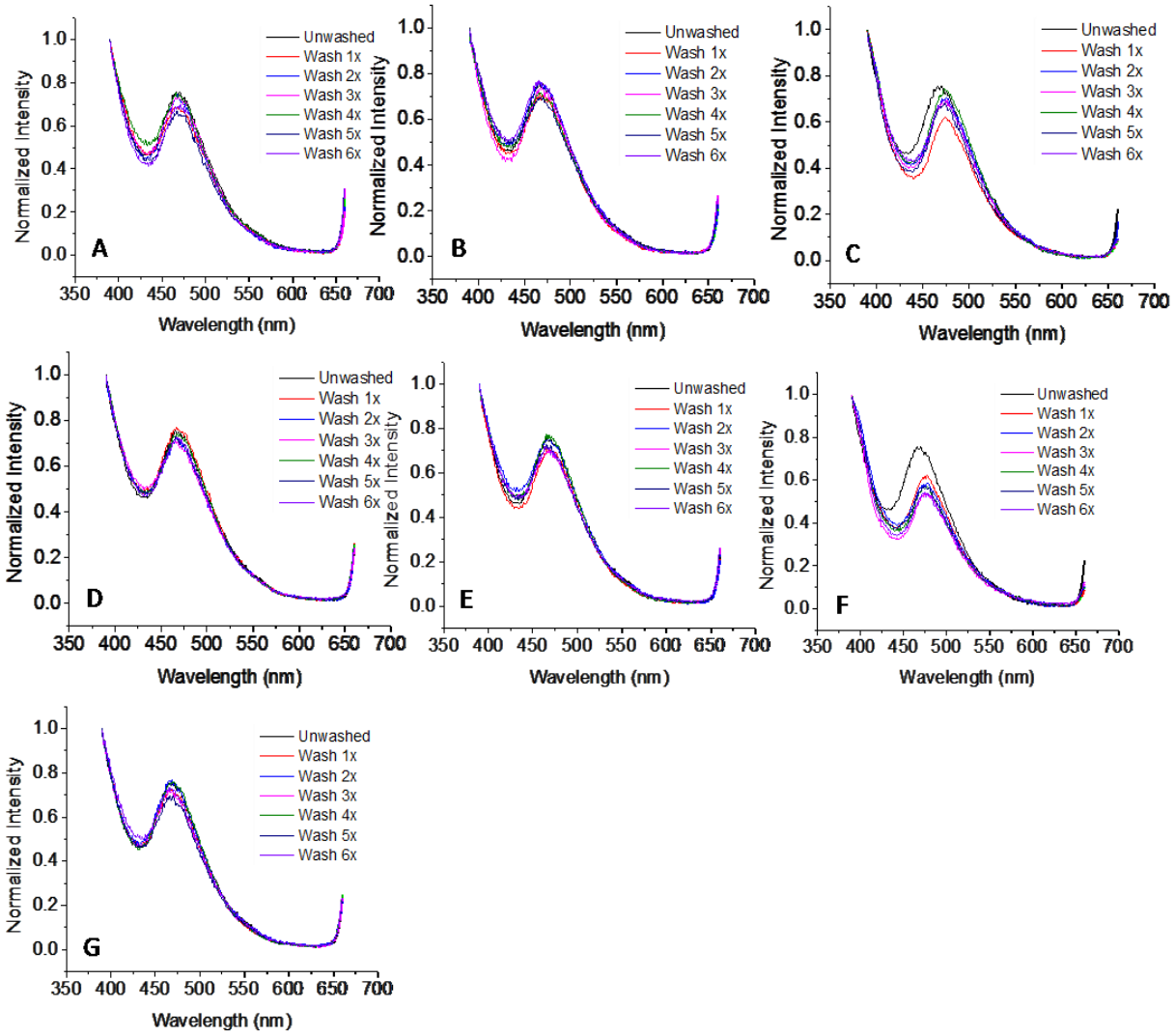

Figure C2. Emission spectra (350 nm excitation) of Acrylic 864 fibers dyed with BG4 and washed with A) All, B) Cheer, C) Oxiclean, D) Purex, E) Tide (L), F) Tide (P) and G)Wisk.

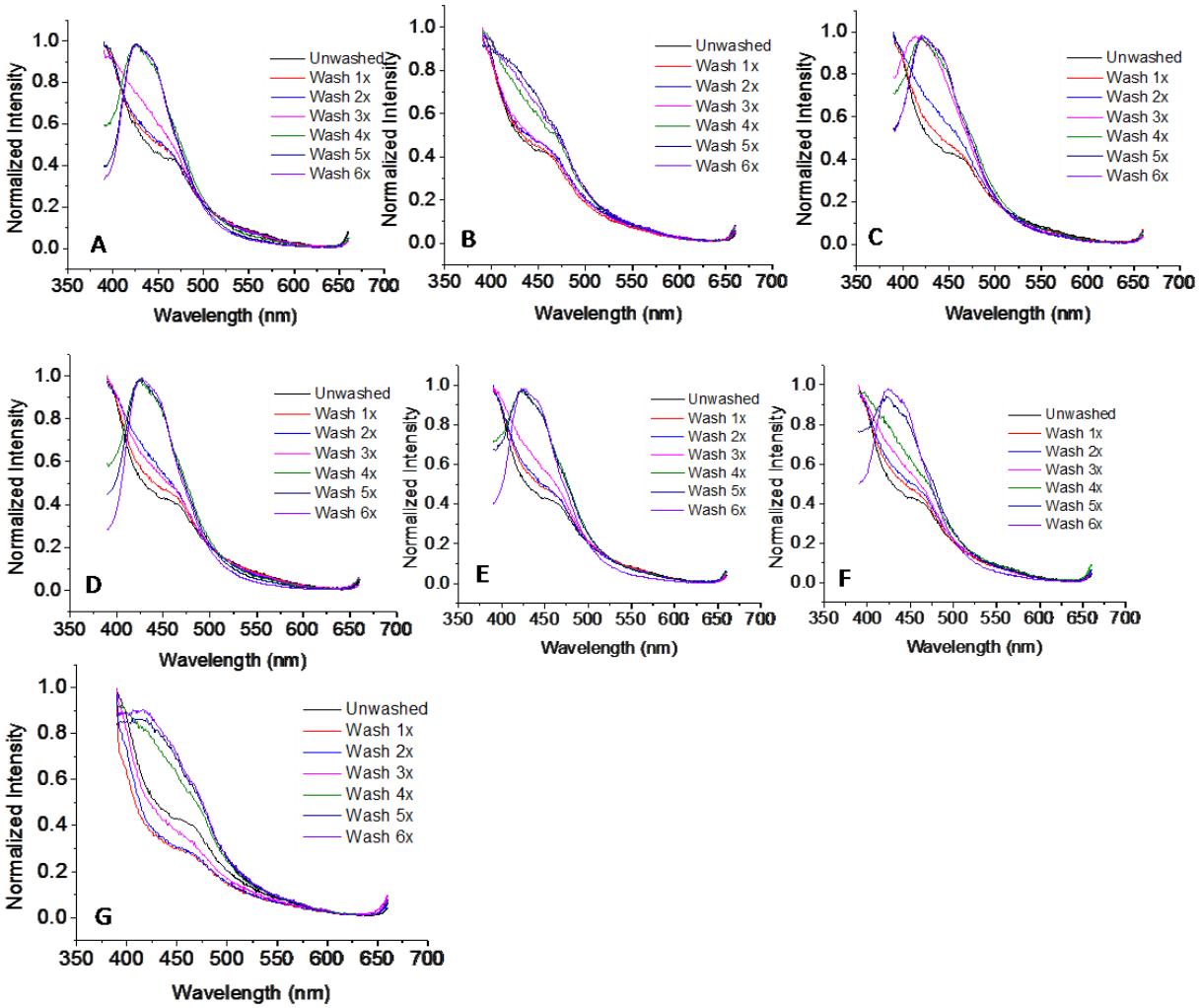

Figure C3. Emission spectra (350 nm excitation) of Cotton 400 fibers dyed with DB1 and washed with A) All, B) Cheer, C) Oxiclean, D) Purex, E) Tide (L), F) Tide (P) and G)Wisk.

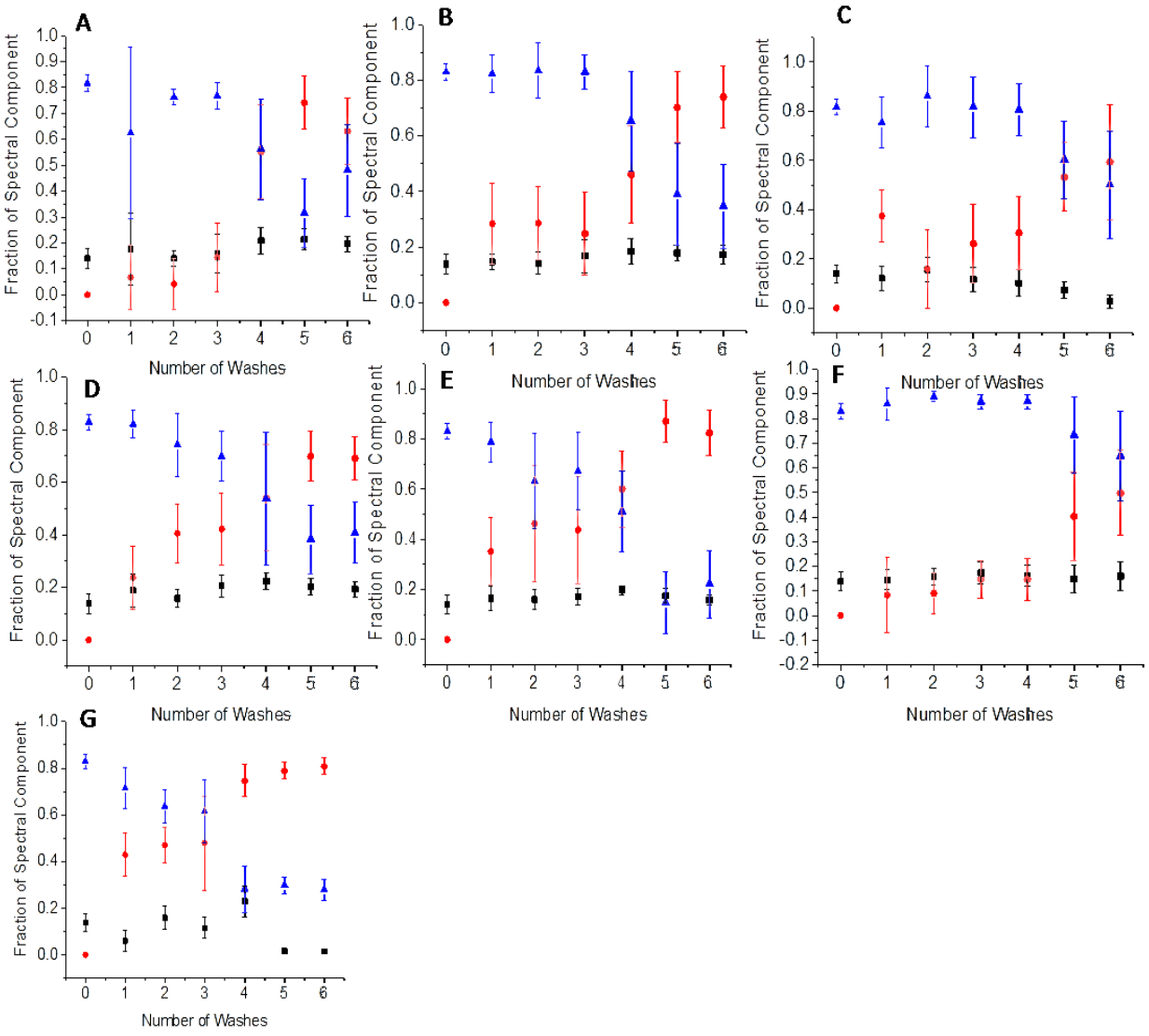

Figure C4. Emission spectra for Nylon 361 fibers dyed with AY 17 were fit to determine the fractional contribution of the dye on the fiber (black squares), undyed fiber (blue triangles) and detergent (red circles). The plots are for fibers washed with A) All, B) Cheer, C) Oxiclean, D) Purex, E) Tide (L), F) Tide (P) and G) Wisk.

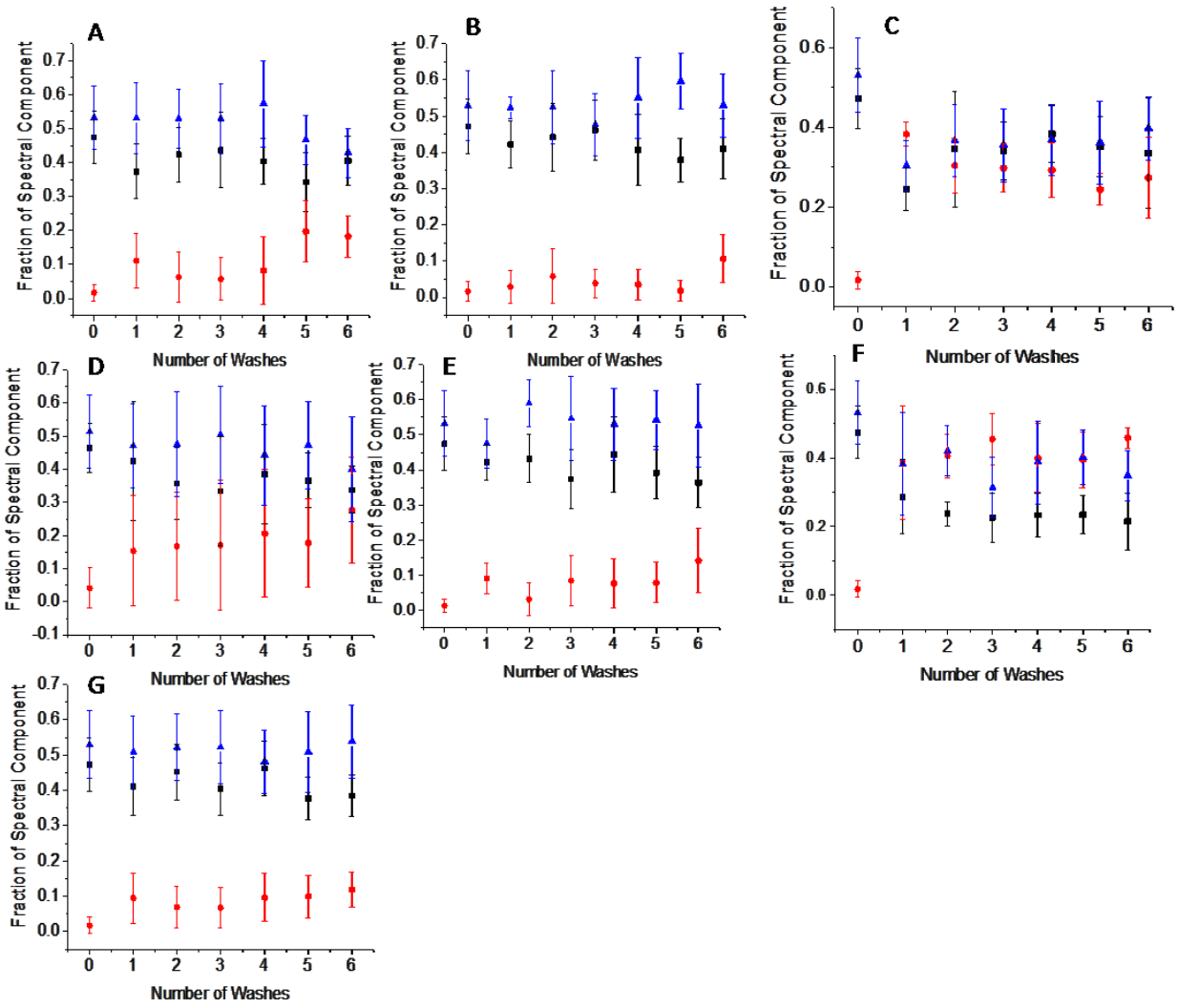

Figure C5. Emission spectra for Acrylic 864 fibers dyed with BG 4 were fit to determine the fractional contribution of the dye on the fiber (black squares), undyed fiber (blue triangles) and detergent (red circles). The plots are for fibers washed with A) All, B) Cheer, C) Oxiclean, D) Purex, E) Tide (L), F) Tide (P) and G)Wisk.

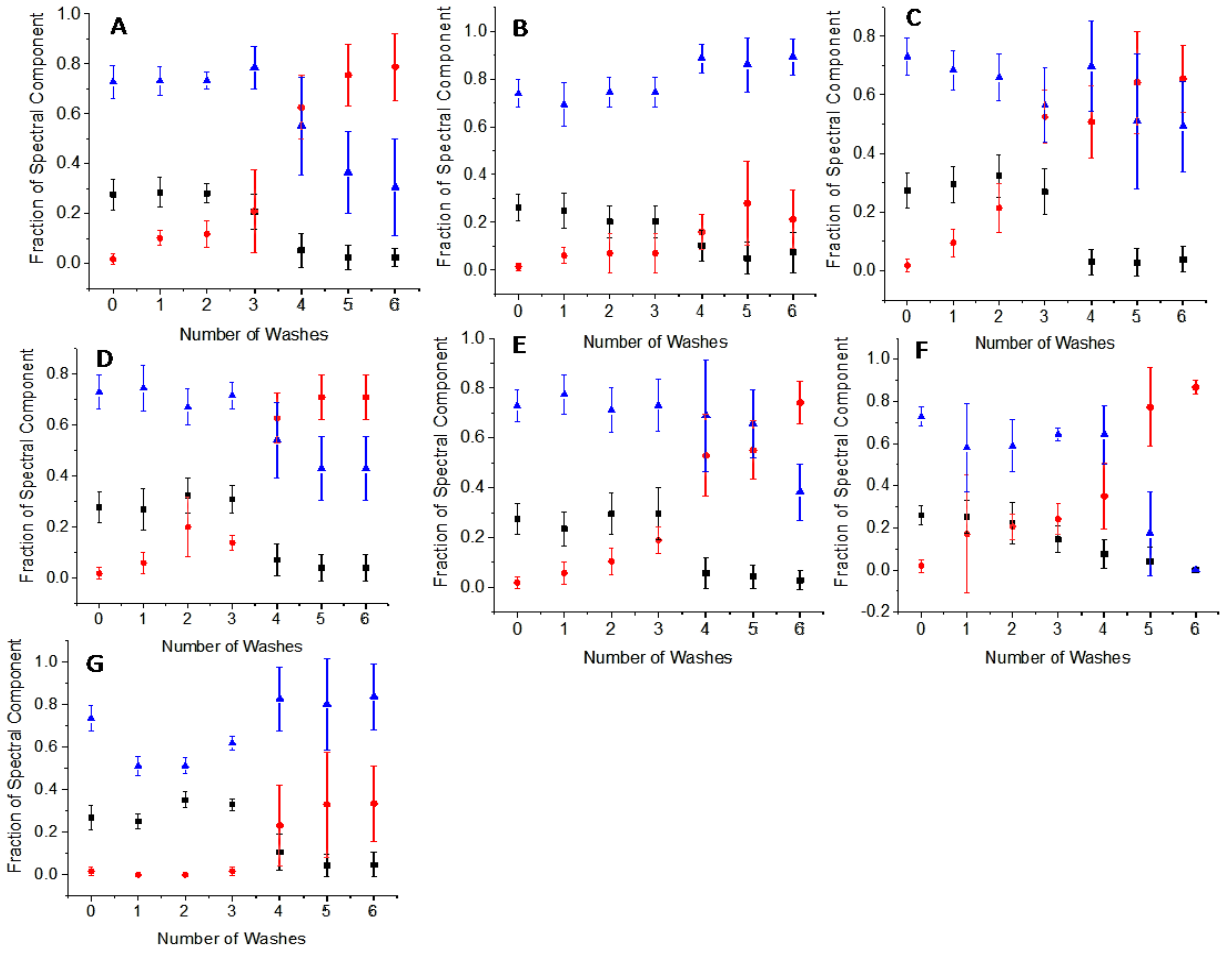

Figure C6. Emission spectra for Cotton 400 fibers dyed with DB 1 were fit to determine the fractional contribution of the dye on the fiber (black squares), undyed fiber (blue triangles) and detergent (red circles). The plots are for fibers washed with A) All, B) Cheer, C) Oxiclean, D) Purex, E) Tide (L), F) Tide (P) and G)Wisk.

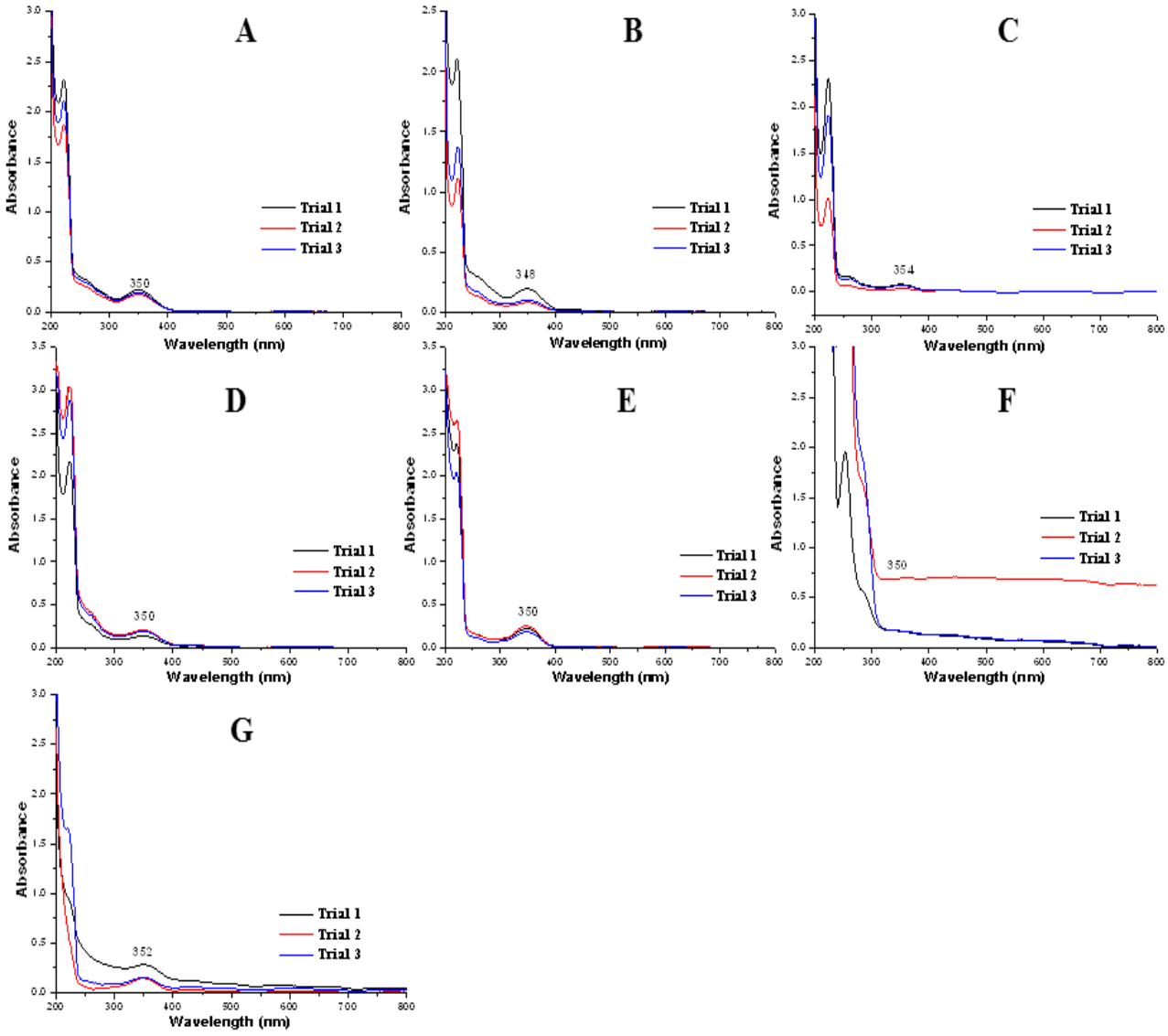

Figure C7. Absorbance recordings from detergent solutions (three trials recorded per detergent) belonging to All (A), Cheer (B), Purex (C), Tide liquid (D), Wisk (E), Tide powder (F) and Oxiclean (G).

APPENDIX D: SUPPLEMENTAL INFORMATION FOR CHAPTER 5

This section contains cluster plots for all combinations of detergent pairs on acrylic and nylon fibers. Absorbance spectra of the whitening agents were acquired by preparing samples of the detergents based on the manufacturers recommendations for use with a 40L washing size. The concentrations were 1.31 mL/L (All), 1.15 mL/L (Cheer), 0.94 g/L (Oxiclean), 1.11 mL/L (Purex), 1.53 mL/L (Tide liquid), 1.29 g/L (Tide powder) and 1.15 mL/L (Wisk). The detergents were placed in a rotary shaker until dissolved and the solutions placed in a 1-cm quartz cuvette for measuring absorbance. Absorbance data were collected using a Cary 50 spectrophotometer (Agilent Technologies, Santa Clara CA). The instrument is equipped with a 75-watt pulsed Xenon lamp with spectral radiance 190-1100 nm. A monochrometer and 2-nm bandpass filter were used for wavelength selection and a beam-splitter with two silicon photodiode detectors used to quantify the absorbance. The spectra are shown below in figure D1.

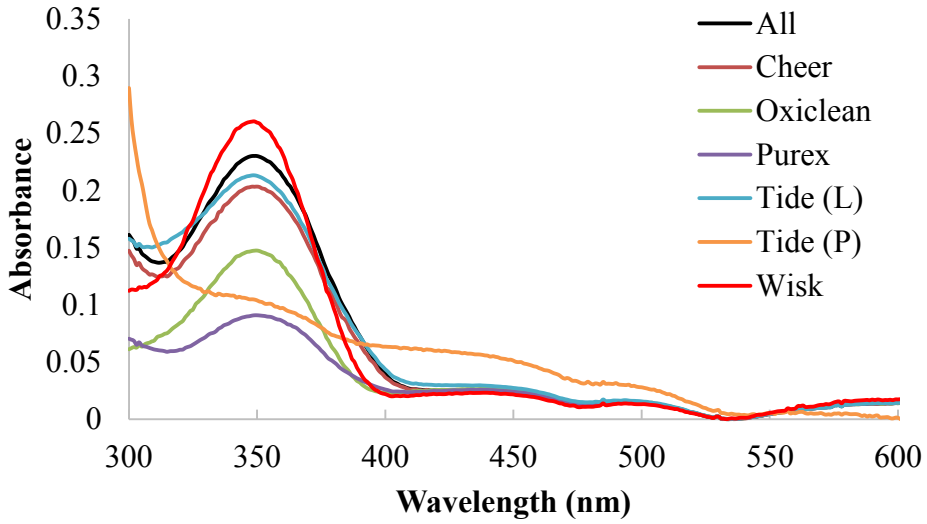

Figure D1. Absorbance spectra for the detergents in solution. All the detergents absorb light at 350 nm, the wavelength selected for fluorescence excitation.

Fluorescence spectra of the undyed fibers were also collected with the procedure utilized in the previous section. The spectra from 10 fibers of each type (acrylic and nylon) were averaged and plotted along with the background from a clean quartz slide. The spectrum from the undyed fibers alone is large compared to that of the background as seen in the figure below.

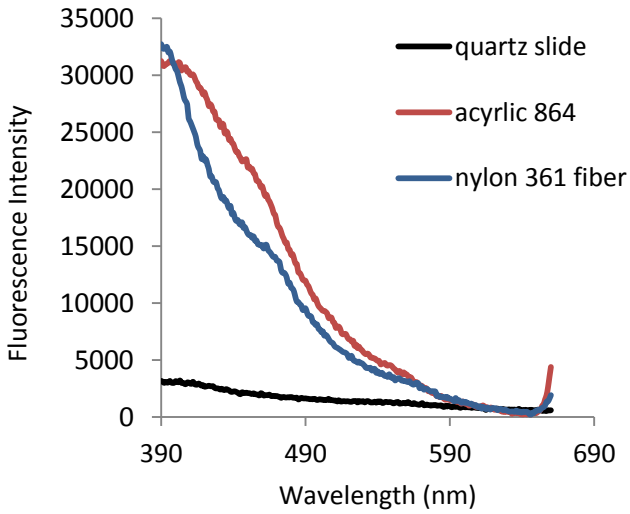

Figure D2. Fluorescence emission spectra of undyed fibers with 350 nm excitation.

Fluorescence spectra were acquired from single fibers drawn from bulk samples of textiles composed of acrylic 864 (dyed with basic green 4) and nylon 361 (dyed with acid yellow 17). These textile samples were laundered five or six times with detergents All, Cheer, Oxiclean, Purex, Tide (liquid), Tide (powder), and Wisk. The fluorescence emission spectra from the detergents on the fibers compared using principal component cluster analysis. Training sets were constructed from spectra of fibers that had been laundered five times, with validation spectra from other fibers laundered either five or six times.

For the analysis, spectra for two different detergent types were compared and the resulting cluster plots are shown for each comparison pair. Boundaries around the training clusters represent the ellipse fitted to the training set shape, with the major and minor axes of the ellipse representing three standard deviations of the scatter of the ellipse. Figures C3 to C7 show comparisons of detergents on nylon 361 fibers dyed with acid yellow 17. Figures C8 to C12 show comparisons of detergents on acrylic 864 fibers dyed with basic green 4.

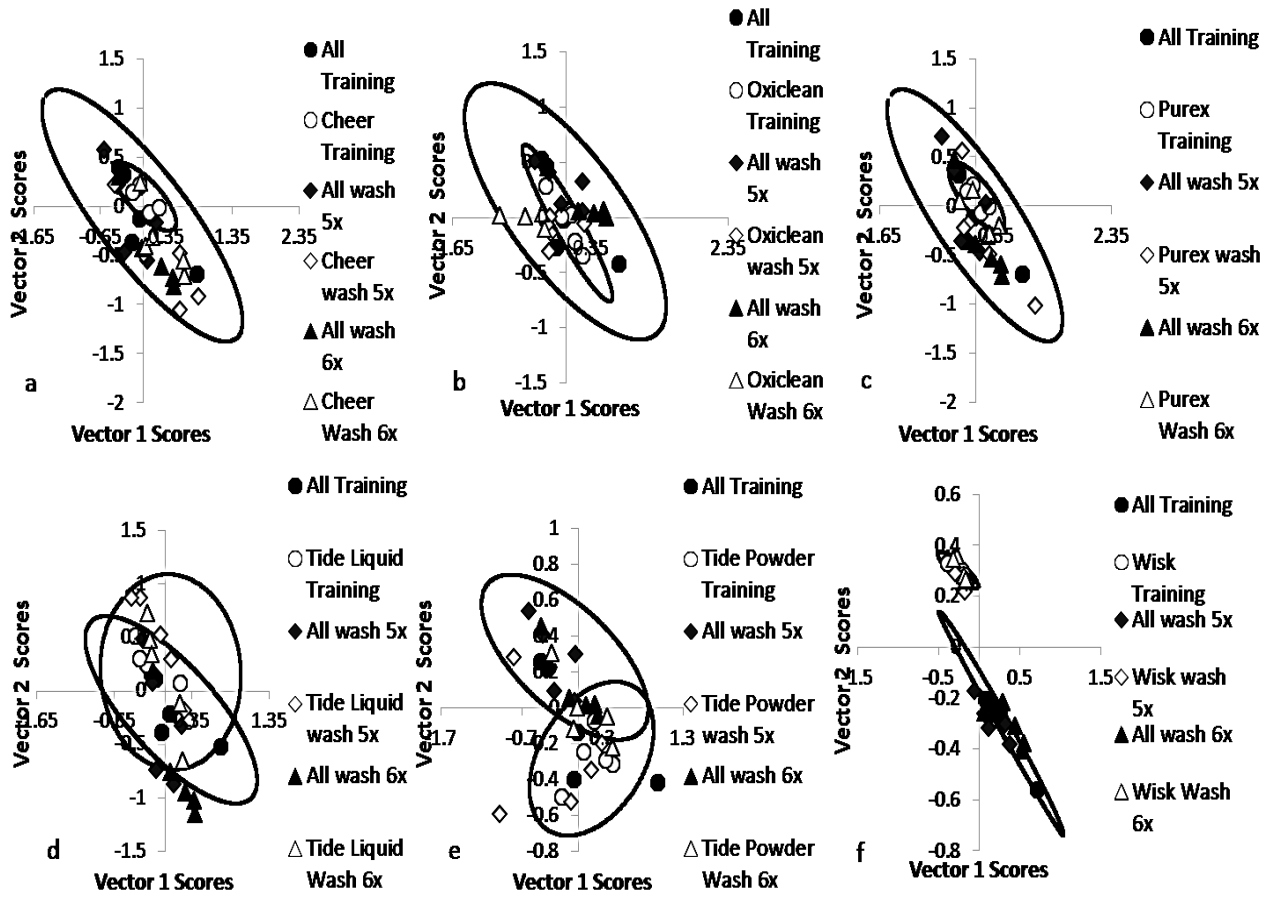

Figure D3. Plots for nylon 361 fibers dyed with AY17, comparing fibers washed with detergent All with fibers washed with a) Cheer, b) Oxiclean, c) Purex, d) Tide liquid, e) Tide powder, and f) Wisk.

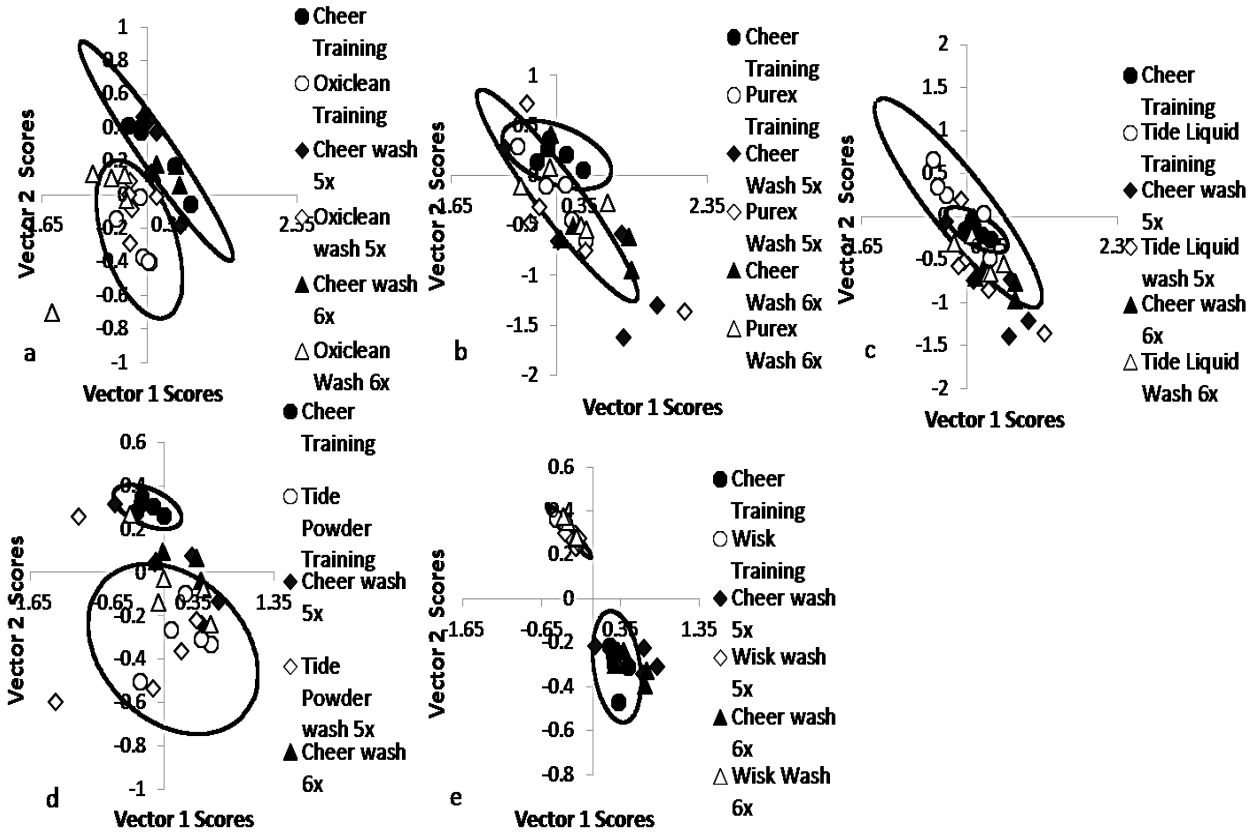

Figure D4. Plots for nylon 361 fibers dyed with AY17, comparing fibers washed with detergent Cheer with fibers washed with a) Oxiclean, b) Purex, c) Tide liquid, d) Tide powder, and e) Wisk. Note that the comparison for All and Cheer is found in Figure D3.

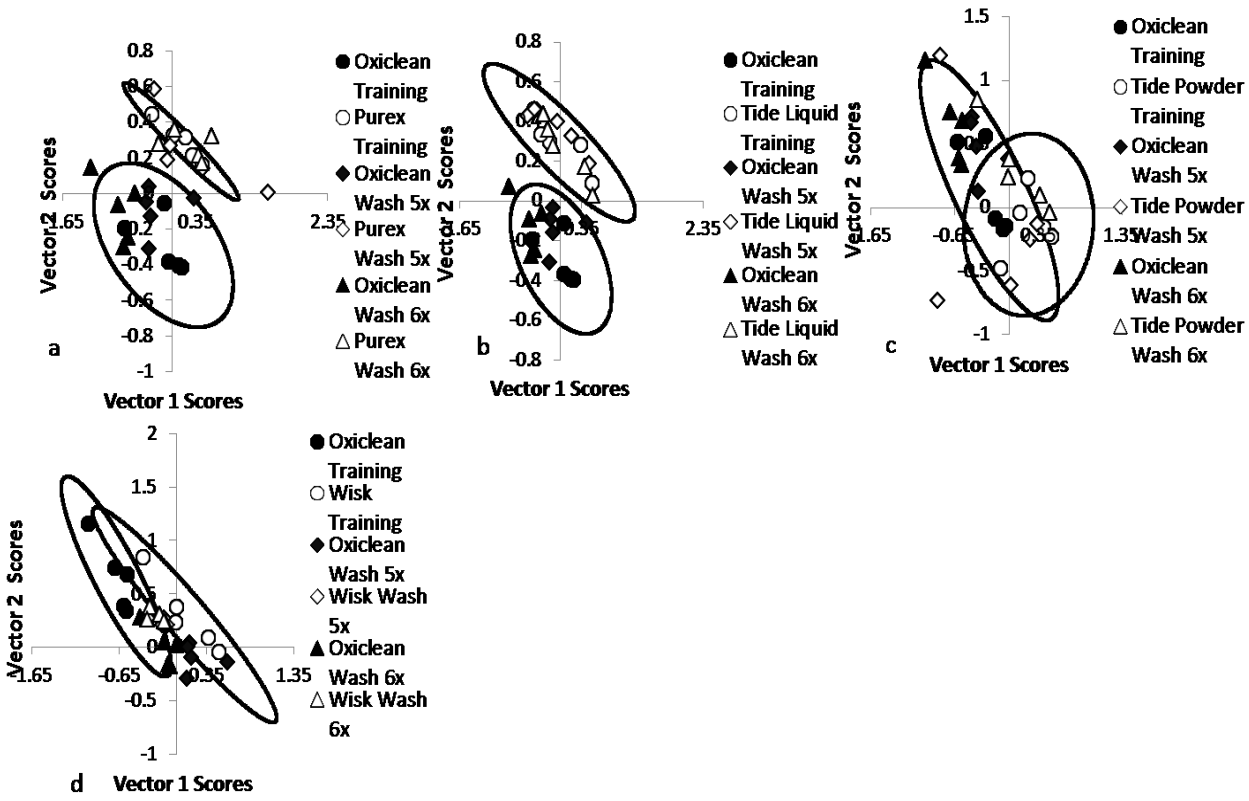

Figure D5. Plots for nylon 361 fibers dyed with AY17, comparing fibers washed with detergent Oxiclean with fibers washed with a) Purex, b) Tide liquid, c) Tide powder, and d) Wisk. Note that the comparisons of Oxiclean with All and Cheer are found in Figure D3 and D4, respectively.

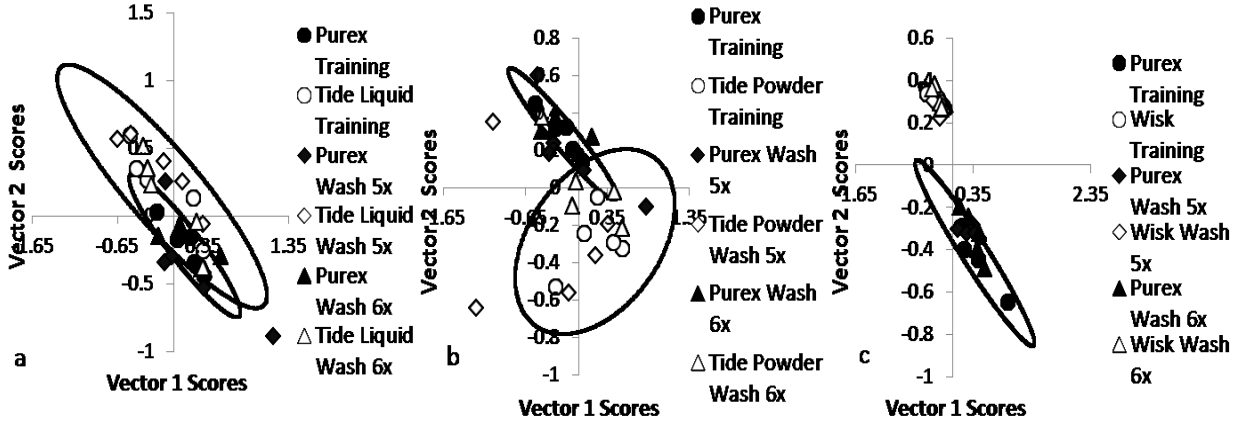

Figure D6. Plots for nylon 361 fibers dyed with AY17, comparing fibers washed with detergent Purex with fibers washed with a) Tide liquid, b) Tide powder, and c) Wisk. Note that the comparisons of Purex with All, Cheer, and Oxiclean are found in Figure D3, D4, and D5 respectively.

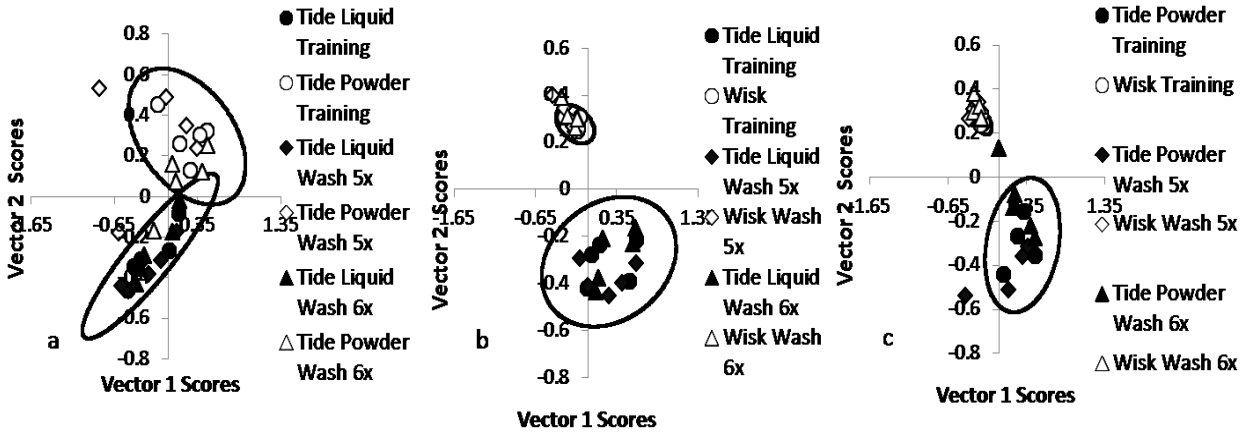

Figure D7. Plots for nylon 361 fibers dyed with AY17, comparing fibers washed with a) detergent Tide (liquid) and Tide (powder), b) fibers washed with Tide liquid and Wisk, and c) fibers washed with Tide (powder) and Wisk.

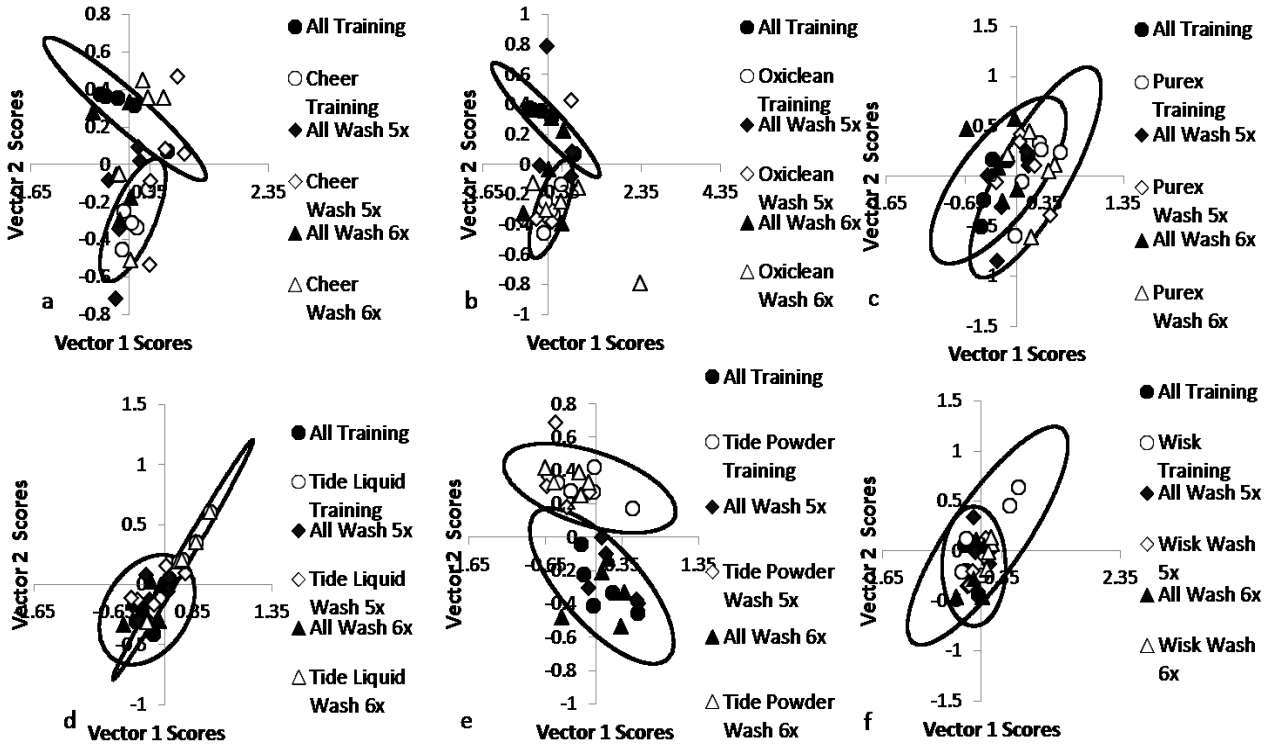

Figure D8. Plots for acrylic 864 fibers dyed with BG4, comparing fibers washed with detergent All with fibers washed with a) Cheer, b) Oxiclean, c) Purex, d) Tide liquid, e) Tide powder, and f) Wisk.

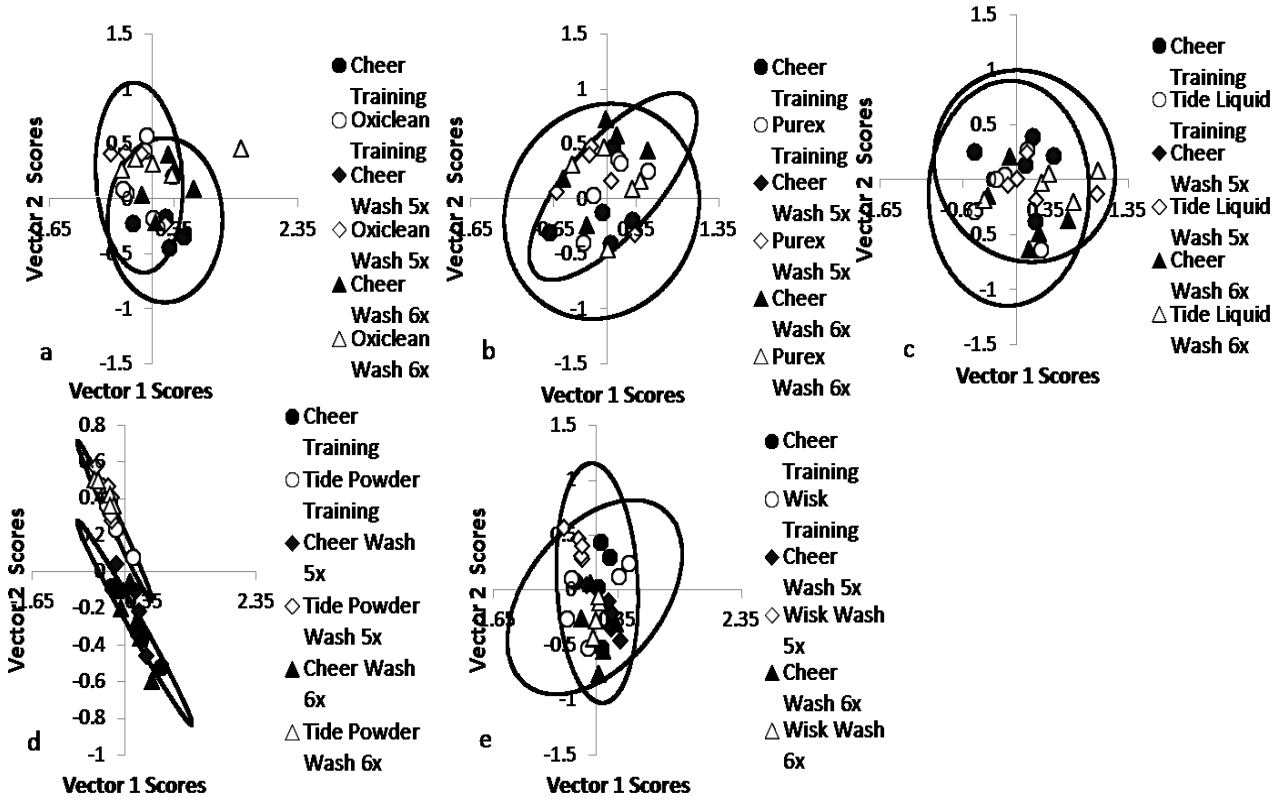

Figure D9. Plots for acrylic 864 fibers dyed with BG4, comparing fibers washed with detergent Cheer with fibers washed with a) Oxiclean, b) Purex, c) Tide liquid, d) Tide powder, and e) Wisk. Note that the comparison for All and Cheer is found in Figure D8.

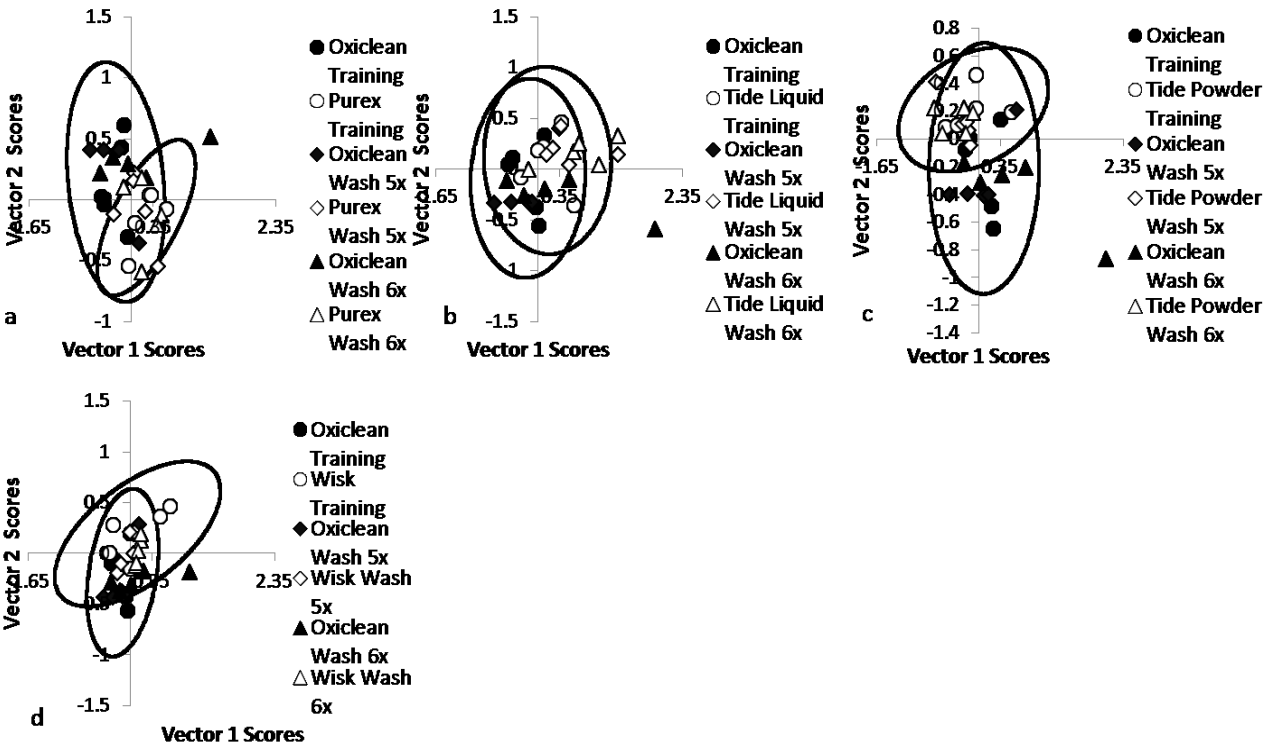

Figure D10. Plots for acrylic 864 fibers dyed with BG4, comparing fibers washed with detergent Oxiclean with fibers washed with a) Purex, b) Tide liquid, c) Tide powder, and d) Wisk. Note that the comparisons of Oxiclean with All and Cheer are found in Figure D8 and D9, respectively.

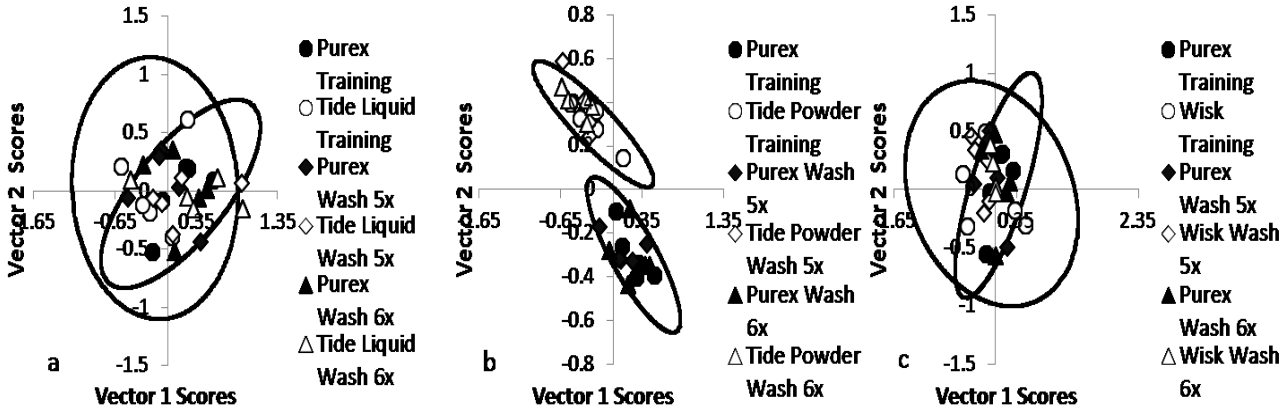

Figure D11. Plots for acrylic 864 fibers dyed with BG4, comparing fibers washed with detergent Purex with fibers washed with a) Tide liquid, b) Tide powder, and c) Wisk. Note that the comparisons of Purex with All, Cheer, and Oxiclean are found in Figure D8, D9, and D10 respectively.

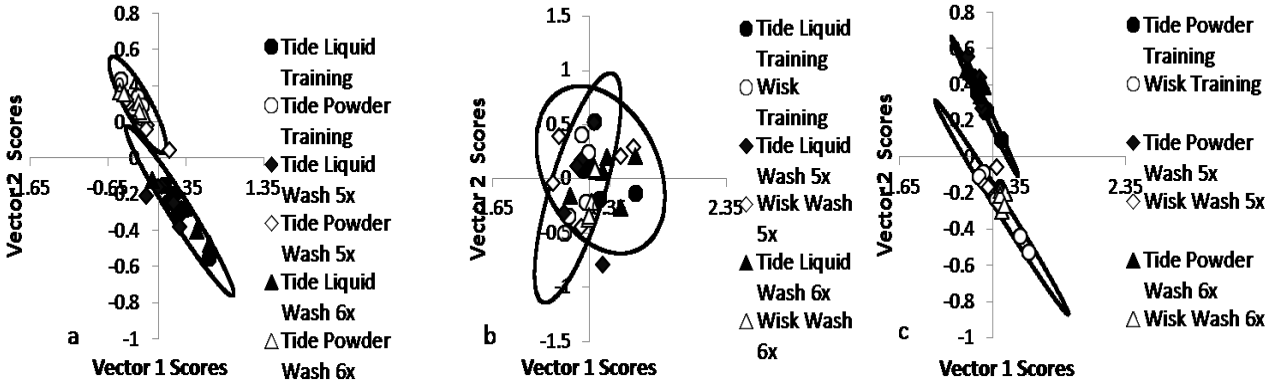

Figure D12. Plots for acrylic fibers dyed with BG4, comparing fibers washed with a) detergent Tide (liquid) and Tide (powder), b) fibers washed with Tide liquid and Wisk, and c) fibers washed with Tide (powder) and Wisk.

APPENDIX E: REPRODUCIBILITY WITHIN EEMs FROM TEN FIBERS OF A SINGLE CLOTH PIECE

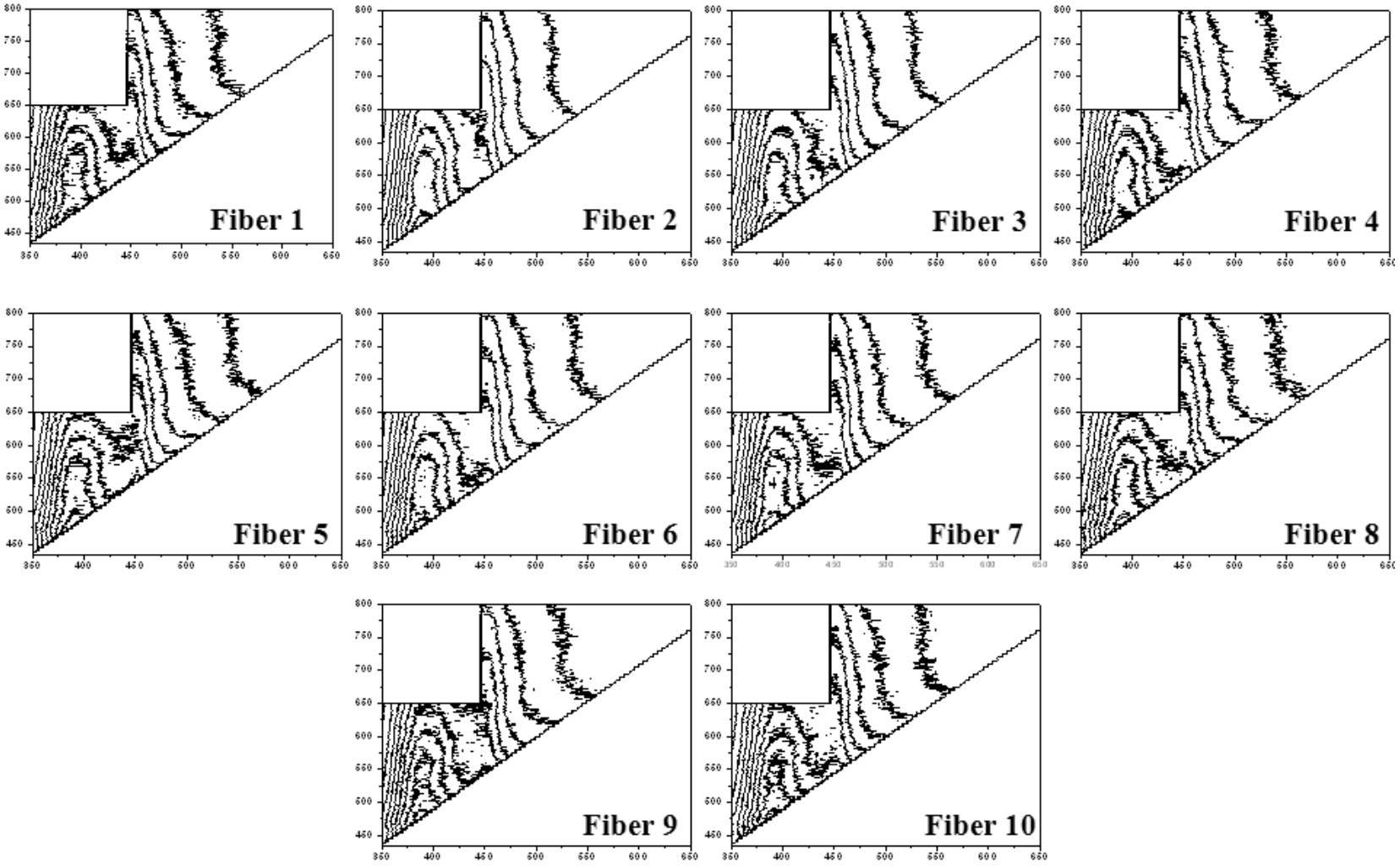

Figure D1. Reproducibility of EEMs recorded from ten fibers on a nylon 361 cloth piece dyed with Acid yellow 17 dye

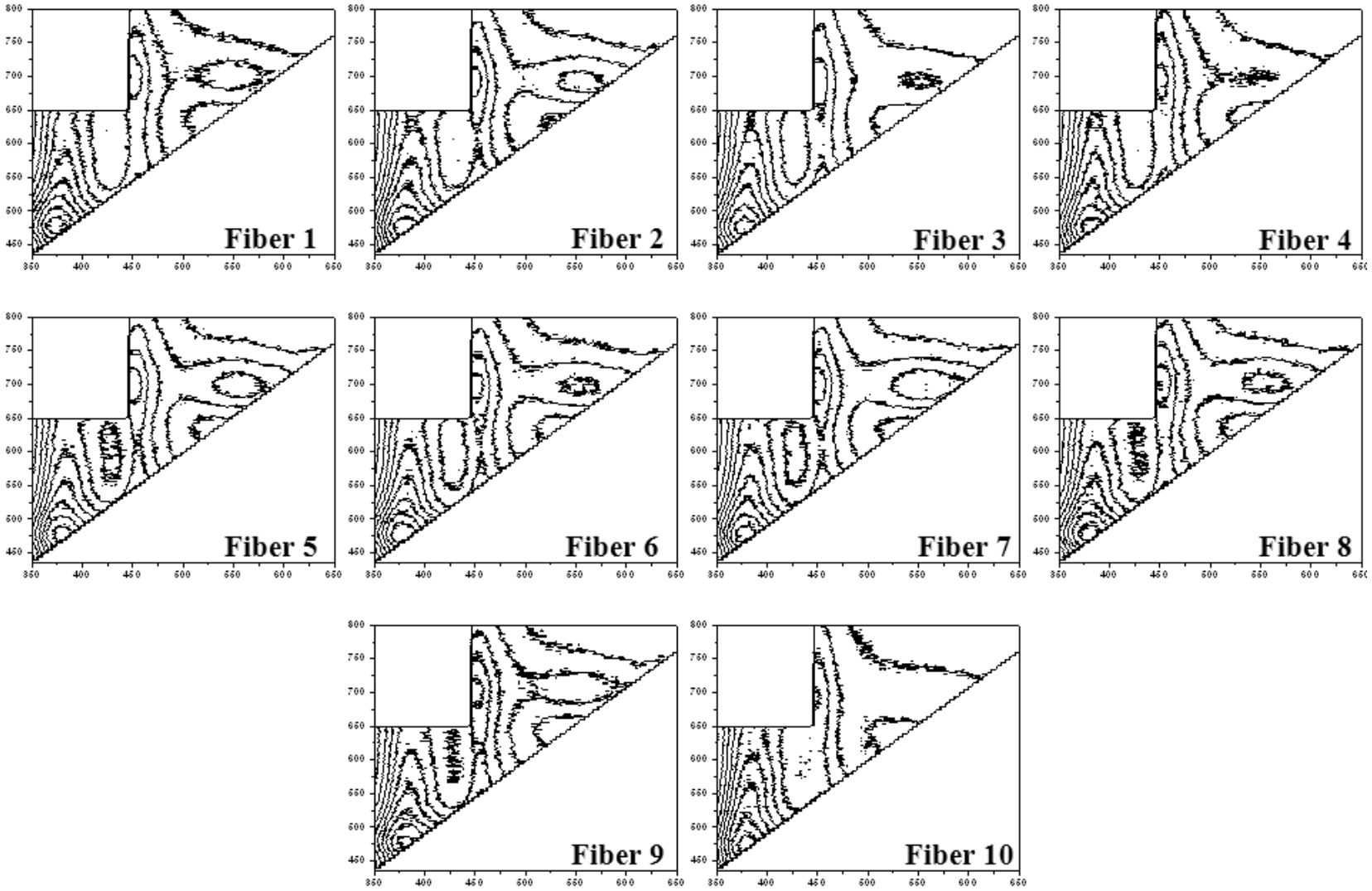

Figure D2. Reproducibility of EEMs recorded from ten fibers on an acrylic 864 cloth piece dyed with Basic green 4 dye

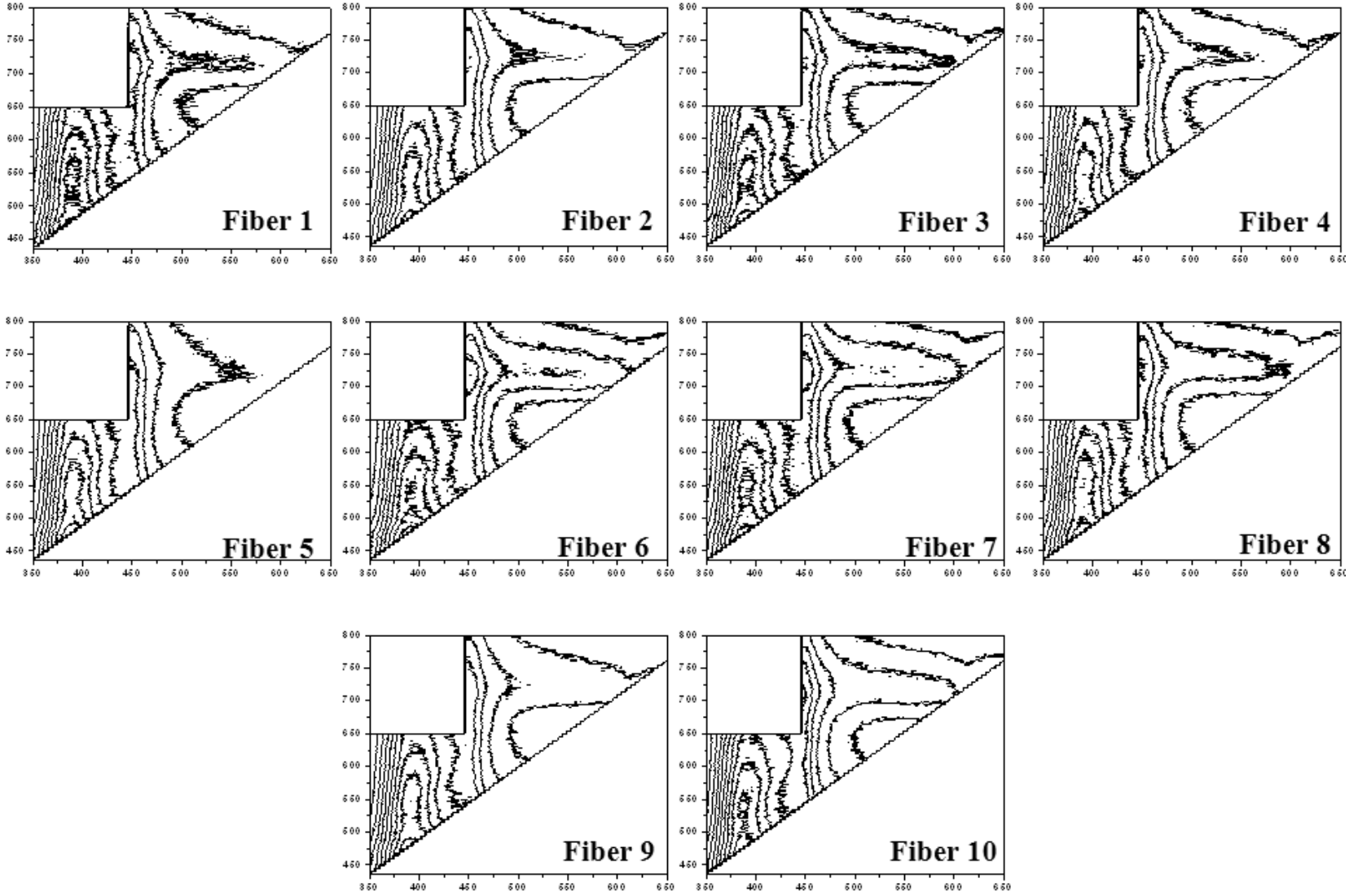

Figure D3. Reproducibility of EEMs recorded from ten fibers on a cotton 400 cloth piece dyed with Direct blue 1 dye

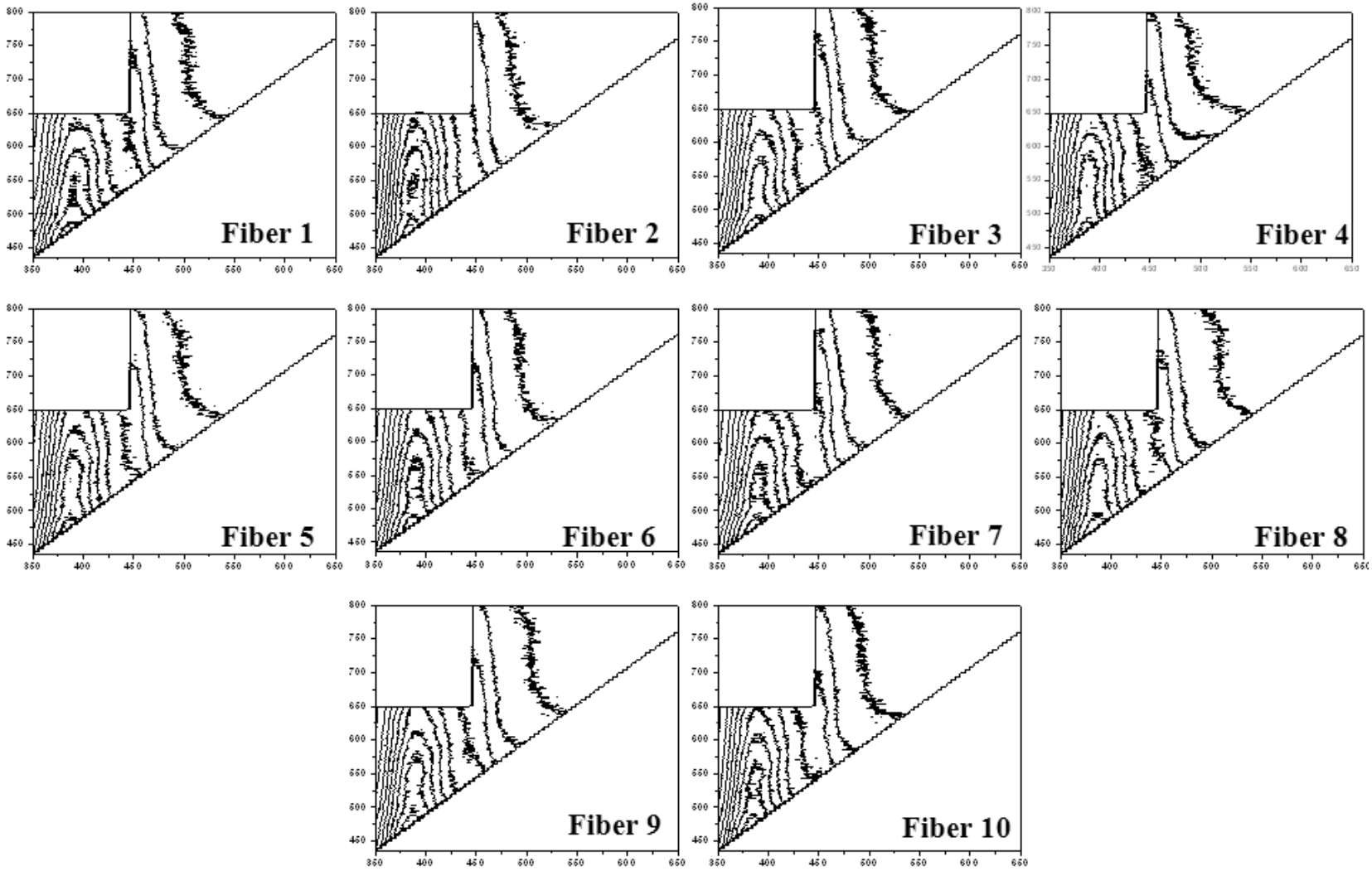

Figure D4. Reproducibility of EEMs recorded from ten fibers from an undyed nylon 361 cloth piece

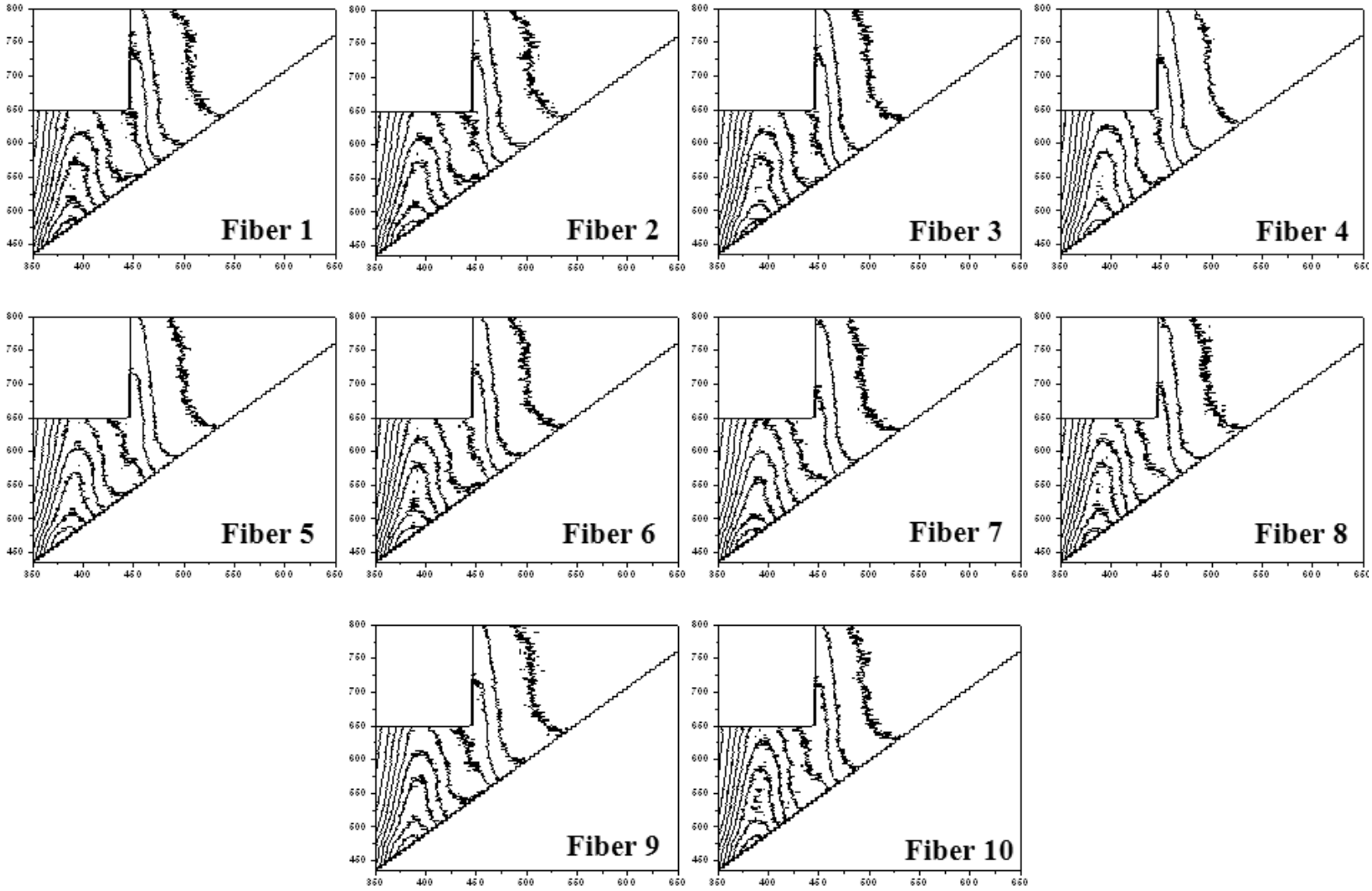

Figure D5. Reproducibility of EEMs recorded from ten fibers from an undyed acrylic 864 cloth piece

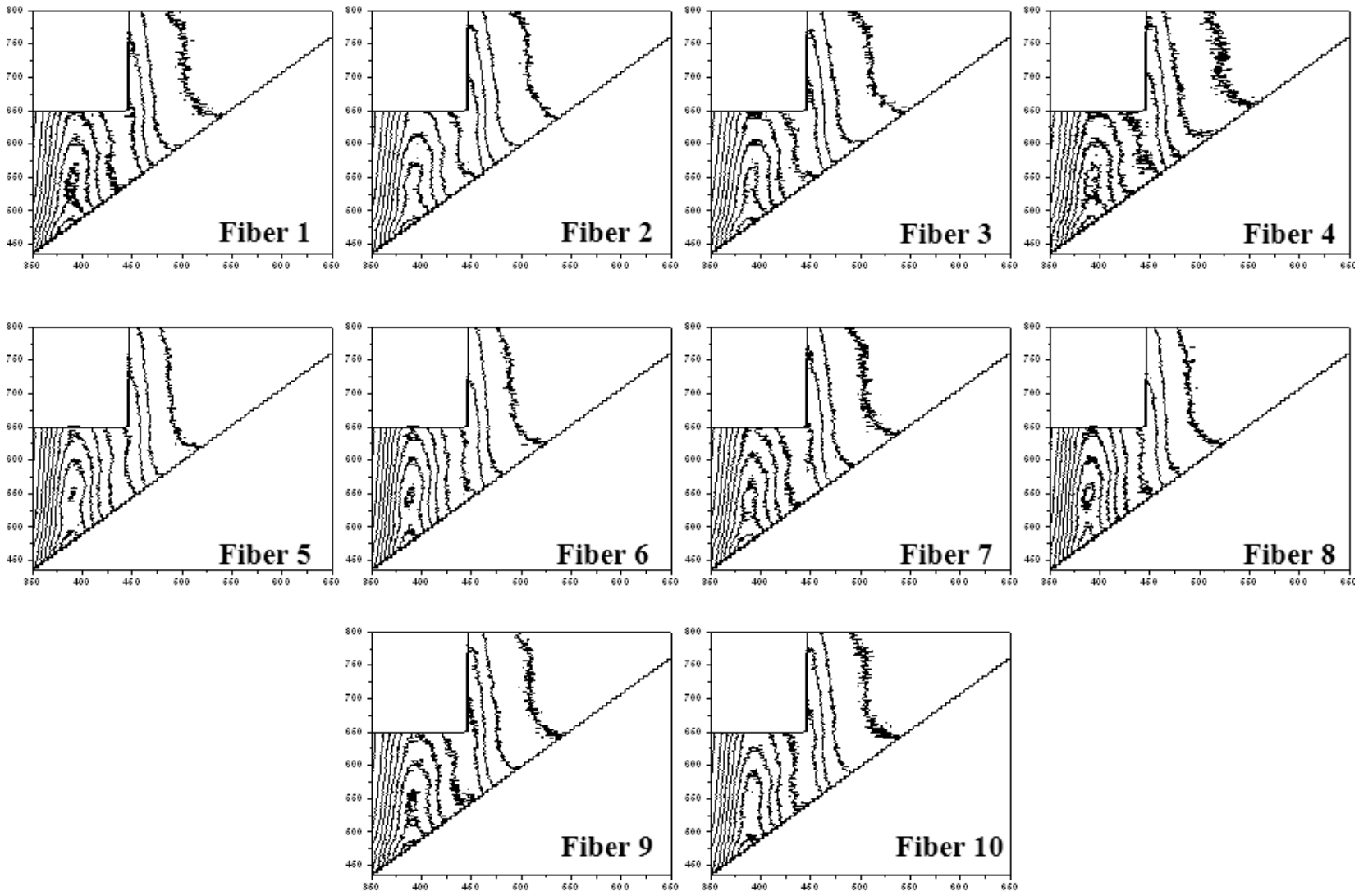

Figure D6. Reproducibility of EEMs recorded from ten fibers from an undyed cotton 400 cloth piece

APPENDIX F: REPRODUCIBILITY WITHIN EEMs FROM TEN SPOTS ON SINGLE INDISTINGUSHABLE FIBERS

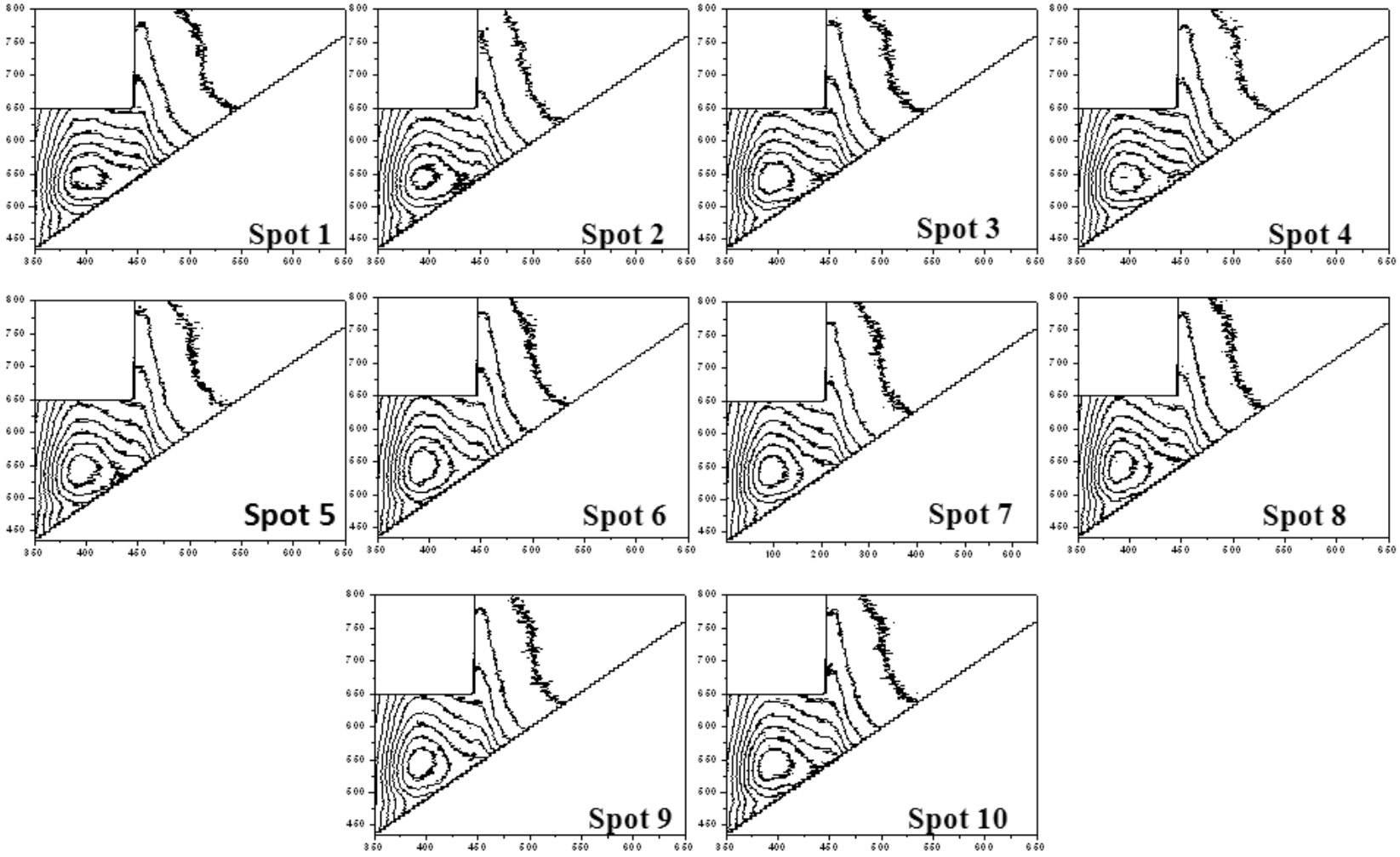

Figure E1. Reproducibility of EEMs recorded from ten spots on a single Acid yellow 17 dyed fiber

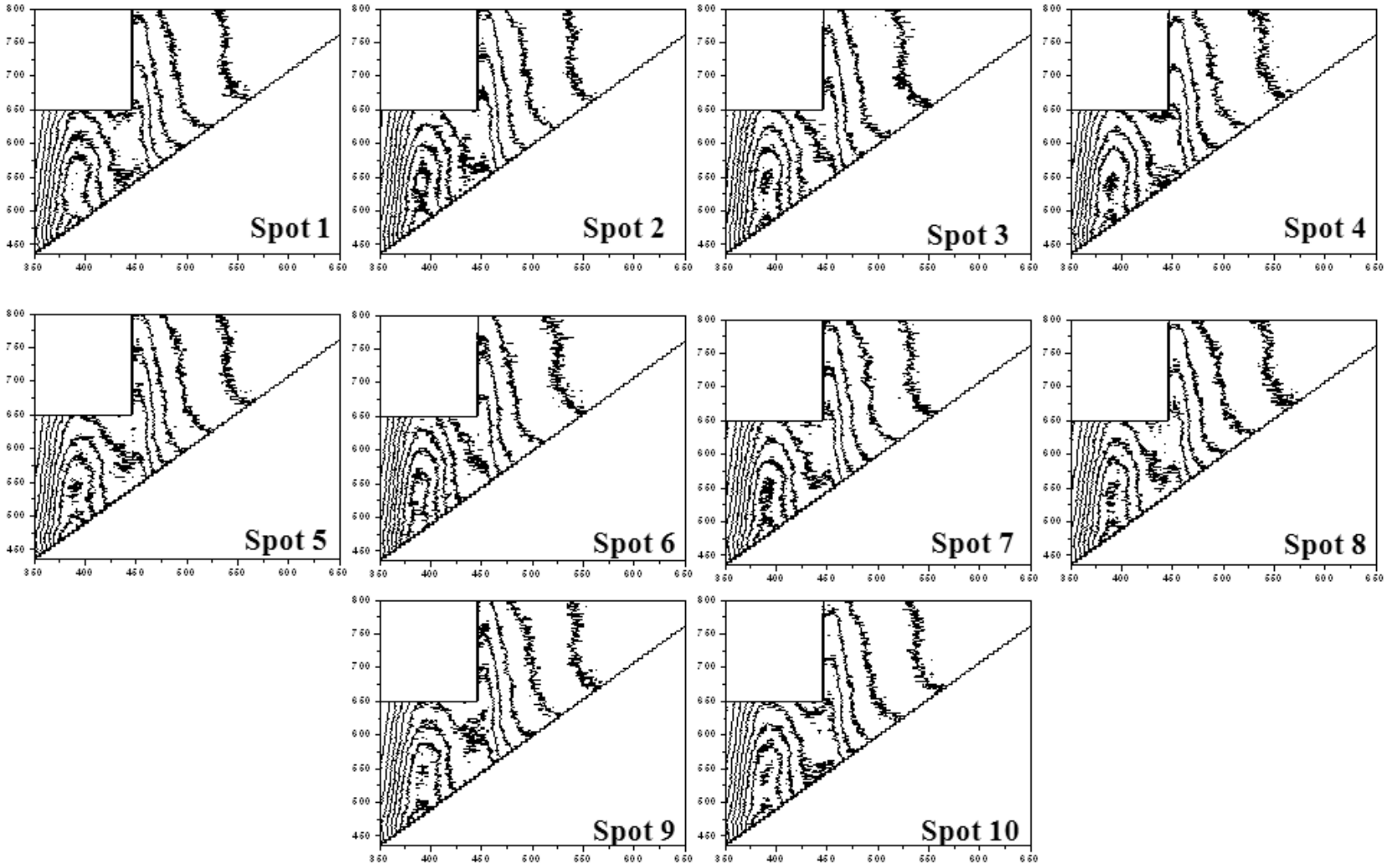

Figure E2. Reproducibility of EEMs recorded from ten spots on a single Acid yellow 23 dyed fiber

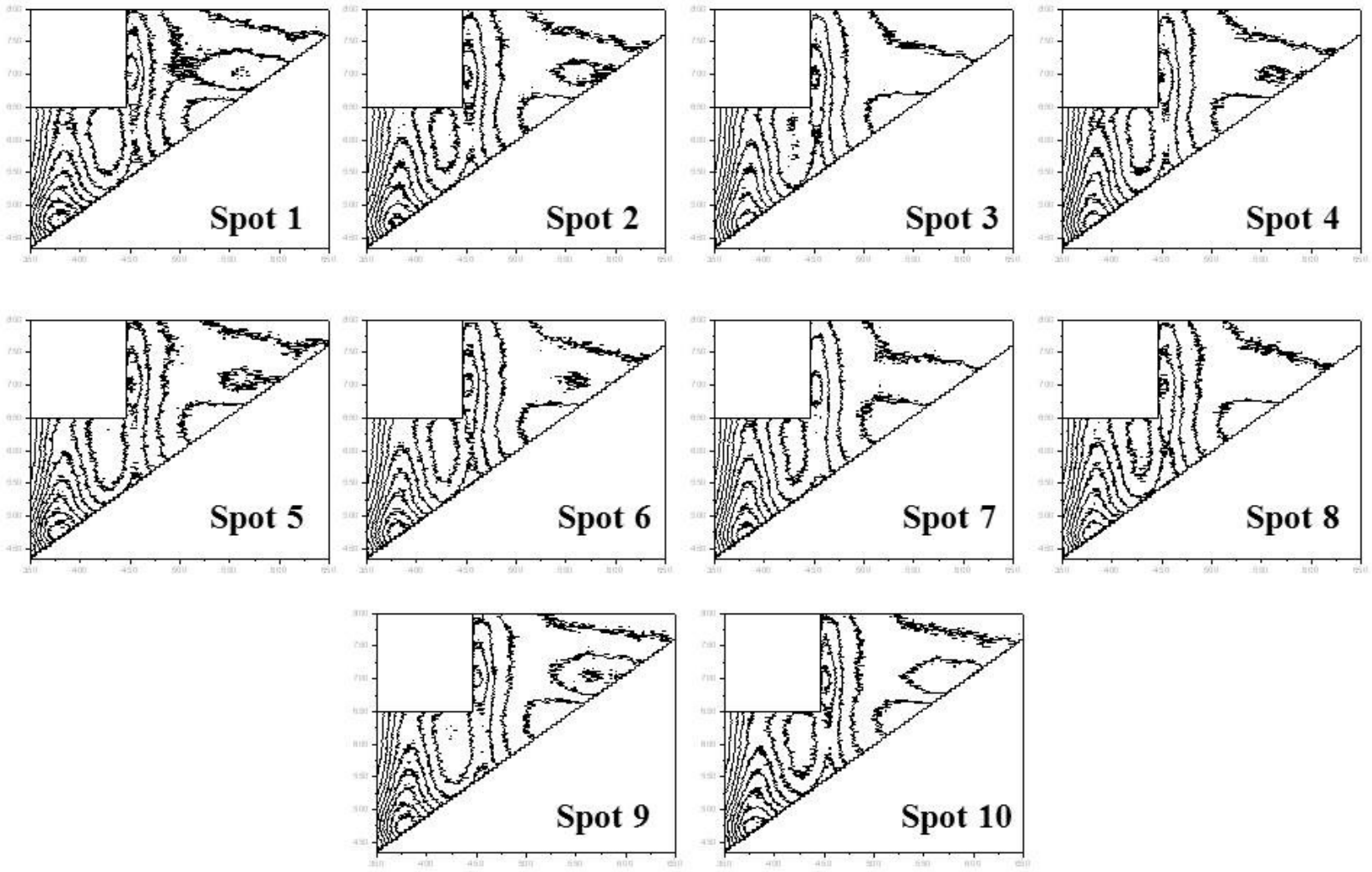

Figure E3. Reproducibility of EEMs recorded from ten spots on a single Basic green 1 dyed fiber

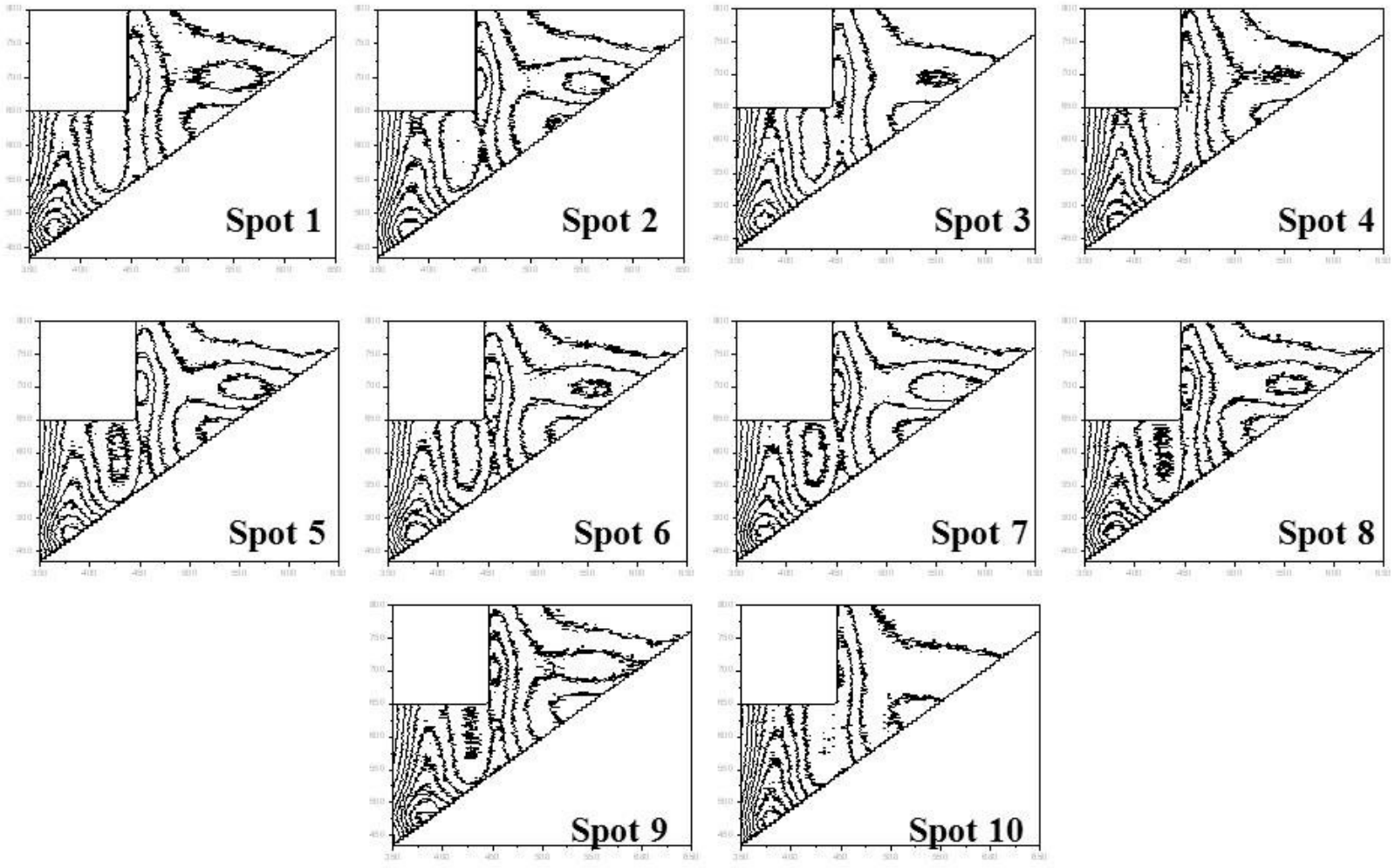

Figure E4. Reproducibility of EEMs recorded from ten spots on a single Basic green 4 dyed fiber

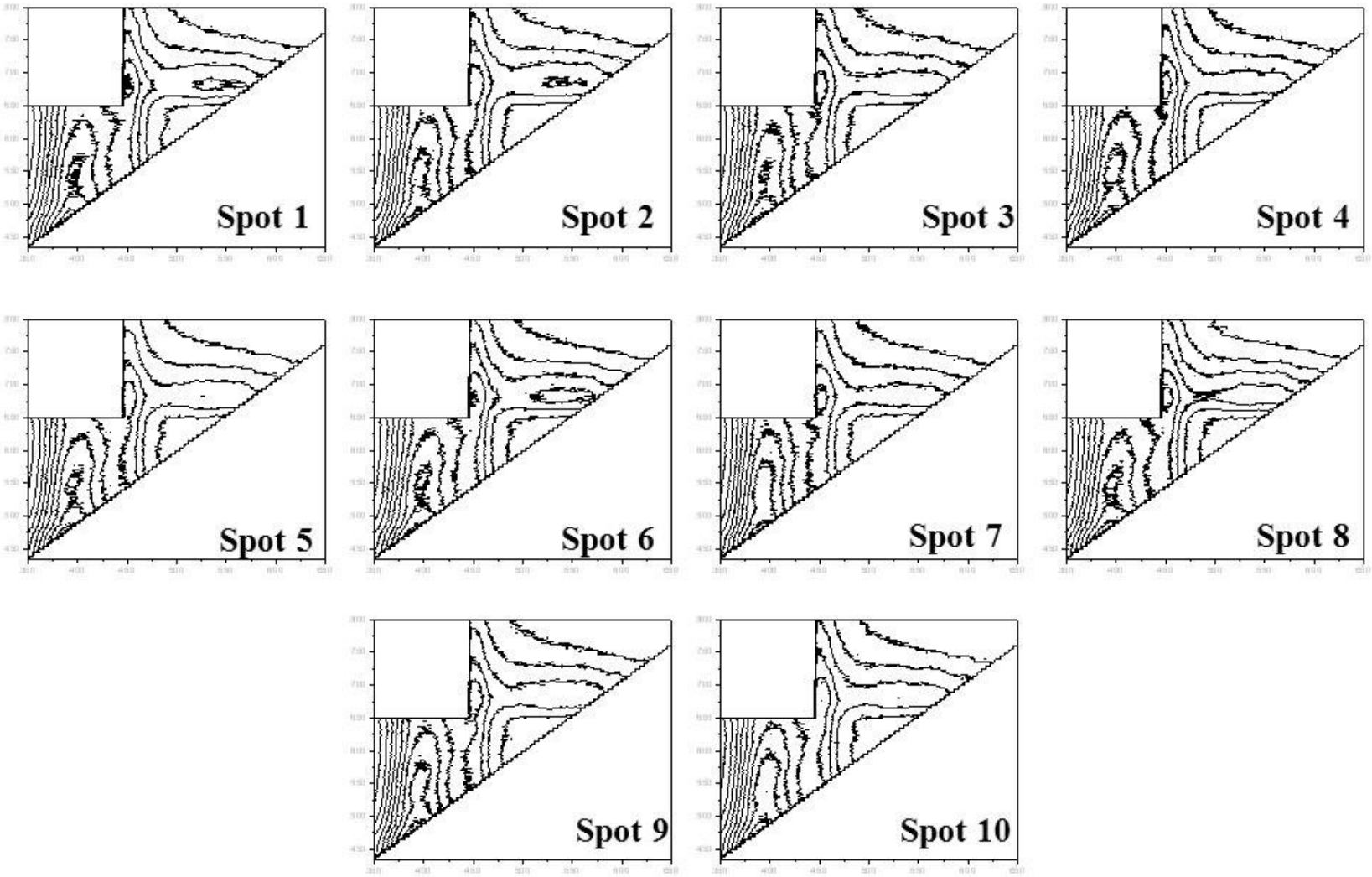

Figure E5. Reproducibility of EEMs recorded from ten spots on a single Disperse blue 3 dyed fiber

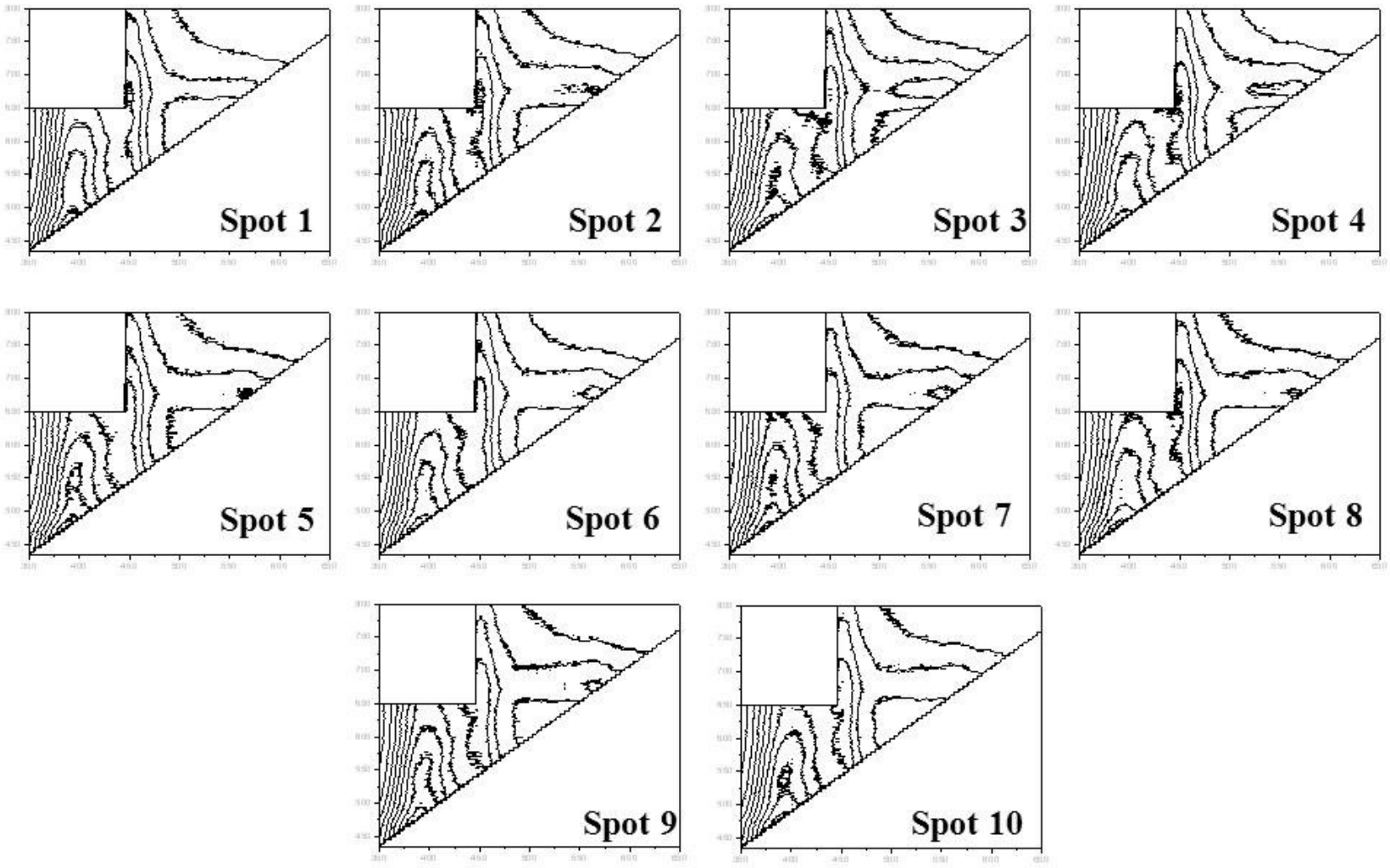

Figure E6. Reproducibility of EEMs recorded from ten spots on a single Disperse blue 14 dyed fiber

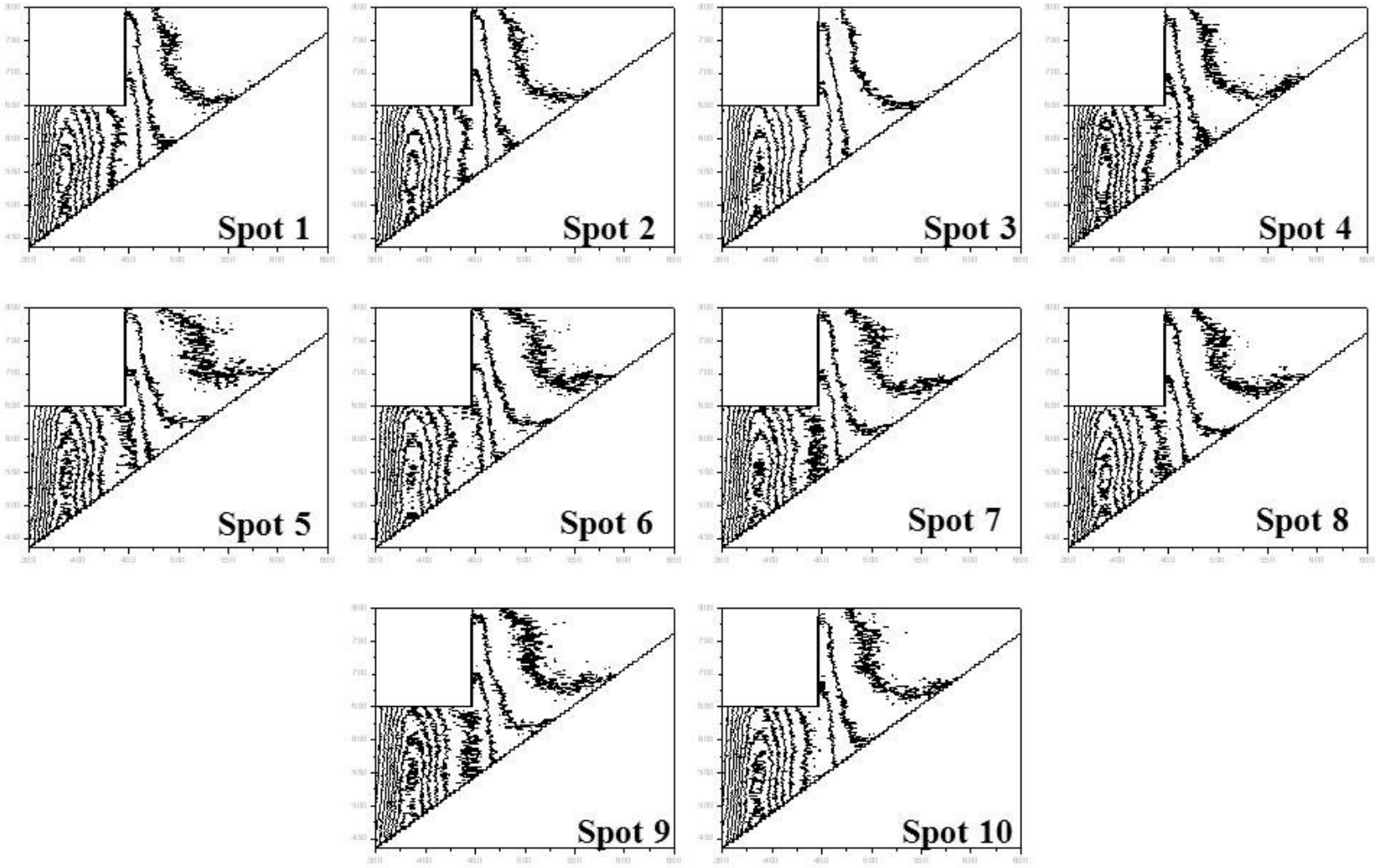

Figure E7. Reproducibility of EEMs recorded from ten spots on a single Disperse red 1 dyed fiber

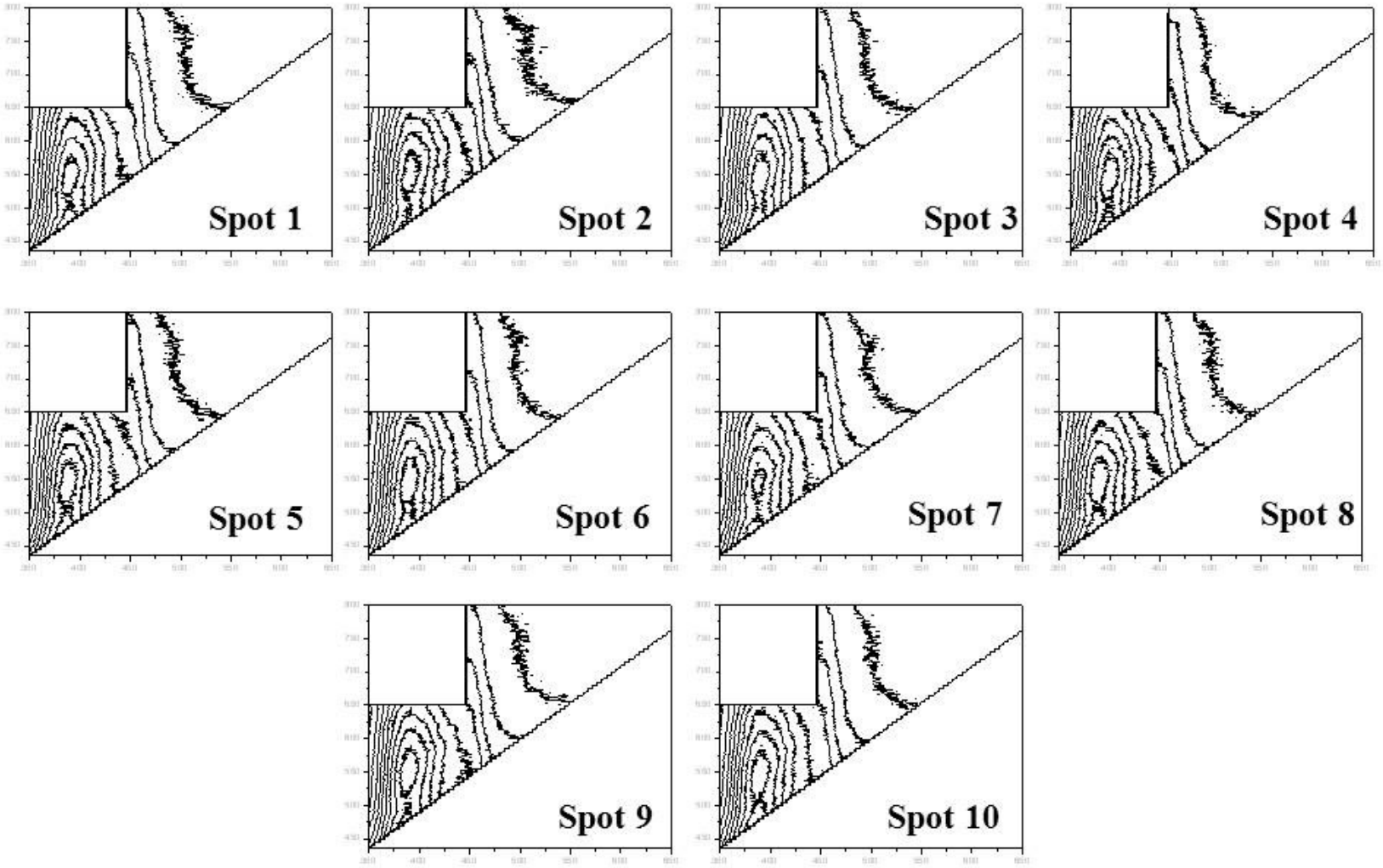

Figure E8. Reproducibility of EEMs recorded from ten spots on a single Disperse red 19 dyed fiber

APPENDIX G: SUPPLEMENTAL INFORMATION FOR CHAPTER 7

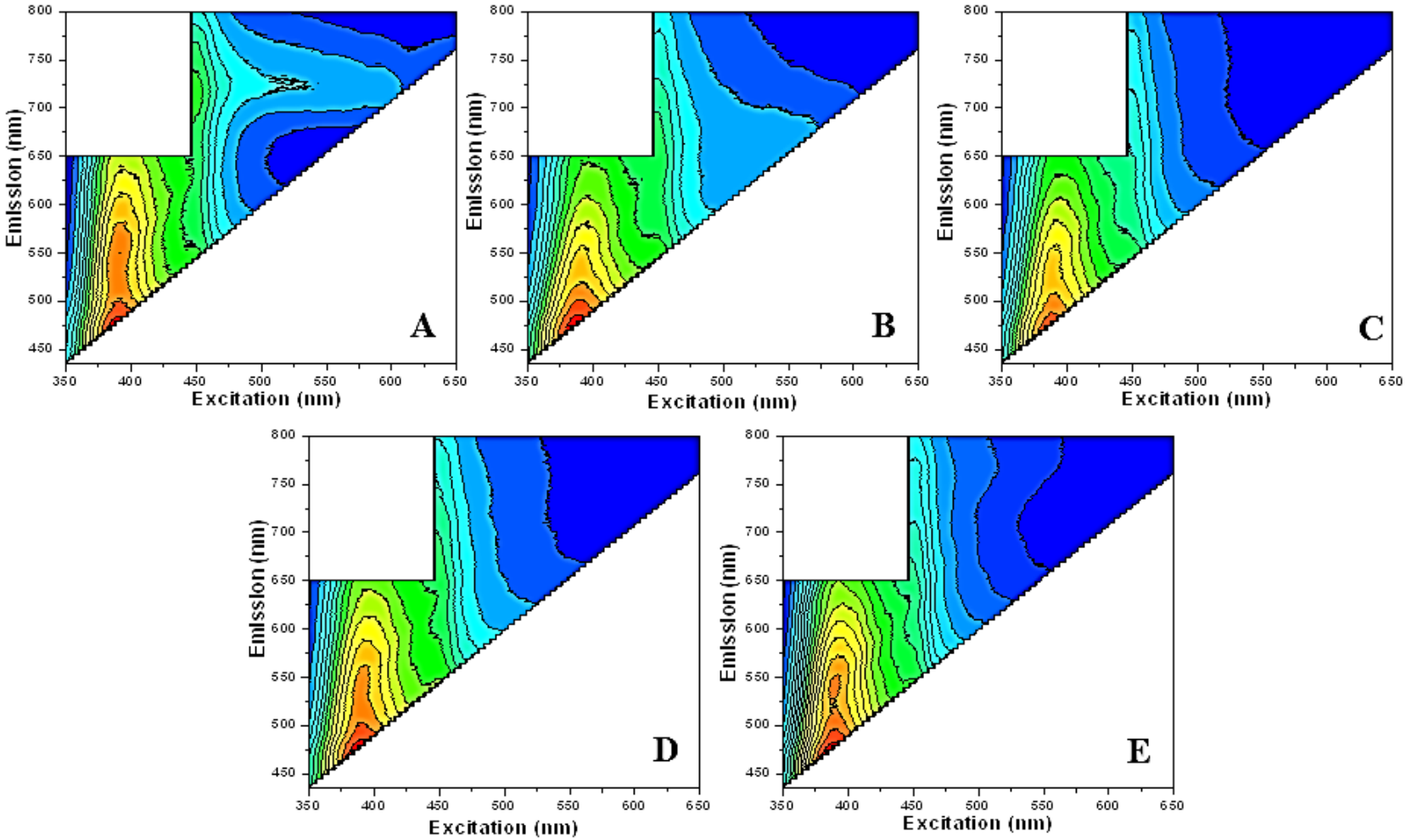

Figure F1. Contour plots of averaged EEMs from ten Direct Blue 1 dyed Cotton 400 textile fibers exposed to Arizona (dry) weather condition for 0 months (A), 3 months (B), 6 months (C), 9 months (D), and 12 months (E).

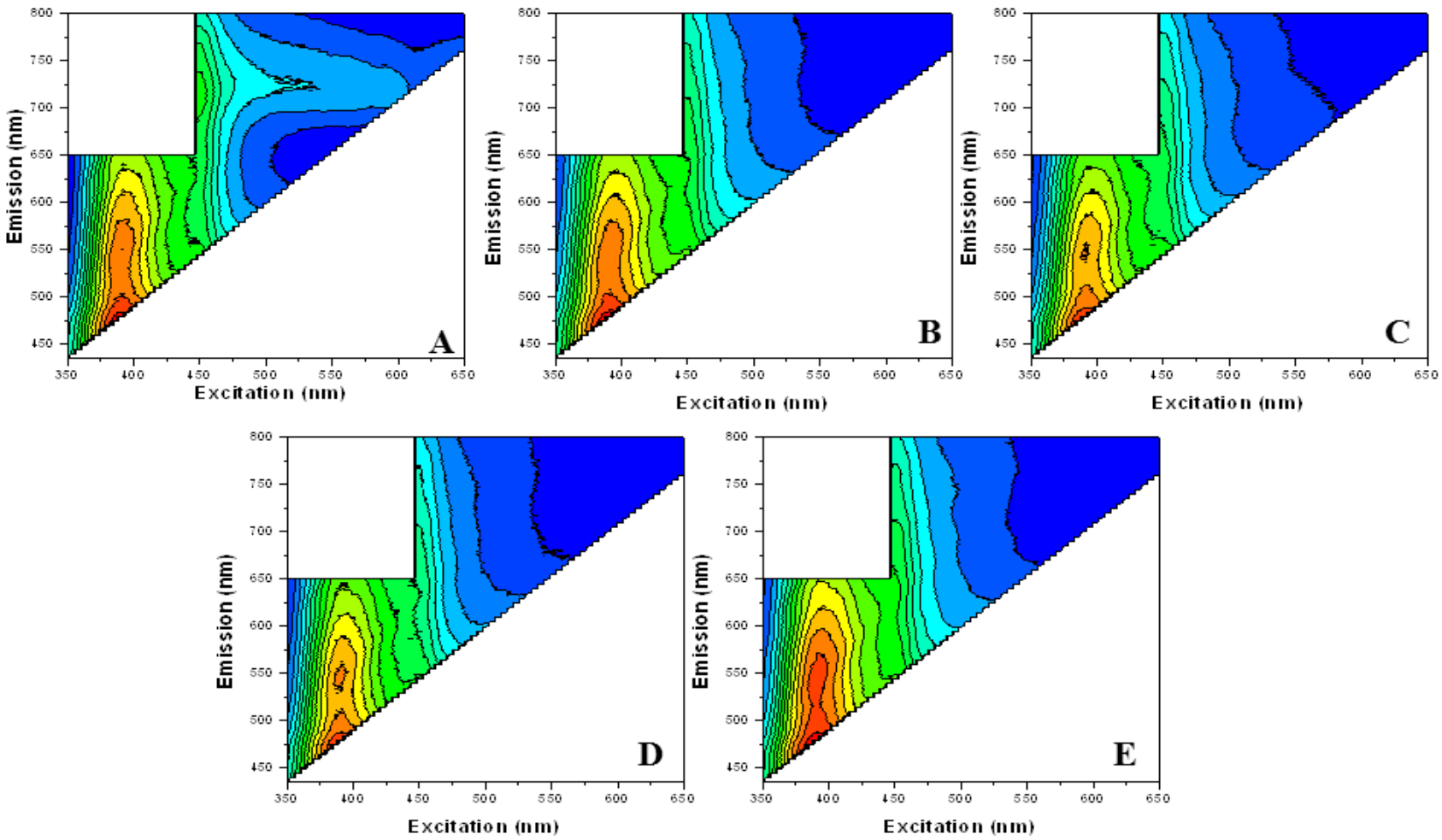

Figure F2. Contour plots of averaged EEMs from ten Direct Blue 1 dyed Cotton 400 textile fibers exposed to Florida (humid) weather condition for 0 months (A), 3 months (B), 6 months (C), 9 months (D), and 12 months (E).

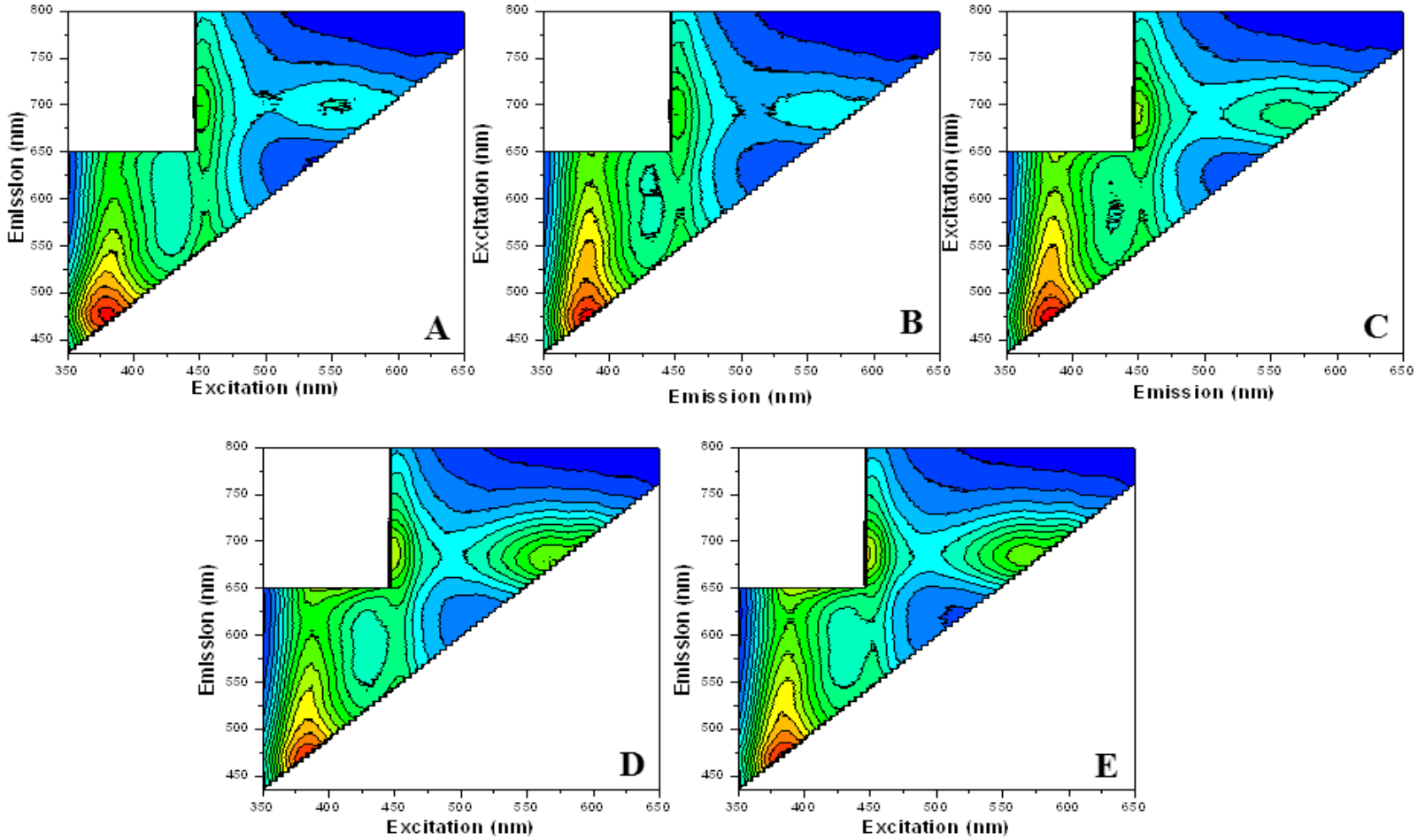

Figure F3. Contour plots of averaged EEMs from ten Basic green 4 dyed Acrylic 864 textile fibers exposed to Arizona (dry) weather condition for 0 months (A), 3 months (B), 6 months (C), 9 months (D), and 12 months (E).

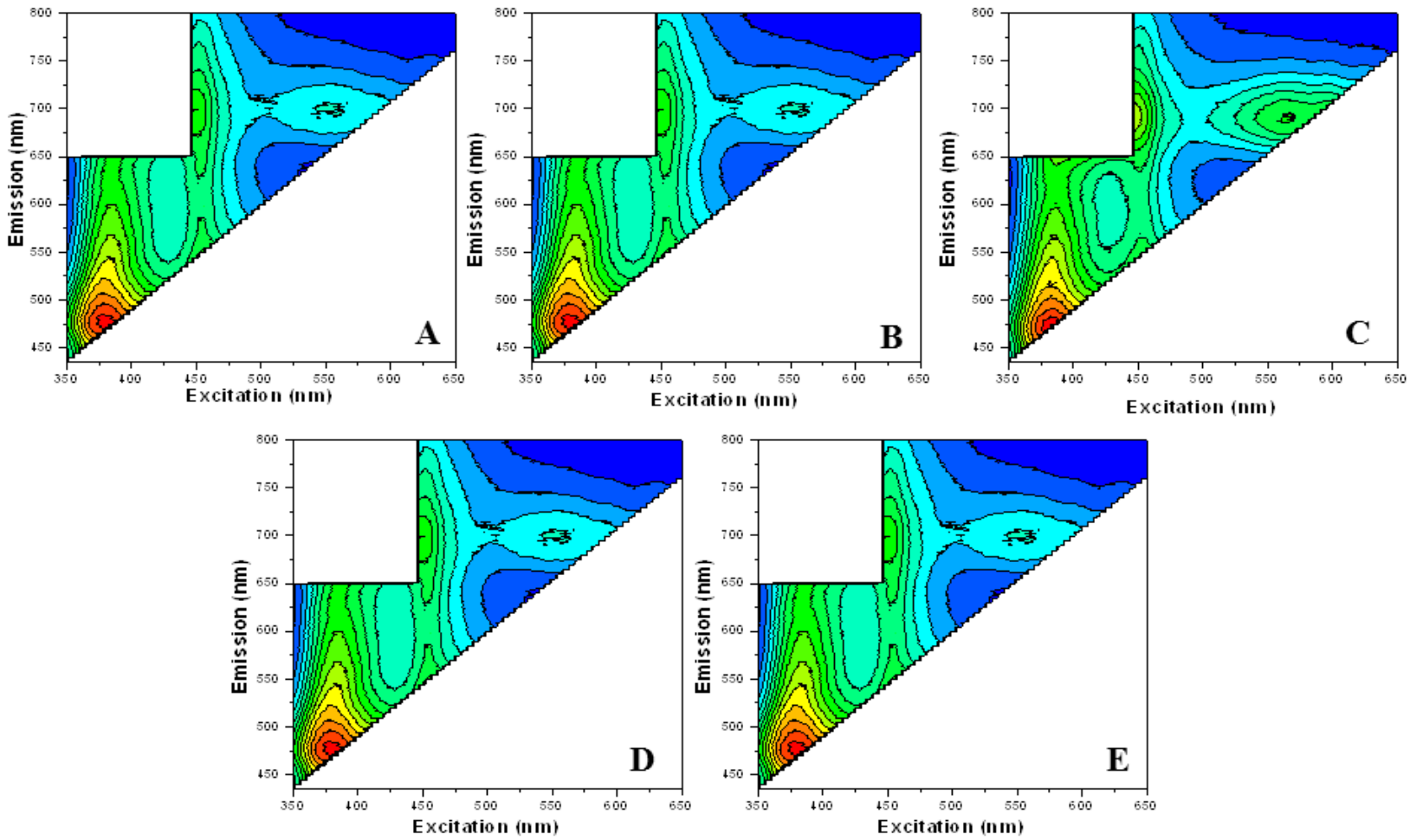

Figure F4. Contour plots of averaged EEMs from ten Basic green 4 dyed Acrylic 864 textile fibers exposed to Florida (humid) weather condition for 0 months (A), 3 months (B), 6 months (C), 9 months (D), and 12 months (E).

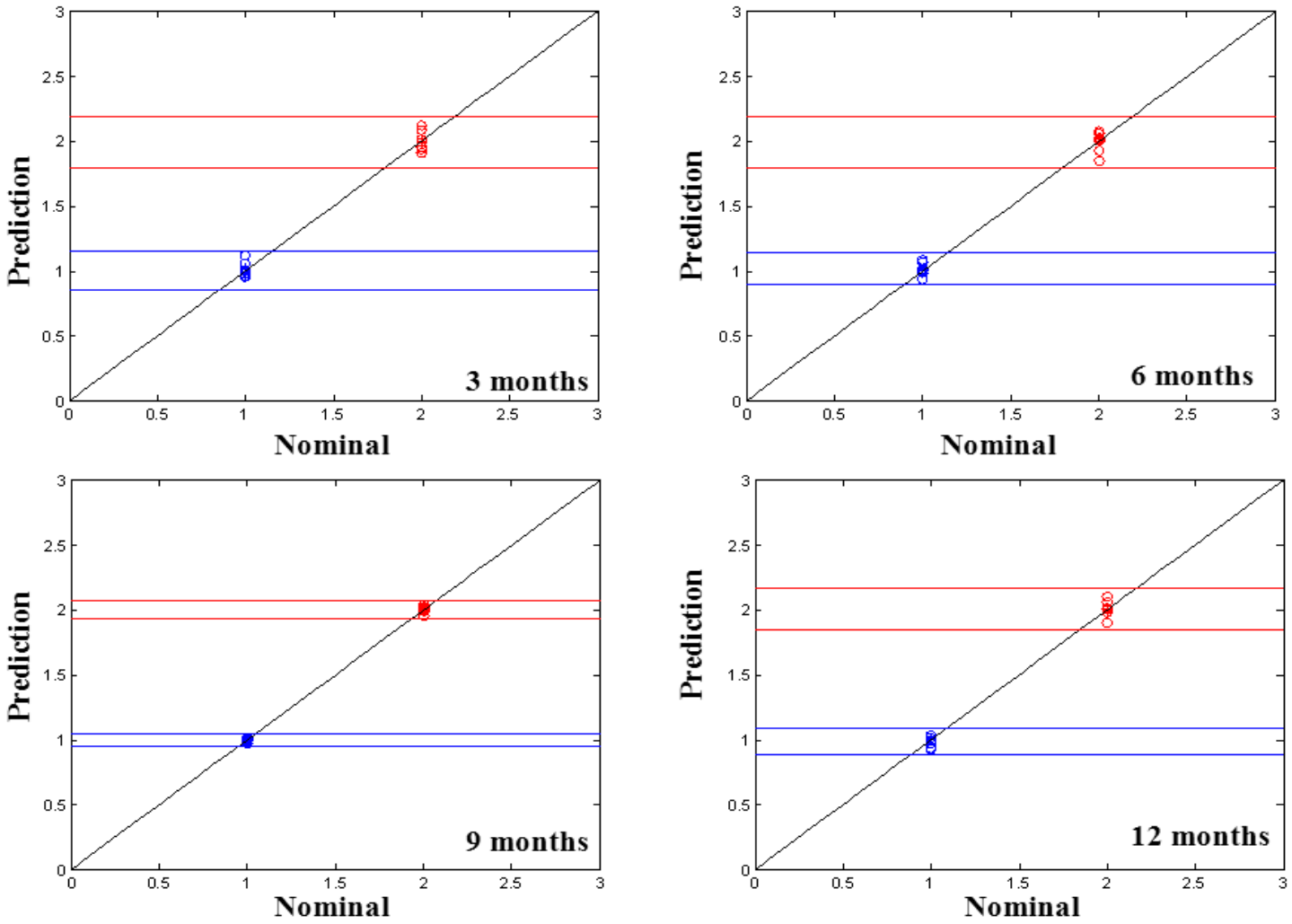

Figure F5. DU-PLS plots (3 component model) for the predicted versus nominal coded values for 10 fibers of AY17 dyed N361 exposed to Arizona (7 calibration samples = blue circles; 3 validation samples = blue crosses) versus 10 fibers of AY17 dyed N361 exposed to Florida (7 calibration samples = red circles; 3 validation samples = red crosses) weathering conditions under different time intervals of exposure.

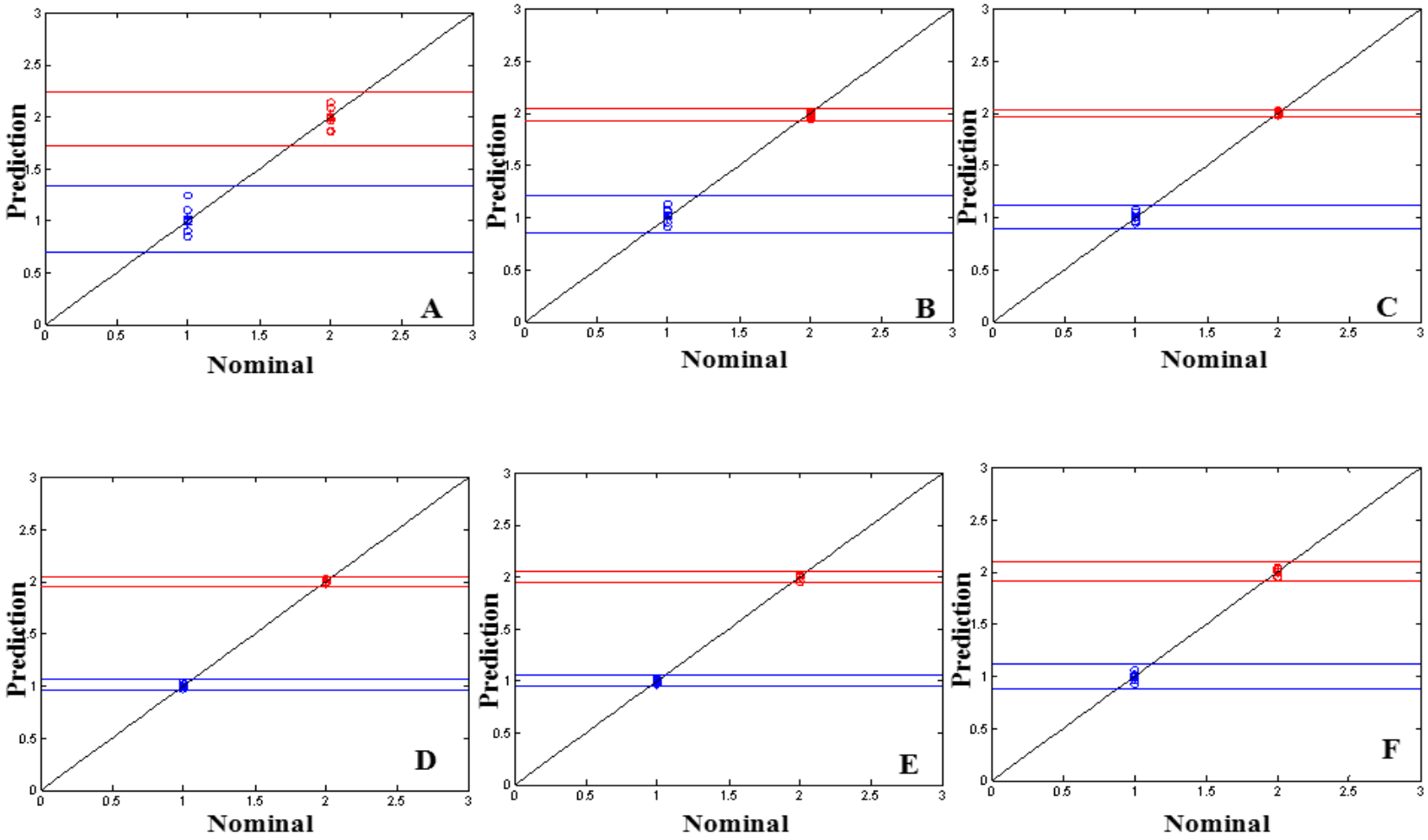

Figure F6. DU-PLS plots (3 component model) for the predicted versus nominal coded values of AY17 dyed N361 fibers exposed under different time intervals within Arizona's (dry) weathering conditions. 20 fibers were examined per exposure out of which 14 fibers were used as calibration samples (circles) whereas 6 fibers were used for validation (crosses). The plots represent: (A) 3 months (blue) versus 6 months (red); (B) 3 months (blue) versus 9 months (red); (C) 3 months (blue) versus 12 months (red); (D) 6 months (blue) versus 9 months (red); (E) 6 months (blue) versus 12 months (red); and (F) 9 months (blue) versus 12 months (red).

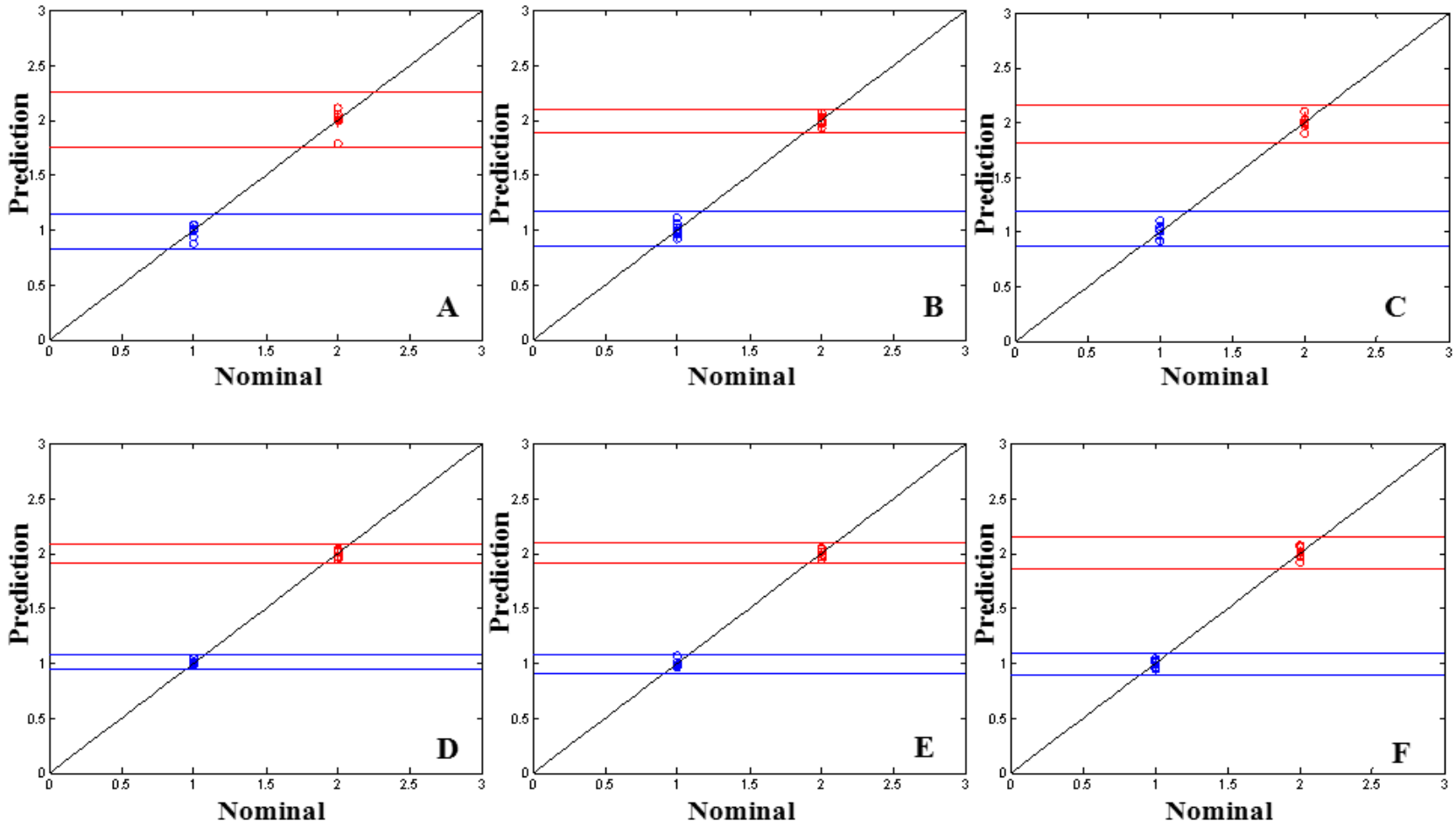

Figure F7. DU-PLS plots (3 component model) for the predicted versus nominal coded values of AY17 dyed N361 fibers exposed under different time intervals within Florida's (humid) weathering conditions. 20 fibers were examined per exposure out of which 14 fibers were used as calibration samples (circles) whereas 6 fibers were used for validation (crosses). The plots represent: (A) 3 months (blue) versus 6 months (red); (B) 3 months (blue) versus 9 months (red); (C) 3 months (blue) versus 12 months (red); (D) 6 months (blue) versus 9 months (red); (E) 6 months (blue) versus 12 months (red); and (F) 9 months (blue) versus 12 months (red).

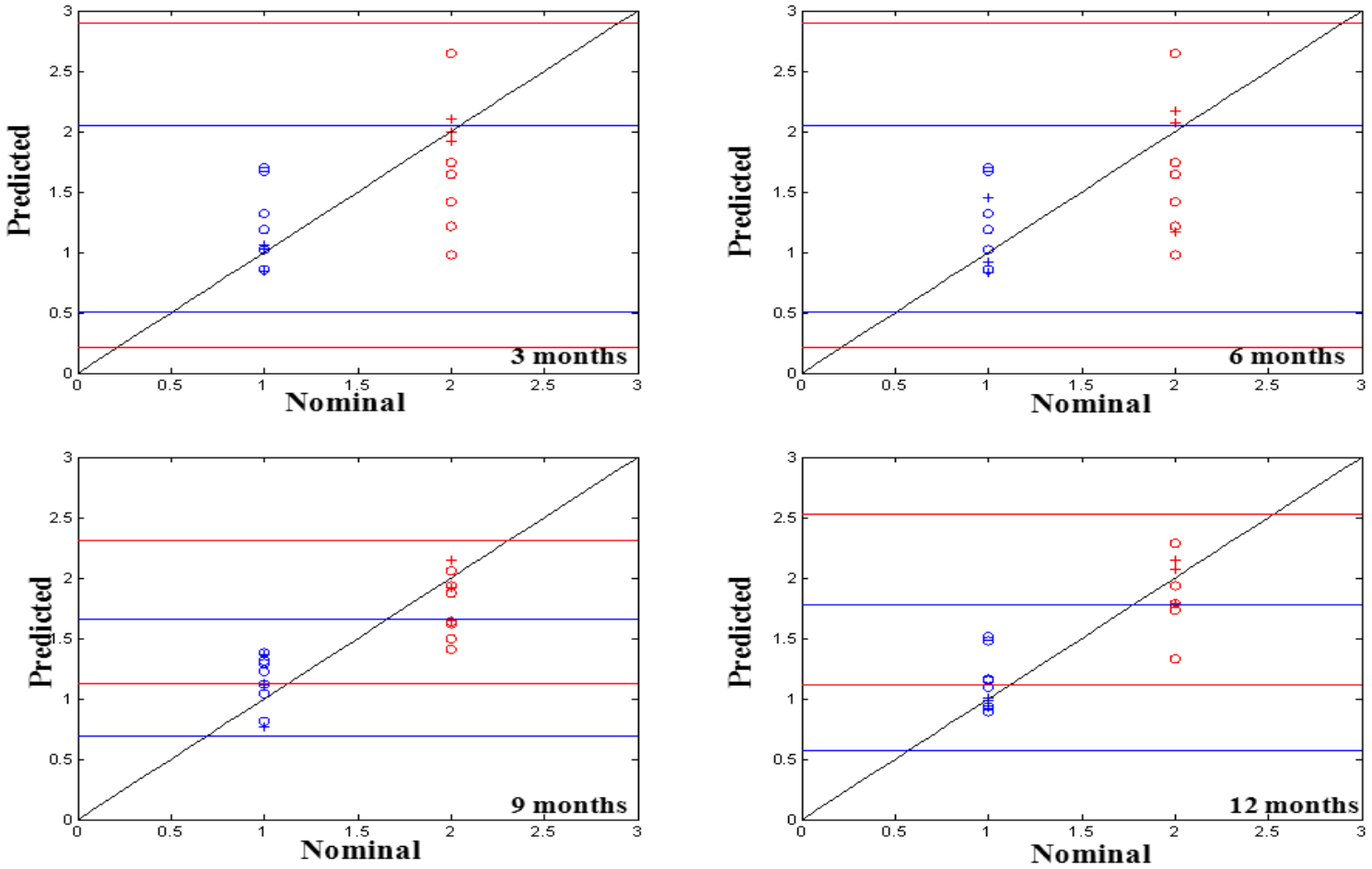

Figure F8. DU-PLS plots (3 component model) for the predicted versus nominal coded values for 10 fibers of BG4 dyed A864 exposed to Arizona (7 calibration samples = blue circles; 3 validation samples = blue crosses) versus 10 fibers of BG4 dyed A864 exposed to Florida (7 calibration samples = red circles; 3 validation samples = red crosses) weathering conditions under different time intervals of exposure.

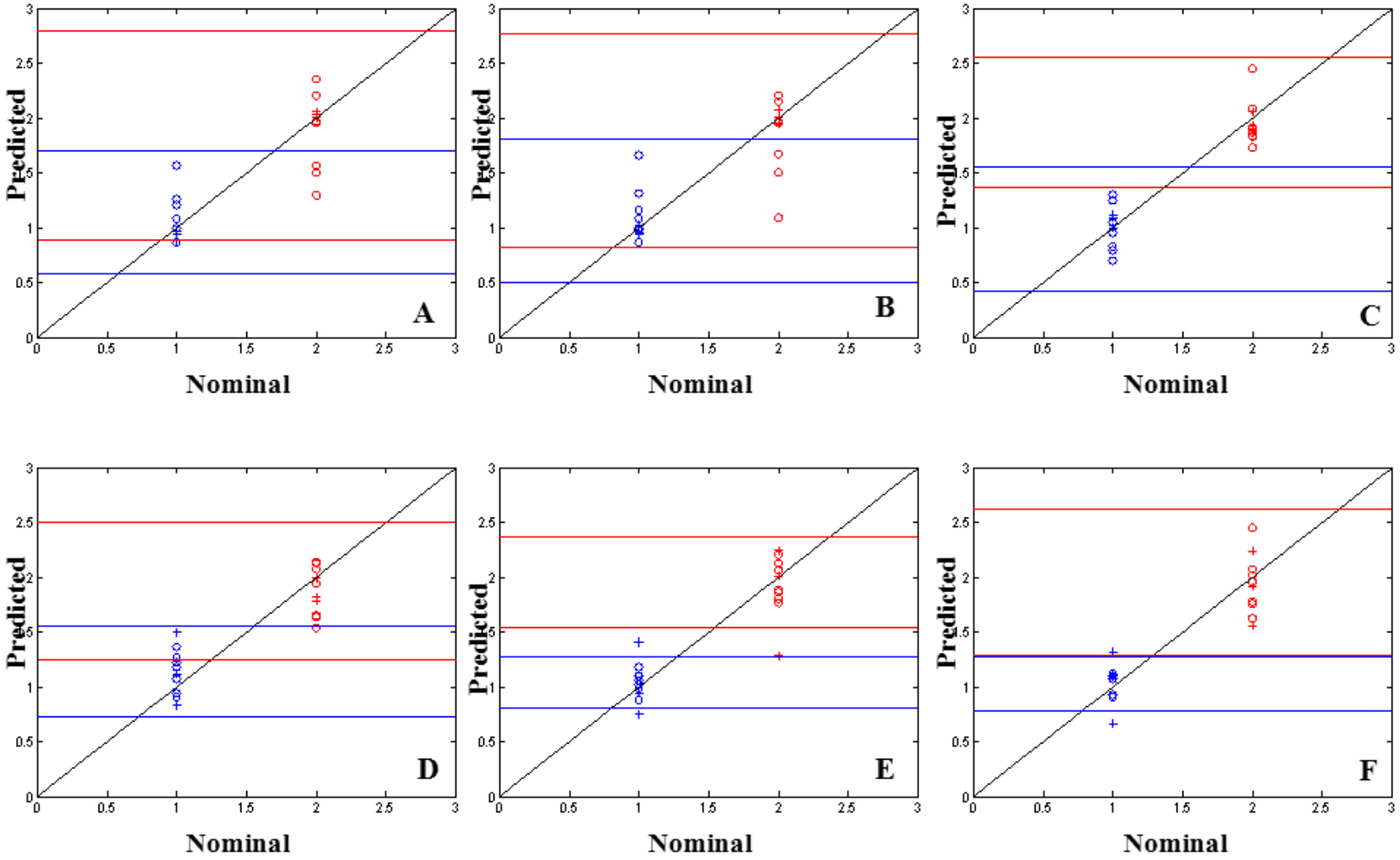

Figure F9. DU-PLS plots (3 component model) for the predicted versus nominal coded values of BG4 dyed A864 fibers exposed under different time intervals within Arizona's (dry) weathering conditions. 20 fibers were examined per exposure out of which 14 fibers were used as calibration samples (circles) whereas 6 fibers were used for validation (crosses). The plots represent: (A) 3 months (blue) versus 6 months (red); (B) 3 months (blue) versus 9 months (red); (C) 3 months (blue) versus 12 months (red); (D) 6 months (blue) versus 9 months (red); (E) 6 months (blue) versus 12 months (red); and (F) 9 months (blue) versus 12 months (red).

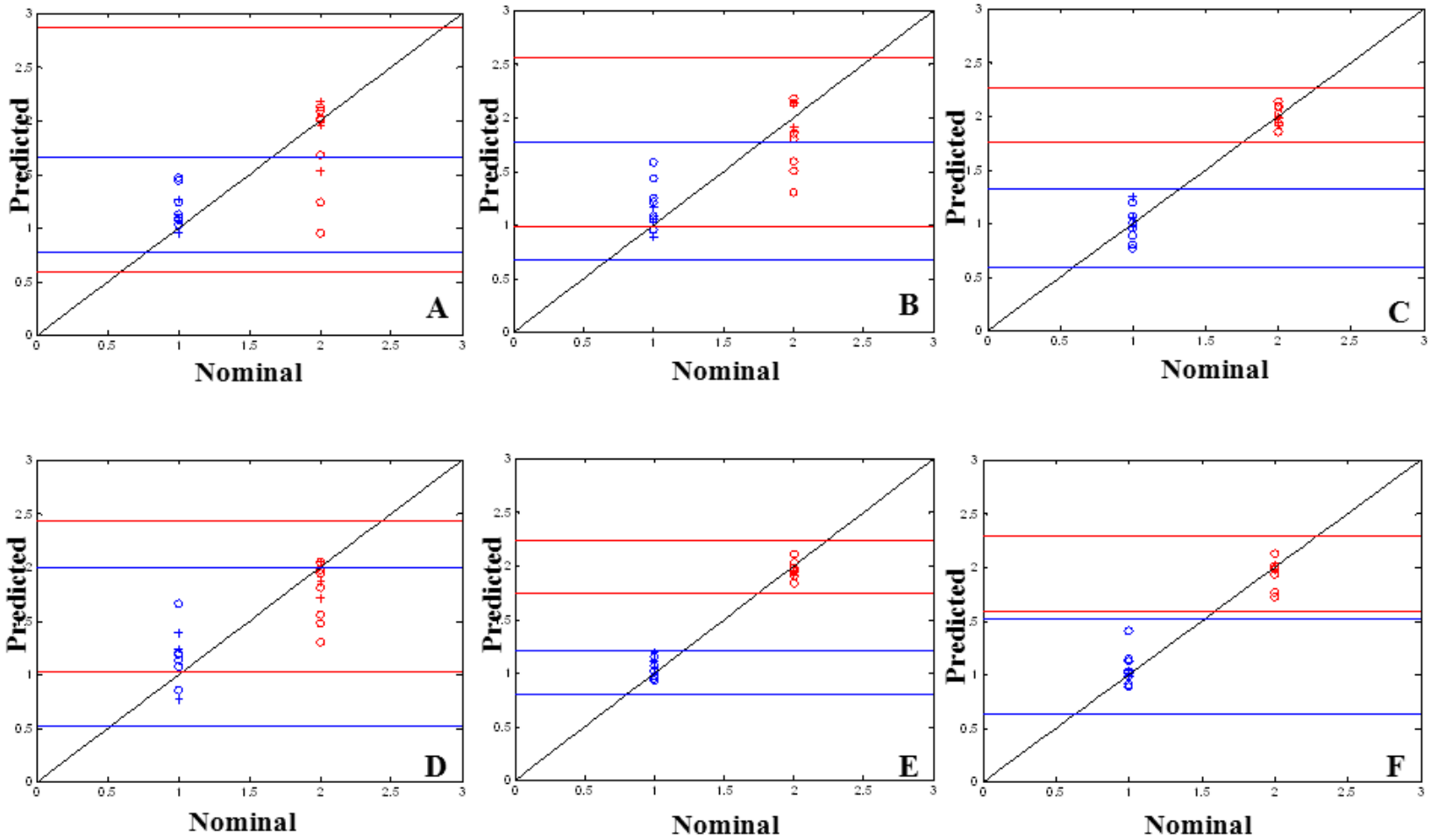

Figure F10. DU-PLS plots (3 component model) for the predicted versus nominal coded values of BG4 dyed A864 fibers exposed under different time intervals within Florida's (humid) weathering conditions. 20 fibers were examined per exposure out of which 14 fibers were used as calibration samples (circles) whereas 6 fibers were used for validation (crosses). The plots represent: (A) 3 months (blue) versus 6 months (red); (B) 3 months (blue) versus 9 months (red); (C) 3 months (blue) versus 12 months (red); (D) 6 months (blue) versus 9 months (red); (E) 6 months (blue) versus 12 months (red); and (F) 9 months (blue) versus 12 months (red).

APPENDIX H: COPYRIGHT PERMISSIONS

Copyright permission for *Applied Spectroscopy*; N. Mujumdar, E. C. Heider, A. D. Campiglia; Enhancing textile fiber identification with detergent fluorescence; Copyright © 2015, SAGE Publications.

Home | Account Info | Help | Live Chat

Title:	Enhancing Textile Fiber Identification with Detergent Fluorescence:
Author:	Nirvani Mujumdar, Emily C. Heider, Andres D. Campiglia
Publication:	Applied Spectroscopy
Publisher:	SAGE Publications
Date:	12/01/2015

Copyright © 2015, © SAGE Publications

Logged in as:

Nirvani Mujumdar

LOGOUT

Gratis Reuse

- Without further permission, as the Author of the journal article you may:
  - post the accepted version (version 2) on your personal website, department's website or your institution's repository. You may NOT post the published version (version 3) on a website or in a repository without permission from SAGE.
  - post the accepted version (version 2) of the article in any repository other than those listed above 12 months after official publication of the article.
  - use the published version (version 3) for your own teaching needs or to supply on an individual basis to research colleagues, provided that such supply is not for commercial purposes.
  - use the accepted or published version (version 2 or 3) in a book written or edited by you. To republish the article in a book NOT written or edited by you, permissions must be cleared on the previous page under the option 'Republish in a Book/Journal' by the publisher, editor or author who is compiling the new work.
- When posting or re-using the article electronically, please link to the original article and cite the DOI.
- All other re-use of the published article should be referred to SAGE. Contact information can be found on the bottom of our 'Journal Permissions' page.

Copyright permission for *Analytical and Bioanalytical Chemistry*; E. C. Heider, N. Mujumdar, A. D. Campiglia; Identification of detergents for forensic fiber analysis; Copyright © 2016, Springer-Verlag Berlin Heidelberg.

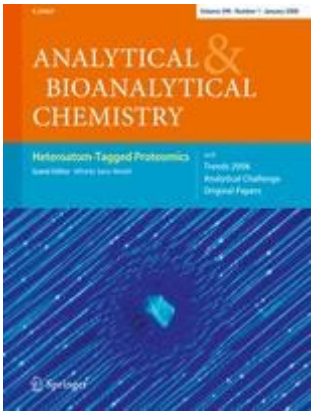

Title:	Identification of detergents for forensic fiber analysis
Author:	Emily C. Heider
Publication:	Analytical and Bioanalytical Chemistry
Publisher:	Springer
Date:	Jan 1, 2016
Copyright © 2016, Springer-Verlag Berlin Heidelberg	

This Agreement between Nirvani Mujumdar ("You") and Springer ("Springer") consists of your license details and the terms and conditions provided by Springer and Copyright Clearance Center.

Your confirmation email will contain your order number for future reference.

Get the printable license.

License Number	3953780497981
License date	Sep 21, 2016
Licensed Content Publisher	Springer
Licensed Content Publication	Analytical and Bioanalytical Chemistry
Licensed Content Title	Identification of detergents for forensic fiber analysis
Licensed Content Author	Emily C. Heider
Licensed Content Date	Jan 1, 2016
Type of Use	Thesis/Dissertation
Portion	Full text
Number of copies	1
Author of this Springer	Yes and you are a contributor of the new work
Order reference number	
Title of your thesis /	MULTIDIMENSIONAL ROOM-TEMPERATURE

dissertation	FLUORESCENCE MICROSCOPY FOR THE NONDESTRUCTIVE ANALYSIS OF FORENSIC TRACE TEXTILE FIBERS
Expected completion date	Dec 2016
Estimated size(pages)	250

Requestor Location	ORLANDO, FL 32826 United States Attn: Nirvani Mujumdar

Copyright permission for *Analytical Chemistry*; A. M. de la Pena, N. Mujumdar, E. C. Heider, H. C. Goicoechea; D. M. de la Pena, A. D. Campiglia; Identification of detergents for forensic fiber analysis; Copyright © 2016, ACS Publications.

Permission to use figures 1.3 and 1.4 in this dissertation; Copyright © 2009, Elsevier.

Chapter: 11 Analysis of dyes using chromatography
Book: Identification of Textile Fibers
Author: S.W. Lewis
Publisher: Elsevier
Date: Jan 1, 2009

Order Completed
Thank you for your order.

This Agreement between Nirvani Mujumdar ("You") and Elsevier ("Elsevier") consists of your order details and the terms and conditions provided by Elsevier and Copyright Clearance Center.

License number	Reference confirmation email for license number
License date	Sep 23, 2016
Licensed Content Publisher	Elsevier
Licensed Content Publication	Elsevier Books
Licensed Content Title	Identification of Textile Fibers
Licensed Content Author	S.W. Lewis
Licensed Content Date	2009
Licensed Content Volume	n/a
Licensed Content Issue	n/a
Licensed Content Pages	21
Type of Use	reuse in a thesis/dissertation
Portion	figures/tables/illustrations
Number of figures/tables/illustrations	2
Format	both print and electronic
Are you the author of this Elsevier chapter?	No
Will you be translating?	No
Order reference number	
Original figure numbers	11.8, 11.9

Title of your thesis/dissertation	MULTIDIMENSIONAL ROOM-TEMPERATURE FLUORESCENCE MICROSCOPY FOR THE NONDESTRUCTIVE ANALYSIS OF FORENSIC TRACE TEXTILE FIBERS
Expected completion date	Dec 2016
Estimated size (number of pages)	250
Elsevier VAT number	GB 494 6272 12
	Nirvani Mujumdar
Requestor Location	ORLANDO, FL 32826 United States Attn: Nirvani Mujumdar

LIST OF REFERENCES

(1) ASCLD/LAB. 2016.

(2) Taupin, J. M., and Cwiklik, C. *Scientific Protocols for Forensic Examination of Clothing*; CRC Press: Boca Raton, FL, 2011.

(3) Goodpaster, J. V.; Liszewski, E. A. *Analytical and bioanalytical chemistry* **2009**, *394*, 2009.

(4) Farah, S.; Kunduru, K. R.; Tsach, T.; Bentolila, A.; Domb, A. J. *Polym Advan Technol* **2015**, *26*, 785.

(5) Meleiro, P. P.; Garcia-Ruiz, C. *Appl Spectrosc Rev* **2016**, *51*, 258.

(6) Cho, L.-L. *Forensic Science Journal* **2007**, *6*, 55.

(7) Abbott, L. C.; Batchelor, S. N.; Smith, J. R. L.; Moore, J. N. *Forensic science international* **2010**, *202*, 54.

(8) Wiggins, K. G. *Journal of forensic sciences* **2001**, *46*, 1303.

(9) Robertson, J., Grieve, M. *Forensic Examination of Fibres*; Taylor & Francis, Ltd. : London, UK., 1999.

(10) Robertson, J. *Forensic Examination of Fibres*; Ellis Horwood Ltd. : West Sussex, England, 1992.

(11) Robertson, J., and Grieve, M. *Forensic examination of fibers*; 2nd ed.; CRC press: New York, 1999.

(12) Taupin, J. M. *Journal of forensic sciences* **1996**, *41*, 697.

(13) David, S. K., and Pailthorpe, M. T. *Classification of textile fibres: production, structure, and properties.*; 2nd ed.; CRC Press: New York, NY., 1999.

(14) Rendle, D. F. *Chemical Society reviews* **2005**, *34*, 1021.

(15) Blackledge, R. D. *Forensic Analysis on the Cutting Edge*; John Wiley & Sons, Inc. : Hoboken, New Jersey, 2007.

(16) Robertson, J., and Grieve, M. *Forensic examination of fibres*; Taylor & Francis, Ltd. : London, UK. , 1999.

(17) Zollinger, H. *Color chemistry: Synthesis, properties and applications of organic dyes and pigments*; 3rd ed.; Wiley-VCH.: Zurich, Switzerland.

(18) Skoog, D. A., Holler, F. J., and Crouch, S. R. *Principles of instrumental analysis*; 6th ed.; Thomson Brookes/Cole: Belmont, CA, 2007.

(19) Akbari, A.; Remigy, J. C.; Aptel, P. *Chem Eng Process* **2002**, *41*, 601.

(20) Robertson, J., and Grieve, M. *Forensic examination of fibres*; CRC Press: New York, NY, 1999.

(21) *Fiber economics bureau*, 2016.

(22) Thomas, J.; Buzzini, P.; Massonnet, G.; Reedy, B.; Roux, C. *Forensic science international* **2005**, *152*, 189.

(23) Grieve, M. C. *Journal of forensic sciences* **1983**, *28*, 877.

(24) Bell, S. *Encyclopedia of Forensic Science: Facts on file* New York, 2008.

(25) Grieve, M. C.; Wiggins, K. G. *Journal of forensic sciences* **2001**, *46*, 835.

(26) SWGMAT. Introduction to Forensic Fiber Examination. *Fiber Guidelines.* https://www.fbi.gov/about-us/lab/forensic-science-communications/fsc/april1999/houcktoc.htm/houckch1.htm.

(27) Robertson, J. a. G., M. *Forensic examination of fibres*; 2nd ed.; CRC Press: New York, 1999.

(28) Cochran, K. H.; Barry, J. A.; Muddiman, D. C.; Hinks, D. *Analytical chemistry* **2013**, *85*, 831.

(29) SWGMAT. A Forensic Fiber Examiner Training Program. *Fiber Subgroup*, 2004. https://www.fbi.gov/about-us/lab/forensic-science-communications/fsc/april2005/standards/SWGMAT_fiber_training_program.pdf.

(30) De Wael, K.; Gason, F. G. C. S. J.; Baes, C. A. V. *Journal of forensic sciences* **2008**, *53*, 168.

(31) Robertson, J., and Grieve, M. *Forensic examination of fibres*; 2nd ed.; CRC Press: New York, 1999.

(32) Torok, P.; Higdon, P. D.; Wilson, T. 1998; Vol. 3261, p 22.

(33) Finzi, L.; Dunlap, D. D. In *eLS*; John Wiley & Sons, Ltd: 2001.

(34) Palmer, R.; Chinherende, V. *Journal of forensic sciences* **1996**, *41*, 802.

(35) Pawley, J. *Handbook of Biological Confocal Microscopy*; Springer US, 2010.

(36) Prasad, V.; Semwogerere, D.; Weeks, E. R. *J Phys-Condens Mat* **2007**, *19*.

(37) Kirkbride, K. P.; Tridico, S. R. *Forensic science international* **2010**, *195*, 28.

(38) Lepot, L.; De Wael, K.; Gason, F.; Gilbert, B. *Sci Justice* **2008**, *48*, 109.

(39) Song, Y.; Srinivasarao, M.; Tonelli, A.; Balik, C. M.; McGregor, R. *Macromolecules* **2000**, *33*, 4478.

(40) Méndez-Vilas, A. *Current Microscopy Contributions to Advances in Science and Technology*; Formatex Research Center, 2012.

(41) Vitez, I. M.; Newman, A. W.; Davidovich, M.; Kiesnowski, C. *Thermochim Acta* **1998**, *324*, 187.

(42) Bisbing, R. E. *The Forensic Laboratory Hand Book: Procedures and Practice*, 2007.

(43) Robertson, J., and Grieve, M. *Forensic examination of fibres*; 2nd ed.; CRC press: New York, 1999.

(44) Robertson, J., and Grieve, M. *Forensic Examination of Fibres*; 2nd ed.; CRC Press: New York, 1999

(45) Robson, D. *Journal of the Forensic Science Society* **1994**, *34*, 187.

(46) Grieve, M. C.; Cabiness, L. R. *Forensic science international* **1985**, *29*, 129.

(47) Grieve, M. C. *Sci Justice* **1995**, *35*, 179.

(48) Tungol, M. W., Bartick, E. G., and Montaser, A. *Forensic Examination of Synthetic Textile Fibers* New York, 1995.

(49) Robertson, J., and Grieve, M. *Forensic Examination of Fibres*; CRC Press: New York, 1999.

(50) Macrae, R.; Dudley, R. J.; Smalldon, K. W. *Journal of forensic sciences* **1979**, *24*, 117.

(51) Appalaneni, K.; Heider, E. C.; Moore, A. F. T.; Campiglia, A. D. *Analytical chemistry* **2014**, *86*, 6774.

(52) de la Pena, A. M.; Mujumdar, N.; Heider, E. C.; Goicoechea, H. C.; de la Pena, D. M.; Campiglia, A. D. *Analytical chemistry* **2016**, *88*, 2967.

(53) Weaver, J. W. *Analytical Methods for a Textile Laboratory*; 3rd ed.; American Association of Textile Chemists and Colorists: Research Triangle Park, N.C. , 1984.

(54) Grieve, M. C.; Dunlop, J.; Haddock, P. *Journal of forensic sciences* **1990**, *35*, 301.

(55) Wiggins, K. G.; Cook, R.; Turner, Y. J. *Journal of forensic sciences* **1988**, *33*, 998.

(56) Wiggins, K. G.; Crabtree, S. R.; March, B. M. *Journal of forensic sciences* **1996**, *41*, 1042.

(57) Houck, M. M. *Identification of Textile Fibres*; 1st ed.; Woodhead Publishing Ltd. : Cambridge, UK, 2009.

(58) Beattie, I. B.; Roberts, H. L.; Dudley, R. J. *Forensic science international* **1981**, *17*, 57.

(59) Golding, G. M.; Kokot, S. *Journal of forensic sciences* **1989**, *34*, 1156.

(60) Rendle, D. F.; Crabtree, S. R.; Wiggins, K. G.; Salter, M. T. *J Soc Dyers Colour* **1994**, *110*, 338.

(61) Home, J. M.; Dudley, R. J. *Forensic science international* **1981**, *17*, 71.

(62) Hartshorne, A. W.; Laing, D. K. *Forensic science international* **1984**, *25*, 133.

(63) Macrae, R.; Smalldon, K. W. *Journal of forensic sciences* **1979**, *24*, 109.

(64) Beattie, I. B.; Dudley, R. J.; Smalldon, K. W. *J Soc Dyers Colour* **1979**, *95*, 295.

(65) Cheng, J.; So, W. H.; Watson, N. D.; Caddy, B. *Journal of the Forensic Science Society* **1991**, *31*, 31.

(66) Laing, D. K.; Dudley, R. J.; Hartshorne, A. W.; Home, J. M.; Rickard, R. A.; Bennett, D. C. *Forensic science international* **1991**, *50*, 23.

(67) Resua, R. *Journal of forensic sciences* **1980**, *25*, 168.

(68) Resua, R.; Deforest, P. R.; Harris, H. *Journal of forensic sciences* **1981**, *26*, 515.

(69) Wiggins, K. G.; Holness, J. A.; March, B. M. *Journal of forensic sciences* **2005**, *50*, 364.

(70) Robertson, J. a. G., M. *Forensic Examination of Fibres*; 2nd ed.; CRC Press: Boca Raton, FL, 1999.

(71) Robertson, J. *Forensic Examination of Fibres*; 1st ed.; Taylor & Francis Ltd. : West Sussex, England, 1992.

(72) Petrick, L. M.; Wilson, T. A.; Fawcett, W. R. *Journal of forensic sciences* **2006**, *51*, 771.

(73) Carey, A.; Rodewijk, N.; Xu, X. M.; van der Weerd, J. *Analytical chemistry* **2013**, *85*, 11335.

(74) Kretschmer, K.; Helbig, W. *Journal of forensic sciences* **1992**, *37*, 727.

(75) van Bommel, M. R.; Vanden Berghe, I.; Wallert, A. M.; Boitelle, R.; Wouters, J. *J Chromatogr A* **2007**, *1157*, 260.

(76) Ultra Performance LC: Separation Sciences Redefined. [Online Early Access]. Published Online: 2004. http://www.waters.com/webassets/cms/library/docs/720001136en.pdf.

(77) Hoy, S. J., University of South Carolina, 2013.

(78) Robertson, J. a. G., M. *Forensic Examination of Fibres*; 2nd ed.; CRC Press: New York, 1999.

(79) Croft, S. N.; Hinks, D. *J Soc Dyers Colour* **1992**, *108*, 546.

(80) Siren, H.; Sulkava, R. *J Chromatogr A* **1995**, *717*, 149.

(81) Xu, X.; Leijenhorst, H.; Van den Hoven, P.; De Koeijer, J. A.; Logtenberg, H. *Sci Justice* **2001**, *41*, 93.

(82) Terabe, S.; Otsuka, K.; Ichikawa, K.; Tsuchiya, A.; Ando, T. *Analytical chemistry* **1984**, *56*, 111.

(83) Li, S. F. *Capillary Electrophoresis - Principles, Practice and Applications*; Elseiver: Amsterdam, 1994.

(84) Trojanowicz, M.; Wojcik, L.; Urbaniak-Walczak, K. *Chem Anal-Warsaw* **2003**, *48*, 607.

(85) Dockery, C. R.; Stefan, A. R.; Nieuwland, A. A.; Roberson, S. N.; Baguley, B. M.; Hendrix, J. E.; Morgan, S. L. *Analytical and bioanalytical chemistry* **2009**, *394*, 2095.

(86) Stefan, A. R.; Dockery, C. R.; Baguley, B. M.; Vann, B. C.; Nieuwland, A. A.; Hendrix, J. E.; Morgan, S. L. *Analytical and bioanalytical chemistry* **2009**, *394*, 2087.

(87) Oxspring, D. A.; Smyth, W. F.; Marchant, R. *Analyst* **1995**, *120*, 1995.

(88) Agilent Technologies; https://www.agilent.com/cs/library/primers/Public/5990-6969EN%20GPC%20SEC%20Chrom%20Guide.pdf.

(89) Mcgee, W. W.; Coraine, K.; Strimaitis, J. *J Liq Chromatogr* **1979**, *2*, 287.

(90) Weisskopf, K. *J Polym Sci Pol Chem* **1988**, *26*, 1919.

(91) Montaudo, G.; Montaudo, M. S.; Puglisi, C.; Samperi, F. *Analytical chemistry* **1994**, *66*, 4366.

(92) Drott, E. E.; Mendelso.Ra *Separ Sci* **1971**, *6*, 137.

(93) Farah, S.; Tsach, T.; Bentolila, A.; Domb, A. J. *Talanta* **2014**, *123*, 54.

(94) Thompson, M. *High-performance liquid chromatography/mass spectrometry (LC/MS)*, AMC Technical Briefs, 2008.

(95) Ho, C.; Lam, C.; Chan, M.; Cheung, R.; Law, L.; Lit, L.; Ng, K.; Suen, M.; Tai, H. *Clinical Biochemist Reviews* **2003**, *24*, 3.

(96) Huang, M.; Yinon, J.; Sigman, M. E. *Journal of forensic sciences* **2004**, *49*, 238.

(97) Huang, M.; Russo, R.; Fookes, B. G.; Sigman, M. E. *Journal of forensic sciences* **2005**, *50*, 526.

(98) Yinon, J.; Saar, J. *J Chromatogr* **1991**, *586*, 73.

(99) Arpino, P. *Mass Spectrom Rev* **1992**, *11*, 3.

(100) Pozniak, B. P.; Cole, R. B. *Journal of the American Society for Mass Spectrometry* **2007**, *18*, 737.

(101) Tuinman, A. A.; Lewis, L. A.; Lewis, S. A. *Analytical chemistry* **2003**, *75*, 2753.

(102) Morgan, S. L., Nieuwland, A. A., Mubarek, C. R., Hendrix, J. E., Enlow, E. M., and Vasser, B. J. In *Proceedings of the European Fibres Group Annual Meeting* Prague, Czechoslovakia, 2004.

(103) Yinon, J. *Forensic Applications of Mass Spectrometry*; CRC Press: Boca Raton, FL, 1994.

(104) Hughes, J. C.; Wheals, B. B.; Whitehouse, M. J. *Forensic Sci* **1977**, *10*, 217.

(105) Causin, V.; Marega, C.; Schiavone, S.; Della Guardia, V.; Marigo, A. *J Anal Appl Pyrol* **2006**, *75*, 43.

(106) Armitage, S.; Saywell, S.; Roux, C.; Lennard, C.; Greenwood, P. *Journal of forensic sciences* **2001**, *46*, 1043.

(107) Karas, M.; Kruger, R. *Chem Rev* **2003**, *103*, 427.

(108) Burnum, K. E.; Frappier, S. L.; Caprioli, R. M. *Annu Rev Anal Chem* **2008**, *1*, 689.

(109) Reyzer, M. L.; Caprioli, R. M. *Curr Opin Chem Biol* **2007**, *11*, 29.

(110) Berry, K. A. Z.; Hankin, J. A.; Barkley, R. M.; Spraggins, J. M.; Caprioli, R. M.; Murphy, R. C. *Chem Rev* **2011**, *111*, 6491.

(111) Castellino, S.; Groseclose, M. R.; Wagner, D. *Bioanalysis* **2011**, *3*, 2427.

(112) Cramer, R. *Advances in MALDI and Laser-Induced Soft Ionization*; Springer: Switzerland, 2016.

(113) Barry, J. A.; Groseclose, M. R.; Robichaud, G.; Castellino, S.; Muddiman, D. C. *International journal of mass spectrometry* **2015**, *377*, 448.

(114) Jurinke, C.; Oeth, P.; van den Boom, D. *Molecular Biotechnology* **2004**, *26*, 147.

(115) Welker, M.; Fastner, J.; Erhard, M.; von Dohren, H. *Environ Toxicol* **2002**, *17*, 367.

(116) Rader, H. J.; Schrepp, W. *Acta Polym* **1998**, *49*, 272.

(117) Soltzberg, L. J.; Hagar, A.; Kridaratikorn, S.; Mattson, A.; Newman, R. *Journal of the American Society for Mass Spectrometry* **2007**, *18*, 2001.

(118) Cochran, K. H.; Barry, J. A.; Robichaud, G.; Muddiman, D. C. *Analytical and bioanalytical chemistry* **2015**, *407*, 813.

(119) Barry, J. A.; Muddiman, D. C. *Rapid Commun Mass Sp* **2011**, *25*, 3527.

(120) Robichaud, G.; Barry, J. A.; Garrard, K. P.; Muddiman, D. C. *Journal of the American Society for Mass Spectrometry* **2013**, *24*, 92.

(121) Robichaud, G.; Barry, J. A.; Muddiman, D. C. *Journal of the American Society for Mass Spectrometry* **2014**, *25*, 319.

(122) Eyring, M. B. *Visile Microscopical SPectrophotometry in the Forensic Sciences*; 2nd ed.; Regents/Prentice Hall: Upper Saddle River, NJ, 1993; Vol. 1.

(123) Biermann, T. W. *Sci Justice* **2007**, *47*, 68.

(124) Grieve, M. C.; Biermann, T.; Davignon, M. *Sci Justice* **2003**, *43*, 5.

(125) Grieve, M. C.; Biermann, T. W.; Davignon, M. *Sci Justice* **2001**, *41*, 245.

(126) Grieve, M. C.; Biermann, T. W.; Schaub, K. *Sci Justice* **2006**, *46*, 15.

(127) Palmer, R.; Hutchinson, W.; Fryer, V. *Sci Justice* **2009**, *49*, 12.

(128) Suzuki, S.; Suzuki, Y.; Ohta, H.; Sugita, R.; Marumo, Y. *Sci Justice* **2001**, *41*, 107.

(129) Wiggins, K.; Holness, J. A. *Sci Justice* **2005**, *45*, 93.

(130) Grieve, M. C.; Biermann, T. W.; Schaub, K. *Sci Justice* **2005**, *45*, 13.

(131) Wiggins, K.; Drummond, P. *Sci Justice* **2005**, *45*, 157.

(132) Almer, J., McAnsh, E., and Doupe, B. *Canadian Society of Forensic Science Journal* **2010**, *43*, 16.

(133) Was-Gubala, J.; Starczak, R. *Spectrochim Acta A* **2015**, *142*, 118.

(134) Tungol, M. W.; Bartick, E. G.; Montaser, A. *Journal of forensic sciences* **1991**, *36*, 1027.

(135) Tungol, M. W.; Bartick, E. G.; Montaser, A. *Spectrochim Acta B* **1991**, *46*, E1535.

(136) Tungol, M. W.; Bartick, E. G.; Montaser, A. *Applied Spectroscopy* **1993**, *47*, 1655.

(137) Miller, J. V.; Bartick, E. G. *Appl Spectrosc* **2001**, *55*, 1729.

(138) Suzuki, E. *Forensic Applications of Infrared Spectroscopy*; Regents/Prentice Hall: Upper Saddle River, NJ, 1993.

(139) Gilbert, C.; Kokot, S. *Vib Spectrosc* **1995**, *9*, 161.

(140) Kokot, S.; Crawford, K.; Rintoul, L.; Meyer, U. *Vib Spectrosc* **1997**, *15*, 103.

(141) Causin, V.; Marega, C.; Guzzini, G.; Marigo, A. *Applied Spectroscopy* **2004**, *58*, 1272.

(142) Causin, V.; Marega, C.; Schiavone, S.; Marigo, A. *Forensic science international* **2005**, *151*, 125.

(143) Jochem, G.; Lehnert, R. J. *Sci Justice* **2002**, *42*, 215.

(144) Osterberg, M.; Schmidt, U.; Jaaskelainen, A. S. *Colloid Surface A* **2006**, *291*, 197.

(145) Buzzini, P.; Massonnet, G. *Journal of forensic sciences* **2015**, *60*, 712.

(146) Massonnet, G.; Buzzini, P.; Jochem, G.; Stauber, M.; Coyle, T.; Roux, C.; Thomas, J.; Leijenhorst, H.; Van Zanten, Z.; Wiggins, K.; Russell, C.; Chabli, S.; Rosengarten, A. *Journal of forensic sciences* **2005**, *50*, 1028.

(147) Edwards, H. G. M.; Farwell, D. W.; Webster, D. *Spectrochim Acta A* **1997**, *53*, 2383.

(148) De Wael, K.; Baes, C.; Lepot, L.; Gason, F. *Sci Justice* **2011**, *51*, 154.

(149) Wiggins, K. G. *Analytical and bioanalytical chemistry* **2003**, *376*, 1172.

(150) Koons, R. D. *Journal of forensic sciences* **1996**, *41*, 199.

(151) Prange, A.; Reus, U.; Boddeker, H.; Fischer, R.; Adolf, F. P. *Anal Sci* **1995**, *11*, 483.

(152) Sano, T.; Suzuki, S. *Forensic science international* **2009**, *192*, E27.

(153) Shackley, M. S. In *X-Ray Fluorescence Spectrometry (XRF) in Geoarchaeology*; Shackley, S. M., Ed.; Springer New York: New York, NY, 2011, p 7.

(154) Weaver, J. W. *Analytical Methods for a Textile Laboratory*; 3rd ed.; American Association of Textile Chemists and Colorists: Research Triangle Park, N.C. , 1984.

(155) Piccolo, B.; Mitcham, D.; Tripp, V. W.; Oconnor, R. T. *Appl Spectrosc* **1966**, *20*, 326.

(156) Flynn, K.; O'Leary, R.; Roux, C.; Reedy, B. J. *Journal of forensic sciences* **2006**, *51*, 586.

(157) Keen, I. P.; White, G. W.; Fredericks, P. M. *Journal of forensic sciences* **1998**, *43*, 82.

(158) Kokot, S.; Tuan, N. A.; Rintoul, L. *Appl Spectrosc* **1997**, *51*, 387.

(159) Jurdana, L. E.; Ghiggino, K. P.; Nugent, K. W.; Leaver, I. H. *Text Res J* **1995**, *65*, 593.

(160) White, P. C.; Munro, C. H.; Smith, W. E. *Analyst* **1996**, *121*, 835.

(161) Lakowicz, J. R. *Principles of fluorescence spectroscopy*; New York : Kluwer Academic/Plenum, 1999.

(162) Mujumdar, N.; Heider, E. C.; Campiglia, A. D. *Appl Spectrosc* **2015**, *69*, 1390.

(163) Gray, F. M.; Smith, M. J.; Silva, M. B. *J Chem Educ* **2011**, *88*, 476.

(164) Bergfjord, C.; Holst, B. *Ultramicroscopy* **2010**, *110*, 1192.

(165) Kirkbride, K. T., M. *Infrared Microscopy of Fibers*; 2nd ed.; CRC: New York, 1999.

(166) Causin, V.; Marega, C.; Guzzini, G.; Marigo, A. *Journal of forensic sciences* **2005**, *50*, 887.

(167) Grieve, M. C.; Dunlop, J.; Haddock, P. *Journal of forensic sciences* **1988**, *33*, 1332.

(168) Challinor, J. M. *Fiber Identification by Pyrolysis Techniques*; 2nd ed.; CRC: New York, 1999.

(169) Robertson, J. *Other methods of colour analysis: high performance liquid chromatography.* ; 2nd ed. Boca Raton, 1999.

(170) Huang, M.; Yinon, J.; Sigman, M. E. *Journal of forensic sciences* **2004**, *49*, 238.

(171) Li-Ling, C. *Forensic Science Journal* **2007**, *6*, 8.

(172) Zhou, C. Z.; Li, M.; Garcia, R.; Crawford, A.; Beck, K.; Hinks, D.; Griffis, D. P. *Analytical chemistry* **2012**, *84*, 10085.

(173) Massonnet, G.; et al. *Forensic science international* **2012**, *222*, 200.

(174) Cantrell, S.; Roux, C.; Maynard, P.; Robertson, J. *Forensic science international* **2001**, *123*, 48.

(175) Ingle, J., J. D. and Crouch, S. R. *Spectrochemical Analysis*; Prentice Hall: Upper Saddle River, NJ, 1988.

(176) Lichtman, J. W.; Conchello, J. A. *Nat Methods* **2005**, *2*, 910.

(177) da Silva, J. C. G. E.; Tavares, M. J. C. G.; Tauler, R. *Chemosphere* **2006**, *64*, 1939.

(178) DaCosta, R. S.; Andersson, H.; Wilson, B. C. *Photochem Photobiol* **2003**, *78*, 384.

(179) Warner, I. M.; Christian, G. D.; Davidson, E. R.; Callis, J. B. *Analytical chemistry* **1977**, *49*, 564.

(180) Warner, I. M.; Davidson, E. R.; Christian, G. D. *Analytical chemistry* **1977**, *49*, 2155.

(181) Lowrie, C. N.; Jackson, G. *Forensic science international* **1991**, *50*, 111.

(182) Pounds, C. A. *Journal of the Forensic Science Society* **1975**, *15*, 127.

(183) Sermier, F. M.; Massonnet, G.; Buzzini, P.; Fortini, A.; Gason, F.; De Wael, K.; Rovas, P. *Forensic science international* **2006**, *160*, 102.

(184) Casadio, F.; Leona, M.; Lombardi, J. R.; Van Duyne, R. *Accounts of chemical research* **2010**, *43*, 782.

(185) Leona, M.; Stenger, J.; Ferloni, E. *J Raman Spectrosc* **2006**, *37*, 981.

(186) Kirkbirde, K.; Tungol, M. W. *Infrared Microspectroscopy of Fibers*; 2nd ed.; CRC: New York, 1999.

(187) Petrick, L. M.; Wilson, T. A.; Fawcett, W. R. *Journal of Forensic Science* **2006**, *51*, 771.

(188) Huang, M.; Russo, R.; Fookes, B. G.; Sigman, M. E. *Journal of Forensic Science* **2005**, *50*, 1.

(189) Tuinman, A. A.; Lewis, L. A.; Lewis, S., Samuel A. *Analytical Chemistry* **2003**, *75*, 2753.

(190) Laing, D. K.; Hartshorne, A. W.; Harwood, R. J. *Forensic Science International* **1986**, *30*, 65.

(191) Markstrom, L. J.; Mabbott, G. A. *Forensic Science International* **2011**, *209*, 108.

(192) Was-Gubala, J.; Starczak, R. *Applied Spectroscopy* **2015**, *69*, 296.

(193) Nakamura, R.; Tanaka, Y.; Ogata, A.; Naruse, M. *Analytical Chemistry* **2009**, *81*, 5691.

(194) Bowen, A.; Stoney, D. *J Forensic Sci* **2013**, *58*, 789.

(195) Tripp, V., W.; Piccolo, B.; Mitcham, D.; O'Connor, R. T. *Textile Res J* **1964**, *34*, 773.

(196) Burg, A. W.; Rohovsky, M.; Kensler, C. J. *CRC Critical Reviews in Environmental Control* **1977**, *7*, 91.

(197) Stana, K. K.; Pohar, C.; Ribitsch, V. *Colloid Polym Sci* **1995**, *273*, 1174.

(198) Was-Gubala, J. *Science and Justice* **2009**, *49*, 165.

(199) Was-Gubala, J.; Grzesiak, E. *Science and Justice* **2010**, *50*, 55.

(200) Hendel, I.; Nevo, A. *Econometrica* **2006**, *74*, 1637.

(201) Heider, E. C.; Barhoum, M.; Peterson, E. M.; Schaefer, J.; Harris, J. M. *Appl Spectrosc* **2010**, *64*, 37.

(202) Malinowski, E. R. *Journal of Chemometrics* **1988**, *3*, 49.

(203) St. Martin's Press: New York, 1964.

(204) Oien, C. T. Clearwater, FL U.S.A., 2007.

(205) Miller, J. V.; Bartick, E. G. *Appl. Spectrosc.* **2001**, *55*, 1729.

(206) Grieve, M. *Fibres and their Examination in Forensic Science*; Springer-Verlag: Berlin, 1990; Vol. 4.

(207) Goodpaster, J. V.; Liszewski, E. A. *Analytical Bioanalytical Chemistry* **2009**, *394*, 2009.

(208) Laing, D. K.; Hartshorne, A. W.; Harwood, R. J. *Forensic Sci. Int.* **1986**, *30*, 65.

(209) Markstrom, L. J.; Mabbott, G. A. *Forensic Sci. Int.* **2011**, *209*, 108.

(210) Was-Gubala, J.; Starczak, R. *Appl. Spectrosc.* **2015**, *69*, 296.

(211) Was-Gubala, J. *Forensic Sci. Int.* **1997**, *85*, 51.

(212) Ledbetter, N. L.; Walton, B. L.; Davila, P.; Hoffmann, W. D.; Ernest, R. R.; Verbeck, G. F. *J Forensic Sci* **2010**, *55*, 1219.

(213) Reuland, D. J.; Trinler, W. A. *J Forensic Sci. Soc.* **1980**, *20*, 111.

(214) Luongo, G.; Thorsén, G.; Östman, C. *Anal. Bioanal. Chem.* **2014**, *406*, 2747.

(215) Antal, B.; Kuki, Á.; Nagy, L.; Nagy, T.; Zsuga, M.; Kéki, S. *Anal. Bioanal. Chem* **2016**, *408*, 5189.

(216) Micali, G.; Curro, P.; Calabro, G. *Analyst* **1984**, *109*, 155.

(217) Loyd, J. B. F. *J Forensic Sci Soc* **1977**, *17*, 145.

(218) Hartshorne, A. W.; Laing, D. K. *Forensic Sci. Int.* **1991**, *51*, 239.

(219) Shu, W.-C.; Ding, W.-H. *Journal of the Chinese Chemical Society* **2009**, *56*, 797.

(220) Martinez, A. M.; Kak, A. C. *IEEE Trans Pattern Analysis and Machine Intelligence* **2001**, *23*, 228.

(221) Malinowski, E. R. *J Chemom* **1988**, *3*, 49.

(222) Malinowski, E. R. *J Chemometr* **1989**, *3*, 49.

(223) *The Warren Commission's Report*; St. Martin's Press: New York, 1964.

(224) Deadman, H. A. Fiber Evidence and the Wayne Williams Trial - I, US Government Document J1.14/8a:F44. [Online Early Access]. Published Online: 1984. http://www.fbi.gov

(225) Oien, C. T.; Symposium, T. E., Ed. Clearwater, FL, 2007.

(226) Brettell, T. A.; Butler, J. M.; Saferstein, R. *Analytical chemistry* **2005**, *77*, 3839.

(227) Abraham, D.; Grieve, R. B.; Oaks, J. A. *Experimental parasitology* **1990**, *70*, 314.

(228) Wiggins, K. *Thin layer chromatographic analysis for fibre dyes*; 2nd ed.; CRC Press: New York, 1999.

(229) Wiggins, K.; Holness, J. A. *Sci Justice* **2005**, *45*, 93.

(230) Griffin, R. S., J. *Other methods of colour analysis: high performance liquid chromatography*; 2nd ed. Boca Raton, FL, 1999.

(231) Trojanowicz, M. W., L. ; Urbaniak-walczak, K. *Chemical Analysis* **2003**, *48*, 607.

(232) Xu, X. L., H.; Van den Hoven, P.; De Koeijer, J.A.; Logtenberg, H. *Sci Justice* **2001**, *41*, 93.

(233) Petrick, L. M.; Wilson, T. A.; Ronald Fawcett, W. *Journal of forensic sciences* **2006**, *51*, 771.

(234) Soltzberg, L. J.; Hagar, A.; Kridaratikorn, S.; Mattson, A.; Newman, R. *Journal of the American Society for Mass Spectrometry* **2007**, *18*, 2001.

(235) Stefan, A. R.; Dockery, C. R.; Baguley, B. M.; Vann, B. C.; Nieuwland, A. A.; Hendrix, J. E.; Morgan, S. L. *Analytical and bioanalytical chemistry* **2009**, *394*, 2087.

(236) Tuinman, A. A.; Lewis, L. A.; Lewis, S. A., Sr. *Analytical chemistry* **2003**, *75*, 2753.

(237) Abu-Rous, M.; Varga, K.; Bechtold, T.; Schuster, K. C. *J Appl Polym Sci* **2007**, *106*, 2083.

(238) Muller, M.; Murphy, B.; Burghammer, M.; Snigireva, I.; Riekel, C.; Gunneweg, J.; Pantos, E. *Appl Phys a-Mater* **2006**, *83*, 183.

(239) Bro, R. *Chemometr Intell Lab* **1997**, *38*, 149.

(240) Arruda, A. F.; Yu, S. J.; Campiglia, A. D. *Talanta* **2003**, *59*, 1199.

(241) Indahl, U. G. *J Chemometr* **2014**, *28*, 508.

(242) Barker, M.; Rayens, W. *J Chemometr* **2003**, *17*, 166.

(243) Brereton, R. G.; Lloyd, G. R. *J Chemometr* **2014**, *28*, 213.

(244) Ouertani, S. S.; Mazerolles, G.; Boccard, J.; Rudaz, S.; Hanafi, M. *Chemometr Intell Lab* **2014**, *133*, 25.

(245) de Almeida, M. R.; Correa, D. N.; Rocha, W. F. C.; Scafi, F. J. O.; Poppi, R. J. *Microchem J* **2013**, *109*, 170.

(246) Wehrens, R.; Putter, H.; Buydens, L. M. C. *Chemometr Intell Lab* **2000**, *54*, 35.

(247) Perez, N. F.; Ferre, J.; Boque, R. *Chemometr Intell Lab* **2009**, *95*, 122.

(248) Ballabio, D.; Consonni, V. *Anal Methods-Uk* **2013**, *5*, 3790.

(249) Olivieri, A. C.; Wu, H. L.; Yu, R. Q. *Chemometr Intell Lab* **2009**, *96*, 246.

(250) Olivieri, A. C. E., G. M. *Practical Three-Way Calibration*; 2nd ed.; Elsevier: Amsterdam, 2014.

(251) Kemsley, E. K. *Trac-Trend Anal Chem* **1998**, *17*, 24.

(252) Christensen, J. H.; Hansen, A. B.; Mortensen, J.; Andersen, O. *Analytical chemistry* **2005**, *77*, 2210.

(253) Guimet, F.; Boque, R.; Ferre, J. *Chemometr Intell Lab* **2006**, *81*, 94.

(254) Damiani, P. C.; Duran-Meras, I.; Garcia-Reiriz, A.; Jimenez-Giron, A.; de la Pena, A. M.; Olivieri, A. C. *Analytical chemistry* **2007**, *79*, 6949.

(255) Bro, R.; Kiers, H. A. L. *J Chemometr* **2003**, *17*, 274.

(256) Slotani, M. *Annals of the Institute of Statistical Mathematics* **1964**, *16*, 135.

(257) Haaland, D. M.; Thomas, E. V. *Analytical chemistry* **1988**, *60*, 1193.

(258) Slaten, B. L.; Smith, B. F. *J Appl Polym Sci* **1979**, *23*, 367.

(259) Thanki, P. N.; Singh, R. P. *Polymer* **1998**, *39*, 6363.

(260) Shearer, J. C.; Peters, D. C.; Kubic, T. A. *Trac-Trend Anal Chem* **1985**, *4*, 246.

(261) Lee, H. C., Palmbach, T. and Miller, M. T. *Henry Lee's Crime Scene Handbook*; 1st ed.; Academic Press: Barcelona, Spain, 2001.

(262) Bedenko, V. E.; Stefanskaya, I. V.; Tropanikhin, I. Y.; Erokhina, A. E. *Fibre Chem+* **2015**, *47*, 58.

(263) Imaizumi, A.; Yoshizumi, K.; Fujita, T. *Environ Technol* **2004**, *25*, 451.

(264) Saheb, D. N.; Jog, J. P. *Adv Polym Tech* **1999**, *18*, 351.

(265) Tylli, H.; Forsskahl, I.; Olkkonen, C. *J Photoch Photobio A* **1993**, *76*, 143.

(266) Pal, S. K.; Thakare, V. B.; Singh, G.; Verma, M. K. *Indian J Fibre Text* **2011**, *36*, 145.

(267) Daruwall, Eh.; Dsilva, A. P.; Mehta, A. C. *Text Res J* **1967**, *37*, 147.

(268) Barry, R., and Chorley, R. *Atmosphere, Weather and Climate*; 9th ed.; Routledge: New York, NY, 2010.

(269) Olivieri, A. C.; Escandar, G. M.; de la Pena, A. M. *Trac-Trend Anal Chem* **2011**, *30*, 607.